Negative Ion Electron Capture Dissociation (niECD): A Novel Tandem Mass Spectrometric Technique

by

Ning Wang

A dissertation submitted in partial fulfillment
of the requirements for the degree of
Doctor of Philosophy
(Chemistry)
in the University of Michigan
2014

Doctoral Committee:

Professor Kristina I. Håkansson, Chair
Professor Philip C. Andrews
Professor Robert T. Kennedy
Assistant Professor Brandon T. Ruotolo

To My Dear Family

Acknowledgements

My first and deepest appreciation goes to my advisor, Dr. Kristina Håkansson, for her continuous guidance and support in all stages of this thesis. I would like to thank all her contributions of time, ideas, and funding that make my Ph.D. experience productive and rewarding. Her enthusiasm, passion and vast knowledge have inspired me to overcome all the challenges in my Ph.D. pursuit. One simply could not wish for a better or friendlier advisor.

I would also like to thank my dissertation committee members, Dr. Robert Kennedy, Dr. Philip Andrews, and Dr. Brandon Ruotolo. Their insightful comments, valuable suggestions, encouragement and critiques were of essence to this thesis.

The members of Håkansson group have contributed immensely to my personal and professional life at the University of Michigan. The group has always been a source of friendships and good advice. I thank all the past and current group members: Hyun Ju Yoo, Bo Wang, Hangtian Song, Wen Zhou, Chris Rath, Katie Hersberger, Di Gao, Wendi Hale, Tao Jiang, Phil McClory, Kevin Ileka, and Jordan Stern for their great encouragement and for making this lab a friendly environment to work. I couldn't have survived the graduate school without them.

My research was funded by a National Science Foundation (NSF) grant, a Margaret & Herman Sokol Graduate Summer Research Fellowship, a Chemistry Research

Excellence Award, and financial support from Department of Chemistry at the University of Michigan through teaching assistantship.

In addition, I would like to thank my friends in the United States, China and other parts of the world, who offered me joy and help. I am deeply grateful to my closest friend in Ann Arbor, Lu Tian, who was always a great support in all my struggles and frustration.

Last but not least, I would like to thank my family for their constant love and care. I would not have made this far without them. For my parents, Qing Wang and Yueqin Qi, whose unconditional love provided me inspiration and was my driving force. For my loving, supportive, encouraging and patient husband, Jialiang Yan, who has helped me make everything possible.

Ning Wang

April 20, 2014

Ann Arbor, Michigan

Table of Contents

List of Figures

List of Schemes

List of Abbreviations

CAD	Collision activated dissociation
CCK	Cholecystokinin
CCKS	Sulfated cholecystokinin
CEM	Chain ejection model
CHEF	Correlated harmonic excitation fields
CI	Chemical ionization
CRM	Charged residue model
DABCO	1,4-diazabicyclo[2.2.2]octane
DTSSP	3,3'-dithiobis (sulfosuccinimidyl propionate)
ECD	Electron capture dissociation
EDD	Electron detachment dissociation
EID	Electron ionization dissociation
ESI	Electrospray ionization
ETD	Electron transfer dissociation
FT-ICR	Fourier transform ion cyclotron resonance
IEM	Ion evaporation model
IRMPD	Infrared multiphoton dissociation
IVR	Intramolecular vibrational-energy redistribution
LC	Liquid chromatography
MALDI	Matrix-assisted laser desorption/ionization
MS	Mass spectrometry
MS/MS or MS^n	Tandem mass spectrometry
m/z	Mass-to-charge ratio
Nano ESI	Nano electrospray ionization
NETD	Negative electron transfer dissociation
NHS	*N*-hydroxysuccinimide
niECD	Negative ion electron capture dissociation
pI	Isoelectric point
PNGase F	Peptide-N-glycosidase F
ppm	Parts-per-million
ppb	Parts-per-billion

PSD	Post-source decay
PTM	Post-translational modification
PTR	Proton transfer reaction
Q	Quadrupole
RP-HPLC	Reverse-phase high performance liquid chromatography
rf	Radio frequency
S/N	Signal to noise
SORI-CAD	Sustained off-resonance irradiation collision activated dissociation
SPE	Solid-phase extraction
T	Tesla, a unit of magnetic field
TMAA	Trimethylammoniumacetyl
TMPP	Tris(2,4,6-trimethoxyphenyl) phosphonium
TOF	Time of flight
UVPD	Ultraviolet photodissociation

Abstract

Negative Ion Electron Capture Dissociation (niECD): a Novel Tandem Mass Spectrometric Technique

by

Ning Wang

Chair: Kristina I. Håkansson

Electron capture dissociation (ECD) and electron transfer dissociation (ETD) are powerful tandem mass spectrometry (MS/MS) techniques for biomolecular structural elucidation. However, one drawback of ECD/ETD is that they require multiply positively charged precursor ions, possibly precluding analysis of acidic molecules such as phospho-, sulfopeptides, and sialylated glycopeptides.

Electron attachment to anions appears unlikely due to Coulomb repulsion. However, we found that such an intriguing reaction is indeed feasible within a narrow energy range (3.5-6.5 eV). The resulting charge-*increased* radicals further undergo dissociation analogous to ECD/ETD, thus constituting a novel MS/MS technique that we termed negative ion electron capture dissociation (niECD). niECD of phospho- and sulfopeptides yields predictable $c'/z^{\bullet}$-type backbone fragments without loss of phosphoric

acid or sulfonate.

Fragmentation pattern similarities between niECD and ECD indicate that niECD proceeds through a mechanism related to that of ECD. We proposed that gas-phase zwitterionic structures are necessary for successful niECD and that a positive charge is required to serve as the electron capture site, or to promote electron capture. N-terminal acetylation, which should reduce the probability of zwitterion formation, results in decreased niECD efficiency and introduction of fixed positive charge tags, which should promote zwitterion formation, enables niECD of peptides which could not undergo niECD in their unmodified forms. niECD efficiency also decreases with decreasing zwitterion propensity for five sets of synthetic peptides, further supporting the zwitterion mechanism.

niECD was further applied to peptide chains bound by natural disulfide bonds or disulfide-containing cross-linkers. niECD of disulfide-linked peptides again results in very similar fragmentation patterns as those from ECD. S-S bond cleavage constitutes the preferred fragmentation pathway, producing characteristic fragments, which allow rapid detection of disulfide-linked peptides. Analogous to cation ECD, niECD of both N-linked and O-linked sialylated glycopeptides, which are readily deprotonated in negative ion mode, exhibits peptide backbone fragmentation with retention of labile glycans.

Overall, the research presented in this thesis contributes to an increased understanding of the mechanism and utility of niECD, thereby allowing this unique approach to be developed into a valuable analytical tool for structural analysis of important biological samples.

Chapter 1

Introduction

1.1 Mass Spectrometry-Based Proteomics

In this post-genomic era where the name of the game has become proteomics, our knowledge of biological systems continues to expand and progress. The human genome has been predicted to comprise between 20,000 and 25,000 protein-coding genes.[1-3] By contrast, the human proteome is vastly more complex with the total number of proteins estimated to be over 1 million.[4] Complete characterization of the proteome, which encompasses identification and structural characterization of proteins and their complexes, quantitation of protein expression under different treatments or environmental conditions, as well as determination of post-translational modifications (PTMs), remains a tremendous challenge. PTMs constitute a variety of covalent modifications (e.g., phosphorylation, glycosylation, acetylation, and disulfide formation) to a protein after its

translation and are key factors that exponentially increase the diversity and complexity of the proteome.[5] More than 400 different PTMs have been described. PTMs are required for changes in protein subcellular location, complexation, degradation, signal transduction, and regulatory control of enzymatic function.[6] Identifying the type and location of these protein modifications is a first step in understanding their regulatory potential.

Mass spectrometry (MS) has evolved into a formidable tool for dissecting the primary structures as well as the PTMs of proteins.[7-9] In MS-based proteomics experiments, there are two complementary approaches: bottom-up and top-down.[10-13] Currently, the "bottom-up" approach is the gold standard when analyzing protein(s) by mass spectrometry due to its high-throughput protein identification, well-developed MS instrumentation and software.[14] Bottom-up proteomics has multiple implementations. For example, proteins can first be separated by liquid chromatography (LC) and/or electrophoresis, followed by proteolytic digestion into peptides (1-3 kDa). The protease typically used to digest proteins is trypsin, which cleaves C-terminal to arginine and lysine. The resulting peptides are then separated by reverse-phase (RP) HPLC, introduced into a mass spectrometer as peptide cations and subjected to tandem mass spectrometry (MS/MS) analysis to obtain sequence information.[10, 15] The most widely used method for bottom-up MS/MS data analysis is a database search[16, 17] in which experimental precursor ion mass and product ion masses are compared with predicted peptide fragment masses from a genome-derived database to identify the corresponding protein.[18-20] Alternatively, "shotgun" proteomics relies on enzymatic digestion of protein mixtures without the need for prior protein fractionation/separation.[21-24] Highly

complex samples containing hundreds of thousands of peptides are then analyzed directly by online LC/MS (typically by two orthogonal stationary phases such as cation exchange and reverse phase chromatography) and MS/MS. Some benefits associated with the bottom-up approach are that peptides are readily solubilized and separated, tasks that are considerably more difficult for proteins. It also provides higher sensitivity and throughput than the top-down method. However, only a small percentage of the digested peptides are normally detected, leading to limited protein sequence coverage by identified peptides. An additional drawback of bottom-up includes ambiguity of the origin for redundant peptide sequences (the protein inference problem).

In contrast to the bottom-up approach, the "top-down" approach, which analyzes intact proteins directly without prior digestion, has emerged as an attractive alternative, particularly for the analysis of protein PTMs.[25-28] In top-down proteomics, gas-phase proteins are isolated and fragmented in a mass spectrometer, yielding masses of both the intact proteins and their fragment ions for protein identification. It has been shown that labile PTM loss occurs to a smaller extent in top-down compared with bottom-up analysis.[25, 29, 30] Thus, the identity and location of each PTM can be more frequently deduced in top-down experiments according to its characteristic mass discrepancy relative to unmodified amino acid residues. Advantages of the top-down approach are higher sequence coverage of target proteins[31] and improved PTM characterization.[25, 32] In theory, the top down approach can provide a complete description of the primary structure of proteins, locate all PTMs, and reveal any correlations between these modifications. However, it has proven difficult to produce extensive fragmentation of intact protein ions, particularly from large proteins. Electron-based fragmentation

reactions, such as electron capture dissociation (ECD)[33] and electron transfer dissociation (ETD),[34, 35] can fragment proteins more effectively than conventional collision activated dissociation (CAD) and retain labile PTMs.[36] They have become the preferred fragmentation methods in top-down experiments. Ultraviolet photodissociation (UVPD) has also been implemented for characterization of intact proteins, leading to near-complete fragmentation of proteins up to 29 kDa.[37] Nevertheless, there are other technological obstacles to the top-down method, which prevent it from widespread use. For instance, front-end separation of intact proteins is more challenging than the separation of peptide mixtures. This challenge means that larger quantities of protein are required and the analytical throughput as well as efficiency is still a major challenge for top-down experiments. In addition, instruments with higher resolution and high mass accuracy, such as FT-ICR and Orbitrap, are essential in top-down proteomics to resolve isotopic envelopes of co-eluting proteins and isotopic distributions from peptides of different charge states.

1.2 Fourier Transform Ion Cyclotron Resonance Mass Spectrometry

1.2.1 FT-ICR Overview

Fourier transform ion cyclotron resonance mass spectrometry (FT-ICR MS) was first introduced in 1974 by Comisarow and Marshall.[38, 39] It offers the highest mass resolving power[40, 41] and mass measurement accuracy[41] of all mass analyzers, making it a superior choice for biological applications such as proteomics[42-45] and analysis of extremely complex organic mixtures such as petroleum.[46] One factor contributing to this high FT-ICR performance is a highly uniform magnetic field with a stability of a few

parts per billion (ppb) per hour. The cyclotron frequency of a charged species in such a magnetic field constitutes a unique signature for ions of a particular mass-to-charge ratio. This cyclotron frequency can be measured very accurately because the observation time can be as long as several seconds with no influence of ion kinetic energy spread. Another advantage of the FT-ICR mass analyzer is its capability of various MS/MS activation techniques, allowing identification of analytes not only by their intact molecular weight, but also their dissociation patterns (discussed in details in Section 1.4).

All FT-ICR mass analyzers are equipped with three main components: a superconducting magnet, an analyzer cell (ICR cell), and an ultrahigh vacuum system.[47] The performance parameters, such as mass resolving power, mass accuracy, dynamic range, and upper mass limit, improve linearly or quadratically with increasing magnetic field strength in FT-ICR mass spectrometers.[48, 49] Thus, instruments with higher field have broader applications, yielding more informative data, and permitting experiments on systems with greater complexity. Currently, commercially available magnet sizes produced for FT-ICR MS instruments are 4.7 T, 7 T, 9.4 T, 12 T, and 15 T. In addition, two 21 T FT-ICR superconducting magnet systems are under construction for the USA National High Magnetic Field Laboratory (NHMFL) and the Pacific Northwest National Laboratory (PNNL). The ICR cell, where ions are stored, mass analyzed, and detected is the heart of FT-ICR instruments and is discussed shortly in the following section. An ultrahigh vacuum system (in the region of 10^{-9} – 10^{-10} Torr) provided by cryogenic or turbo molecular pumps is required in FT-ICR mass spectrometers to generate long-lasting signal and to achieve ultrahigh mass resolution.[47, 50] Differential pumping stages are

typically applied to gradually decrease the pressure from atmospheric to ultrahigh vacuum in the ICR cell.

1.2.2 General FT-ICR Principle

In FT-ICR, the mass-to-charge (m/z) ratio of an analyte ion is determined based on its frequency of cyclotron motion in a highly homogenous magnetic field.[47, 50-54] In a magnetic field, **B**, an ion with velocity **v** and charge q = ze in which e is the elementary charge and z is the number of elementary charges, experiences the Lorentz force, which is perpendicular to both the ion velocity and the magnetic field.

$$\boldsymbol{F} = ze\mathbf{v} \times \mathbf{B} \qquad (1)$$

The Lorentz force causes the ion to travel in a circular trajectory perpendicular to the magnetic field, and is counterbalanced by the centrifugal force, which is defined by the ion mass, m, the ion velocity, v_{xy}, in the *x*-*y*-plane (perpendicular to the magnetic field), and the radius of the circular orbit, *r*.

$$F = m\frac{{v_{xy}}^2}{r} = zev_{xy}B \qquad (2)$$

By introducing the angular frequency $\omega = v/r$, the following equation can be derived:

$$\omega = \frac{zeB}{m} \qquad (3)$$

The cyclotron frequency *f* equals $\omega/2\pi$ and the cyclotron equation (4) is obtained by dividing equation (3) by 2π.

$$f = \frac{zeB}{2\pi m} \qquad (4)$$

Therefore, each ion of a certain m/z ratio has a unique cyclotron frequency in a given magnetic field. This relation is the governing principle in FT-ICR MS. One important feature of equation (4) is that this characteristic cyclotron frequency is independent of ion velocity and kinetic energy, eliminating the need for "focusing" ions as encountered in most other mass spectrometers.[47, 50]

The cyclotron motion described above is detected in an ICR cell, which can adopt different geometries.[53, 55] A common design is the cylindrical cell (see Figure 1.1), consisting of six electrodes: one front and one back trapping electrode positioned perpendicular to the magnetic field, two opposing excitation electrodes, and two opposing detection electrodes. Once inside the ICR cell, ions are trapped axially by the two end trapping plates with small DC potentials in addition to being confined radially by the Lorentz force. The trapping plate configuration creates a potential well that allows ions to oscillate axially between the trapping electrodes whilst maintaining their cyclotron motion.[50]

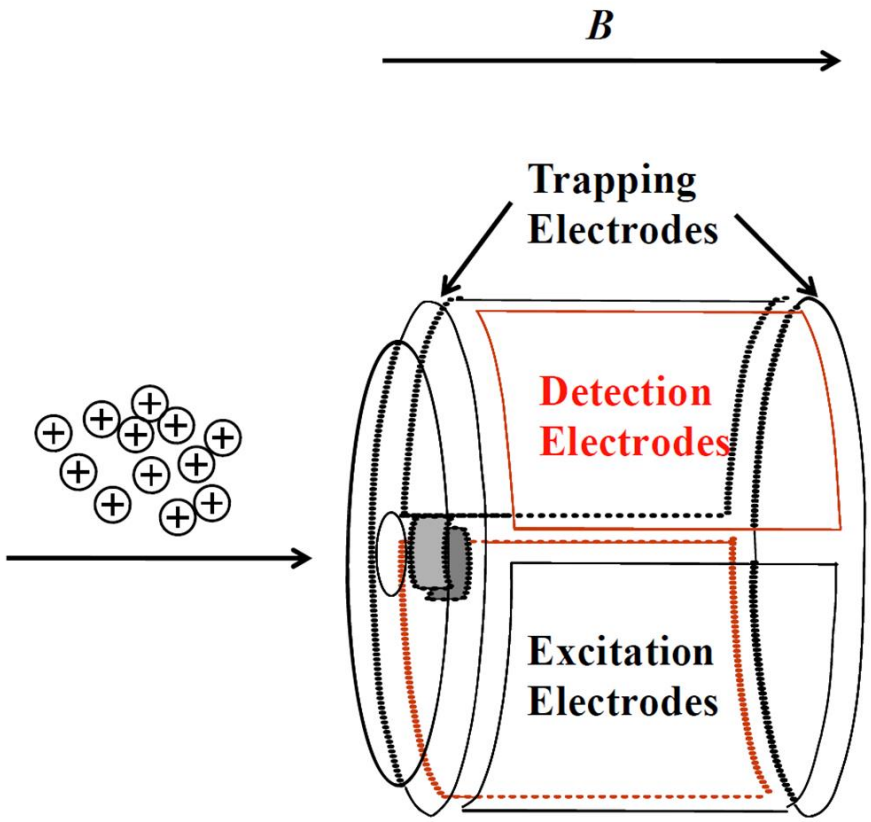

Figure 1.1. Schematic representation of a closed cylindrical ICR cell. Two trapping plates are mounted perpendicular to the magnetic field at both ends of the ICR cell. Detection and excitation electrodes are positioned 180^{o} out of phase (alternating) on the ICR cell wall. The direction of ion motion and the magnetic field are indicated with arrows.

Under initial conditions, ions typically have small cyclotron orbit radius (<1 mm) due to their low kinetic energy and cannot induce a measurable image current in the detection plates. In addition, ions have random cyclotron phase, which may generate zero net image current. This lack of signal is due to ions with the same cyclotron frequency but different phase inducing image current simultaneously in each of the detection plates and thus canceling each other out.[47, 55] To obtain a detectable signal, the ions must be excited coherently by applying a spatially uniform electric field, which oscillates at the cyclotron frequency of a given m/z ratio. This field is introduced via the

excitation electrodes.[47] Ions in resonance with the applied frequency absorb energy and spiral outwards to a larger cyclotron radius. All ions with the same m/z ratio are coherently excited and undergo cyclotron motion as a compact "ion packet". In practice, a broadband excitation, involving a rapid frequency sweep or chirp over a relatively wide range of frequencies, is usually performed to allow simultaneous detection of all ions of interest.[50] When ion packets pass near each electrode, alternating image currents are induced in the two opposing detection electrodes. The image current, recorded for a predetermined period of time, is then amplified and digitized to generate a time-domain signal or transient. This time-domain signal, which contains all the frequencies of ion packets in the cell, is converted to frequency-domain spectra via discrete Fourier transformation. Spectral frequencies are then converted to m/z ratios by applying equation (4). A schematic view of FT-ICR detection is shown in Figure 1.2.

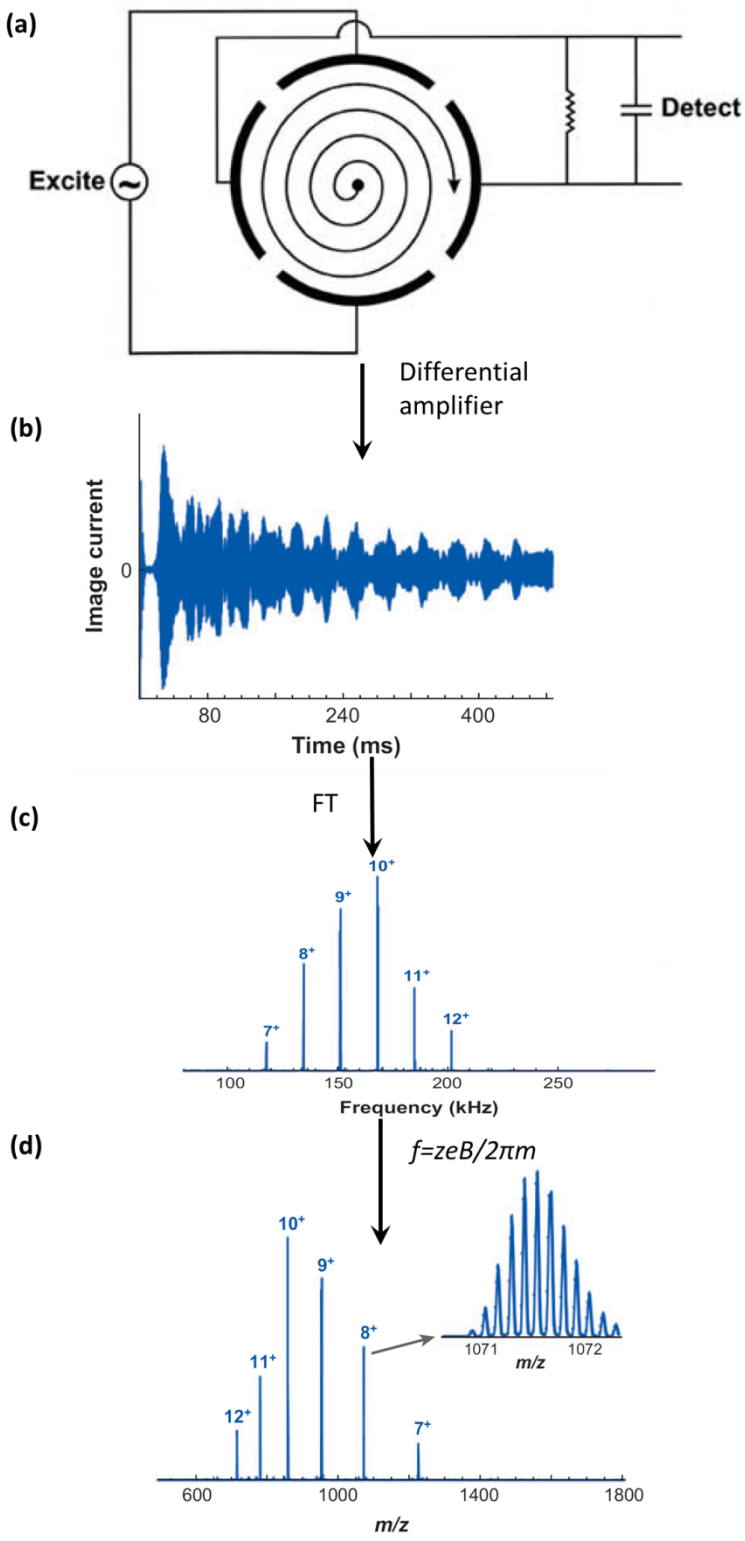

Figure 1.2. (a) Schematic diagram of ion excitation and detection inside the ICR cell. An rf voltage waveform containing the resonance frequency of the ion is applied to the pair of excitation plates. An image current of the orbiting ion cloud is detected on the

pair of detection plates. (b) The time-domain signal recorded by image current detection from two opposing detection electrodes. (c) Frequency-domain signal obtained from the time-domain signal via fast Fourier transformation. (d) m/z spectrum obtained by converting frequencies to m/z ratios. Adapted from Marshall.[56]

In FT-ICR MS, the signal from ions of a given m/z ratio is linearly proportional to the number of ions and to the radius of the ion motion.[47, 57] At least 100 charges of a specific m/z ratio are required to induce a measurable current.[58] The resolving power is proportional to the acquisition period for the time-domain transient.[47] The longer the image current is recorded, the higher resolving power the mass spectrum has. However, the time-domain transient duration is in turn limited by magnetic and electric field imperfection, ion-neutral collisions, and ion-ion interactions.[59-62] Inherently, ion detection in FT-ICR MS is non-destructive and a wide m/z range can be detected simultaneously.

1.2.3 FT-ICR Instrumentation

Schematic diagrams of our two 7 Tesla Fourier transform ion cyclotron resonance mass spectrometers (Bruker Daltonics, Billerica, MA) are shown in Figure 1.3. The Apex instrument incorporates an electrospray ion source, dual ion funnels, an external quadrupole (Q), a hexapole collision cell, high voltage ion transfer optics, and the ICR cell located in the homogeneous region of a magnetic field. Electrospray ionization (ESI) is the most commonly used ionization technique coupled with FT-ICR MS for biomolecule analysis[63, 64] and its principles are described in detail in Section 1.3. The dual stage ion funnels located after the ESI source improve ion transmission and therefore increase sensitivity.[65, 66] They are comprised of a series of ring electrodes with applied RF fields and a gradient DC potential, resulting in effective focusing and

transmission of ions from regions of high pressure to low pressure. The quadrupole can act as a mass filter which allows mass selection of precursor ions. The following hexapole collision cell is used for mass-selective ion accumulation,[67] or to perform external CAD (see Section 1.4.1). A series of ion transfer optics positioned after the collision cell is necessary to overcome the magnetic mirror effect and to transport ions into the ICR cell.[68] The mass analyzer is an infinity cell, which has a common cylindrical geometry design with equipotential-line-segmented trapping plates. An indirectly heated hollow cathode (HeatWave, Watsonville, CA),[69] mounted on the rear side of the ICR cell, provides electrons for ion-electron reactions such as ECD and negative ion ECD (niECD; see Section 1.4.3). A 10.6 μm CO_2 IR laser (Synrad, Mukilteo, WA) is used for infrared multiphoton dissociation (IRMPD). The SolariX instrument shares a similar design with Apex, except that the high voltage ion transfer optics is replaced with a transfer hexapole, accounting for an order of magnitude increase in sensitivity. A chemical ionization (CI) source is also coupled to the SolariX instrument after the dual ion funnels, to produce radical reagents for ETD, negative ETD (NETD) or proton transfer reaction (PTR) events.

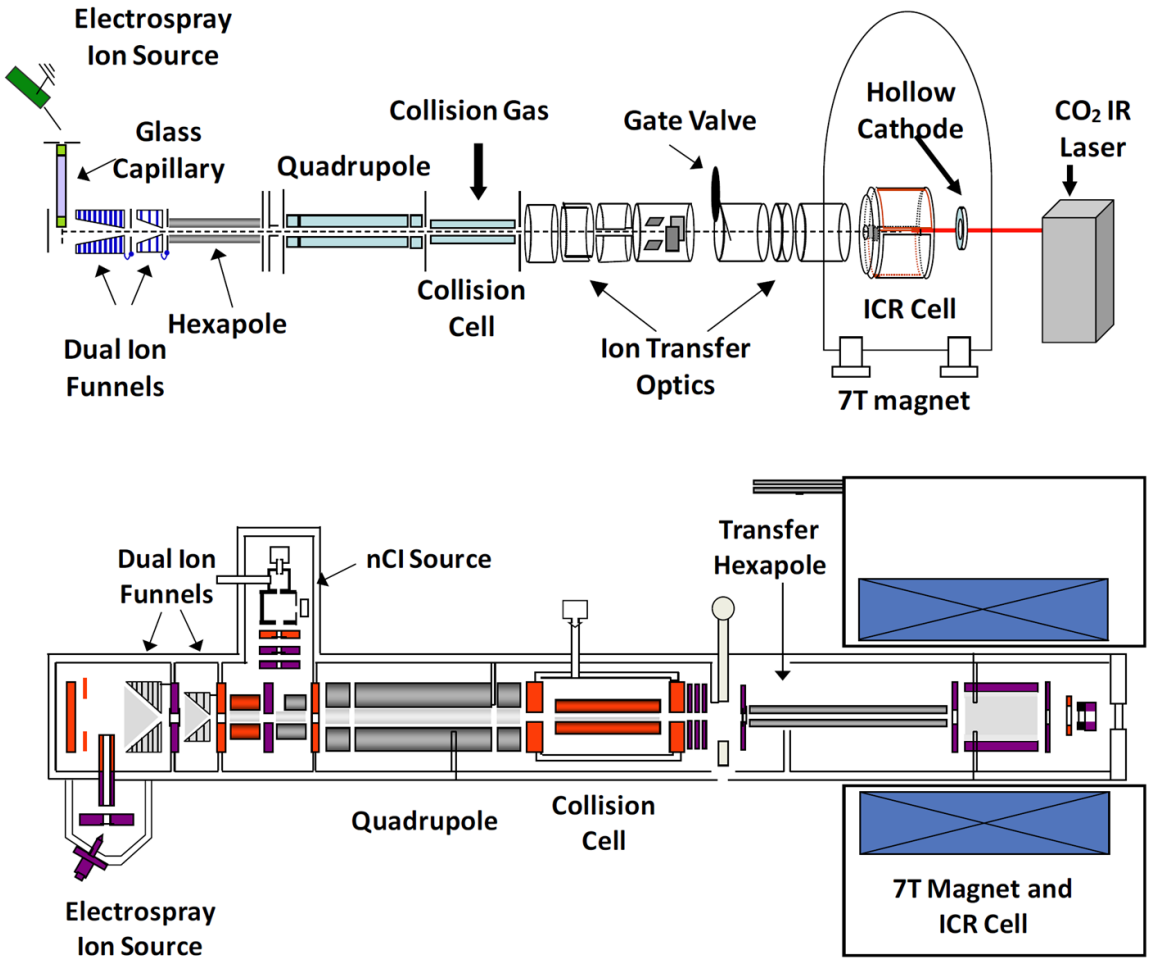

Figure 1.3. Schematic diagrams (top, Bruker Apex; bottom, Bruker Solarix) of 7 T Q-FT-ICR mass spectrometers in our lab. The instruments are equipped with an ESI source, dual stage ion funnels, a quadrupole mass filter, a hexapole collision cell for CAD, and a cylindrical infinity ICR cell as mass analyzer.

1.3 Electrospray Ionization (ESI)

Ionization of the analyte is the first step in any mass spectrometric analysis. It is the advent of "soft" ionization techniques, in particular electrospray ionization (ESI)[70, 71] and matrix-assisted laser desorption/ionization (MALDI),[72] that made mass spectrometry the preferred method in proteomics applications. These soft ionization methods allow for the ionization of large non-volatile biomolecules in their intact form. In this thesis, ESI is used exclusively. During ESI, samples are typically prepared in an

easily evaporated solvent, such as a mixture of water and volatile organic solvent, with a small amount of acid or base to promote protonation or deprotonation, respectively. As shown in Figure 1.4, the sample solution is pushed through a capillary needle to which a high electric potential (3-6 kV) is applied. Depending on the polarity of the electric field, either cations or anions will accumulate at the tip of the needle. Due to the Coulomb repulsion between the ions, and the pull of the electric field, the analyte solution overcomes the surface tension and forms a Taylor cone[73] that emits a spray of charged droplets. Hot drying gas or a heated mass spectrometer inlet is often used to promote solvent evaporation from the droplets. As desolvation of the droplets is continuing, droplet radii decrease and the charge density increases. When the radius of a droplet reaches the Rayleigh limit,[74-76] the Coulomb repulsion exceeds the surface tension and leads to Coulomb fission, releasing smaller offspring droplets. The repetitive Coulomb fission process eventually results in the molecular ions containing either a single charge or multiple charges ready for MS analysis.

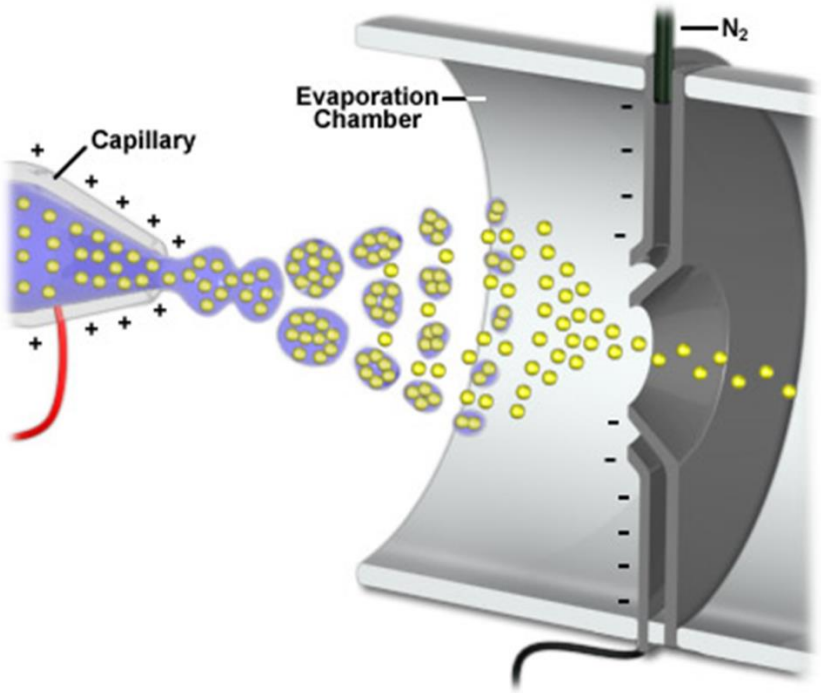

Figure 1.4. A diagram of electrospray ionization (positive ion mode used as an example). See more information at http://www.magnet.fsu.edu/education/tutorials/tools/ionization_esi.html

The final generation of desolvated ions from droplets in ESI is not yet fully resolved. There are two major theories. Iribarne and Thomson proposed the ion evaporation model (IEM),[77] which states that prior to complete desolvation, the field strength at the droplet surface becomes large enough to eject ions directly from the droplet surface into the gas phase. The charged residue model (CRM)[78, 79] introduced by Dole and coworkers suggests that droplets undergo successive cycles of solvent evaporation and Coulomb fission at the Rayleigh limit until a single residual analyte ion is left. Complete evaporation of the solvent finally yields the analyte with the charges that the final droplet carried. Generally, it is believed that small ions are produced through IEM[80, 81] whereas larger ions, such as globular proteins, are formed by CRM.[82, 83] More recently, a chain ejection model (CEM) has been proposed for unfolded proteins by Konermann and co-

workers.[84, 85] Upon unfolding, proteins become more hydrophobic and migrate to the droplet surface. One chain terminus then gets expelled into the vapor phase, followed by stepwise sequential ejection of the remaining protein. A schematic diagram illustrating these three mechanisms is shown in Figure 1.5.

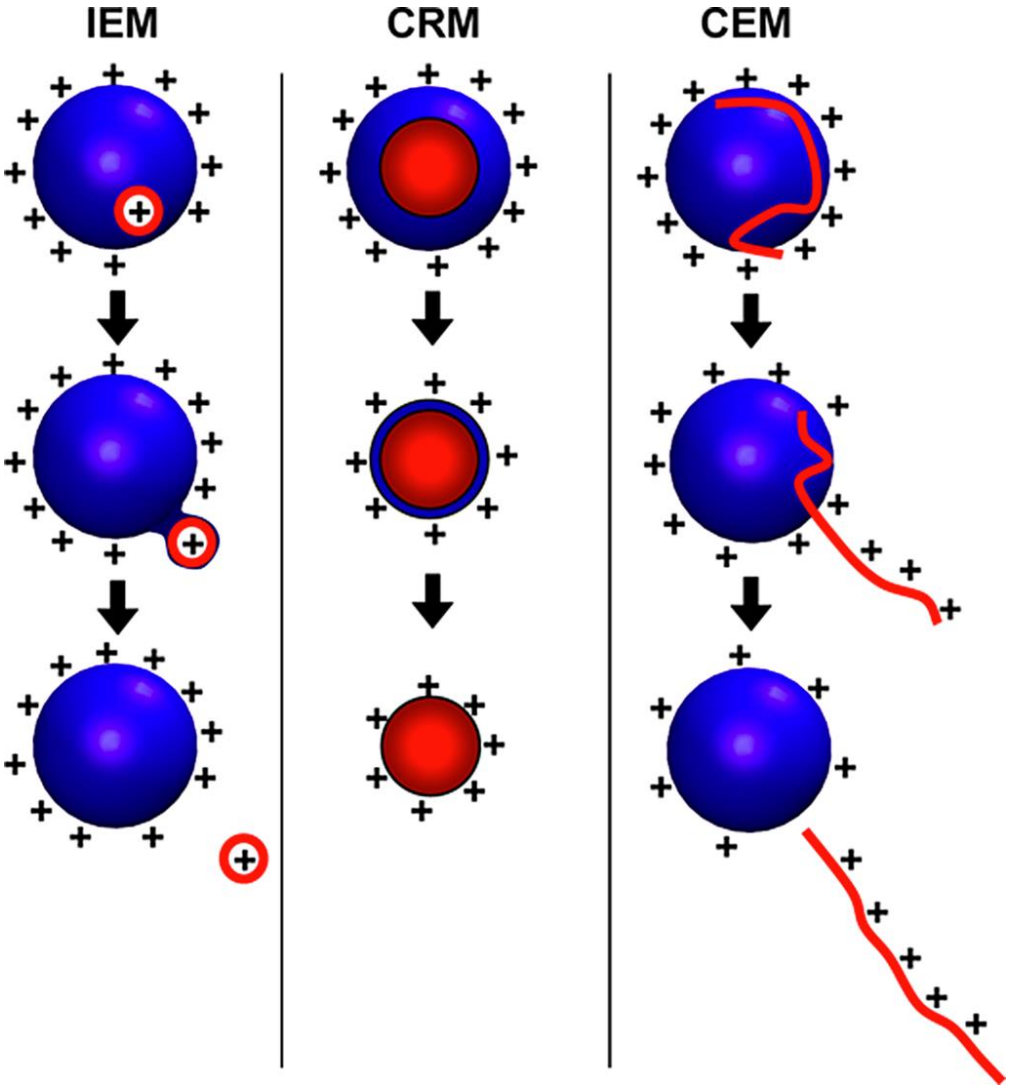

Figure 1.5. A schematic representation of the possible pathways for ion formation from a charged liquid droplet. This figure is reproduced from Konermann with permission.[86] (a) IEM: small ion ejection from a charged nanodroplet. (b) CRM: release of a globular protein into the gas phase. (c) CEM: ejection of an unfolded protein.

One characteristic of ESI is that it can produce multiply charged ions, effectively extending the mass range of mass analyzers and making detection of large molecules

possible with most mass analyzers. Multiple charging is particularly beneficial in FT-ICR instruments where generated image current is directly proportional to charge state and higher charge states can enhance the signal-to-noise ratio.[87] Furthermore, resolving power, mass accuracy and limits of detection in FT-ICR MS are all improved in the low m/z region.[47] In addition, certain MS/MS techniques such as ECD (Section 1.4.3) and electron detachment dissociation (EDD, Section 1.4.5) require multiply charged precursor ions. Contrary to ESI, MALDI typically produces singly-charged ions.

1.4 Tandem Mass Spectrometry (MS/MS or MS^n)

Because soft ionization techniques such as ESI primarily yield peptide or protein ions with little or no fragmentation in the source, subsequent tandem mass spectrometric activation is usually required to provide additional information regarding the primary structure of the analytes. In tandem mass spectrometry (MS/MS or MS^n),[51, 88] ions of a selected m/z ratio (precursor ions) are isolated and dissociated by different ion activation techniques to generate fragment ions whose m/z values are then measured. Based on the masses of the fragment ions, more detailed structural information of the precursor ions, such as peptide sequence information, can be deduced. Tandem MS experiments can be performed tandem in space, such as in triple quadrupole instruments, or in time, such as in FT-ICR mass spectrometers.

Effective ion activation is essential in MS/MS experiment, and ultimately defines what types of products are produced.[9, 22, 89, 90] Activation can be achieved in various ways: via collisions with gases or surfaces, absorption of IR or UV photons, or activation by ion-electron reactions. For confident sequencing of interrogated peptides, the ideal activation method should cleave between every backbone position to produce a

homologous series of peptide fragment ions that differ in mass by one amino acid. Scheme 1.1 illustrates the common types of peptide fragment ions observed from different activation techniques, based on the nomenclature proposed by Roepstorff and Fohlman.[91] The success of a proteomics experiment often depends on the choice of ion activation technique and several of these techniques are described in detail below.

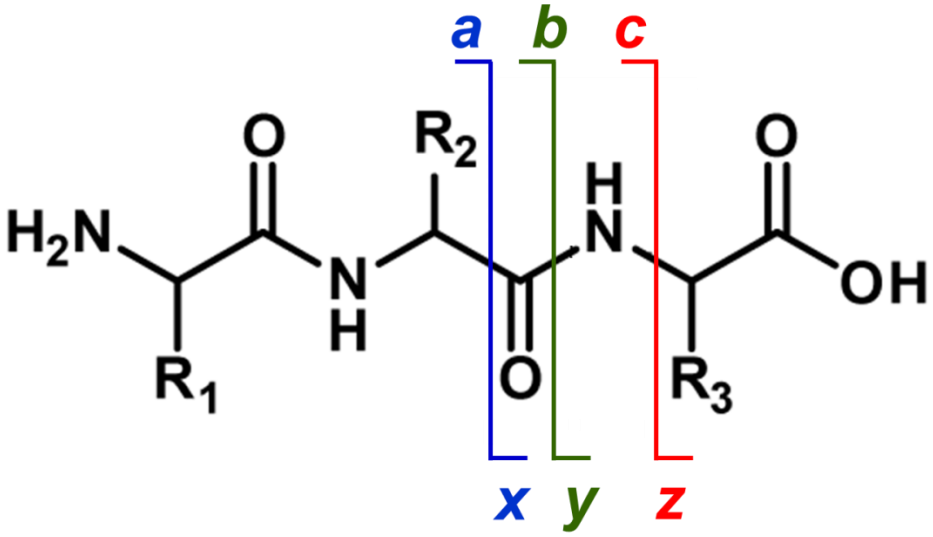

Scheme 1.1. Nomenclature for peptide/protein fragment ions in tandem mass spectrometry. Adapted from Roepstorff and Fohlman.[91]

MS/MS in Positive Ion Mode

The vast majority of MS/MS research, both experimental and fundamental, concerns positively charged analytes. Ion activation methods for protonated species are well-established for the determination of peptide/protein identity and sequence.[92, 93] This widespread use of positive ion mode is a result of standard "bottom-up" protocols involving the use of trypsin as an enzyme, which yields peptides with at least two basic (protonation) sites (i.e., N-terminus and arginine or lysine at C-terminus). In addition,

conventional LC-MS/MS-based peptide analysis in high-throughput proteomic analysis is conducted using acidic mobile phases, which facilitate ionization in positive ion mode.

1.4.1 Positive Ion Mode CAD

Collision-activated dissociation in positive ion mode remains the most prevalent method used to dissociate peptide ions for subsequent sequence analysis.[94] During CAD, a precursor ion population undergoes inelastic collisions with inert gases such as argon, helium or nitrogen, resulting in energy transfer and ultimately internal excitation of the precursor ion, as shown in Scheme 1.2.[95, 96] CAD is typically divided into two energy regimes: high-energy CAD (kiloeV range) and low-energy CAD (1-100 eV range). High-energy CAD typically occurs in sector and TOF instruments and ion excitation is mainly electronic,[97] whereas low-energy CAD is mostly observed in multipoles and trapping devices, such as ion traps and FT-ICR instruments and excitation is generally vibrational.[98] In this thesis, only low-energy CAD is applied and the acronym "CAD" refers to low-energy CAD.

$$[M + nH]^{n+} + \textbf{collision} \rightarrow [M + nH]^{n+}* \rightarrow \text{fragments}$$

Scheme 1.2. Fragmentation pathway in positive CAD. M denotes the neutral precursor ion, H denotes a proton, n denotes the number of protons, and the asterisk denotes excitation.

Low-energy CAD is considered a "slow-heating" fragmentation method. Ion activation is achieved through multiple collisions, each depositing a small amount of energy and causing the internal energy of the precursor ion to increase progressively. This energy is distributed throughout the ion via intramolecular vibrational-energy redistribution (IVR) until the threshold of dissociation is reached.[90, 99] Thus, CAD tends

to cleave the weakest bonds within the molecule and the product ions are formed through the lowest energy pathways.[100] In a gas-phase peptide ion, the preferred sites of cleavage are the amide (C-N) bonds of the peptide backbone, resulting in formation of *b* ions from the N-terminus and *y*-type fragments from the C-terminus (Scheme 1.1).[91] Low-energy CAD can be further divided into "beam-type" and "ion trap-type". Beam-type CAD employs an electric field to accelerate the precursor ions and is typically performed in a triple quadrupole or hydrid quadrupole/TOF configuration. On our hybrid FT-ICR mass spectrometers, it is achieved in the hexapole located after the quadrupole. In ion trap-type CAD, kinetic energy of precursor ions is raised by resonant excitation. This type of fragmentation is also available in ICR-cells via ICR-sustained off-resonance irradiation (SORI) CAD, in which selected ions are excited by a slightly off-resonance waveform.[101] Generally, ion trap-type CAD involves lower energy per collision and thus occurs over much longer timescales than beam-type CAD.

The generally accepted fragmentation mechanism for peptide CAD is the "mobile proton" model.[92, 102-104] According to this model, protons are initially located at basic sites, such as basic side chains or the N-terminus of peptides, and are internally solvated by amide oxygens or nitrogens. Following activation, the proton becomes "mobile" and migrates from the basic sites to the solvation sites. Protonation of the amide nitrogen weakens the amide bond and increases the electrophilicity of the adjacent carbonyl, which is then subjected to nucleophilic attack by either the neighboring amide oxygen (the oxazolone pathway)[105] or the nitrogen (the diketopiperazine pathway).[106] Random dissociation of the amide linkages along the peptide backbone allows interpretation of the amino acid sequence. However, enhanced cleavages can occur near certain amino acids,

such as N-terminal to proline, C-terminal to histidine and C-terminal to acidic residues when no mobile proton is available,[103, 107, 108] and suppress other backbone fragments from forming.

Despite its wide implementation, one major limitation of CAD is its poor applicability in PTM analysis. Many PTMs are more labile than the backbone amide bond and are readily lost upon collisional activation, thus rendering localization of their site of attachment a challenging task.[109] Additionally, when a labile group such as a phosphate group is present in a peptide or protein, the CAD spectrum is often dominated by loss of the PTM. This dissociation channel preempts peptide backbone bond cleavages, resulting in poor sequence coverage. Furthermore, structural scrambling can occur in CAD experiments, producing misleading structural information. For example, Palumbo and Reid showed that, in low-energy (i.e., ion-trap type) CAD, a phosphate group can migrate to a different site in the peptide in a rearrangement reaction,[110] causing ambiguous site assignments. Other reports state that this phenomenon is not prevalent in typical data-dependent liquid chromatography (LC)/CAD/MS/MS analysis[111, 112] but such analyses still suffer from preferential PTM loss.

1.4.2 IRMPD

In infrared multiphoton dissociation ,[113] precursor ions are irradiated with an IR laser beam and vibrationally excited by absorbing multiple photons. IRMPD is well suited for ion traps[114] and FT-ICR instruments,[69, 115] which allow sufficient interaction time between ions and photons. The most frequently used IR laser is a CO_2 laser operating at 10.6 μm,[116, 117] although tunable CO_2 laser can also be implemented.[118, 119] Because the energy transferred by each photon is around 0.1 eV,[114] absorption of

hundreds or even thousands of IR photons by the precursor ion is required before effective activation and fragmentation. Thus, IRMPD is another type of slow-heating technique and produces peptide fragment ions (*b*- and *y*-type) similar to CAD. One advantage of IRMPD over CAD in an FT-ICR instrument is that no collision gas is introduced into ICR cell during IRMPD and therefore the vacuum is not deteriorated, which is essential for high resolving power in FT-ICR.

1.4.3 ECD and ETD

Different from the vibrational techniques discussed above, electron capture dissociation [36, 120-124] and electron transfer dissociation [34, 125-128] activate peptide ions through ion-electron or ion-ion reactions. In ECD, multiply charged precursor cations are irradiated with low-energy electrons (<1 eV), resulting in charge-reduced radicals from electron capture. This intermediate undergoes rapid radical-driven dissociation into unique product ions. For peptides, *c*- and *z*-type backbone fragments are generated in ECD by cleaving the backbone N-Cα bonds rather than amide bonds. Disulfide bonds, which are fairly stable under other ion activation conditions, are also preferentially cleaved by ECD.[33] ECD is primarily implemented in FT-ICR mass analyzers to allow trapping of both electrons and precursor cations. The discovery of ETD by Hunt and co-workers made electron-based dissociation available in relatively inexpensive and radiofrequency (rf)-based ion trap instruments by using a different source of electrons.[34] In ETD, instead of free electrons, anion electron carriers are used to transfer electrons to multiply charged cationic precursors, producing odd-electron charge-reduced species and subsequent product ions similar to those in ECD. Anion reagents frequently used in ETD are anthracene,[34] fluoranthene[129] and azobenzene[130] as they have low electron

affinities, thus allowing efficient electron transfer to the precursor peptide ion. The overall ECD and ETD reaction schemes are illustrated in Scheme 1.3.

$$[M + nH]^{n+} + \mathbf{e}^{-}\ \mathbf{(<1\ eV)} \rightarrow [M + nH]^{(n-1)+\bullet} \rightarrow \text{fragments}$$

$$[M + nH]^{n+} + \mathbf{A}^{-\bullet} \rightarrow [M + nH]^{(n-1)+\bullet} + A \rightarrow \text{fragments}$$

Scheme 1.3. Fragmentation routes in ECD (top) and ETD (bottom). For ECD and ETD, n must be greater than two. In ETD, A denotes the electron carrier.

The exact mechanism of ECD is still a subject of debate.[33, 131-137] According to the "hot hydrogen" or "Cornell" mechanism conceived by McLafferty and coworkers,[33] electron capture occurs at a protonated site, e.g., a lysine ε-ammonium group, an arginine guanidinium group, a histidine imidazolium ring, or an N-terminal ammonium group, solvated onto one or several backbone carbonyls. Neutralization of the charged site releases a hot hydrogen atom that is transferred to the nearby backbone carbonyl, yielding an aminoketyl radical. This intermediate rapidly dissociates via N–Cα bond cleavage to form N-terminal *c*-type product ions and C-terminal *z*-type product ions (Scheme 1.4). An alternative theory (the "Utah-Washington" or amide superbase" mechanism) was proposed by Turecek and co-workers and by Simons and co-workers.[135, 136, 138] In this model, the electron is directly captured into the π* orbital of a backbone amide, producing an excited amide group with high basicity (superbase) that can abstract a proton from a nearby chemical group. Such direct electron attachment can be thermodynamically facilitated by positive charges located in spatial proximity (Coulomb stabilization). The resulting aminoketyl radical undergoes facile N-Cα bond cleavage with very low energy barrier, leading to the formation of *c*- and *z*-ions, as illustrated in Scheme 1.5. It is further suggested that both mechanisms could be valid, depending on

the nature of charge carriers (e.g., lysine versus arginine).[136, 139] Zubarev and co-workers have also suggested that electron capture may occur at a neutral intramolecular hydrogen bond with subsequent hydrogen transfer to the backbone carbonyl.[137] There is evidence that the fragmentation mechanism of ETD is similar to ECD, although thermodynamically an additional barrier is present as an electron has to leave the radical anion.[140, 141]

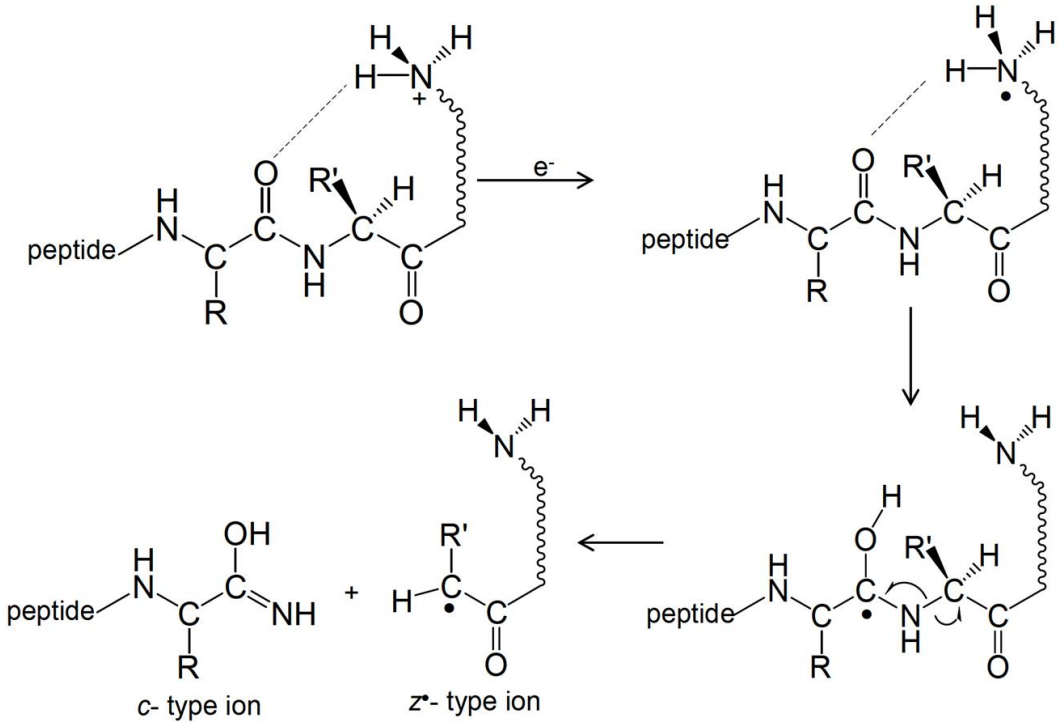

Scheme 1.4. The hot hydrogen mechanism for ECD of peptides. Scheme adapted from references.[139, 142]

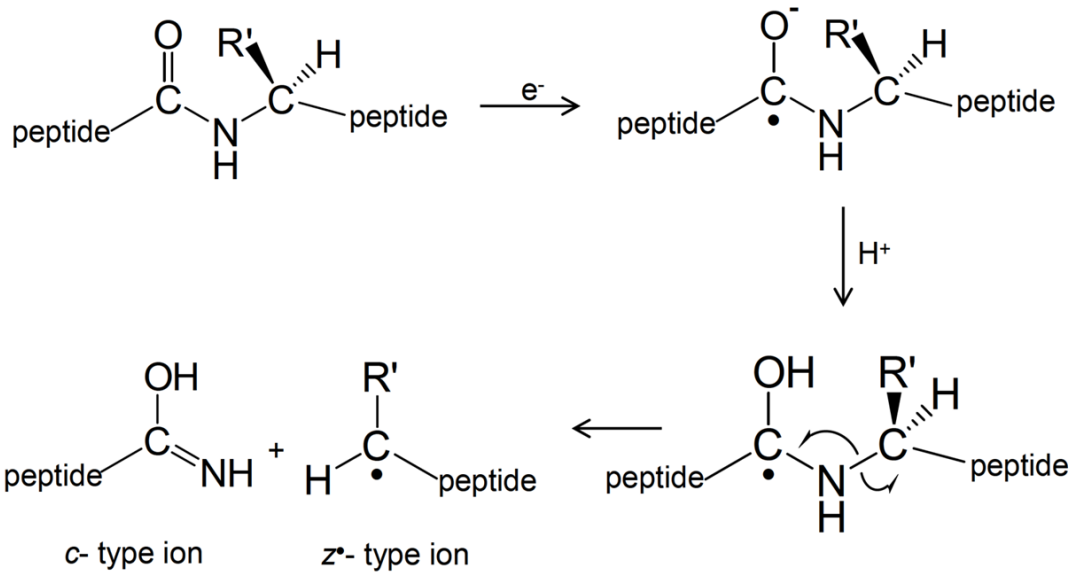

Scheme 1.5. The amide superbase mechanism for ECD of peptides. Reproduced from a reference.[139]

ECD/ETD are highly complementary to the slow heating methods such as CAD. The fundamentally distinct fragmentation mechanisms associated with these techniques result in different backbone bond cleavages, i.e., *c*/*z*-type product ions for ECD/ETD, *b*/*y*-type ions for CAD/IRMPD, as well as different fragmentation preferences. It is often advantageous to perform ECD and CAD as a duet to take advantage of this complementarity of the two methods. Moreover, combination of MS/MS data from both ECD and CAD of the same sample increases the confidence of peak assignment by utilizing the so-called "golden" product pairs with characteristic mass differences, and consequently leads to more reliable protein identifications in both database searching methods and de novo sequencing.[143] In addition, higher sequence coverage is generally obtained from ECD/ETD alone versus CAD alone,[144, 145] presumably because ECD/ETD can cleave peptide backbone bonds more randomly. Another major attraction of

ECD/ETD for peptide/protein analysis is their ability to generate extensive peptide backbone bond cleavages while leaving the PTMs intact,[146-150] which is particularly difficult for the very labile phosphorylation, glycosylation, and sulfation. Thus, ECD/ETD have developed into key techniques for PTM identification and localization.

One disadvantage of ECD/ETD is that they are only applicable to positively charged precursor ions with at least two charges, because capture of an electron reduces total charge by one and neutrals are not detectable in mass spectrometers. Moreover, ECD/ETD efficiency is charge-state dependent, favoring higher charge states.[128, 151-153]

MS/MS in Negative Ion Mode

Although much less information is available concerning the fragmentation of deprotonated peptides, there are compelling reasons to pursue MS/MS techniques in negative ion mode. One reason for less than 100% sequence coverage in detecting digested peptides by the bottom-up mass spectrometry approach is the use of only positive polarity. However, 45% of all human protein sequences and most common PTMs, such as phosphorylation, sulfation, and sialylated glycosylation, are acidic. They can readily form anions but produce no or little signal in the positive mode. This is especially true in mixtures where competition for charge results in suppression of less basic species. Thus, the extension of analytical strategies to include negative ion mode should offer improved sensitivity and amino acid sequence coverage of proteins. Further, some important PTMs, including phosphorylation and sulfation, are much more labile in cations than in anions, and can get easily lost during ionization and ion activation in positive ion mode.[154, 155] Moreover, negatively charged peptide ions can undergo unique dissociation processes that provide additional information for peptide identification and

sequencing. Therefore, in principle, negative ion analysis should be able to provide complementary structural information, especially for acidic analytes.

1.4.4 Negative Ion Mode CAD

The fragmentation pattern of peptide anions in CAD is quite different from that of their positive ion counterparts. Thus, complementary product ions and amino acid sequence information are often obtained in negative ion mode.[156] In addition, CAD of deprotonated phosphopeptides has been found to reveal information regarding the site specific location of the phosphorylation when consecutive threonine and serine residues are present.[157] However, compared with positive ion CAD, CAD of negatively charged species is typically more complex, less predictable, and the fragmentation behaviors are less understood.[158] Complex product ion patterns, corresponding to backbone *a*, *b*, *c*, *x*, *y*, *z* ions, side chain losses as well as internal ion fragments can all be observed in negative ion CAD, which often requires extensive manual interpretation of the tandem mass spectra.[156, 159-161] The simplest fragmentation pathways for peptide anions involve cleavages of the amide backbone unit, producing fragments similar to *b*- and *y*-type ions in corresponding positive ion spectra.[158] C-terminal *y* ions which probably contain the negative charge at the C-terminus are usually more common and more abundant than the N-terminal *b* ions. In addition, the presence of certain residues, e.g., Asp, Asn, Glu, and Gln, significantly affects dissociation by cleaving the N-Cα backbone bond of these residues accompanied by abundant neutral loss of H_2O (Asp/Glu) and NH_3 (Asn/Gln).[162] Ser and Thr residues also undergo pronounced cleavages of their side chains, i.e., characteristic loss of CH_2O from Ser and MeCHO from Thr, which often dominate the spectra.[156] These prominent neutral losses from amino acid side chains lead to

insufficient peptide sequence information. In fact, sixteen out of twenty natural amino acids exhibit some type of neutral loss in negative ion mode CAD.[158] For acidic peptides, the likely deprotonation sites are acidic residues and the terminal carboxylic acid. Fragment ions are preferentially formed from cleavage adjacent to these acidic residues. Neutral loss (e.g., NH_3, CH_3, H_2O, and CO_2) is also prevalent from both the parent ions and fragment ions.[159] Overall, despite the increasing understanding of the dissociation pattern in negative ion CAD of peptides, spectra are generally complicated by abundant side-chain losses, neutral losses from the parent ion, and internal ion fragments.

1.4.5 EDD

As an electron-mediated technique operating in negative ion mode, electron detachment dissociation was first discovered by Zubarev and co-workers in 2001.[163] In EDD, instead of capturing a low-energy electron, negatively charged precursor ions are bombarded with higher-energy electrons (10-30 eV), resulting in electron ejection/detachment from the precursor ions and formation of charge-reduced but oxidized radical anions. For peptides, the electron-deficient radical intermediates mainly undergo Cα-C bond cleavages leading to the formation of *a*-, and *x*-ions as well as neutral loss (e.g., CO_2 loss).[163, 164] The EDD fragmentation scheme is shown in Scheme 1.6. EDD is useful for the analysis of acidic peptides, including phospho-, sulfopeptides, and peptides containing multiple acidic residues. Similar to ECD/ETD, EDD has shown the ability to preserve labile PTMs, such as phosphorylation and sulfation.[163, 165-167] For instance, the site of sulfation was deduced from the EDD spectrum of the sulfated peptide caerulein.[163] Despite the value of EDD, it is not a very efficient fragmentation process

due to its limited reaction cross section between negatively charged peptides and electrons. Consequently, accumulation of tens or hundreds of summed mass spectra is often required to obtain satisfactory mass spectral quality.[167-169] In addition, multiply negatively charged ions are a prerequisite in EDD because it is initiated by a charge-reduction process.

$$[M - nH]^{n-} + \mathbf{e}^{-}\ \mathbf{(>10\ eV)} \rightarrow [M - nH]^{(n-1)-\bullet *} + 2e^{-} \rightarrow \text{fragments}$$

Scheme 1.6. Fragmentation scheme in EDD. Similar to ECD/ETD, n here must be greater than 2.

1.4.6 NETD

Negative electron transfer dissociation is the ion-ion analog of EDD. In NETD, an electron is transferred from the multiply deprotonated precursor ion to a radical cation with high electron affinity, as demonstrated in Scheme 1.7.[170] The resulting charge-reduced precursor radical fragments into predominantly EDD-like *a*• and *x* ions. In the initial NETD work, xenon radical cations ($Xe^{+\bullet}$) were employed to abstract electrons and promote radical formation for subsequent dissociation. However, this reaction results in PTM loss and neutral loss of CO_2 which adds complexity to the spectra.[170] More recent work by Polfer and co-workers with alternative NETD reagents (fluoranthene) showed that the labile phosphorylation could be retained.[171]

$$[M - nH]^{n-} + \mathbf{A}^{+\bullet} \rightarrow [M - nH]^{(n-1)-\bullet} + A \rightarrow \text{fragments}$$

Scheme 1.7. Fragmentation pathway in NETD. A denotes the radical cation.

1.4.7 niECD

Negative ion electron capture dissociation is a novel negative ion mode MS/MS technique discovered in our lab and is also the focus of this dissertation. Detailed discussions of its discovery, fundamental studies, and applications are presented in the following chapters. In a nutshell, it is a fragmentation technique for anions analogous to ECD for cations. In niECD, electrons with a narrow energy range (3.5–6.5 eV) can be captured by a negatively charged peptide ion to form a charge-increased radical that fragments at N—Cα bonds, producing *c*′ and *z*• peptide ions.[172] The overall fragmentation scheme in niECD can be written as follows (Scheme 1.8):

$$[M - nH]^{n-} + \mathbf{e}^{-}\ \mathbf{(3.5 – 6.5\ eV)} \rightarrow [M - nH]^{(n+1)-\bullet} \rightarrow \text{fragments}$$

Scheme 1.8. Fragmentation route in niECD. For niECD, n can be one or more.

niECD is not only an unusual chemical reaction, but it also holds promise for analytical benefits, including the following: the fragmentation in niECD is similar to conventional positive ion mode ECD (and ETD) and complementary to the traditionally utilized vibrational technique CAD, thus generating significant structural information; labile but crucial PTMs like phosphorylation, are preserved within the fragments, allowing their localization; more importantly, niECD is achieved in negative ion mode where acidic molecules show improved ionization efficiency and less ion suppression; furthermore, the increased charge state generated in niECD improves the sensitivity in image-current-based detection (e.g., in FT-ICR MS) where signal is proportional to charge state.

1.5 Dissertation Overview

The research presented in this dissertation explores the development, mechanism and applicability of the new electron-based fragmentation technique in negative ion mode– niECD. The first (current) chapter provides a broad overview of mass spectrometry-based proteomics, FT-ICR MS used throughout this thesis, the soft ionization technique frequently utilized in biomolecule analysis ESI, and a variety of MS/MS techniques for structural characterization of peptides and proteins in both positive and negative ion modes. Chapter 2 discusses the discovery of niECD: peptide anions can capture an electron within a certain energy range, resulting in charge-increased odd-electron species that undergo ECD-like fragmentation. In this chapter, which has been published in the *Journal of the American Chemical Society* (2011, volume 133, page 16790), phosphorylated and sulfated peptides were investigated by niECD in which extensive *c*- and *z*-type peptide backbone fragments with retention of the labile phosphorylation and sulfation are observed. Following the discovery of this exciting new technique, the curiosity of how it works inspired me to keep investigating the mechanism behind it. The striking similarity of niECD results to positive ion mode ECD led to the hypothesis that gas-phase zwitterionic structures might play a role in niECD. In Chapter 3, the mechanism of niECD is extensively investigated by modifying peptides and carbohydrates with different derivatization techniques to either prevent or promote gas-phase zwitterion formation. To systematically validate this mechanism, five sets of peptides with varying number and positions of charges were also synthesized. niECD efficiency was calculated and compared between different sets of peptides. In Chapters 4 and 5, the applicability of niECD is further expanded to two additional important protein

PTMs: disulfide linkage and glycosylation. In Chapter 4, peptide pairs bound by either natural disulfide bridges or disulfide-containing cross-linkers were characterized by niECD. Preferential disulfide cleavage was observed in niECD, which suggests that it proceeds through similar pathways that are involved in regular ECD. Chapter 5 investigates N-linked and O-linked glycopeptides with both neutral and acidic glycans. Similar to positive mode ECD/ETD, niECD of glycopeptide cleaves primarily at the peptide backbone bonds while leaving the labile glycan intact, which is essential in site-specific analysis of glycoproteins. niECD provides peptide sequence information as well as site information of glycan occupancy simultaneously for glycopeptides. In the end, a summary of all results in this dissertation is presented in Chapter 6, together with future directions. Chapters 3-5 are written in the format of journal articles that will be submitted for publication.

1.6 References

1. Collins, F. S.; Lander, E. S.; Rogers, J.; Waterston, R. H.; Int Human Genome Sequencing, C. Finishing the euchromatic sequence of the human genome. *Nature* **2004**, *431*, 931-945.
2. Lander, E. S.; Int Human Genome Sequencing, C.; Linton, L. M.; Birren, B.; Nusbaum, C.; Zody, M. C.; Baldwin, J.; Devon, K.; Dewar, K.; Doyle, M. *et al*. Initial sequencing and analysis of the human genome. *Nature* **2001**, *409*, 860-921.
3. Venter, J. C.; Adams, M. D.; Myers, E. W.; Li, P. W.; Mural, R. J.; Sutton, G. G.; Smith, H. O.; Yandell, M.; Evans, C. A.; Holt, R. A. The sequence of the human genome. *Science* **2001**, *291*, 1304-1351.
4. Jensen, O. N. Modification-specific proteomics: Characterization of post-translational modifications by mass spectrometry. *Curr. Opin. Chem. Biol.* **2004**, *8*, 33-41.
5. Garavelli, J. S.; Hou, Z. L.; Pattabiraman, N.; Stephens, R. M. The RESID database of protein structure modifications and the NRL-3D sequence-structure database. *Nucleic Acids Res.* **2001**, *29*, 199-201.
6. Mann, M.; Jensen, O. N. Proteomic analysis of post-translational modifications. *Nat. Biotechnol.* **2003**, *21*, 255-261.
7. Kjeldsen, F.; Haselmann, K. F.; Budnik, B. A.; Sorensen, E. S.; Zubarev, R. A. Complete characterization of posttranslational modification sites in the bovine

milk protein PP3 by tandem mass spectrometry with electron capture dissociation at the last stage. *Anal. Chem.* **2003**, *75*, 2355-2361.
8. Aebersold, R.; Goodlett, D. R. Mass spectrometry in proteomics. *Chem. Rev.* **2001**, *101*, 269-295.
9. Aebersold, R.; Mann, M. Mass spectrometry-based proteomics. *Nature* **2003**, *422*, 198-207.
10. Han, X.; Aslanian, A.; Yates III, J. R. Mass spectrometry for proteomics. *Curr. Opin. Chem. Biol.* **2008**, *12*, 483-490.
11. Chait, B. T. Mass spectrometry: Bottom-up or top-down? *Science* **2006**, *314*, 65-66.
12. Bogdanov, B.; Smith, R. D. Proteomics by FTICR mass spectrometry: top down and bottom up. *Mass Spectrom. Rev.* **2005**, *24*, 168-200.
13. Yates, J. R.; Ruse, C. I.; Nakorchevsky, A. Proteomics by mass spectrometry: approaches, advances, and applications. *Annu. Rev. Biomed. Eng.* **2009**, *11*, 49-79.
14. Wiesner, J.; Premsler, T.; Sickmann, A. Application of electron transfer dissociation (ETD) for the analysis of posttranslational modifications. *Proteomics* **2008**, *8*, 4466-4483.
15. Armirotti, A. Bottom-up proteomics. *Curr. Anal. Chem.* **2009**, *5*, 116-130.
16. Eng, J. K.; McCormack, A. L.; Yates, J. R. An approach to correlate tandem mass-spectral data of peptides with amino-acid-sequences in a protein database. *J. Am. Soc. Mass. Spectrom.* **1994**, *5*, 976-989.
17. Perkins, D. N.; Pappin, D. J. C.; Creasy, D. M.; Cottrell, J. S. Probability-based protein identification by searching sequence databases using mass spectrometry data. *Electrophoresis* **1999**, *20*, 3551-3567.
18. Brosch, M.; Swamy, S.; Hubbard, T.; Choudhary, J. Comparison of mascot and X!Tandem performance for low and high accuracy mass spectrometry and the development of an adjusted Mascot threshold. *Mol. Cell. Proteomics* **2008**, *7*, 962-970.
19. Sweet, S. M. M.; Jones, A. W.; Cunningham, D. L.; Heath, J. K.; Creese, A. J.; Cooper, H. J. Database search strategies for proteomic data sets generated by electron capture dissociation mass spectrometry. *J. Proteome Res.* **2009**, *8*, 5475-5484.
20. Tolmachev, A. V.; Monroe, M. E.; Purvine, S. O.; Moore, R. J.; Jaitly, N.; Adkins, J. N.; Anderson, G. A.; Smith, R. D. Characterization of strategies for obtaining confident identifications in bottom-up proteomics measurements using hybrid FTMS instruments. *Anal. Chem.* **2008**, *80*, 8514-8525.
21. Bereman, M. S.; Egertson, J. D.; MacCoss, M. J. Comparison between procedures using SDS for shotgun proteomic analyses of complex samples. *Proteomics* **2011**, *11*, 2931-2935.
22. Washburn, M. P.; Wolters, D.; Yates, J. R. Large-scale analysis of the yeast proteome by multidimensional protein identification technology. *Nat. Biotechnol.* **2001**, *19*, 242-247.
23. Wolters, D. A.; Washburn, M. P.; Yates, J. R. An automated multidimensional protein identification technology for shotgun proteomics. *Anal. Chem.* **2001**, *73*, 5683-5690.
24. MacCoss, M. J.; McDonald, W. H.; Saraf, A.; Sadygov, R.; Clark, J. M.; Tasto, J.

J.; Gould, K. L.; Wolters, D.; Washburn, M.; Weiss, A. *et al*. Shotgun identification of protein modifications from protein complexes and lens tissue. *Proc. Natl. Acad. Sci. U. S. A.* **2002**, *99*, 7900-7905.
25. Siuti, N.; Kelleher, N. L. Decoding protein modifications using top-down mass spectrometry. *Nat. Methods* **2007**, *4*, 817-821.
26. Kelleher, N. L. Top-down proteomics. *Anal. Chem.* **2004**, *76*, 196A-203A.
27. Kellie, J. F.; Tran, J. C.; Lee, J. E.; Ahlf, D. R.; Thomas, H. M.; Haylee, M.; Ntai, I.; Catherman, A. D.; Adam, D.; Durbin, K. R. *et al*. The emerging process of top down mass spectrometry for protein analysis: Biomarkers, protein-therapeutics, and achieving high throughput. *Mol. Biosyst.* **2010**, *6*, 1532-1539.
28. Garcia, B. A. What does the future hold for top down mass spectrometry? *J. Am. Soc. Mass. Spectrom.* **2010**, *21*, 193-202.
29. Meng, F. Y.; Cargile, B. J.; Miller, L. M.; Forbes, A. J.; Johnson, J. R.; Kelleher, N. L. Informatics and multiplexing of intact protein identification in bacteria and the archaea. *Nat. Biotechnol.* **2001**, *19*, 952-957.
30. Reid, G. E.; Stephenson, J. L.; McLuckey, S. A. Tandem mass spectrometry of ribonuclease A and B: N-linked glycosylation site analysis of whole protein ions. *Anal. Chem.* **2002**, *74*, 577-583.
31. Kelleher, N. L.; Lin, H. Y.; Valaskovic, G. A.; Aaserud, D. J.; Fridriksson, E. K.; McLafferty, F. W. Top down versus bottom up protein characterization by tandem high-resolution mass spectrometry. *J. Am. Chem. Soc.* **1999**, *121*, 806-812.
32. Zabrouskov, V.; Han, X. M.; Welker, E.; Zhai, H. L.; Lin, C.; van Wijk, K. J.; Scheraga, H. A.; McLafferty, F. W. Stepwise deamidation of ribonuclease A at five sites determined by top down mass spectrometry. *Biochem.* **2006**, *45*, 987-992.
33. Zubarev, R. A.; Kruger, N. A.; Fridriksson, E. K.; Lewis, M. A.; Horn, D. M.; Carpenter, B. K.; McLafferty, F. W. Electron capture dissociation of gaseous multiply-charged proteins is favored at disulfide bonds and other sites of high hydrogen atom affinity. *J. Am. Chem. Soc.* **1999**, *121*, 2857-2862.
34. Syka, J. E. P.; Coon, J. J.; Schroeder, M. J.; Shabanowitz, J.; Hunt, D. F. Peptide and protein sequence analysis by electron transfer dissociation mass spectrometry. *Proc. Natl. Acad. Sci. U. S. A.* **2004**, *101*, 9528-9533.
35. Coon, J. J.; Ueberheide, B.; Syka, J. E. P.; Dryhurst, D. D.; Ausio, J.; Shabanowitz, J.; Hunt, D. F. Protein identification using sequential ion/ion reactions and tandem mass spectrometry. *Proc. Natl. Acad. Sci. U. S. A.* **2005**, *102*, 9463-9468.
36. Cooper, H. J.; Hakansson, K.; Marshall, A. G. The role of electron capture dissociation in biomolecular analysis. *Mass Spectrom. Rev.* **2005**, *24*, 201-222.
37. Shaw, J. B.; Li, W. Z.; Holden, D. D.; Zhang, Y.; Griep-Raming, J.; Fellers, R. T.; Early, B. P.; Thomas, P. M.; Kelleher, N. L.; Brodbelt, J. S. Complete protein characterization using top-down mass spectrometry and ultraviolet photodissociation. *J. Am. Chem. Soc.* **2013**, *135*, 12646-12651.
38. Comisarow, M. B.; Marshall, A. G. Fourier transform ion cyclotron resonance spectroscopy. *Chem. Phys. Lett.* **1974**, *25*, 282-283.
39. Comisarow, M. B.; Marshall, A. G. Frequency-sweep fourier transform ion cyclotron resonance spectroscopy. *Chem. Phys. Lett.* **1974**, *26*, 489-490.
40. Gorman, J. J.; Wallis, T. P.; Pitt, J. J. Protein disulfide bond determination by mass spectrometry. *Mass Spectrom. Rev.* **2002**, *21*, 183-216.

41. Shi, S. D.-H.; Hendrickson, C. L.; Marshall, A. G. Counting individual sulfur atoms in a protein by ultrahigh-resolution fourier transform ion cyclotron resonance mass spectrometry: Experimental resolution of isotopic fine structure in proteins. *Proc. Natl. Acad. Sci. U.S.A.* **1998**, *95*, 11532-11537.
42. Hakansson, K.; Cooper, H. J.; Hudgins, R. R.; Nilsson, C. L. High resolution tandem mass spectrometry for structural biochemistry. *Curr. Org. Chem.* **2003**, *7*, 1503-1525.
43. Medzihradszky, K. F.; Zhang, X.; Chalkley, R. J.; Guan, S.; McFarland, M. A.; Chalmers, M. J.; Marshall, A. G.; Diaz, R. L.; Allis, C. D.; Burlingame, A. L. Characterization of tetrahymena histone h2b variants and posttranslational populations by electron capture dissociation (ECD) fourier transform ion cyclotron mass spectrometry (FT-ICR MS). *Mol. Cell. Proteomics* **2004**, *3*, 872-886.
44. Cooper, H. J.; Akbarzadeh, S.; Heath, J. K.; Zeller, M. Data-dependent electron capture dissociation FT-ICR mass spectrometry for proteomic analyses. *J. Proteome Res.* **2005**, *4*, 1538-1544.
45. Chalmers, M. J.; Kolch, W.; Emmett, M. R.; Marshall, A. G. Identification and Analysis of Phosphopeptides. *J. Chromatogr. B.* **2004**, *803*, 111-120.
46. Marshall, A. G.; Rodgers, R. P. Petroleomics: The next grand challenge for chemical analysis. *Acc. Chem. Res.* **2004**, *37*, 53-59.
47. Marshall, A. G.; Hendrickson, C. L.; Jackson, G. S. Fourier transform ion cyclotron resonance mass spectrometry: A primer. *Mass Spectrom. Rev.* **1998**, *17*, 1-35.
48. Marshall, A. G.; Guan, S. Advantages of high magnetic field for FT-ICR mass spectrometry. *Rapid Commun. Mass Spectrom.* **1996**, *10*, 1819-1823.
49. Loo, J. A.; Edmonds, C. G.; Udseth, H. R.; Smith, R. D. Effect of reducing disulfide-containing proteins on electrospray ionization mass spectra. *Anal. Chem.* **1990**, *62*, 693-698.
50. Amster, I. J. A tutorial on fourier transform mass spectrometry. *J. Mass Spectrom.* **1996**, *31*, 1325-1337.
51. de Hoffmann, E.; Stroobant, V. *Mass spectrometry - principles and applications*. Third ed.; John Wiley and Sons Ltd: West Sussex, England, **2007**.
52. Marshall, A. G. Milestones in fourier transform ion cyclotron resonance mass spectrometry technique development. *Int. J. Mass Spectrom.* **2000**, *200*, 331-356.
53. Marshall, A. G.; Hendrickson, C. L. Fourier transform ion cyclotron resonance detection: principles and experimental configurations. *Int. J. Mass Spectrom.* **2002**, *215*, 59-75.
54. Heeren, R. M. A.; Kleinnijenhuis, A. J.; McDonnell, L. A.; Mize, T. H. A mini-review of mass spectrometry using high-performance FTICR-MS methods. *Anal. Bioanal. Chem.* **2004**, *378*, 1048-1058.
55. Guan, S.; Marshall, A. G. Ion traps for FT-ICR/MS: Principles and design of geometric and electric configurations. *Int. J. Mass Spectrom. Ion Processes* **1995**, *146/147*, 261-296.
56. Marshall, A. G.; Hendrickson, C. L. High-resolution mass spectrometers. *Annu. Rev. Anal. Chem.* **2008**, *1*, 579-599.
57. Marshall, A. G.; Verdun, F. R. *Fourier transforms in NMR, optical, and mass*

spectrometry: A user's handbook. Elsevier: Amsterdam, **1990**; p 460.
58. Grosshans, P. B.; Marshall, A. G. Theory of ion-cyclotron resonance mass-spectrometry - resonant excitation and radial ejection in orthorhombic and cylindrical ion traps. *Int. J. Mass Spectrom. Ion Processes* **1990**, *100*, 347-379.
59. Comisarow, M. B.; Marshall, A. G. Theory of fourier-transform ion-cyclotron resonance mass-spectroscopy .1. fundamental equations and low-pressure line-shape. *J. Chem. Phys.* **1976**, *64*, 110-119.
60. Guan, S. H.; Li, G. Z.; Marshall, A. G. Effect of ion-neutral collision mechanism on the trapped-ion equation of motion: a new mass spectral line shape for high-mass trapped ions. *Int. J. Mass Spectrom.* **1997**, *167*, 185-193.
61. Mitchell, D. W. Realistic simulation of the ion cyclotron resonance mass spectrometer using a distributed three-dimensional particle-in-cell code. *J. Am. Soc. Mass. Spectrom.* **1999**, *10*, 136-152.
62. Nikolaev, E. N.; Heeren, R. M. A.; Popov, A. M.; Pozdneev, A. V.; Chingin, K. S. Realistic modeling of ion cloud motion in a Fourier transform ion cyclotron resonance cell by use of a particle-in-cell approach. *Rapid Commun. Mass Spectrom.* **2007**, *21*, 3527-3546.
63. Hendrickson, C. L.; Emmett, M. R. Electrospray ionization fourier transform ion cyclotron resonance mass spectrometry. *Annu. Rev. Phys. Chem.* **1999**, *50*, 517-536.
64. Lorenz, S. A.; Maziarz, E. P. I.; Wood, T. D. Electrospray ionization fourier transform mass spectrometry of macromolecules: The first decade. *Appl. Spectrosc.* **1999**, *53*, 18A-36A.
65. Kelly, R. T.; Tolmachev, A. V.; Page, J. S.; Tang, K.; Smith, R. D. The ion funnel: theory, implementations, and applications. *Mass Spectrom. Rev.* **2010**, *29*, 294-312.
66. Tang, K.; Tolmachev, A. V.; Nikolaev, E.; Zhang, R.; Belov, M. E.; Udseth, H. R.; Smith, R. D. Independent control of ion transmission in a jet disrupter dual-channel ion funnel electrospray ionization MS interface. *Anal. Chem.* **2002**, *74*, 5431-5437.
67. Senko, M. W.; Hendrickson, C. L.; Emmett, M. R.; Shi, S. D.-H.; Marshall, A. G. External accumulation of ions for enhanced electrospray ionization fourier transform ion cyclotron resonance mass spectrometry. *J. Am. Soc. Mass Spectrom.* **1997**, *8*, 970-976.
68. Guan, S.; Paša-Tolić, L.; Marshall, A. G.; Xiang, X. Off-axis injection into an ICR ion trap: a means for efficient capture of a continuous beam of externally generated ions. *Int. J. Mass Spectrom. Ion Processes* **1994**, *139*, 75-86.
69. Tsybin, Y. O.; Witt, M.; Baykut, G.; Kjeldsen, F.; Hakansson, P. Combined infrared multiphoton dissociation and electron capture dissociation with a hollow electron beam in fourier transform ion cyclotron resonance mass spectrometry. *Rapid Commun. Mass Spectrom.* **2003**, *17*, 1759-1768.
70. Fenn, J. B.; Mann, M.; Meng, C. K.; Wong, S. F.; Whitehouse, C. M. Electrospray ionization for mass spectrometry of large biomolecules. *Science* **1989**, *246*, 64-71.
71. Fenn, J. B.; Mann, M.; Meng, C. K.; Wong, S. F. Electrospray ionization - principles and practice. *Mass Spectrom. Rev.* **1990**, *9*, 37-70.
72. Tanaka, K.; Waki, H.; Ido, Y.; Akita, S.; Yoshida, Y.; Yoshida, T. Protein and

polymer analyses up to m/z 100 000 by laser ionization time-of-flight mass spectrometry. *Rapid Commun. Mass Spectrom.* **1988**, *2*, 151-153.
73. Taylor, G. Disintegration of water drops in an electric field. *Proc. R. Soc. Lond., Ser. A. Math. Phys. Sci.* **1964**, *280*, 383-397.
74. Rayleigh, L. On the equilibrium of liquid conducting masses charged with electricity. *Philos. Mag.* **1882**, *14*, 184-186.
75. Taflin, D. C.; Ward, T. L.; Davis, E. J. Electrified droplet fission and the Rayleigh limit. *Langmuir* **1989**, *5*, 376-384.
76. Li, K.-Y.; Tu, H.; Ray, A. K. Charge limits on droplets during evaporation. *Langmuir* **2005**, *21*, 3786-3794.
77. Iribarne, J.; Thomson, B. On the evaporation of small ions from charged droplets. *J. Chem. Phys.* **1976**, *64*, 2287-2294.
78. Dole, M.; Mack, L.; Hines, R. Molecular beams of macroions. *J. Chem. Phys.* **1968**, *49*, 2240-2249.
79. Mack, L. L.; Kralik, P.; Rheude, A.; Dole, M. Molecular beams of macroions .2. *J. Chem. Phys.* **1970**, *52*, 4977-&.
80. Nguyen, S.; Fenn, J. B. Gas-phase ions of solute species from charged droplets of solutions. *Proc. Natl. Acad. Sci.* **2007**, *104*, 1111-1117.
81. Gamero-Castano, M.; De La Mora, J. F. Direct measurement of ion evaporation kinetics from electrified liquid surfaces. *J. Chem. Phys.* **2000**, *113*, 815-832.
82. de la Mora, J. F. Electrospray ionization of large multiply charged species proceeds via Dole's charged residue mechanism. *Anal. Chim. Acta* **2000**, *406*, 93-104.
83. Smith, R. D.; Loo, J. A.; Ogorzalek Loo, R. R.; Busman, M.; Udseth, H. R. Principles and practice of electrospray ionization - mass spectrometry for large polypeptide and proteins. *Mass Spectrom. Rev.* **1991**, *10*, 359-451.
84. Konermann, L.; Rodriguez, A. D.; Liu, J. On the formation of highly charged gaseous ions from unfolded proteins by electrospray ionization. *Anal. Chem.* **2012**, *84*, 6798-6804.
85. Ahadi, E.; Konermann, L. Modeling the behavior of coarse-grained polymer chains in charged water droplets: implications for the mechanism of electrospray ionization. *J. Phys. Chem. B* **2012**, *116*, 104-112.
86. Konermann, L.; Ahadi, E.; Rodriguez, A. D.; Vahidi, S. Unraveling the mechanism of electrospray ionization. *Anal. Chem.* **2013**, *85*, 2-9.
87. Fung, Y. M. E.; Adams, C. M.; Zubarev, R. A. Electron ionization dissociation of singly and multiply charged peptides. *J. Am. Chem. Soc.* **2009**, *131*, 9977-9985.
88. Downard, K. *Mass spectrometry: A foundation course*. Royal Society of Chemistry: Cambridge, UK, **2004**.
89. de Godoy, L. M. F.; Olsen, J. V.; Cox, J.; Nielsen, M. L.; Hubner, N. C.; Frohlich, F.; Walther, T. C.; Mann, M. Comprehensive mass-spectrometry-based proteome quantification of haploid versus diploid yeast. *Nature* **2008**, *455*, 1251-U1260.
90. Sleno, L.; Volmer, D. A. Ion activation methods for tandem mass spectrometry. *J. Mass Spectrom.* **2004**, *39*, 1091-1112.
91. Roepstorff, P.; Fohlman, J. Proposal for a common nomenclature for sequence ions in mass-spectra of peptides. *Biomed. Mass Spectrom.* **1984**, *11*, 601-601.
92. Biemann, K.; Martin, S. A. MS/MS of peptides. *Mass Spectrom. Rev.* **1987**, *6*, 1-

76.
93. Hunt, D. F.; Yates, J. R.; Shabanowitz, J.; Winston, S.; Hauer, C. R. Protein sequencing by tandem mass-spectrometry. *Proc. Natl. Acad. Sci. U. S. A.* **1986**, *83*, 6233-6237.
94. McLuckey, S. A. Principles of collisional activation in analytical mass spectrometry. *J. Am. Soc. Mass Spectrom.* **1992**, *3*, 599-614.
95. Papayannopoulos, I. A. The interpretation of collision induced dissociation tandem mass spectra of peptides. *Mass Spectrom. Rev.* **1995**, *14*, 49-73.
96. Hayes, R. N.; Gross, M. L. Collision Induced Dissociation. *Methods Enzymol.* **1990**, *193*, 237-263.
97. Yamaoka, H.; Dong, P.; Durup, J. Energetics of collision-induced dissociations C2H2+- C2H++H and C2H2+- H++C2H. *J. Chem. Phys.* **1969**, *51*, 3465-&.
98. Schwartz, R. N.; Slawsky, Z. I.; Herzfeld, K. F. Calculation of vibrational relaxation times in gases. *J. Chem. Phys.* **1952**, *20*, 1591-1599.
99. Stannard, P. R.; Gelbart, W. M. Intramolecular vibrational-energy redistribution. *J. Phys. Chem.* **1981**, *85*, 3592-3599.
100. McLuckey, S. A.; Goeringer, D. E. Slow heating methods in tandem mass spectrometry. *J. Mass Spectrom.* **1997**, *35*, 461-474.
101. Gauthier, J. W.; Trautman, T. R.; Jacobson, D. B. Sustained off-resonance irradiation for CAD Involving FTMS - CAD technique that emulates infrared multiphoton dissociation. *Anal. Chim. Acta* **1991**, *246*, 211-225.
102. Dongre, A. R.; Jones, J. L.; Somogyi, A.; Wysocki, V. H. Influence of peptide composition, gas-phase basicity, and chemical modification on fragmentation efficiency: Evidence for the mobile proton model. *J. Am. Chem. Soc.* **1996**, *118*, 8365–8374.
103. Wysocki, V. H.; Tsaprailis, G.; Smith, L. L.; Breci, L. A. Special feature: Commentary - mobile and localized protons: A framework for understanding peptide dissociation. *J. Mass Spectrom.* **2000**, *35*, 1399-1406.
104. Paizs, B.; Suhai, S. Fragmentation pathways of protonated peptides. *Mass Spectrom. Rev.* **2005**, *24*, 508-548.
105. Vaisar, T.; Urban, J. Gas-phase fragmentation of protonated mono-N-methylated peptides. Analogy with solution-phase acid-catalyzed hydrolysis. *J. Mass Spectrom.* **1998**, *33*, 505-524.
106. Eckart, K.; Holthausen, M. C.; Koch, W.; Spiess, J. Mass spectrometric and quantum mechanical analysis of gas-phase formation, structure, and decomposition of various b(2) ions and their specifically deuterated analogs. *J. Am. Soc. Mass. Spectrom.* **1998**, *9*, 1002-1011.
107. Huang, Y. Y.; Triscari, J. M.; Tseng, G. C.; Pasa-Tolic, L.; Lipton, M. S.; Smith, R. D.; Wysocki, V. H. Statistical characterization of the charge state and residue dependence of low-energy CID peptide dissociation patterns. *Anal. Chem.* **2005**, *77*, 5800-5813.
108. Huang, Y. Y.; Tseng, G. C.; Yuan, S. S.; Pasa-Tolic, L.; Lipton, M. S.; Smith, R. D.; Wysocki, V. H. A data-mining scheme for identifying peptide structural motifs responsible for different MS/MS fragmentation intensity patterns. *J. Proteome Res.* **2008**, *7*, 70-79.
109. Witze, E. S.; Old, W. M.; Resing, K. A.; Ahn, N. G. Mapping protein post-

translational modifications with mass spectrometry. *Nat. Methods* **2007**, *4*, 798-806.
110. Palumbo, A. M.; Reid, G. E. Evaluation of gas-phase rearrangement and competing fragmentation reactions on protein phosphorylation site assignment using collision induced dissociation-MS/MS and MS3. *Anal. Chem.* **2008**, *80*, 9735-9747.
111. Mischerikow, N.; Altelaar, A. M.; Navarro, J. D.; Mohammed, S.; Heck, A. Comparative assessment of site assignments in CID and ETD spectra of phosphopeptides discloses limited relocation of phosphate groups. *Mol. Cell. Proteomics* **2010**, *9*, 2140-2148.
112. Aguiar, M.; Haas, W.; Beausoleil, S. A.; Rush, J.; Gygi, S. P. Gas-phase rearrangements do not affect site localization reliability in phosphoproteomics data sets. *J. Proteome Res.* **2010**, *9*, 3103-3107.
113. Basov, N. G.; Markin, E. P.; Oraevskii, A. N.; Pankratov, A. V.; Skachkov, A. N. Stimulation of chemical processes by infrared laser radiation. *ZhETF Pisma Redaktsiiu* **1971**, *14*, 251.
114. Brodbelt, J. S.; Wilson, J. J. Infrared multiphoton dissociation in quadrupole ion traps. *Mass Spectrom. Rev.* **2009**, *28*, 390-424.
115. Little, D. P.; Speir, J. P.; Senko, M. W.; O'Connor, P. B.; McLafferty, F. W. Infrared multiphoton dissociation of large multiply-charged ions for biomolecule sequencing. *Anal. Chem.* **1994**, *66*, 2809-2815.
116. Adamson, J. T.; Hakansson, K. Infrared multiphoton dissociation and electron capture dissociation of high-mannose type glycopeptides. *J. Proteome Res.* **2006**, *5*, 493-501.
117. Yang, J.; Hakansson, K. Characterization of oligodeoxynucleotide fragmentation pathways in infrared multiphoton dissociation and electron detachment dissociation by fourier transform ion cyclotron double resonance. *Eur. J. Mass Spectrom.* **2009**, *15*, 293-304.
118. Polfer, N. C.; Valle, J. J.; Moore, D. T.; Oomens, J.; Eyler, J. R.; Bendiak, B. Differentiation of isomers by wavelength-tunable infrared multiple photon dissociation mass spectrometry: Application to glucose-containing disaccharides. *Anal. Chem.* **2006**, *78*, 670-679.
119. Vala, M.; Szczepanski, J.; Oomens, J.; Steill, J. D. H-2 ejection from polycyclic aromatic hydrocarbons: Infrared multiphoton dissociation study of protonated 1,2-dihydronaphthalene. *J. Am. Chem. Soc.* **2009**, *131*, 5784-5791.
120. Zubarev, R. A.; Kelleher, N. L.; McLafferty, F. W. Electron capture dissociation of multiply charged protein cations. A nonergodic process. *J. Am. Chem. Soc.* **1998**, *120*, 3265-3266.
121. McLafferty, F. W.; Horn, D. M.; Breuker, K.; Ge, Y.; Lewis, M. A.; Cerda, B.; Zubarev, R. A.; Carpenter, B. K. Electron capture dissociation of gaseous multiply charged ions by fourier transform ion cyclotron resonance. *J. Am. Soc. Mass Spectrom.* **2001**, *12*, 245-249.
122. Zubarev, R. A. Reactions of polypeptide ions with electrons in the gas phase. *Mass Spectrom. Rev.* **2003**, *22*, 57-77.
123. Zubarev, R. A. Electron capture dissociation tandem mass spectrometry. *Curr. Opin. Biotechnol.* **2004**, *15*, 12-16.

124. Bakhtiar, R.; Guan, Z. Q. Electron capture dissociation mass spectrometry in characterization of peptides and proteins. *Biotechnol. Lett.* **2006**, *28*, 1047-1059.
125. Coon, J. J.; Syka, J. E. P.; Schwartz, J. C.; Shabanowitz, J.; Hunt, D. F. Anion dependence in the partitioning between proton and electron transfer in ion/ion reactions. *Int. J. Mass Spectrom.* **2004**, *236*, 33-42.
126. Molina, H.; Horn, D. M.; Tang, N.; Mathivanan, S.; Pandey, A. Global proteomic profiling of phosphopeptides using electron transfer dissociation tandem mass spectrometry. *Proc. Natl. Acad. Sci. U. S. A.* **2007**, *104*, 2199-2204.
127. Good, D. M.; Wirtala, M.; McAlister, G. C.; Coon, J. J. Performance characteristics of electron transfer dissociation mass spectrometry. *Mol. Cell. Proteomics* **2007**, *6*, 1942-1951.
128. Pitteri, S. J.; Chrisman, P. A.; Hogan, J. M.; McLuckey, S. A. Electron transfer ion/ion reactions in a three-dimensional quadrupole ion trap: reactions of doubly and triply protonated peptides with SO2. *Anal. Chem.* **2005**, *77*, 1831-1839.
129. Chi, A.; Huttenhower, C.; Geer, L. Y.; Coon, J. J.; Syka, J. E. P.; Bai, D. L.; Shabanowitz, J.; Burke, D. J.; Troyanskaya, O. G.; Hunt, D. F. Analysis of phosphorylation sites on proteins from Saccharomyces cerevisiae by electron transfer dissociation (ETD) mass spectrometry. *Proc. Natl. Acad. Sci. U. S. A.* **2007**, *104*, 2193-2198.
130. Xia, Y.; Gunawardena, H. P.; Erickson, D. E.; McLuckey, S. A. Effects of cation charge-site identity and position on electron-transfer dissociation of polypeptide cations. *J. Am. Chem. Soc.* **2007**, *129*, 12232-12243.
131. Breuker, K.; Oh, H. B.; Lin, C.; Carpenter, B. K.; McLafferty, F. W. Nonergodic and conformational control of the electron capture dissociation of protein cations. *Proc. Natl. Acad. Sci. U.S.A.* **2004**, *101*, 14011-14016.
132. Jones, J. W.; Sasaki, T.; Goodlett, D. R.; Turecek, F. Electron capture in spin-trap capped peptides. An experimental example of ergodic dissociation in peptide cation-radicals. *J. Am. Soc. Mass Spectrom.* **2007**, *18*, 432-444.
133. Leib, R. D.; Donald, W. A.; Bush, M. F.; O'Brien, J. T.; Williams, E. R. Internal energy deposition in electron capture dissociation measured using hydrated divalent metal ions as nanocalorimeters. *J. Am. Chem. Soc.* **2007**, *129*, 4894-4895.
134. Turecek, F. N-c-alpha bond dissociation energies and kinetics in amide and peptide radicals. Is the dissociation a non-ergodic process? *J. Am. Chem. Soc.* **2003**, *125*, 5954-5963.
135. Sobczyk, M.; Anusiewicz, W.; Berdys-Kochanska, J.; Sawicka, A.; Skurski, P.; Simons, J. Coulomb-assisted dissociative electron attachment: Application to a model peptide. *J. Phys. Chem. A* **2005**, *109*, 250-258.
136. Syrstad, E. A.; Turecek, F. Toward a general mechanism of electron capture dissociation. *J. Am. Soc. Mass Spectrom.* **2005**, *16*, 208-224.
137. Patriksson, A.; Adams, C.; Kjeldsen, F.; Raber, J.; van der Spoel, D.; Zubarev, R. A. Prediction of N-C-alpha bond cleavage frequencies in electron capture dissociation of trp-cage dications by force-field molecular dynamics simulations. *Int. J. Mass Spectrom.* **2006**, *248*, 124-135.
138. Sawicka, A.; Skurski, P.; Hudgins, R. R.; Simons, J. Model calculations relevant to disulfide bond cleavage via electron capture influenced by positively charged groups. *J. Phys. Chem. B* **2003**, *107*, 13505-13511.

139. Chen, X. H.; Turecek, F. The arginine anomaly: Arginine radicals are poor hydrogen atom donors in electron transfer induced dissociations. *J. Am. Chem. Soc.* **2006**, *128*, 12520-12530.
140. Gunawardena, H. P.; He, M.; Chrisman, P. A.; Pitteri, S. J.; Hogan, J. M.; Hodges, B. D.; McLuckey, S. A. Electron transfer versus proton transfer in gas-phase ion/ion reactions of polyprotonated peptides. *J. Am. Chem. Soc.* **2005**, *127*, 12627-12639.
141. Kjeldsen, F.; Giessing, A. M. B.; Ingrell, C. R.; Jensen, O. N. Peptide sequencing and characterization of post-translational modifications by enhanced ion-charging and liquid chromatography electron-transfer dissociation tandem mass spectrometry. *Anal. Chem.* **2007**, *79*, 9243-9252.
142. Anusiewicz, I.; Berdys-Kochanska, J.; Simons, J. Electron attachment step in electron capture dissociation (ECD) and electron transfer dissociation (ETD). *J. Phys. Chem. A* **2005**, *109*, 5801-5813.
143. Savitski, M. M.; Nielsen, M., L.; Kjeldsen, F.; Zubarev, R. A. Proteomics-grade de novo sequencing approach. *J. Proteome Res.* **2005**, *4*, 2348-2354.
144. Kruger, N. A.; Zubarev, R. A.; Horn, D. M.; McLafferty, F. W. Electron capture dissociation of multiply charged peptide cations. *Int. J. Mass Spectrom.* **1999**, *185/186/187*, 787-793.
145. Zubarev, R. A.; Horn, D. M.; Fridriksson, E. K.; Kelleher, N. L.; Kruger, N. A.; Lewis, M. A.; Carpenter, B. K.; McLafferty, F. W. Electron capture dissociation for structural characterization of multiply charged protein cations. *Anal. Chem.* **2000**, *72*, 563-573.
146. Shi, S. D.-H.; Hemling, M. E.; Carr, S. A.; Horn, D. M.; Lindh, I.; McLafferty, F. W. Phosphopeptide/phosphoprotein mapping by electron capture dissociation mass spectrometry. *Anal. Chem.* **2001**, *73*, 19-22.
147. Stensballe, A.; Norregaard-Jensen, O.; Olsen, J. V.; Haselmann, K. F.; Zubarev, R. A. Electron capture dissociation of singly and multiply phosphorylated peptides. *Rapid Commun. Mass Spectrom.* **2000**, *14*, 1793-1800.
148. Hakansson, K.; Cooper, H. J.; Emmett, M. R.; Costello, C. E.; Marshall, A. G.; Nilsson, C. L. Electron capture dissociation and infrared multiphoton dissociation MS/MS of an N-glycosylated tryptic peptide yield complementary sequence information. *Anal. Chem.* **2001**, *73*, 4530-4536.
149. Mirgorodskaya, E.; Roepstorff, P.; Zubarev, R. A. Localization of O-glycosylation sites in peptides by electron capture dissociation in a fourier transform mass spectrometer. *Anal. Chem.* **1999**, *71*, 4431-4436.
150. McAlister, G. C.; Phanstiel, D.; Good, D. M.; Berggren, W. T.; Coon, J. J. Implementation of electron transfer dissociation on a hybrid linear ion trap-orbitrap mass spectrometer. *Anal. Chem.* **2007**, *79*, 3525-3534.
151. Kalli, A.; Hakansson, K. Electron capture dissociation of highly charged proteolytic peptides from Lys N, Lys C and Glu C digestion. *Mol. Biosyst.* **2010**, *6*, 1668-1681.
152. Kalli, A.; Håkansson, K. Comparison of the electron capture dissociation fragmentation behavior of doubly and triply protonated peptides from trypsin, Glu-C, and chymotrypsin digestion. *J. Proteome Res.* **2008**, *7*, 2834-2844.
153. Good, D. M.; Wirtala, M.; McAlister, G. C.; Coon, J. J. Performance

characteristics of electron transfer dissociation mass spectrometry. *Mol. Cell. Proteomics* **2007**, *6*, 1942-1951.
154. Liu, H.; Hakansson, K. Electron capture dissociation of tyrosine O-sulfated peptides complexed with divalent metal cations. *Anal. Chem.* **2006**, *78*, 7570-7576.
155. Medzihradszky, K. F.; Guan, S.; Maltby, D. A.; Burlingame, A. L. Sulfopeptide fragmentation in electron capture and electron transfer dissociation. *J. Am. Soc. Mass Spectrom.* **2007**, *18*, 1617-1624.
156. Brinkworth, C. S.; Dua, S.; Bowie, J. H. Backbone cleavages of M-H (-) anions of peptides. New backbone cleavages following cyclisation reactions of a C-terminal CONH (-) group with Ser residues and the use of the gamma backbone cleavage initiated by Gin to differentiate between Lys and Gin residues. *Eur. J. Mass Spectrom.* **2002**, *8*, 53-66.
157. Edelson-Averbukh, M.; Pipkorn, R.; Lehmann, W. D. Analysis of protein phosphorylation in the regions of consecutive serine/threonine residues by negative ion electrospray collision-induced dissociation. Approach to pinpointing of phosphorylation sites. *Anal. Chem.* **2007**, *79*, 3476-3486.
158. Bowie, J. H.; Brinkworth, C. S.; Dua, S. Collision-induced fragmentations of the (M-H)(-) parent anions of underivatized peptides: an aid to structure determination and some unusual negative ion cleavages. *Mass Spectrom. Rev.* **2002**, *21*, 87-107.
159. Ewing, N. P.; Cassady, C. J. Dissociation of multiply charged negative ions for hirudin (54-65), fibrinopeptide B, and insulin A (oxidized). *J. Am. Soc. Mass Spectrom.* **2001**, *12*, 105-116.
160. Harrison, A. G. Sequence-specific fragmentation of deprotonated peptides containing H or alkyl side chains. *J. Am. Soc. Mass. Spectrom.* **2001**, *12*, 1-13.
161. Harrison, A. G. Effect of phenylalanine on the fragmentation of deprotonated peptides. *J. Am. Soc. Mass. Spectrom.* **2002**, *13*, 1242-1249.
162. Brinkworth, C. S.; Dua, S.; McAnoy, A. M.; Bowie, J. H. Negative ion fragmentations of deprotonated peptides: backbone cleavages directed through both Asp and Glu. *Rapid Commun. Mass Spectrom.* **2001**, *15*, 1965-1973.
163. Budnik, B. A.; Haselmann, K. F.; Zubarev, R. A. Electron detachment dissociation of peptide DI-ANIONS: an electron-hole recombination phenomenon. *Chem. Phys. Lett.* **2001**, *342*, 299-302.
164. Anusiewicz, I.; Jasionowski, M.; Skurski, P.; Simons, J. Backbone and side-chain cleavages in electron detachment dissociation (EDD). *J. Phys. Chem. A* **2005**, *109*, 11332-11337.
165. Kjeldsen, F.; Silivra, O. A.; Ivonin, I. A.; Haselmann, K. F.; Gorshkov, M.; Zubarev, R. A. C(alpha)-C backbone fragmentation dominates in electron detachment dissociation of gas-phase polypeptide polyanions. *Chem. Eur. J.* **2005**, *11*, 1803-1812.
166. Kleinnijenhuis, A. J.; Kjeldsen, F.; Kallipolitis, B.; Haselmann, K. F.; Jensen, O. N. Analysis of Histidine Phosphorylation Using Tandem MS and Ion-Electron Reactions. *Anal. Chem.* **2007**, 7450-7456.
167. Kweon, H. K.; Hakansson, K. Metal oxide-based enrichment combined with gas-phase ion-electron reactions for improved mass spectrometric characterization of

protein phosphorylation. *J. Proteome Res.* **2008**, *7*, 745-755.
168. Yang, J.; Hakansson, K. Characterization and optimization of electron detachment dissociation fourier transform ion cyclotron resonance mass spectrometry. *Int. J. Mass Spectrom.* **2008**, *276*, 144-148.
169. Wolff, J. J.; Chi, L.; Linhardt, R. J.; Amster, I. J. Distinguishing glucuronic from iduronic acid in glycosaminoglycan tetrasaccharides by using electron detachment dissociation. *Anal. Chem.* **2007**, *79*, 2015-2022.
170. Coon, J. J.; Shabanowitz, J.; Hunt, D. F.; Syka, J. E. P. Electron transfer dissociation of peptide anions. *J. Am. Soc. Mass Spectrom.* **2005**, *16*, 880-882.
171. Huzarska, M.; Ugalde, I.; Kaplan, D. A.; Hartmer, R.; Easterling, M. L.; Polfer, N. C. Negative electron transfer dissociation of deprotonated phosphopeptide anions: Choice of radical cation reagent and competition between electron and proton transfer. *Anal. Chem.* **2010**, *82*, 2873-2878.
172. Yoo, H. J.; Wang, N.; Zhuang, S.; Song, H.; Hakansson, K. Negative-ion electron capture dissociation: radical-driven fragmentation of charge-increased gaseous peptide anions. *J. Am. Chem. Soc.* **2011**, *133*, 16790-16793.

Chapter 2

Discovery of Negative Ion Electron Capture Dissociation (niECD) and Its Application towards Phospho- and Sulfopeptides

2.1 Introduction

Gas-phase ion-electron and ion-ion reactions continue to increase their impact as ion activation methods in tandem mass spectrometry (MS/MS). Examples include electron capture dissociation (ECD),[1,2] electron transfer dissociation (ETD),[3] electron detachment dissociation (EDD),[4-7] negative electron transfer dissociation (NETD),[8, 9] electron induced dissociation,[10-12] and electron ionization dissociation (EID[13]; not to be confused with electron induced dissociation that shares the same acronym). The most prominent of these electron-mediated techniques are ECD and the fundamentally similar ETD, which are powerful alternatives to conventional collision activated dissociation

(CAD). Major advantages of ECD and ETD include that fragmentation patterns are complementary to those observed in positive ion mode CAD, frequently providing more extensive peptide sequence information and, importantly, not involving loss of post-translational modifications (PTMs). Labile PTMs, such as phosphorylation[14, 15] and glycosylation,[16, 17] are preserved upon backbone product ions during ECD/ETD, allowing PTM sites to be determined. By contrast, PTM characterization is often challenging with the slow-heating technique CAD. In CAD, labile PTMs are preferentially cleaved, rendering localization of their site of attachment difficult.[18] More recently, electron ionization and subsequent extensive dissociation (electron ionization dissociation, EID) has been reported following irradiation of $[M + nH]^{n+}$ ($n \geq 1$) peptide cations with fast electrons (at least 10 eV higher than the cation ionization energy, i.e., >20 eV).[13] Such irradiation causes double ionization to $[M + nH]^{(n + 2)+}$ followed by electron capture to form electronically excited $[M + nH]^{(n + 1)+\bullet *}$ ions, which dissociate via both side-chain losses and backbone fragmentation.

Despite the significant developments of various activation methods for biomolecular ions (also including photodissociation[19-23]), the vast majority of MS/MS research deals with cationic analytes. ECD, ETD, and EID all involve positively-charged precursor ions with at least two charges for ECD and ETD because capture/transfer of an electron reduces total charge by one and mass spectrometers cannot detect neutrals. Furthermore, the efficiency of ECD/ETD is dependent on the charge state and precursor ions with high charge states are more favorable.[24-27] However, generation of multiply-charged cations is challenging for acidic analytes, including peptides with important PTMs such as phosphorylation and sulfation, particularly from mixtures for which competition for

charge results in suppression of less basic species. Moreover, some PTMs, such as sulfation, are much more labile in cations than in anions and sulfonate groups are readily lost in both ECD[28, 29] and ETD.[29] Thus, alternative MS/MS techniques operating in negative ion mode are desired. The limited use of negative ion MS/MS is due to complications with anion dissociation chemistry: CAD of peptide anions typically results in PTM loss,[30, 31] similar to cation CAD. Furthermore, backbone fragmentation in negative ion CAD is more complex and less predictable than in positive ion mode,[32] frequently yielding little analytically useful information. Electron-based techniques operating in negative ion mode include EDD and NETD. The former technique has low fragmentation efficiency[7] and dominant structurally non-informative CO_2 loss for peptide dissociation. The latter technique can result in PTM loss due to the energy release from charge reduction.[8] Both EDD and NETD yield backbone $a^{\bullet}$- and *x*-type product ions but also involve structurally uninformative neutral losses as major fragmentation pathways. More recent work by Huzarska and Polfer with different NETD reagents (fluoranthene) shows that PTMs can be preserved.[9] In addition, both techniques require multiply-charged anions as precursor ions. Meta-stable atom-activated dissociation (MAD),[33, 34] also believed to involve radical-driven dissociation, was recently shown to yield complementary fragmentation to both CAD, ECD, and EDD with little PTM loss for peptide anions.[35] All these factors indicate that developing an alternative MS/MS technique for anions analogous to ECD/ETD for cations is highly desirable.

Intuitively, electron capture by negatively-charged gaseous peptide ions appears unlikely due to Coulomb repulsion. However, previous work has shown attachment of 2-

3 eV electrons from a heated filament to singly-charged fullerene anions to form dianions in a Fourier transform ion cyclotron resonance (FT-ICR) mass spectrometer.[36] Electron transfer to unmodified[37] and fluorinated[38] fullerene anions has also been observed in high-energy (keV) collisions with atomic and molecular targets. We argued that such a phenomenon may also be feasible for peptide anions at a certain mass-to-charge (m/z) ratio and an appropriate electron energy. In order to test this hypothesis, coumarin-tagged peptides were first investigated in our lab, based on work by O'Connor and co-workers who showed that coumarin tags act as radical traps in conventional positive ion mode ECD.[39] After careful optimization of the electron energy, we found that abundant charge-increased radical species, $[M + \text{coumarin} - H]^{2-\bullet}$, generated from capture of electrons by singly-deprotonated coumarin-tagged peptides, were observed within a rather narrow energy range (3.5–6.5 eV). Electron capture occurred most efficiently upon irradiation with 4.5 eV electrons (corresponding to a cathode bias voltage of 6 V).[40] These preliminary data demonstrate the feasibility of electron capture by peptide anions. However, the generated doubly-charged radical anions appeared stable to further dissociation, consistent with the previously observed behavior of coumarin-tagged peptides[39] and peptides containing other electron predators[41, 42] in conventional ECD, and with the previously observed fullerene dianions.[36] In addition, further activation (MS^3) of the generated $[M + \text{coumarin} - H]^{2-\bullet}$ radical species through 10.6 μm infrared multiphoton dissociation (IRMPD)[43] mainly resulted in ejection of small structurally uninformative neutrals.[40]

In this Chapter, following the discovery that ~4.5 eV electrons can be captured by coumarin-tagged peptide anions, unmodified peptides are investigated with electron

irradiation in this range. Without a coumarin radical trap, the radical generated from electron capture is unstable and thus may undergo further dissociation, providing more structural information compared with the coumarin-tagged peptides. We were eager to elucidate the fragmentation chemistry associated with this interesting reaction. Particularly, phospho- and sulfopeptide analysis is of great interest. Protein phosphorylation is probably the most extensively studied protein PTM in the literature. It is one of the most widespread regulatory mechanisms found in cells and its reversible and transient nature allows signal transduction pathways to carry out diverse cellular functions.[44, 45] Typically, protein phosphorylation occurs on serine, threonine, or tyrosine side chains and corresponds to covalent attachment of a phosphate group to the protein via protein kinases. For sulfation, tyrosine O-sulfation is the most frequently observed within proteins. It has been implicated in protein-protein interactions of a vast number of membrane- and secreted proteins.[46] O-sulfation is also an important PTM to characterize as its biological significance is less known. For a number of reasons, characterization of phosphorylation and sulfation is much more complex than sole protein identification. In particular, phospho- and sulfopeptides exhibit low ionization efficiency in positive ion mode and are subjected to severe ion suppression by unmodified peptides due to the negatively-charged phosphate and sulfate groups.[47-49] Moreover, sulfate groups are highly labile in positive ion mode.[50, 51] Thus, negative ion mode analysis holds great potential for characterization of both phospho- and sulfopeptides. Herein, phospho- and sulfopeptide anions are subjected to electron irradiation to induce electron capture in negative ion mode.

2.2 Experimental

2.2.1 Reagents

The following peptides were used: neuromedin B (H-GNLWATGHF-NH_2), neurokinin B (H-DMHDFFVGLM-OH), cholecystokinin (CCK, H-DYMGWMDF-NH_2), H-AKPSYP*P*TYK-OH (P* = hydroxyproline), eHWSYGLRPG-NH_2 (e = pyroglutamic acid), exorphin C (H-YPISL-OH), H-RRREEEpSEEEAA-OH, H-KRSpYEEHIP-OH, angiotensin I (H-DRVYIHPFHL-OH), H-RRApSVA-OH, H-TSTEPQpYQPGENL-NH_2, bradykinin 2-9 (H-PPGFSPFR-OH), substance P-OH (H-RPKPQQFFGLM-OH), sulfated cholecystokinin fragment 26-33 (CCKS, H-DsYMGWMDF-NH_2), and hirudin fragment 55-65 (H-DFEEIPEEsYLQ-OH). Most peptides were purchased from Sigma-Aldrich (St. Louis, MO), except H-TSTEPQpYQPGENL-NH_2 (which was from Millipore, Billerica, MA), CCKS and hirudin (from Advanced ChemTech, Louisville, NY). Bovine milk α-casein was obtained from Sigma-Aldrich (St. Louis, MO). Trypsin was from Promega (Madison, WI).

2.2.2 Sample Preparation

Trypsin digestion of α-casein was performed for 12 h at 37 ℃ at an enzyme/substrate ratio of 1:50. The tryptic peptides H-YLGYLEQLLR-OH (α-casein 106-115), H-FALPQYLK-OH (α-casein 189-196), H-TVDMEpSTEVFTK-OH (α-casein 153-164), H-DIGpSEpSTEDQAMEDIK-OH (α-casein 58-73), and H-VPQLEIVPNpSAEER-OH (α-casein 121-134) were subjected to MS/MS. Phosphopeptide enrichment[52] was performed with ZrO_2 microtips (Glygen, Columbia, MD), when necessary. 5-10 μM

peptide solutions were prepared in 50/50 (v/v, H_2O/isopropanol) with 0.1 % triethylamine.

2.2.3 FT-ICR Mass Spectrometry

Negatively-charged peptide ions were generated by external electrospray ionization (ESI) at 70 μL/h (Apollo II ion source, Bruker Daltonics, Billerica, MA). All experiments were performed with a 7 Tesla quadrupole (Q)-FT-ICR mass spectrometer (APEX-Q, Bruker Daltonics) as previously described.[6] All data were obtained in negative ion mode. For ESI, N_2 was used as both nebulizing gas (5 L/s) and drying gas (2.5 L/s). The drying gas temperature was set to 200˚C. Briefly, ions produced by ESI were mass-selectively externally accumulated in a hexapole for 0.2-3 s, transferred via high voltage ion optics, and captured in the ICR cell by dynamic trapping. This accumulation sequence was looped three times to improve precursor ion abundance. For MS/MS experiments, mass-selective external accumulation of negatively-charged peptide ions was performed. For negative ion electron capture dissociation (niECD), mass selectively accumulated peptide ions were irradiated for 10-20 s (later shortened to 0.5-2 s) with 4.5-5.5 eV electrons (corresponding to a cathode bias voltage of 6-7 V) provided by an indirectly heated hollow dispenser cathode.[53] A lens electrode located in front of the hollow cathode was kept 1.5 V more positive than the cathode bias voltage. For isolation of radical species produced from electron capture by negatively-charged peptide ions, correlated harmonic excitation fields (CHEF)[54] was used inside the ICR cell. Collision activated dissociation was performed in an external hexapole at a collision cell DC offset of 20-40 V with argon as collision gas. All mass spectra were acquired with XMASS software (version 6.1, Bruker Daltonics) in broadband mode from m/z 200 to 3000 with 256K data points and summed over 10-32 scans.

2.2.4 Data Analysis

Data processing was performed with the MIDAS analysis software[55]. Data were zero filled once, Hanning apodized, and exported to Microsoft Excel for internal frequency-to-mass calibration with a two-term calibration equation[56]. Peaks in MS^n were assigned within 10 ppm error after internal calibration. Typically, internal calibration was performed with precursor ions and their electron-capture species as calibrants. Product ions were not assigned unless the S/N ratio was at least 3.

2.3 Results and Discussion

2.3.1 Discovery of niECD

Figure 2.1(a) shows 4.5 eV electron irradiation of a singly-deprotonated unmodified peptide with the sequence AKPSYP*P*TYK (P* represents hydroxyproline). Similar to the coumarin-tagged peptides described in the introduction, a charge-increased radical anion, $[M - H]^{2-\bullet}$, is observed at half the m/z ratio of the precursor ion and the zoomed-in view of this peak is shown in the inset of Figure 2.1(a). However, in contrast to the coumarin-tagged peptides, four c'-type and two $z^{\bullet}$-type product ions (Zubarev nomenclature)[57] from backbone N-C_α bond cleavage were also detected, strikingly similar to the types of fragments observed in positive ion mode ECD. We termed this phenomenon negative ion electron capture dissociation (niECD). The charge-increased radial species from AKPSYP*P*TYK was also isolated in the ICR cell to verify that this product was not an artifact at twice the ICR frequency of the precursor ion, as shown in Figure 2.1(b).

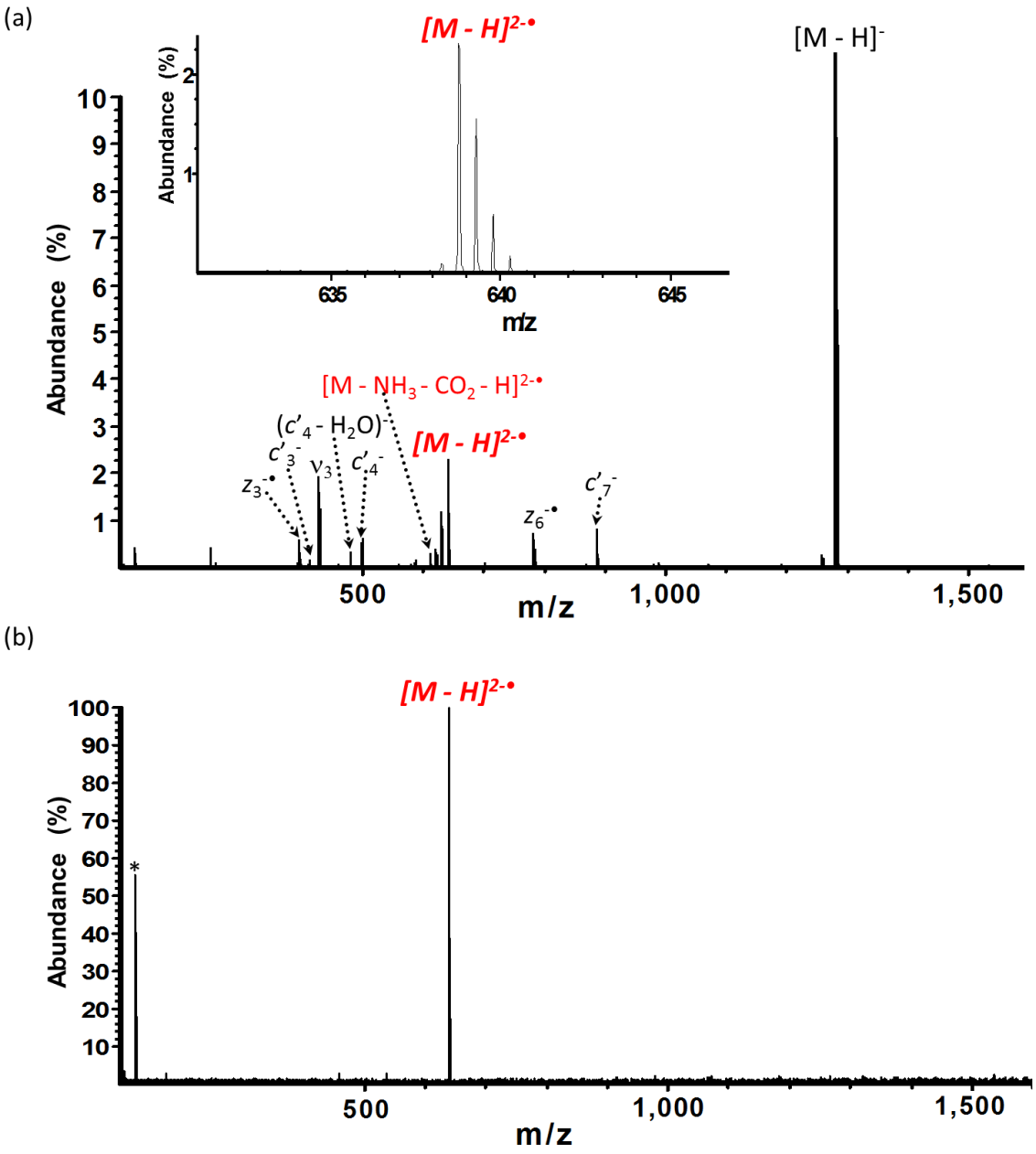

Figure 2.1. (a) niECD (~4.5 eV electrons, 20 s irradiation, 10 scans) of singly-deprotonated underivatized peptide AKPSYP*P*TYK (P* = hydroxyproline). *c*- and *z*-type peptide backbone fragments were produced. The inset shows the zoomed-in view of the electron capture species. (b) The charge-increased radical ion produced from electron capture in (a) was isolated inside the ICR cell to confirm that it is not the second harmonic peak.

2.3.2 niECD of Phospho- and Sulfopeptides

After the discovery of this exciting new technique, we moved on to study phospho- and sulfopeptides because negative ion mode should be a more logical choice for characterization of acidic molecules. First, phosphopeptides obtained from tryptic digestion of α-casein were examined. niECD of a singly-deprotonated serine-phosphorylated peptide is shown in Figure 2.2(a). ~4.5 eV electron irradiation yielded an abundant ammonia-deficient charge-increased radical, $[M - NH_3 - H]^{2-\bullet}$, as the major product. Remarkably, three doubly-charged *c*- and *z*-type sequence ions were observed from the singly-charged precursor ion. Many singly-charged *c/z* ions were also produced and virtually complete sequence coverage could be obtained from the niECD spectrum. More importantly, no phosphate or phosphoric acid loss was observed. Retention of the labile modification upon the peptide backbone fragments points to the serine residue as the site of phosphorylation. By contrast, such fragments were absent in CAD of the same singly deprotonated species. Only two backbone *y* ions were observed in the CAD spectrum, one of which did not contain the phosphate moiety (Figure 2.2(b)). Peptide sequencing as well as modification site determination was not possible based on the CAD fragmentation pattern.

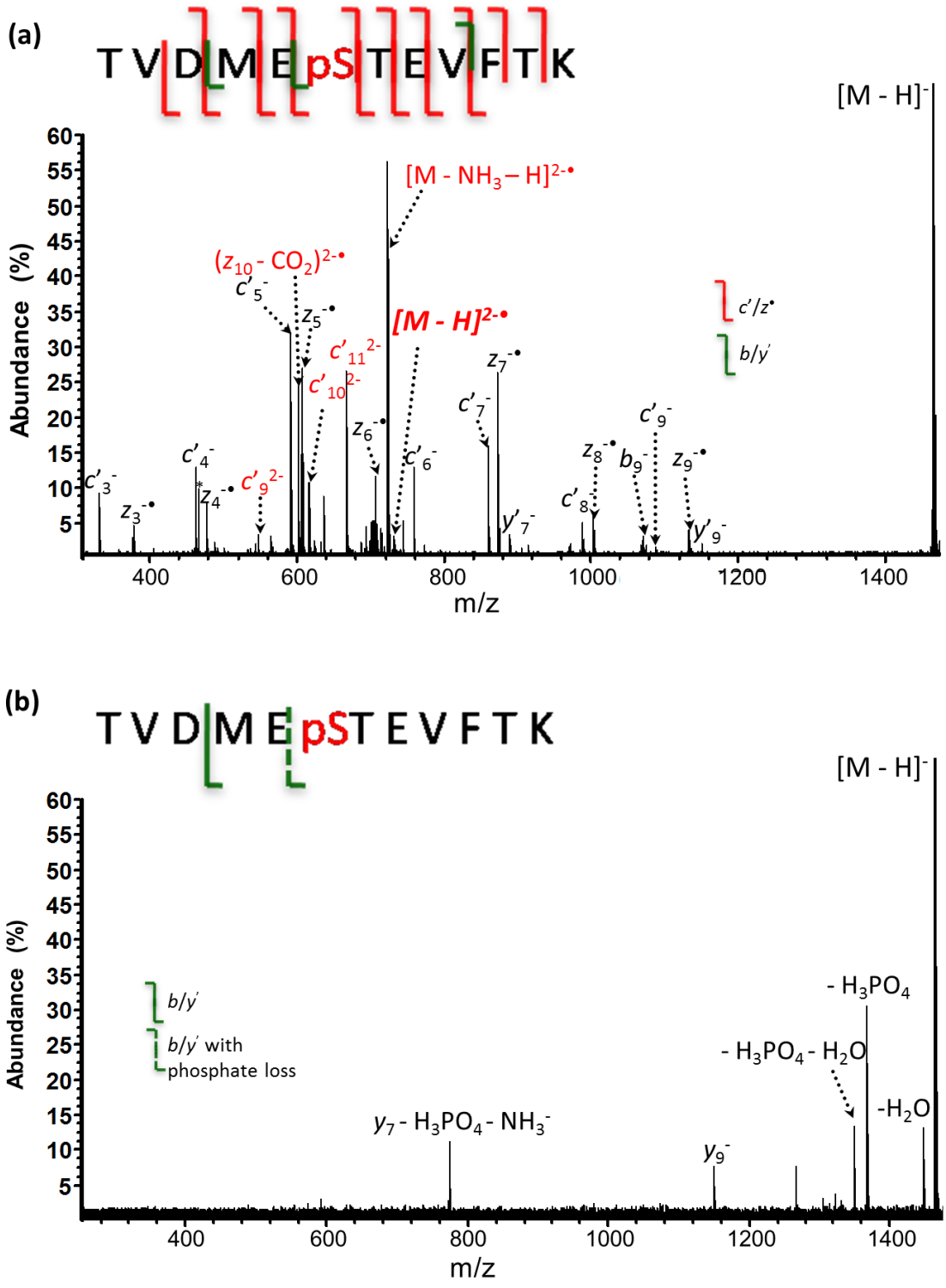

Figure 2.2. (a) niECD of an α-casein tryptic phosphopeptide. 10 s electron irradiation was applied towards the singly-deprotonated singly-phosphorylated peptide (~4.5 eV electrons, 10 scans). (b) Negative ion mode CAD (32 V collision voltage, 10 scans) of the same phosphopeptide. The charge-increased products are marked in red.

niECD of a doubly-deprotonated and doubly-phosphorylated α-casein tryptic peptide is shown in Figure 2.3. For doubly-charged precursor ions, the optimum niECD electron energy is slightly higher than for singly-charged precursor ions; ~5.5 rather than ~4.5 eV electrons were utilized, consistent with increased Coulomb repulsion. The fragmentation efficiency was also lower for doubly-charged precursor ions, however, a charge-increased triply-charged radical, $[M - 2H]^{3-\bullet}$, was observed along with four other charge-increased products and many doubly-charged *c*/*z* ions. Again, phosphate or phosphoric acid loss is absent for this phosphopeptide.

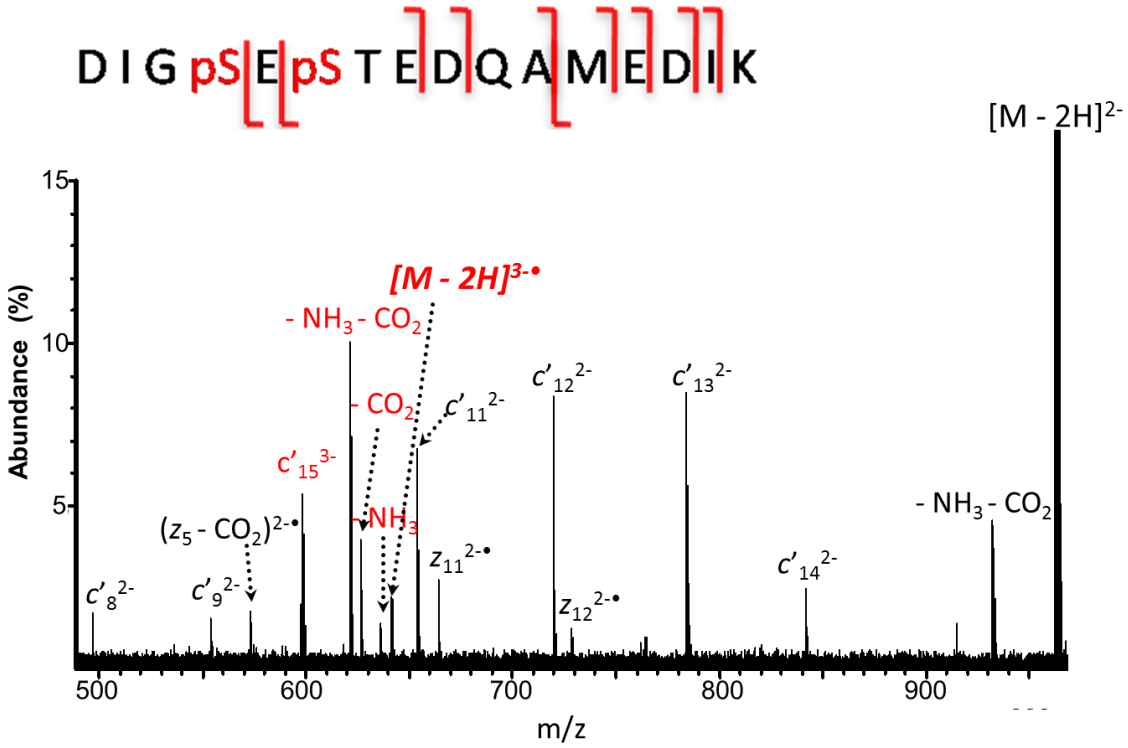

Figure 2.3. niECD (~5.5 eV electrons, 20 s irradiation, 10 scans) of a doubly-deprotonated and doubly-phosphorylated phosphopeptide from trypsin digestion of α-casein.

Figure 2.4 shows the MS/MS spectra of a tyrosine-sulfated peptide (cholecystokinin, CCKS). Sulfation is even more labile in the gas phase than phosphorylation and this modification is frequently lost in positive ion mode, even without ion activation. Thus, negative ion mode in which sulfotyrosine is more stable and shows higher ionization efficiency is preferred compared with positive ion mode analysis. EDD has shown some success for sulfate localization in sulfopeptides,[4] however, backbone fragmentation competes with neutral loss of CO_2 and SO_3. In niECD, extensive series of *c/z* backbone fragments were produced (Figure 2.4(a)). No sulfonate loss occurred and virtually complete sequence coverage was observed. In comparison, when subjected to negative mode CAD, neutral loss of the sulfonate group and additional water loss were the only products, leading to minimal peptide structural information (Figure 2.4(b)).

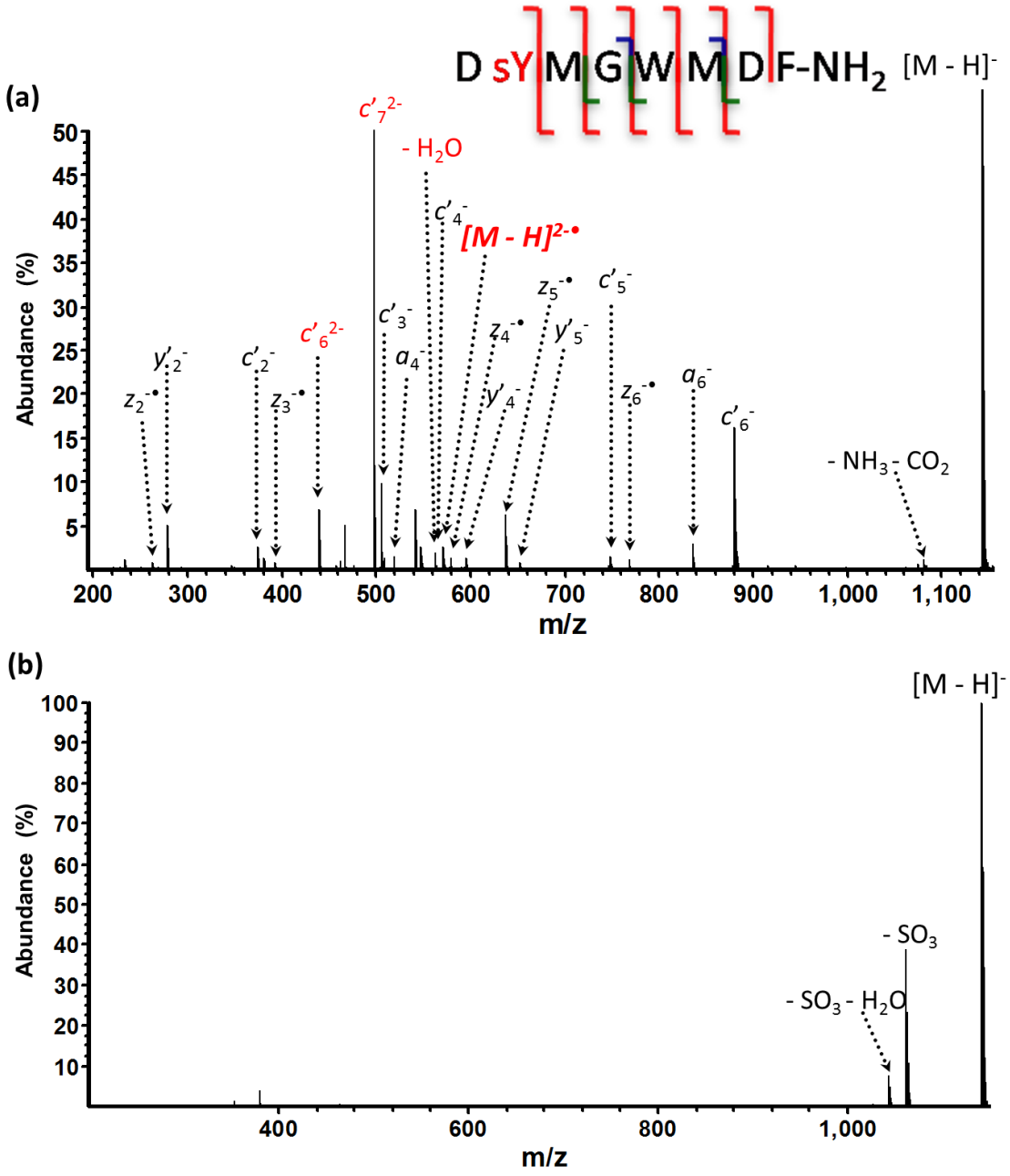

Figure 2.4. (a) niECD of sulfated cholecystokinin (CCKS; ~4.5 eV electrons, 20 s, 10 scans). (b) Negative ion mode CAD (20 V collision voltage, 10 scans) of the same sulfopeptide.

In addition to the examples shown above, several other phospho- and sulfopeptides were subjected to niECD and the corresponding spectra were compared to negative ion mode CAD of the same species. These data are summarized in Table 2.1. For all the phospho- and sulfopeptides studied, niECD provides primarily *c*- and *z*-type peptide

backbone fragments, significantly more extensive peptide sequence coverage than negative mode CAD, and phosphorylation and sulfation is retained. The only phosphopeptide we analyzed that did not undergo niECD (or electron capture by the singly-deprotonated anion) had the sequence H-RRApSVA-OH. This resistance to niECD is likely due to the smaller molecular weight and thus decreased favorability for accommodating two negative charges in the gas phase.

z	m/z	MS/MS: niECD	MS/MS: CAD
-1	1236.541		
-1	1568.634		
-1	1540.632	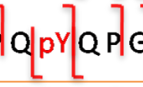	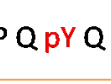
-1	1658.780		
-1	1464.597		
-1	1141.342		
-2	962.335		-
-2	1029.403	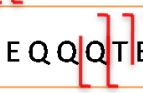	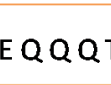

Table 2.1. Comparison of niECD and CAD for phospho- and sulfopeptide anions. Backbone N-C_α bond cleavages to yield $c'/z^\bullet$ ions are indicated with red lines and backbone amide bond cleavages to yield b/y' ions are indicated with green lines. Dashed lines indicate accompanying phosphate or phosphoric acid loss. Lack of indicated fragments in CAD is due to extensive neutral losses (e.g., HPO_3, H_3PO_4, SO_3, and H_2O).

2.3.3 niECD of Unmodified Peptides

In addition to phosphorylated and sulfated peptides, a number of unmodified peptides were also investigated by niECD. Table 2.2 summarizes the niECD outcome of

these unmodified peptides. In contrast to phospho- and sulfopeptides for which all but one short peptide showed extensive fragmentation in niECD, several singly-deprotonated unmodified peptides did not capture electrons, including the larger (>1 kDa) peptides cholecystokinin, neurokinin B, substance P-OH, and neuromedin B. One common characteristic of these four peptides is a lack of either strongly basic or strongly acidic residues, or both, thus reducing the probability of gas-phase zwitterionic structures. Furthermore, previous work by Creese and Cooper[58] and by Woods et al.[59] has shown that gas-phase zwitterionic structures are favored for phosphopeptides,[58, 59] which also undergo favorable niECD (Figure 2.2 and 2.3, Table 1). These observations, along with the striking similarity of niECD spectra to positive ion mode ECD/ETD spectra suggest that zwitterionic structures may play an important role for successful niECD with electron capture either occurring at or being directed by the positively-charged site.[60-62] In addition, work by Vasil'ev and coworkers involving electron capture by neutral gaseous peptides,[63] showed somewhat different product ion spectra with a larger variety of product ion types compared to niECD, further suggesting that charged sites may play a role in niECD.

z	m/z	Peptide name	Peptide sequence	$[M-H]^{2-\cdot}$ observed?
-1	590.320	Exorphin C	H-Y P I S L-OH	No
-1	902.452	Bradykinin 2-9	H-P P G F S P F R-OH	No
-1	977.547	α-casein 189-196	H-F A L P Q Y L K-OH	No
-1	1061.387	CCK	H-D Y M G W M D F-NH_2	No
-1	1209.507	Neurokinin B	H-D M H D F F V G L M-OH	No
-1	1346.704	Substance P	H-R P K P Q Q F F G L M-OH	No
-1	1131.504	Neuromedin B	H-G N L W A T G H F M-NH_2	No
-1	1180.566		e H W S Y G L R P G-NH_2	Yes
-1	1265.690	α-casein 106-115	H-Y L G Y L E Q L L R-OH	Yes
-1	1277.567		H-A K P S Y P* P* T Y K-OH	Yes
-1	1294.669	Angiotensin I	H-D R V Y I H P F H L-OH	Yes

Table 2.2. Electron irradiation of a selection of unmodified peptides. Contrary to phospho- and sulfopeptides, electron capture was not consistently observed. e = pyroglutamic acid, P* = hydroxyproline.

2.3.4 Optimization of niECD Conditions

All peptide niECD spectra shown above were acquired with irradiation times between 10 and 20 s. Such long irradiation times were customary in the early days of ECD,[64] however, they are not practical for, e.g., on-line coupling to LC and for limiting sample quantities. Later on, niECD was performed at higher cathode heating current than previously used (1.9 vs. 1.8 A). At the corresponding higher temperature, larger electron numbers are generated and remarkably faster niECD was possible. In Figure 2.5, niECD of the singly-deprotonated sulfopeptide hirudin (H-DFEEIPEEsYLQ-OH) was performed with shorter irradiation time. With 2 s irradiation, abundant and extensive *c* and *z* ions were produced, resulting in high sequence coverage (Figure 2.5(a)). niECD efficiency decreased with decreased irradiation time, as shown in Figures 2.5(b) and 2.5(c).

However, even with irradiation time as short as 0.5 s, an acceptable niECD spectrum was obtained with the same sequence coverage compared to 2 s irradiation. These irradiation times are shorter than or comparable to typical irradiation times in EDD, a technique that has already been coupled on-line with LC.[65] Based on these data, we believe significant optimization of niECD still remains before reaching its true potential. It is also interesting to note that niECD so far shows superior performance on the Apex instrument as compared to the SolariX instrument. The main difference between the two instruments is the ion transfer optics between the external hexapole collision cell and the ICR cell (high voltage transfer optics vs. hexapole). The former solution results in higher ion loss and also higher axial and radial kinetic energy spread. Manipulation of precursor ion kinetic energy may also affect niECD performance.

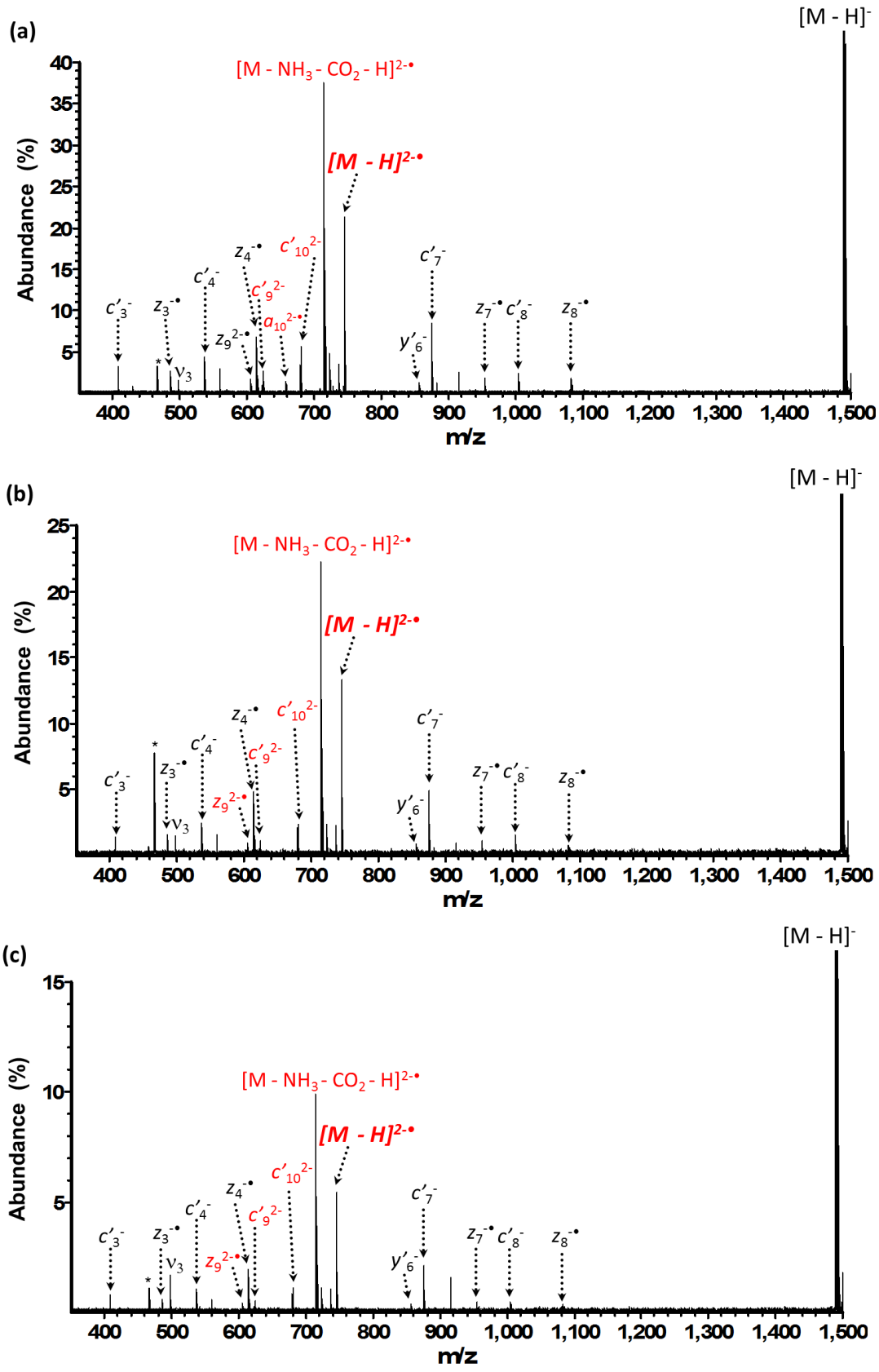
(a)
[M - H]-
[M - NH3 - CO2 - H]2-•
[M - H]2-•
Abundance (%)
m/z
(b)
[M - H]-
[M - NH3 - CO2 - H]2-•
[M - H]2-•
Abundance (%)
m/z
(c)
[M - H]-
[M - NH3 - CO2 - H]2-•
[M - H]2-•
Abundance (%)
m/z

Figure 2.5. niECD (4.5 eV) at shorter irradiation times: (a) 2 s, (b) 1 s and (c) 500 ms. 10 scans were summed for the singly-deprotonated sulfopeptide hirudin (H-DFEEIPEEsYLQ-OH). niECD efficiency decreased with decreased irradiation time. However, even with 500 ms irradiation, an niECD spectrum with acceptable product abundance and sequence coverage could be obtained.

2.4 Conclusion

In summary, we show that peptide anions ($[M - nH]^{n-}$, $n \geq 1$) could capture electrons within a rather narrow energy range (~3.5–6.5 eV), resulting in radical species with increased charge state, and yielding peptide fragmentation (niECD) analogous to that observed in regular cation ECD and ETD. Predictable $c'/z^{\bullet}$-type product ions from N-C_α backbone bond cleavage were observed without loss of labile PTMs. For all the peptide examples we studied, higher sequence coverage was obtained in niECD compared with conventional CAD. Increased charge improves signal-to-noise ratios in FT-ICR MS because generated image current is proportional to charge state.[13] niECD allows *de novo* sequencing of acidic peptides that show improved ionization in negative mode compared with positive mode, e.g., peptides with biologically important PTMs such as phosphorylation and sulfation. Further, niECD is compatible with (but not limited to) singly-charged peptides, which allows coupling with MALDI. Gas-phase zwitterionic structures appear to play an important role in this novel MS/MS technique.

2.5 References

1. Cooper, H. J.; Hakansson, K.; Marshall, A. G. The role of electron capture dissociation in biomolecular analysis. *Mass Spectrom. Rev.* **2005**, *24*, 201-222.
2. Zubarev, R. A.; Kelleher, N. L.; McLafferty, F. W. Electron capture dissociation of multiply charged protein cations. A nonergodic process. *J. Am. Chem. Soc.* **1998**, *120*, 3265-3266.
3. Syka, J. E. P.; Coon, J. J.; Schroeder, M. J.; Shabanowitz, J.; Hunt, D. F. Peptide

and protein sequence analysis by electron transfer dissociation mass spectrometry. *Proc. Natl. Acad. Sci. U. S. A.* **2004**, *101*, 9528-9533.
4. Budnik, B. A.; Haselmann, K. F.; Zubarev, R. A. Electron detachment dissociation of peptide DI-ANIONS: an electron-hole recombination phenomenon. *Chem. Phys. Lett.* **2001**, *342*, 299-302.
5. Wolff, J. J.; Chi, L.; Linhardt, R. J.; Amster, I. J. Distinguishing glucuronic from iduronic acid in glycosaminoglycan tetrasaccharides by using electron detachment dissociation. *Anal. Chem.* **2007**, *79*, 2015-2022.
6. Yang, J.; Mo, J.; Adamson, J. T.; Hakansson, K. Characterization of oligodeoxynucleotides by electron detachment dissociation fourier transform ion cyclotron resonance mass spectrometry. *Anal. Chem.* **2005**, *77*, 1876-1882.
7. Kweon, H. K.; Hakansson, K. Metal oxide-based enrichment combined with gas-phase ion-electron reactions for improved mass spectrometric characterization of protein phosphorylation. *J. Proteome Res.* **2008**, *7*, 745-755.
8. Coon, J. J.; Shabanowitz, J.; Hunt, D. F.; Syka, J. E. P. Electron transfer dissociation of peptide anions. *J. Am. Soc. Mass Spectrom.* **2005**, *16*, 880-882.
9. Huzarska, M.; Ugalde, I.; Kaplan, D. A.; Hartmer, R.; Easterling, M. L.; Polfer, N. C. Negative electron transfer dissociation of deprotonated phosphopeptide anions: Choice of radical cation reagent and competition between electron and proton transfer. *Anal. Chem.* **2010**, *82*, 2873-2878.
10. Budnik, B. A.; Haselmann, K. F.; Elkin, Y. N.; Gorbach, V. I.; Zubarev, R. A. Applications of electron-ion dissociation reactions for analysis of polycationic chitooligosaccharides in fourier transform mass spectrometry. *Anal. Chem.* **2003**, *75*, 5994-6001.
11. Cody, R. B.; Freiser, B. S. Electron-impact excitation of ions from organics - alternative to collision-induced dissociation. *Anal. Chem.* **1979**, *51*, 547-551.
12. Kalli, A.; Grigorean, G.; Hakansson, K. Electron induced dissociation of singly deprotonated peptides. *J. Am. Soc. Mass Spectrom.* **2011**, *22*, 2209-2221.
13. Fung, Y. M. E.; Adams, C. M.; Zubarev, R. A. Electron ionization dissociation of singly and multiply charged peptides. *J. Am. Chem. Soc.* **2009**, *131*, 9977-9985.
14. Shi, S. D.-H.; Hemling, M. E.; Carr, S. A.; Horn, D. M.; Lindh, I.; McLafferty, F. W. Phosphopeptide/phosphoprotein mapping by electron capture dissociation mass spectrometry. *Anal. Chem.* **2001**, *73*, 19-22.
15. Stensballe, A.; Norregaard-Jensen, O.; Olsen, J. V.; Haselmann, K. F.; Zubarev, R. A. Electron capture dissociation of singly and multiply phosphorylated peptides. *Rapid Commun. Mass Spectrom.* **2000**, *14*, 1793-1800.
16. Hakansson, K.; Cooper, H. J.; Emmett, M. R.; Costello, C. E.; Marshall, A. G.; Nilsson, C. L. Electron capture dissociation and infrared multiphoton dissociation MS/MS of an N-glycosylated tryptic peptide yield complementary sequence information. *Anal. Chem.* **2001**, *73*, 4530-4536.
17. Mirgorodskaya, E.; Hassan, H.; Clausen, H.; Roepstorff, P. Mass spectrometric determination of o-glycosylation sites using beta-elimination and partial acid hydrolysis. *Anal. Chem.* **2001**, *73*, 1263-1269.
18. Witze, E. S.; Old, W. M.; Resing, K. A.; Ahn, N. G. Mapping protein post-translational modifications with mass spectrometry. *Nat. Methods* **2007**, *4*, 798-806.

19. Thompson, M. S.; Cui, W. D.; Reilly, J. P. Fragmentation of singly charged peptide ions by photodissociation at l = 157 nm. *Angew. Chem. Int. Ed.* **2004**, *43*, 4791-4794.
20. Kalcic, C. L.; Gunaratne, T. C.; Jonest, A. D.; Dantus, M.; Reid, G. E. Femtosecond laser-induced ionization/dissociation of protonated peptides. *J. Am. Chem. Soc.* **2009**, *131*, 940-942.
21. Polfer, N. C. Infrared multiple photon dissociation spectroscopy of trapped ions. *Chem. Soc. Rev.* **2011**, *40*, 2211-2221.
22. Brodbelt, J. S. Shedding light on the frontier of photodissociation. *J. Am. Soc. Mass Spectrom.* **2011**, *22*, 197-206.
23. Moon, J. H.; Yoon, S. H.; Kim, M. S. Photodissociation of singly protonated peptides at 193 nm investigated with tandem time-of-flight mass spectrometry. *Rapid Commun. Mass Spectrom.* **2005**, *19*, 3248-3252.
24. Good, D. M.; Wirtala, M.; McAlister, G. C.; Coon, J. J. Performance characteristics of electron transfer dissociation mass spectrometry. *Mol. Cell. Proteomics* **2007**, *6*, 1942-1951.
25. Kalli, A.; Hakansson, K. Comparison of the electron capture dissociation fragmentation behavior of doubly and triply protonated peptides from trypsin, GLU-C, and chymotrypsin digestion. *J. Proteome Res.* **2008**, *7*, 2834-2844.
26. Kalli, A.; Hakansson, K. Electron capture dissociation of highly charged proteolytic peptides from Lys N, Lys C and Glu C digestion. *Mol. Biosyst.* **2010**, *6*, 1668-1681.
27. Pitteri, S. J.; Chrisman, P. A.; Hogan, J. M.; McLuckey, S. A. Electron transfer ion/ion reactions in a three-dimensional quadrupole ion trap: Reactions of doubly and triply protonated peptides with SO2 center dot. *Anal. Chem.* **2005**, *77*, 1831-1839.
28. Liu, H.; Hakansson, K. Electron capture dissociation of tyrosine O-sulfated peptides complexed with divalent metal cations. *Anal. Chem.* **2006**, *78*, 7570-7576.
29. Medzihradszky, K. F.; Guan, S.; Maltby, D. A.; Burlingame, A. L. Sulfopeptide fragmentation in electron capture and electron transfer dissociation. *J. Am. Soc. Mass Spectrom.* **2007**, *18*, 1617-1624.
30. Neubauer, G.; Mann, M. Parent ion scans of large molecules. *J. Mass Spectrom.* **1997**, *32*, 94-98.
31. Huddleston, M. J.; Annan, R. S.; Bean, M. F.; Carr, S. A. Selective detection of phosphopeptides in complex mixtures by electrospray liquid chromatography mass spectrometry. *J. Am. Soc. Mass Spectrom.* **1993**, *4*, 710-717.
32. Bowie, J. H.; Brinkworth, C. S.; Dua, S. Collision-induced fragmentations of the (M-H)(-) parent anions of underivatized peptides: an aid to structure determination and some unusual negative ion cleavages. *Mass Spectrom. Rev.* **2002**, *21*, 87-107.
33. Misharin, A. S.; Silivra, O. A.; Kjeldsen, F.; Zubarev, R. A. Dissociation of peptide ions by fast atom bombardment in a quadrupole ion trap. *Rapid Commun. Mass Spectrom.* **2005**, *19*, 2163-2171.
34. Berkout, V. D. Fragmentation of singly protonated peptides via interaction with metastable rare gas atoms. *Anal. Chem.* **2009**, *81*, 725-731.

35. Cook, S. L.; Jackson, G. P. Metastable atom-activated dissociation mass spectrometry of phosphorylated and sulfonated peptides in negative ion mode. *J. Am. Soc. Mass Spectrom.* **2011**, *22*, 1088-1099.
36. Hartig, J.; Blom, M. N.; Hampe, O.; Kappes, M. M. Electron attachment to negative fullerene ions: a fourier transform mass spectrometric study. *Int. J. Mass Spectrom.* **2003**, *229*, 93-98.
37. Liu, B.; Hvelplund, P.; Nielsen, S. B.; Tomita, S. Formation of C-60(2-) dianions in collisions between C-60(-) and Na atoms. *Phys. Rev. Lett.* **2004**, *92*, 168301.
38. Boltalina, O. V.; Hvelplund, P.; Larsen, M. C.; Larsson, M. O. Electron capture by C60F35- in collisions with atomic and molecular targets. *Phys. Rev. Lett.* **1998**, *80*, 5101–5104.
39. Belyayev, M. A.; Cournoyer, J. J.; Lin, C.; O'Connor, P. B. The effect of radical trap moieties on electron capture dissociation spectra of substance P. *J. Am. Soc. Mass Spectrom.* **2006**, *17*, 1428-1436.
40. Yoo, H. J.; Wang, N.; Zhuang, S.; Song, H.; Hakansson, K. Negative-ion electron capture dissociation: radical-driven fragmentation of charge-increased gaseous peptide anions. *J. Am. Chem. Soc.* **2011**, *133*, 16790-16793.
41. Jones, A. W.; Mikhailov, V. A.; Iniesta, J.; Cooper, H. J. Electron capture dissociation mass spectrometry of tyrosine nitrated peptides. *J. Am. Soc. Mass Spectrom.* **2010**, *21*, 268-277.
42. Sohn, C. H.; Chung, C. K.; Yin, S.; Ramachandran, P.; Loo, J. A.; Beauchamp, J. Probing the mechanism of electron capture and electron transfer dissociation using tags with variable electron affinity. *J. Am. Chem. Soc.* **2009**, *131*, 5444-5459.
43. Bomse, D. S.; Woodin, R. L.; Beauchamp, J. L. Molecular activation with low-intensity cw infrared laser radiation - multiphoton dissociation of ions derived from diethyl ether. *J. Am. Chem. Soc.* **1979**, *101*, 5503-5512.
44. Manning, G.; Plowman, G. D.; Hunter, T.; Sudarsanam, S. Evolution of protein kinase signaling from yeast to man. *Trends Biochem. Sci* **2002**, *27*, 514-520.
45. Zhang, H.; Zha, X.; Tan, Y.; Hornbeck, P. V.; Mastrangelo, A. J.; Alessi, D. R.; Polakiewicz, R. D.; Comb, M. J. Phosphoprotein analysis using antibodies broadly reactive against phosphorylated motifs. *J. Biol. Chem.* **2002**, *277*, 39379-39387.
46. Kehoe, J. W.; Bertozzi, C. R. Tyrosine sulfation: A modulator of extracellular protein-protein interactions. *Chem. Biol.* **2000**, *7*, R57-R61.
47. Ishihama, Y.; Wei, F.-Y.; Aoshima, K.; Sato, T.; Kuromitsu, J.; Oda, Y. Enhancement of the efficiency of phosphoproteomic identification by removing phosphates after phosphopeptide enrichment. *J. Proteome Res.* **2007**, *6*, 1139-1144.
48. Marcantonio, M.; Trost, M.; Courcelles, M.; Desjardins, M.; Thibault, P. Combined enzymatic and data mining approaches for comprehensive phosphoproteome analyses application to cell signaling events of interferon-γ-stimulated macrophages. *Mol. Cell. Proteomics* **2008**, *7*, 645-660.
49. Gropengiesser, J.; Varadarajan, B. T.; Stephanowitz, H.; Krause, E. The relative influence of phosphorylation and methylation on responsiveness of peptides to MALDI and ESI mass spectrometry. *J. Mass Spectrom.* **2009**, *44*, 821-831.
50. Kjeldsen, F.; Giessing, A. M. B.; Ingrell, C. R.; Jensen, O. N. Peptide sequencing

and characterization of post-translational modifications by enhanced ion-charging and liquid chromatography electron-transfer dissociation tandem mass spectrometry. *Anal. Chem.* **2007**, *79*, 9243-9252.

51. Mikesh, L. M.; Ueberheide, B.; Chi, A.; Coon, J. J.; Syka, J. E.; Shabanowitz, J.; Hunt, D. F. The utility of ETD mass spectrometry in proteomic analysis. *Biochim. Biophys. Acta* **2006**, *1764*, 1811-1822.
52. Kweon, H. K.; Hakansson, K. Selective zirconium dioxide-based enrichment of phosphorylated peptides for mass spectrometric analysis. *Anal. Chem.* **2006**, *78*, 1743-1749.
53. Tsybin, Y. O.; Witt, M.; Baykut, G.; Kjeldsen, F.; Hakansson, P. Combined infrared multiphoton dissociation and electron capture dissociation with a hollow electron beam in fourier transform ion cyclotron resonance mass spectrometry. *Rapid Commun. Mass Spectrom.* **2003**, *17*, 1759-1768.
54. De Koning, L. J.; Nibbering, N. M. M.; Van Orden, S. L.; Laukien, F. H. Mass selection of ions in a fourier transform ion cyclotron resonance trap using correlated harmonic excitation fields (CHEF). *Int. J. Mass Spectrom.* **1997**, *165*, 209-219.
55. Senko, M. W.; Canterbury, J. D.; Guan, S.; Marshall, A. G. A high-performance modular data system for FT-ICR mass spectrometry. *Rapid Commun. Mass Spectrom.* **1996**, *10*, 1839-1844.
56. Ledford Jr, E. B.; Rempel, D. L.; Gross, M. Space charge effects in fourier transform mass spectrometry. II. mass calibration. *Anal. Chem.* **1984**, *56*, 2744-2748.
57. Kjeldsen, F.; Haselmann, K.; Budnik, B. A.; Jensen, F.; Zubarev, R. A. Dissociative capture of hot electrons by polypeptide polycations: An efficient process accompanied by secondary fragmentation. *Chem. Phys. Lett.* **2002**, *356*, 201-206.
58. Creese, A. J.; Cooper, H. J. The effect of phosphorylation on the electron capture dissociation of peptide ions. *J. Am. Soc. Mass Spectrom.* **2008**, *19*, 1263-1274.
59. Woods, A. S. The mighty arginine, the stable quaternary amines, the powerful aromatics, and the aggressive phosphate: Their role in the noncovalent minuet. *J. Proteome Res.* **2004**, *3*, 478-484.
60. Simons, J. Mechanisms for S-S and N-C-alpha bond cleavage in peptide ECD and ETD mass spectrometry. *Chem. Phys. Lett.* **2010**, *484*, 81-95.
61. Syrstad, E. A.; Turecek, F. Toward a general mechanism of electron capture dissociation. *J. Am. Soc. Mass Spectrom.* **2005**, *16*, 208-224.
62. Zubarev, R. A.; Kruger, N. A.; Fridriksson, E. K.; Lewis, M. A.; Horn, D. M.; Carpenter, B. K.; McLafferty, F. W. Electron capture dissociation of gaseous multiply-charged proteins is favored at disulfide bonds and other sites of high hydrogen atom affinity. *J. Am. Chem. Soc.* **1999**, *121*, 2857-2862.
63. Vasil'ev, Y. V.; Figard, B. J.; Morre, J.; Deinzer, M. L. Fragmentation of peptide negative molecular ions induced by resonance electron capture. *J. Chem. Phys.* **2009**, *131*, 044317.
64. Hakansson, K.; Emmett, M. R.; Hendrickson, C. L.; Marshall, A. G. High sensitivity electron capture dissociation tandem FT-ICR mass spectrometry of microelectrosprayed peptides. *Anal. Chem.* **2001**, *73*, 3605-3610.

65. Kjeldsen, F.; Horning, O. B.; Jensen, S. S.; Giessing, A. M. B.; Jensen, O. N. Towards liquid chromatography time-scale peptide sequencing and characterization of post-translational modifications in the negative ion-mode using electron detachment dissociation tandem mass spectrometry. *J. Am. Soc. Mass Spectrom.* **2008**, *19*, 1156-1162.

Chapter 3

Mechanistic Investigation of Negative Ion Electron Capture Dissociation (niECD)

3.1 Introduction

Electron irradiation has seen a surge of interest as an activation method in tandem mass spectrometry. An electron interacting with a molecular ion can trigger a range of reactions, depending upon the electron energy as well as the polarity of the precursor ion.[1-5] Amongst the several electron-based dissociation techniques in current use, electron capture dissociation (ECD), which involves attachment of low-energy electron (< 1 eV) to multiply-charged cations, has found the broadest applications in the structural analysis of biomolecules.[1, 6-8] In ECD, radical-driven fragmentation of charge-reduced peptide/protein cations yields N-C_α backbone bond cleavage and results in predictable $c'/z^\bullet$-type product ions without loss of labile posttranslational modifications (PTMs). In

parallel with the analytical applications of ECD, there has been much interest in studying its dissociation mechanism. There are two primary mechanisms proposed to explain the ECD outcome for peptides/proteins. In the hot hydrogen model, the electron is proposed to be captured at one of the protonated sites and H$^{\bullet}$ resulting from neutralization is released and recaptured by a nearby carbonyl oxygen atom, yielding an aminoketyl intermediate that dissociates via N-Cα backbone bond cleavage. In the amide-superbase model, it is argued that the electron is first captured in the remote-charge but Coulomb stabilized π* orbital of a backbone amide, generating an aminoketyl anion (a super base), which abstracts a nearby proton. The resulting aminoketyl radical undergoes facile cleavage of the adjacent N-Cα bond with a very low energy barrier.[9, 10]

Attachment of electrons to anions is counterintuitive due to Coulomb repulsion. However, as described in Chapter 2, such an intriguing phenomenon can indeed occur for both singly- and multiply-deprotonated anions within a rather narrow energy range. The resulting charge-*increased* radical intermediates further undergo extensive dissociation and we termed this exciting novel tandem mass spectrometric technique negative ion electron capture dissociation (niECD).[11] The fragmentation patterns observed in niECD of anions are analogous to those in conventional ECD of cations, with mainly *c* and *z*-type product ions for peptides and *d* and *w*-type product ions for oligonucleotides.[11, 12] Analogous to ECD, niECD is valuable for sequencing and characterizing PTMs because peptide fragments from niECD retain labile modifications. As shown in the previous chapter, this novel ion activation method appears particularly promising for analysis of acidic peptides, such as biologically important phospho- and sulfopeptides, which show improved ionization in negative ion mode and are still challenging to analyze with

currently available MS/MS techniques. In addition, the increased charge resulting from niECD improves signal-to-noise ratios in FT-ICR MS instruments because generated image current is proportional to charge state.[4] Furthermore, this feature allows higher fragmentation efficiencies than conventional ECD/ETD; in theory >100%, similar to electron ionization dissociation in which positive ions are further ionized to form more highly charged cationic intermediates.[4] Moreover, niECD is compatible with (but not limited to) singly-charged ions, thus allowing coupling with MALDI.

In summary, niECD shows promise for becoming a powerful MS/MS technique for biomolecular structural elucidation. However, the mechanism of this new technique requires additional investigation. Mechanistic knowledge of the niECD process is essential before it can be routinely applied and reach its full potential. Understanding the fragmentation mechanism also offers the opportunity to design derivatives that control gas-phase chemistry, leading to optimized fragmentation and/or wider application.[13, 14] In addition, gaseous anions exhibit different physics and chemistry compared with the same ions in solution. Fundamental studies of this new phenomenon may also generate novel insights into the gas-phase structures of biomolecular anions which are less understood compared with biomolecular cations. Preliminary data (see Chapter 2) have shown that niECD is not a universal reaction, i.e., there were a number of unmodified peptides that could not undergo niECD. A zwitterion mechanism for niECD was proposed in the previous chapter, stating that zwitterionic gas-phase structures may be necessary for successful niECD with electron capture either occurring at, or being directed by, the positively-charged site. This hypothesis is based on the observation that all the peptides failing to capture an electron lack either strongly basic or strongly acidic

residues in their sequences, and thus they are less likely to form gas-phase zwitterionic structures. In addition, for phosphopeptides, which undergo efficient niECD (see Chapter 2), it has been suggested that they exist as salt-bridged zwitterions in the gas phase.[15, 16] The striking similarity observed between niECD and positive ion mode ECD further indicates that the mechanism of niECD is related to that of ECD[9, 10, 17] and, thus, positively charged sites may play a role in niECD. Furthermore, recent computational work proposes that singly-deprotonated angiotensin II is zwitterionic in the gas phase.[18]

In this Chapter, the presented research strives to verify the zwitterion hypothesis described above and to further explore the fundamental aspects of niECD. In order to test this hypothesis, two different strategies were applied to alter the peptide structures: inhibition of zwitterion formation for peptides that underwent facile niECD, and enhancement of the probability for zwitterion formation for peptides that did not capture an electron. Inhibition of gas-phase zwitterions was realized by removing potential protonation sites, e.g., the peptide N-terminal amine, or deprotonation sites, e.g., phosphate and sulfate groups in phospho- and sulfopeptides. By contrast, gas-phase zwitterionic structures were promoted by chemical derivatization techniques that introduce positive charge-carrying or highly basic groups into the molecules. Fixed charge derivatives have been frequently utilized in mass spectrometry research to improve peptide/protein sequencing and to explore the mechanisms of several fragmentation techniques.[19-22] Various positive charge tags, such as tris (2,4,6-trimethoxyphenyl)phosphonium (TMPP),[19, 20, 23, 24] 2,4,6-trimethylpyridinium,[25, 26] 2,2′-bipyridyl[27], and trimethylammoniumalkyl,[28-30] have been implemented based on their chemical availability or synthetic convenience. With the addition of these tags, cationic

charges are affixed to the peptides at specific sites. Consequently, in order to be detected in negative ion mode, peptides have to become zwitterions. Enhancing zwitterion formation can also be achieved by introducing readily chargeable groups into the peptides, such as the basic guanidino group by various guanidination strategies.[31-35] The niECD fragmentation patterns of unmodified analytes and their derivatized counterparts were then compared.

In addition to chemical labeling techniques, a more systematic approach to probe the niECD mechanism is to synthesize one or more sets of peptides with decreased (or increased) zwitterion probabilities. Herein, niECD measurements were performed on five sets of synthetic peptides with defined sequences to further illuminate the mechanism of this process.

3.2 Experimental

3.2.1 Reagents

Sulfated cholecystokinin (CCKS, H-DsYMGWMDF-NH_2) was purchased from Advanced Chemtech (Louisville, NY). Other peptides used, cholecystokinin (CCK, H-DYMGWMDF-NH_2), substance P-OH (H-RPKPQQFFGLM-OH), phosphopeptide H-KRSpYEEHIP-OH, were from Sigma-Aldrich (St. Louis, MO). The oligosaccharide, disialyl-lacto-N-tetraose (DSLNT), was purchased from V-labs Inc (Covington, LA). Acetic anhydride, barium dioxide ($Ba(OH)_2$), 12.5% (w/v) aqueous trimethylamine solution, iodoacetic anhydride, Girard's T reagent (1-(hydrazinocarbonyl-methyl) trimethylammonium chloride), *S*-methylisothiourea hemisulfate were obtained from Sigma-Aldrich (St. Louis, MO). DABCO (1,4-diazabicyclo[2.2.2]octane)-based *N*-

hydroxysuccinimide (NHS) ester reagent was a generous gift from Dr. Philip Andrews' lab at the University of Michigan. Synthetic peptides were purchased from GenicBio (Shanghai, China).

3.2.2 Sample Preparation

Acetylation

The sulfopeptide CCKS was N-terminally acetylated according to previously published procedures.[36] 200 μL of 25% acetic anhydride in methanol was incubated with 50 μL peptide solution in water for 3 h at room temperature.

Solution-phase Dephosphorylation

3 μL saturated $Ba(OH)_2$ was added to 10 μL of 200 μM phosphopeptide. Next 6 μL water was added and the mixture was then heated to 37 °C for 2 h.

Fixed-charge Derivatization

Trimethylammoniumacetyl (TMAA) derivatization of peptides was performed following the method of Stults and Wetzel.[29] One μL of 40 mM peptide solution was combined with 12 μL of 0.30 M MES buffer (pH 6.0). The mixture was chilled in an ice bath and 5 μL of 0.01 M iodoacetic anhydride in dry THF was injected. The solution was immediately vortexed for 1 min. The tube was returned to the ice bath for another 5 min and then allowed to equilibrate to room temperature for 2-3 min. 5 μL of 12.5% (w/v) aqueous trimethylamine was then immediately added to this solution of iodoacetyl peptide. The mixture was vortexed and the reaction was allowed to proceed for 2 h at 37 °C. During this period, the tube was vortexed every 30 min to ensure adequate mixing.

DABCO-based NHS-ester was incubated with peptides at 5:1 molar ratio in HEPES buffer (pH=7) at room temperature for 20 min.

Girard's T reagent was used to derivatize the model oligosaccharide as described in the previous report by Unterieser and Mischnick.[37] The Girard's T solution was prepared by dissolving 20 μmol Girard's T reagent in 350 μL MeOH and 150 μL acetic acid, and then added to 500 μL aqueous solution of 10 μmol DSLNT. The reaction was performed for 30 min at 40 °C.

Guanidination

N-terminal guanidination reactions were carried out as previously described[38] with some modifications. 1 M *S*-methylisothiourea hemisulfate in 6% NH_4OH (v/v) was combined with 200 μM peptide in 1:1 ratio (v/v) at 65 ℃ for 1 h. The pH was adjusted to 10.5. The mixture was incubated at 65 ℃ for 1 h.

After the reactions, the solvents were removed under vaccum. All the derivatized as well as the synthetic peptides were purified using C18 microtips (Millipore, Billerica, MA). The derivatized DSLNT was purified using graphitized carbon solid-phase extraction (SPE) cartridges (Supelco, Bellefonte, PA). All the samples were dissolved in 1:1 isopropanol/water (v/v) with 0.1% triethylamine for negative ion mode analysis.

3.2.3 FT-ICR Mass Spectrometry

The samples were directly infused via an external Apollo II electrospray ion source (Bruker Daltonics, Billerica, MA) at a flow rate of 70 μL/h in negative ion mode. All experiments were performed with an actively shielded 7 Tesla hybrid quadrupole (Q)-FT-ICR mass spectrometer (APEX-Q, Bruker Daltonics), as previously described.[39] Briefly, ions produced by ESI were accumulated in the first hexapole for 0.05 s, mass-selectively accumulated in the second hexapole collision cell for 0.5-4 s, transferred through high voltage ion optics, and captured in an Infinity ICR cell by dynamic trapping. This

accumulation sequence was looped one to three times to improve precursor ion abundance. For MS/MS experiments, mass-selective external accumulation of negatively-charged precursor ions was performed. For negative ion electron capture dissociation (niECD), the electrons were provided by an indirectly heated hollow dispenser cathode.[40] The cathode heating current was kept at 1.8 A, and the cathode voltage was pulsed to a bias voltage of – 6 V (corresponding to 4.5 eV electrons) for 5-20 s. A lens electrode located in front of the hollow cathode was kept 1.0–1.5 V more positive than the cathode bias voltage. For nozzle-skimmer dissociation, the voltage of skimmer 1 was increased to 120 V to cleave the phosphate or sulfate group (corresponding to phosphoric acid and sulfonate loss, respectively).

3.2.4 Data Analysis

All mass spectra were acquired with XMASS software (version 6.1, Bruker Daltonics) in broadband mode from m/z 200 to 3000 with 256K data points and summed over 10-32 scans. Data processing was performed with the MIDAS analysis software.[41] Data were zero filled once, Hanning apodized, and exported to Microsoft Excel for internal frequency-to-mass calibration with a two-term calibration equation.[42] Typically, internal calibration was performed with precursor ions and their electron-capture species as calibrants. Peaks in MS^n were assigned within 10 ppm error after internal calibration. Product ions were not assigned unless the S/N ratio was at least 3.

3.3 Results and Discussion

3.3.1 Peptide N-terminal Acetylation

Peptide N-terminal acetylation was performed with the goal to prevent peptides with no other basic sites from becoming zwitterionic anions in the gas phase. In this reaction, the potential protonation site at the N-terminal amine is blocked by an acetyl group, thus in theory reducing the probability of gas-phase protonation, required for zwitterion formation in negative ion mode. The tyrosine-sulfated peptide cholecystokinin (CCKS), which typically undergoes favorable niECD, was chosen as a model peptide. Figure 3.1 compares niECD of unmodified and N-terminally acetylated CCKS. As expected, unmodified CCKS demonstrated highly favorable niECD with a fragmentation efficiency of 44%, as shown in Figure 3.1(a). This sulfopeptide does not contain any basic residues. Thus, the most basic site is the N-terminus and zwitterion formation should be less favorable upon acetylation. Consistently, in Figure 3.1(b), niECD efficiency of N-terminally acetylated CCKS was significantly lower (6%) than that of unmodified CCKS. However, electron capture and fragmentation still occurred for the acetylated species, possibly due to protonation of the tryptophan residue.

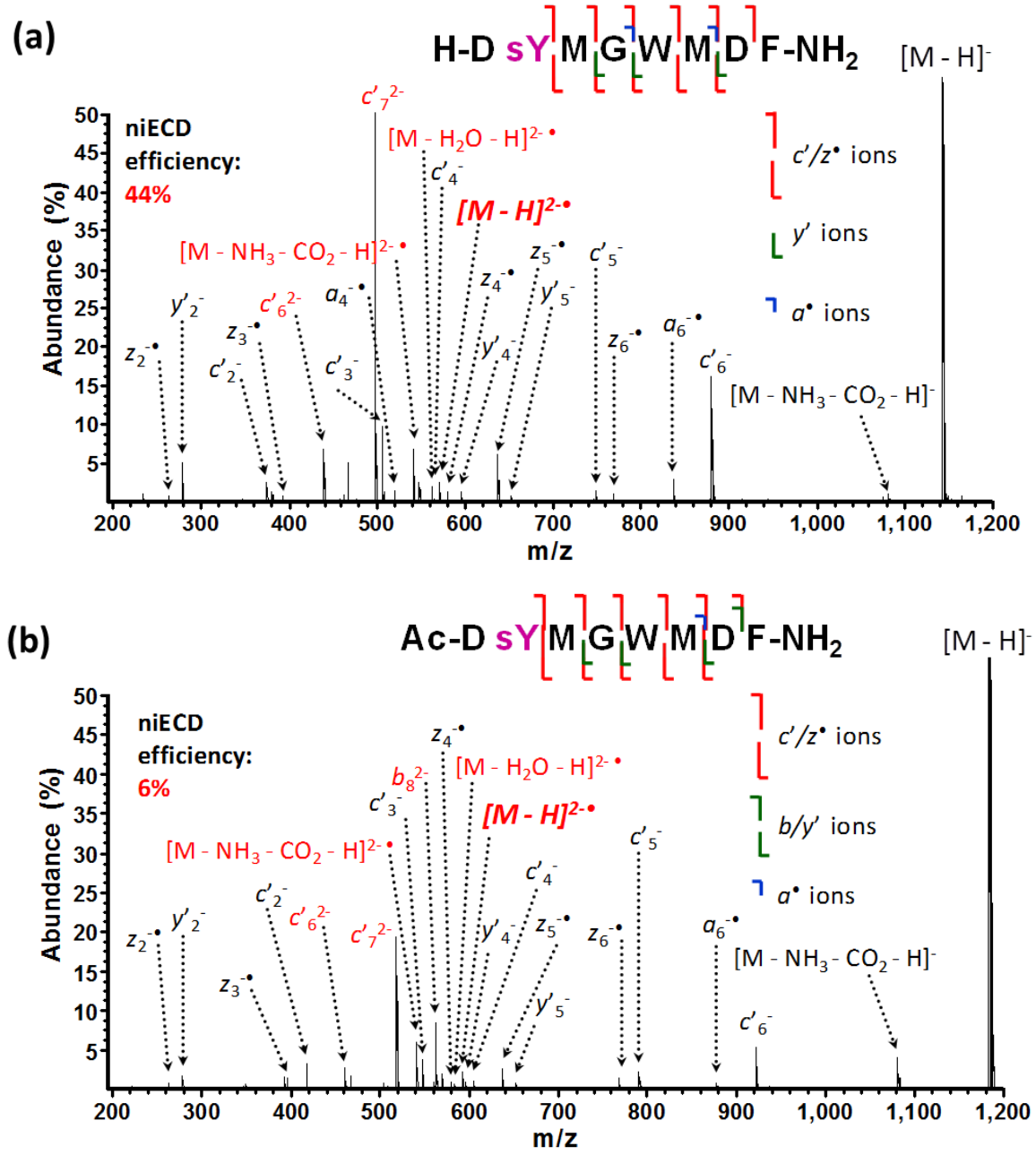

Figure 3.1. (a) niECD of sulfated cholecystokinin (CCKS; ~4.5 eV electrons, 20 s, 10 scans). (b) niECD of N-terminally acetylated CCKS under identical conditions as in (a). Charge-increased product/precursor ions are marked in red. ν_3 = third harmonic.

3.3.2 Peptide Dephosphorylation/Desulfation

Because all the phospho- and sulfopeptides studied in Chapter 2 showed extensive fragmentation in niECD, the effects of the presence of phosphate and sulfate groups were

also investigated. Intriguingly, the non-sulfated version of CCKS (CCK) did not undergo niECD at all (Figure 3.3(a)). Gas-phase desulfation of CCKS via nozzle-skimmer dissociation inside the electrospray ion source eliminated the occurrence of electron capture by the resulting CCK-like peptide as well (data not shown). Phosphopeptides were also examined and one example is shown in Figure 3.2. Irradiation with 4.5 eV electrons was performed for this phosphorylated peptide, resulting in successful electron capture and a series of *c*- and *z*-type backbone fragments from niECD, as demonstrated in Figure 3.2(a). Similar to desulfation, dephosphorylation in the gas phase (Figure 3.2(b), by nozzle skimmer dissociation), or in the solution phase (Figure 3.2(c), by reacting with saturated $Ba(OH)_2$ causing β-elimination of the phosphate group) decreased niECD efficiency. The absence of electron capture, or poorer niECD performance, upon desulfation and dephosphorylation are likely caused by the decreased zwitterion propensity following removal of potential deprotonation sites, corresponding to the acidic phosphate and sulfate groups. This observation is also consistent with the fact that phosphopeptides likely exist as zwitterions in the gas phase.[15, 16]

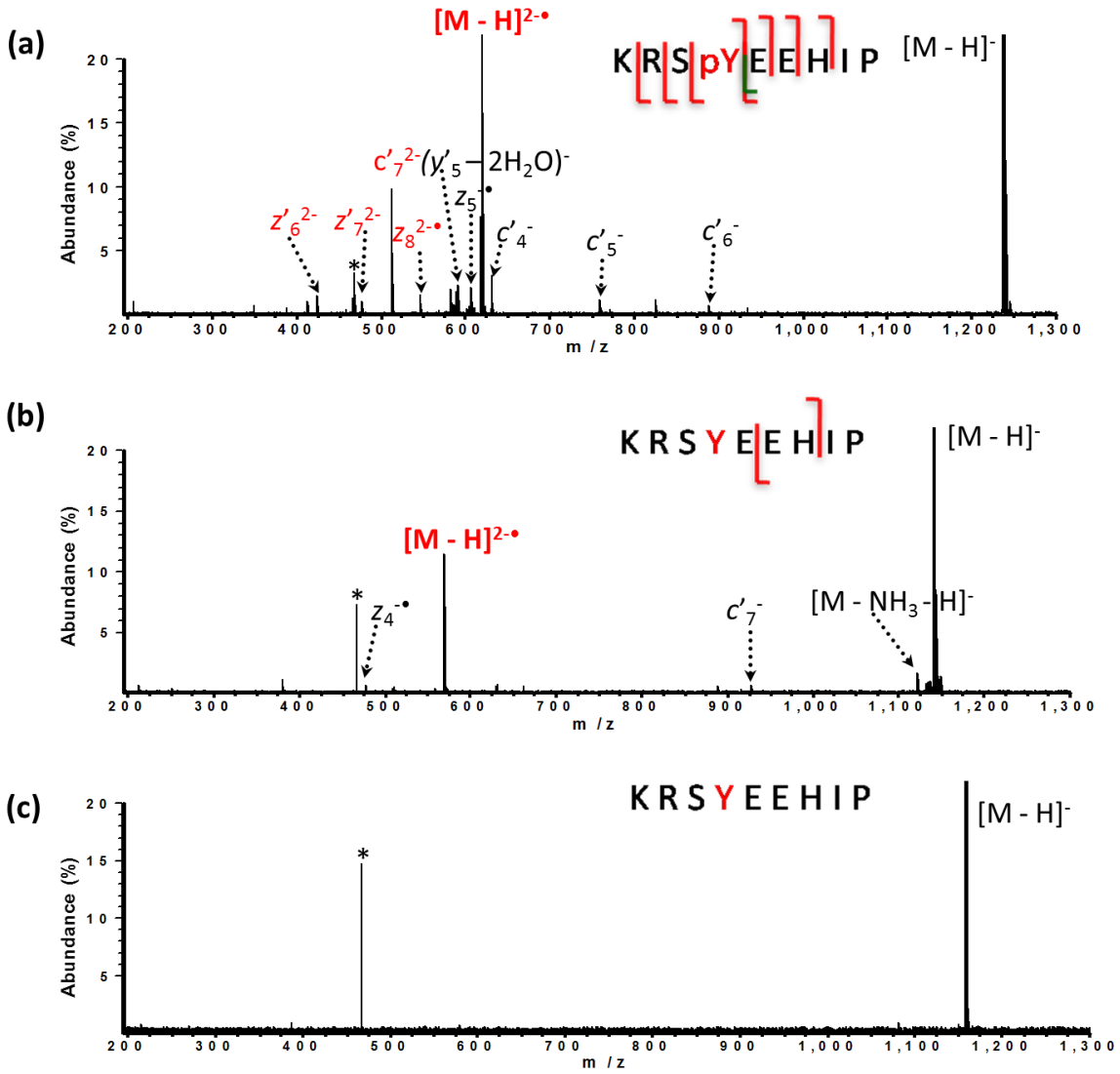

Figure 3.2. Dephosphorylation of a tyrosine-phosphorylated peptide. (A) niECD of the singly deprotonated phosphopeptide. (B) niECD of gas-phase dephosphorylated peptide (phosphate group was removed via in source nozzle-skimmer dissociation followed by quadrupole isolation). (C) niECD of solution-phase dephosphorylated peptide (phosphate group was removed by reacting with saturated $Ba(OH)_2$). All the three niECD experiments were performed with 4.5 eV electrons for 10 s and accumulated for 10 scans. * represents electronic noise.

3.3.3 Peptide Fixed-Positive Charge Derivatization

An alternative approach to examine the zwitterion mechanism is to promote zwitterion formation for peptides that failed to capture an electron. This may be achieved

by attaching a fixed positive charge to the peptides via charge-containing tags. The first fixed-charge tag explored is trimethylammoniumacetyl (TMAA), which contains a positive quaternary group adjacent to three methyl groups. TMMA was placed onto the peptide *N*-terminus through iodoacetylation of the N-terminal amine, followed by further reaction with trimethylamine to produce a quaternary ammonium-derivatized molecule. The TMAA structure as well as the full mass spectrum of the derivatization mixture is shown in Figure 3.3(b). The singly-charged peptide anion carrying a TMAA group, needs to have at least two deprotonation sites. Thus, addition of a permanent cationic charge forces the peptide to form a gas-phase zwitterion. TMAA-modified CCK was isolated and subjected to niECD, as illustrated in Figure 3.3(c). As discussed above, niECD of non-sulfated CCKS (CCK) was not successful. However, introduction of the TMAA tag did enable niECD of CCK. A charge-increased electron capture species, a number of charge-increased product ions as well as a c_5 sequence ion were present in the spectrum. The TMAA derivative was also evaluated with another model peptide, Substance P-OH, which was also unable to undergo electron capture in its unmodified form (Figure 3.4(a)). The niECD spectrum of TMAA-modified Substance P-OH is shown in Figure 3.4(b): quaternary ammonium derivatization also rescued its niECD ability. An abundant charge-increased electron capture signal and two backbone fragments resulting from N-Cα bond cleavages were observed in niECD of TMAA-Substance P-OH. However, for both CCK and Substance P—OH, the presence of the fixed-charge site altered the fragmentation behavior with the dominant pathway corresponding to loss of the tag (trimethylamine), similar to the reported fragmentation behavior of fixed charge-containing peptides in conventional ECD/ETD.[20, 21, 26, 43]

(a) Underivatized CCK:
DYMGWMDF-NH_2

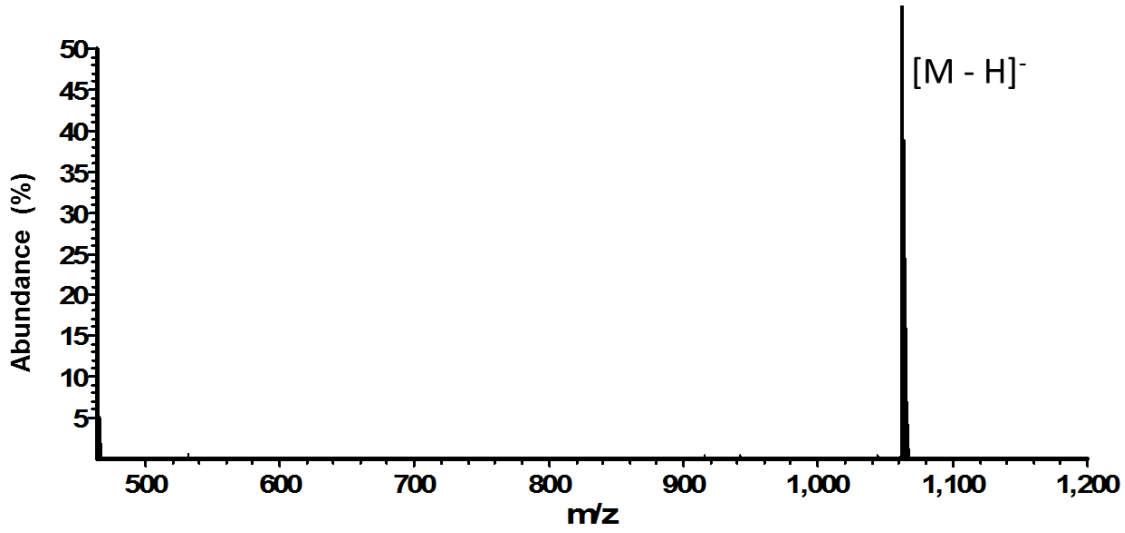

(b) $(CH_3)_3\overset{+}{N}$-CH_2-CO-

Trimethylammoniumacetyl (TMAA)

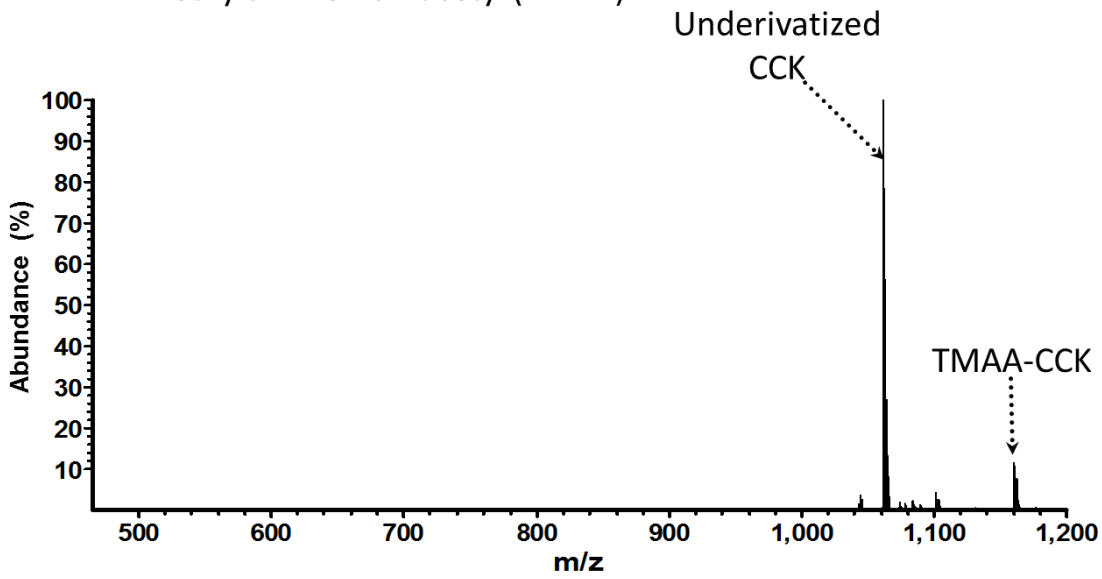

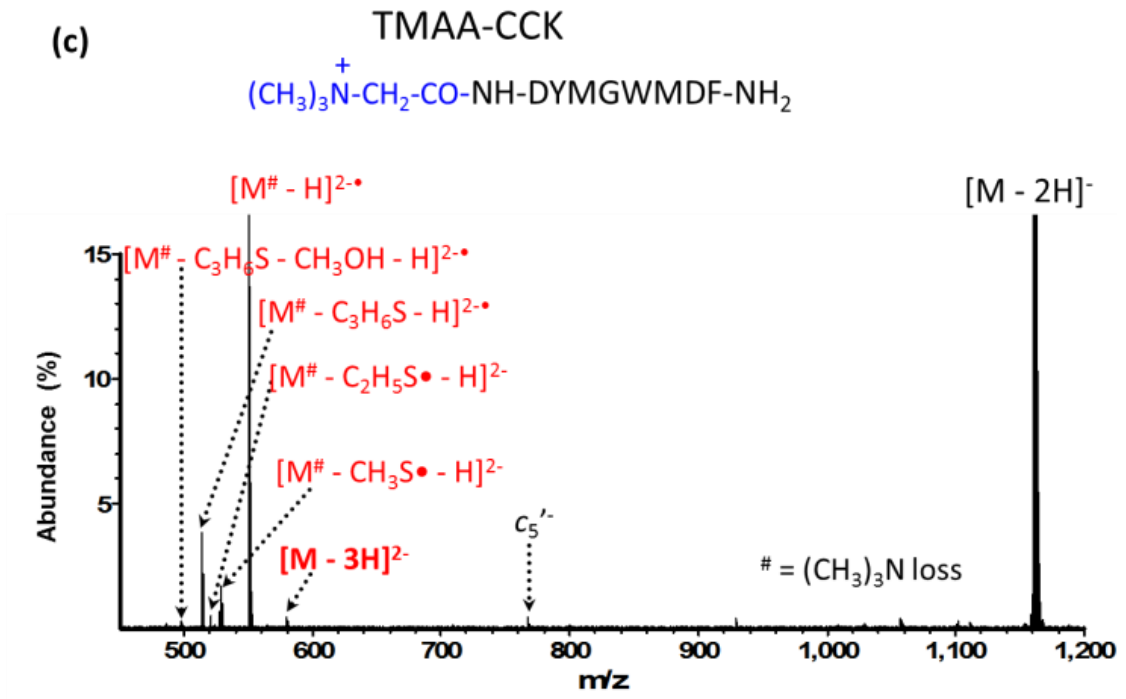

Figure 3.3. A trimethylammoniumacetyl (TMAA) group was attached to the *N*-terminus of the peptide CCK to introduce a fixed positive charge. (a) niECD MS/MS of underivatized CCK (4.5 eV electrons, 20 s, 32 scans). No electron capture was observed. (b) Negative ion mode MS of the reaction mixture after derivatization (10 scans). (c) niECD MS/MS of isolated CCK derivatized by the TMAA tag (4.5 eV electrons, 10 s, 32 scans). Charge-increased product ions are high-lighted in red.

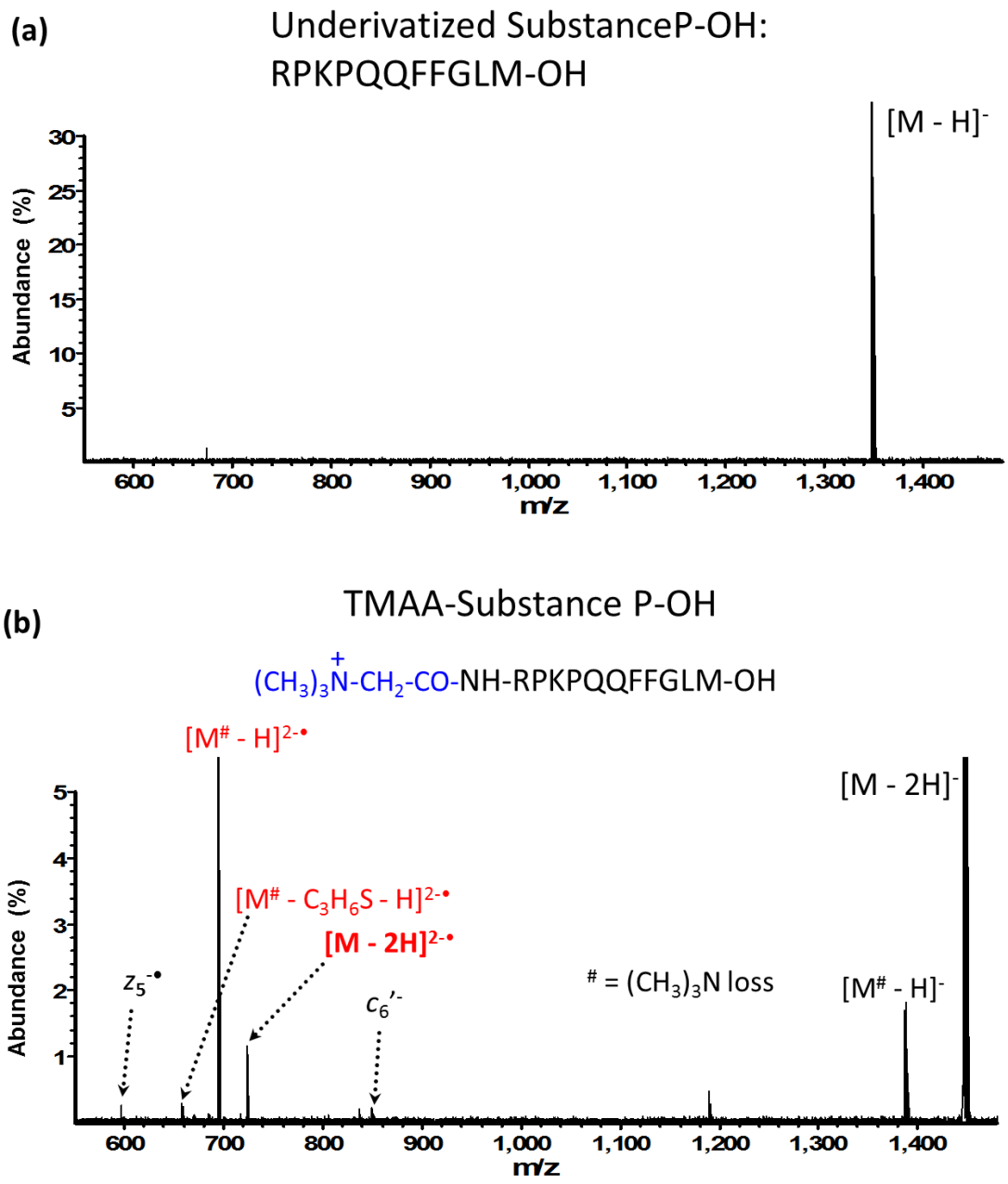

Figure 3.4. Electron irradiation (4.5 eV, 10 s, 32 scans) of substance P-OH without (top) and with (bottom) an N-terminal TMAA fixed-charge tag. The underivatized peptide did not undergo niECD whereas the presence of the tag allowed electron capture and detection of *c*′/*z*•-type ions. Similar to TMAA-derivatized CCK (Figure 3.3(c)), trimethylamine loss is dominant.

We also investigated a second charge-providing tag: another quaternary amine tag but including two intrinsic positive charges in its 1,4-diazabicyclo[2.2.2]octane (DABCO) moiety. The structure of the DABCO-based *N*-hydroxysuccinimide (NHS) ester reagent

is provided in Figure 3.5(a). It specifically reacts with primary amines and was synthesized by Dr. Philip Andrews' group as part of an effective MS-cleavable crosslinking reagent.[44] The DABCO-labeled CCK anion was subjected to niECD, as shown in Figure 3.5(b). In this case, in order to obtain a net charge of -1, the precursor ion has to have three deprotonation sites. Similar to the TMAA tag, the DABCO group allowed electron capture by CCK. However, the major dissociation pathway in niECD was again the elimination of part, or all, of the derivative moiety. No backbone fragmentation was observed, leading to no information regarding the peptide sequence. For the second model peptide, substance P-OH, detection of its DABCO derivative in negative ion mode was unsuccessful, probably because of the much lower acidity of this peptide and thus difficulty to introduce three negative charges.

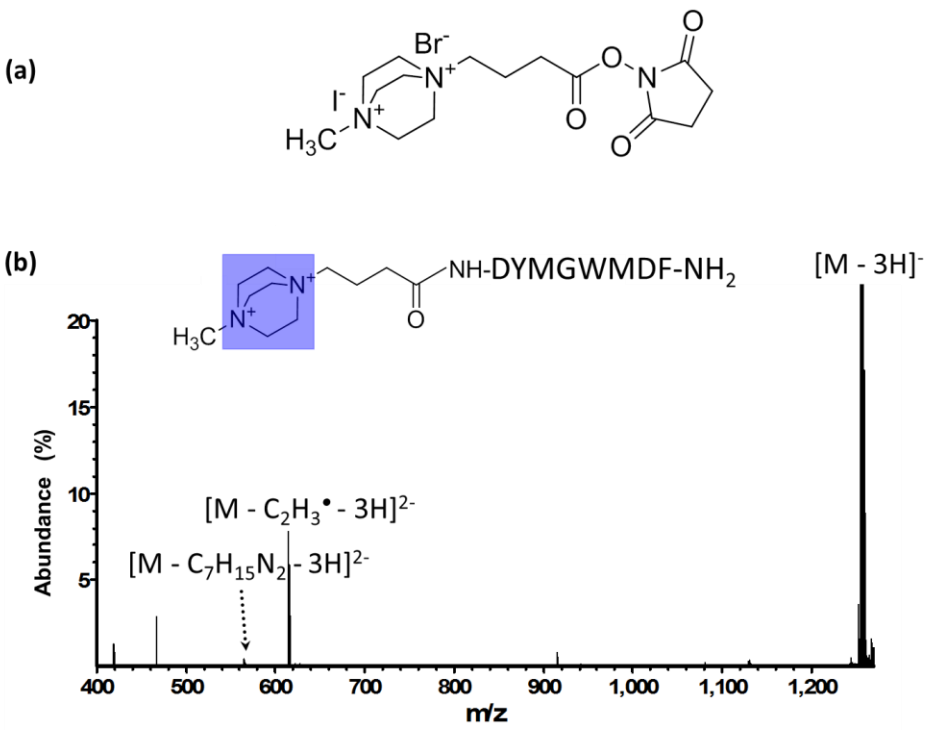

Figure 3.5. (a) Structure of the DABCO-based NHS ester reagent. (b) niECD (4.5 eV, 5 s, 32 scans) of DABCO-modified CCK. The DABCO ring is high-lighted in blue. Partial and entire tag losses were the major product ions.

It is interesting to note that addition of metal ions (Na^+, Ca^{2+}, and Cs^+), which may promote zwitterion formation,[45] did not enable electron capture by CCK (Figure 3.6). Neither did N-terminal tris(2,4,6-trimethoxyphenyl) phosphonium-acetyl (TMPP) derivatization,[11] which introduces a different type of fixed charge, a positive quaternary phosphonium, to the peptide (Figure 3.7). The lack of success for TMPP-Ac derivatization, or metal adduction, may be explained by effective shielding of the positively-charged site by the aromatic groups surrounding the phosphonium, or by the peptide carbonyls wrapping around the metal ion.

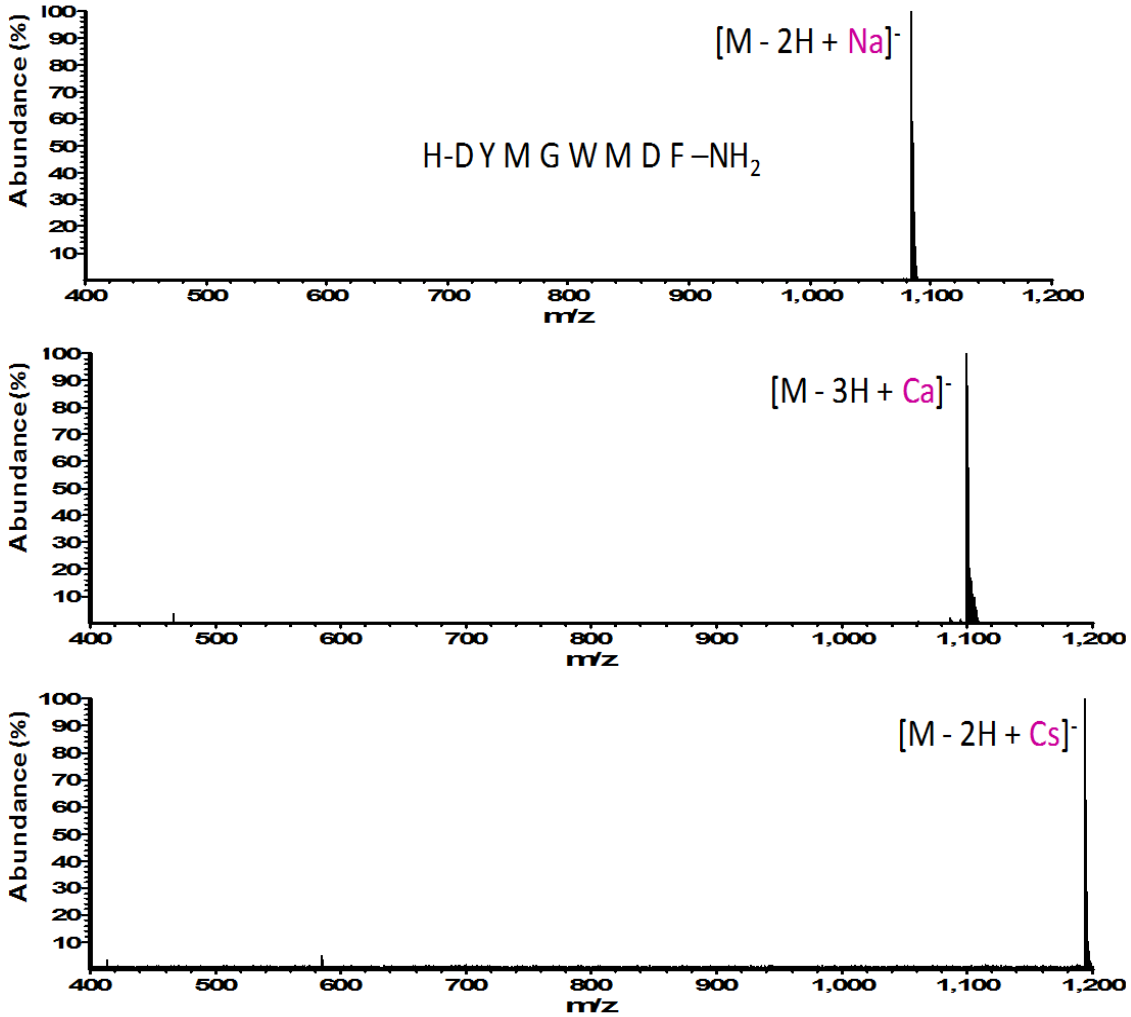

Figure 3.6. Electron irradiation (4.5 eV, 20 s, 10 scans) of metal-adducted CCK. None of the metal complexes underwent niECD.

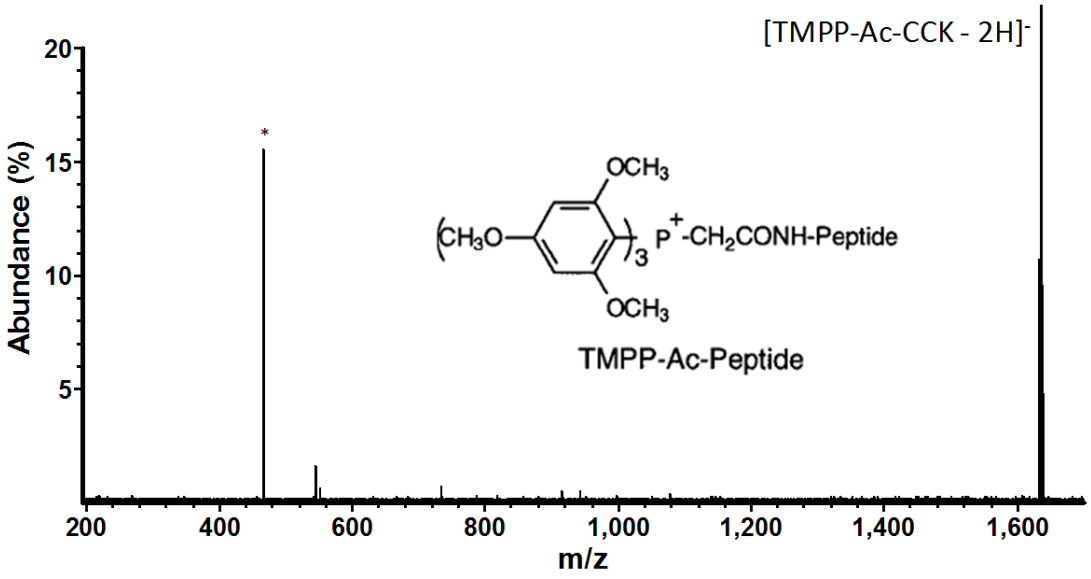

Figure 3.7. Electron irradiation (4.5 eV, 10 s, 10 scans) of tris(2,4,6-trimethoxyphenyl)phosphonium-acetyl (TMPP-Ac)-CCK (see inset for structure). No electron capture was observed.

3.3.4 Oligosaccharide Fixed-Positive Charge Derivatization

Oligosaccharides are particularly challenging to analyze by MS due to their non-linear structures. In addition, they typically lack basic sites and can therefore be difficult to ionize in positive ion mode, particularly for sulfated and sialylated species. Both ECD[46, 47] and EDD[48] have been shown to generate extensive cross-ring cleavages for oligosaccharides, necessary to determine carbohydrate linkage information. However, smaller glycans, particularly *O*-glycans, are difficult to multiply charge. Electron induced dissociation and vacuum ultraviolet photodissociation, which are compatible with singly-charged ions, are being explored as alternative strategies.[49, 50] niECD could fill a need here as well, particularly for acidic carbohydrates, including sialylated and sulfated species, which are known to be altered in cancer.[51-57]

The first attempt to apply niECD towards carbohydrate analysis failed. A branched doubly-sialylated oligosaccharide, disialyl-lacto-N-tetraose (DSLNT), was chosen as a model molecule because it contains two acidic sialic acid residues and should readily get deprotonated in negative ion mode. A diagram depicting the DSLNT structure is shown in the inset of Figure 3.8(a). niECD was applied towards the carbohydrate with and without metal adduction. However, neither form of the DSLNT anion captured an electron (data not shown). If the zwitterion hypothesis is valid, the absence of such a gas-phase structure may explain why niECD was not observed. This oligosaccharide includes two deprotonation sites but lacks a favorable protonation site, and thus has a smaller probability of becoming a zwitterion. In order to overcome this problem, chemical derivatization with Girard's T reagent was performed to enhance the generation of a gas-phase zwitterionic structure. This reagent carries a hydrazide functionality that allows glycan-specific modification and introduces a fixed cationic charge (a quaternary amine center) to the reducing terminus of the glycan (Scheme 3.1). Girard's T derivatization has been reported in many mass spectrometric applications of oligosaccharides to facilitate their ionization, fragmentation and/or quantification.[50, 58, 59] A negative ion ESI-FT-ICR mass spectrum of the reaction mixture with Girard's T and DSLNT is shown in Figure 3.8(a), where the unreacted substrate peak was not observed and thus the DSLNT was converted to its Girard's T derivative at high yield. The niECD fragmentation pattern of Girard's T-treated DSLNT is shown in Figure 3.8(b). As expected, the modified carbohydrate captured an electron very efficiently. However, the dissociation pattern is again not that analytically informative. Pronounced neutral tag loss and several B, C, Y, Z glycosidic fragments, which correspond to terminal sialic acid

loss, were produced. These cleavages are typical for CAD and may result from excess vibrational energy in niECD. Cross-ring fragments did not appear in the spectrum.

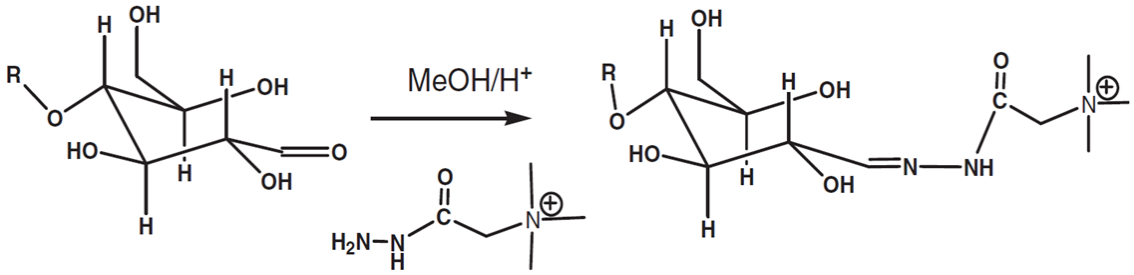

Scheme 3.1. Schematic representation of oligosaccharide reaction with Girard's T reagent (adapted from reference[50]).

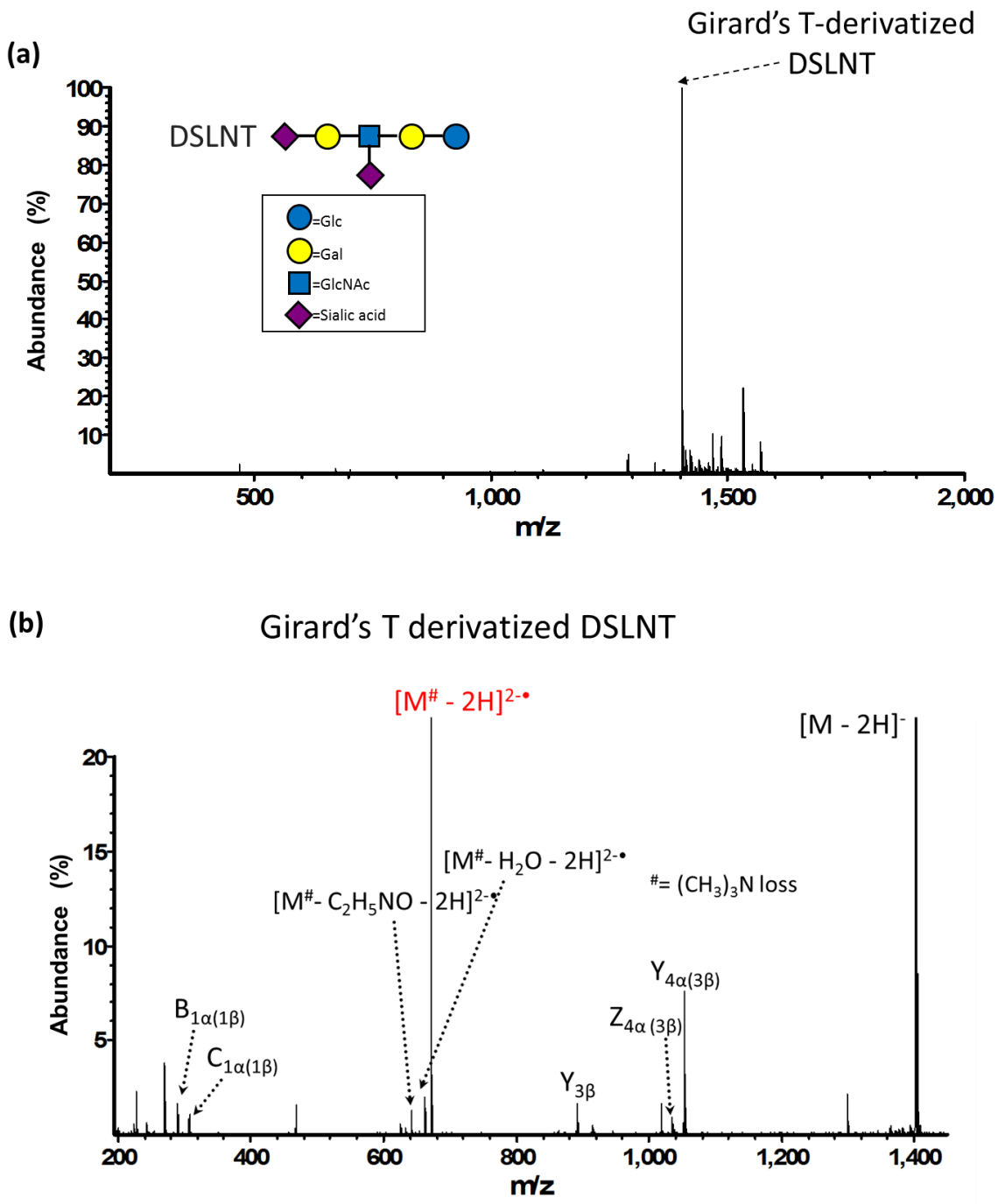

Figure 3.8. The oligosaccharide DSLNT was derivatized by Girard's T reagent. (a) Full mass scan in negative ion mode of the derivatization mixture (10 scans). (b) niECD (4.5 eV, 10 s, 32 scans) of Girard's T-modified DSLNT. The charge-increased electron capture species is marked in red. The letter α refers to the largest branch and the letter β represents the second largest branch of DSLNT.

3.3.5 Peptide Guanidination

Due to the prominent tag loss observed in niECD of fixed charge-tagged peptides, an alternative derivatization method that incorporates a group with high basicity rather than a permanent charge was pursued. Guanidination reaction is a common peptide modification process used to improve the signal intensity of lysine-containing peptides in MALDI, assist peptide sequencing and identification, or enable peptide quantification.[31, 34, 38, 60] In guanidination, the ε-amino groups of lysine residues are converted to guanidino groups, thereby creating more basic homoarginine residues. A similar strategy was adapted here to increase N-terminal basicity by converting the α-amino group to a guanidino group. This change in basicity should enhance N-terminal protonation and thus increase the probability of zwitterion formation. The same model peptide as investigated above, CCK, was examined. As shown in Figure 3.9, electron capture was successfully observed for the guanidinated precursor ion, producing a charge-increased radical intermediate, one *c*-, one *z*-, and one *y*-type backbone fragment. No tag loss was detected. Although relatively more structural information was obtained in this case compared with the above fixed charge-derivatized CCK experiments, the niECD fragmentation efficiency of guanidinated CCK is quite low. This low efficiency is due to the highly inefficient process of N-terminal guanidination, consequently resulting in low precursor ion abundance. Low reaction yield is consistent with previous reports on this modification chemistry.[61, 62] The guanidination reaction specifically targets the ε-amine of lysines, which are less sterically hindered than α-amines of peptide N-termini. Critical factors that affect derivatization efficiency in this reaction, including pH, methylisourea concentration and temperature,[33] were all optimized, but no substantial improvement

was achieved.

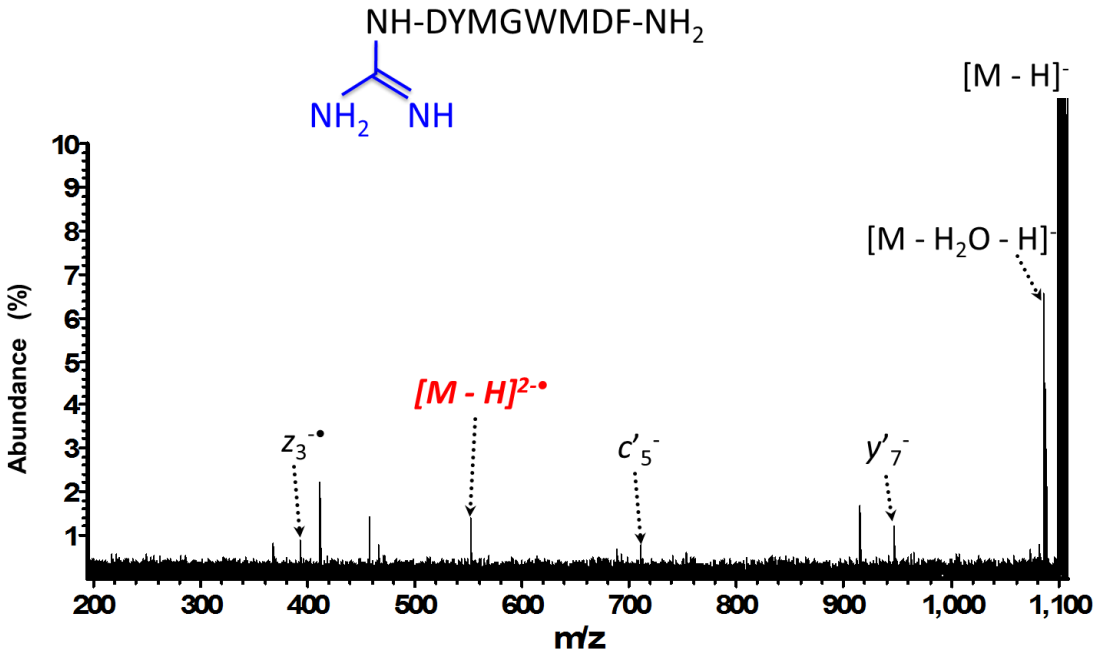

Figure 3.9. niECD (4.5 eV, 32 scans, 5 s irradiation) spectrum of the N-terminally guanidinated peptide CCK. The charge-increased radical is high-lighted in red and several backbone fragments were produced.

3.3.6 Synthetic Peptides

One problem with the natural peptides investigated to date is that they frequently have multiple possible protonation and deprotonation sites. For example, the sulfopeptide CCKS (H-DsYMGWMDF-NH_2), which undergoes highly favorable niECD, has two aspartic acid residues and one sulfate group as likely deprotonation sites and the N-terminus as a likely protonation site. Prediction of the number of gas-phase charged sites (positive and negative) and their location is highly challenging. In order to examine the mechanism more systematically, niECD was applied to several series of synthetic peptides in which the number and positions of charges could be controlled. Peptides were carefully designed around the sequence of the sulfopeptide hirudin (which

undergoes highly efficient niECD). The peptide lengths were chosen so that electron capture will not be disfavored due to excessive increase in charge density upon electron attachment. Five sets of peptides were synthesized and their sequences are listed in Table 3.1.

(a)

1st	Peptide Sequence
P1	DFEEIPEEYLQ
P2	DFYEIPEEYLQ
P3	DFYEIPLEYLQ
P4	DFYLIPLEYLQ
P5	YFYLIPLEYLQ
P6	YFYLIPLSYLQ

(b)

2nd	Peptide Sequence
P7	DFEEIPEEYLK
P8	DFYEIPEEYLK
P9	DFYEIPLEYLK
P10	DFYLIPLEYLK
P11	YFYLIPLEYLK
P12	YFYLIPLSYLK

(c)

3rd	Peptide Sequence
P13	KLFIDYEEPEE
P14	KLFIDYEEPEY
P15	KLFIDYELPEY
P16	KLFIDYLLPEY
P17	KLFIYYLLPEY
P18	KLFIYYLLPSY

(d)

4th	Peptide Sequence
P19	DFEEIPEEYLK*
P20	DFYEIPEEYLK*
P21	DFYEIPLEYLK*
P22	DFYLIPLEYLK*
P23	YFYLIPLEYLK*
P24	YFYLIPLSYLK*

(e)

5th	Peptide Sequence
P25	K*LFIDYEEPEE
P26	K*LFIDYEEPEY
P27	K*LFIDYELPEY
P28	K*LFIDYLLPEY
P29	K*LFIYYLLPEY
P30	K*LFIYYLLPSY

Table 3.1. Five sets of peptides were synthesized based on the sequence of the sulfopeptide hirudin. (a) In the first series, the acidic residues were gradually replaced with more neutral ones from P1 to P6, thus decreasing the probability of zwitterionic structures. (b) P7-12 were synthesized with lysine replacing the C-terminal glutamine in P1-6. (c) For P13-18, the C-terminal lysine in P7-12 was moved to the N-terminus to be located further away from acidic sites. (d) In P19-24, the lysine side chains in P7-12 were converted to more basic guanidino groups. (e) In P25-30, the lysine side chains in P13-18 were converted to guanidinio groups. The acidic residues are marked in purple and the basic ones in blue. K* represents guanidinated lysine.

Among the first six synthetic peptides (Table 3.1(a)), P1 has the same peptide sequence as hirudin but without the sulfate group. This peptide has multiple acidic sites for possible deprotonation and the N-terminus for protonation. Thus, it should have a high chance of being zwitterionic in the gas phase. Consistently, singly deprotonated P1 showed efficient niECD with a fragmentation efficiency of 50% (Figure 3.10(a)). When calculating niECD efficiencies, product ion peak abundances were normalized to charge, summed and divided by the precursor ion abundance in the same spectrum. These experiments were performed in triplicate for all samples. In P2, the acidic glutamic acid residue was replaced with a less acidic tyrosine. This peptide still contains many acidic sites and should still readily form a zwitterion in the gas phase. However, compared with P1, statistically it should have a lower probability of becoming a zwitterion. This change in sequence decreased niECD efficiency to 41%. The probability of a zwitterionic structure was further reduced by gradually replacing acidic residues with more neutral residues (P3-6). The replacement residues were chosen to maintain the peptide masses close to each other, so that the size would not be a factor in the experiments. Consistent with the hypothesis, niECD efficiency decreased from P3 to P6 with decreased zwitterionic propensity. For the singly-charged anion of P6, which is completely composed of neutral residues, it could exist as a zwitterion with one protonation site at the N-terminus, and one deprotonation at the C-terminus. The other site of deprotonation is likely the tyrosine residue, which has been reported to be deprotonated under high pH conditions,[63] or the backbone amide as a means of charge solvation.[64] The lower probability of tyrosine or backbone deprotonation compared with that of more acidic residues leads to lower efficiency (1%) of niECD for P6 (Figure 3.10(b)). niECD mass

spectra of P1 and P6 in the first series are shown in Figure 3.11 as two examples. A dramatic difference between these two spectra is observed: niECD of P1 (the top spectrum) is significantly more efficient than that of P6 (the bottom spectrum) (50% for P1 vs. 1% for P6), resulting in much richer fragmentation and higher sequence coverage (75% for P1 vs. 40% for P6). All the niECD efficiency data of these six peptides are summarized in Figure 3.11(a). In this plot, niECD efficiency is decreasing with decreased zwitterion probability, well correlated with the proposed zwitterion mechanism.

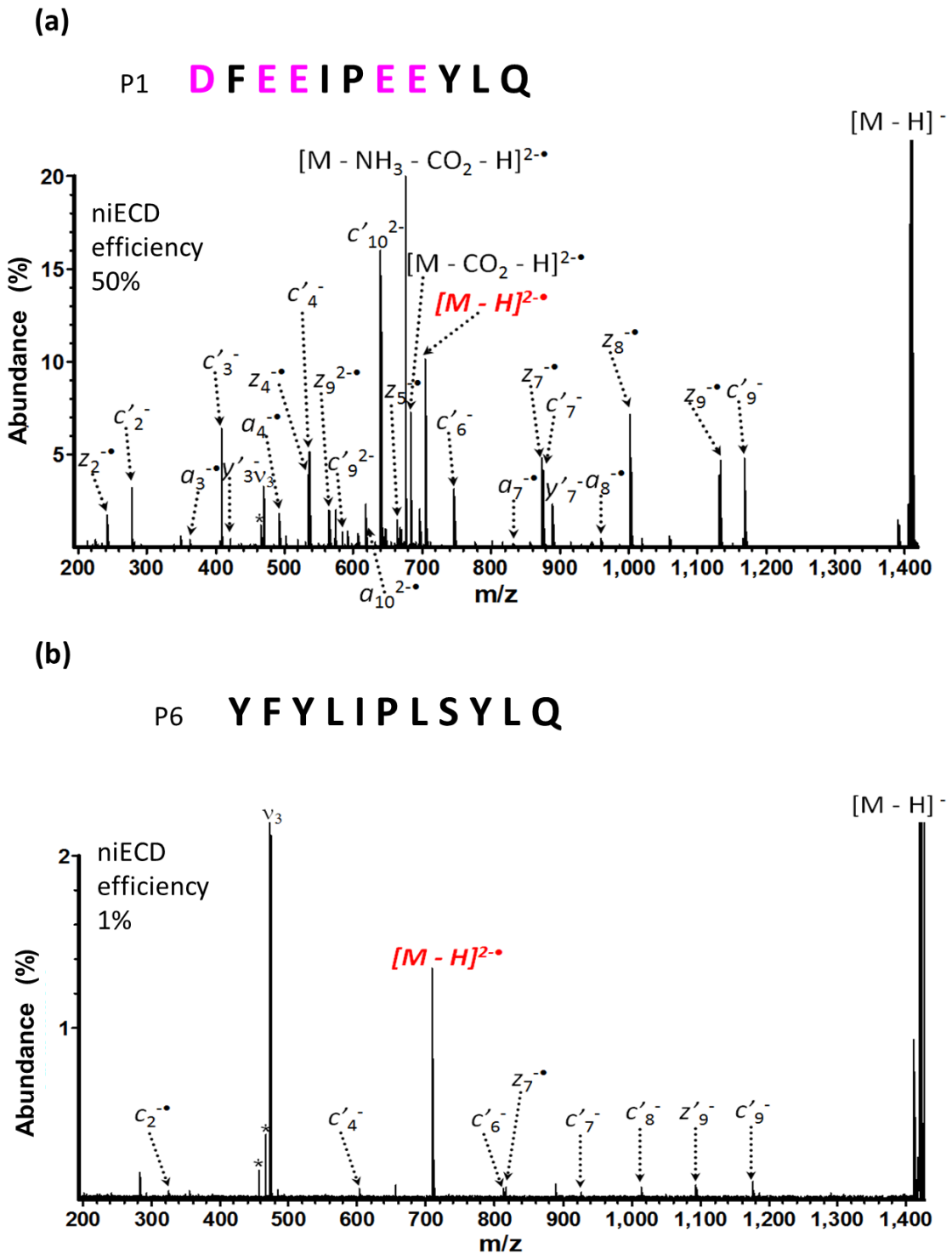

Figure 3.10. niECD (4.5 eV, 16 scans, 5 s irradiation) MS/MS spectra of singly-deprotonated (a) P1 and (b) P6. niECD efficiency decreased from P1 to P6. The electron capture species are high-lighted in red.

Following manipulation of the acidic sites, the effects of the basic sites were investigated as well. The second series of peptides, P7-12 (see their sequences in Table 3.1(b)) was synthesized by replacing the C-terminal glutamine residue in P1-6 with a lysine residue. With more basic residues in the sequences, peptides should have more available sites for protonation and, in principle, zwitterions should form more readily. The niECD efficiencies of P7-12 are also plotted in Figure 3.11(a). Similar to P1-6, the niECD behavior of P7-11 follows the same trend: the efficiency drops as the number of acidic sites drop. Unexpectedly though, the niECD efficiency of P7-12 was lower overall than the corresponding ones for P1-6. We argue that, because the lysine residue is at the C-terminus, a favorable salt bridge could be formed between the lysine side chain and the C-terminal carboxylic acid, rendering the cation less accessible.

To eliminate this potential non-covalent interaction in P7-12, the sequences of the peptides were adjusted and the lysine residue was moved to the N-terminus to be located further away from any acidic sites (P13-18; Table 3.1(c)). In this third series of synthetic peptides, P13 and P14 experienced a significant increase in niECD efficiency, strongly supporting the zwitterion hypothesis, but a decrease in efficiency was observed for P15-18 compared with the corresponding ones for P1-6 (Figure 3.11(a)). This deviation in niECD performance may be rationalized by the gas-phase structural changes of these peptides. Additional experiments, such as ion mobility MS and computational modeling, are necessary to lend more insights into the structural effects of niECD.

In the last two sets of peptides, the basicity of the lysine residue in P7-12 and P13-18 was further enhanced by converting the lysine side chains to guanidino groups through lysine guanidination reaction and thus converting them into arginine-like residues.

niECD was then applied to P19-24 and P25-28 and similar decreasing trends in niECD efficiency were observed for both of these two series (Figure 3.11(b) and 3.11(c)).

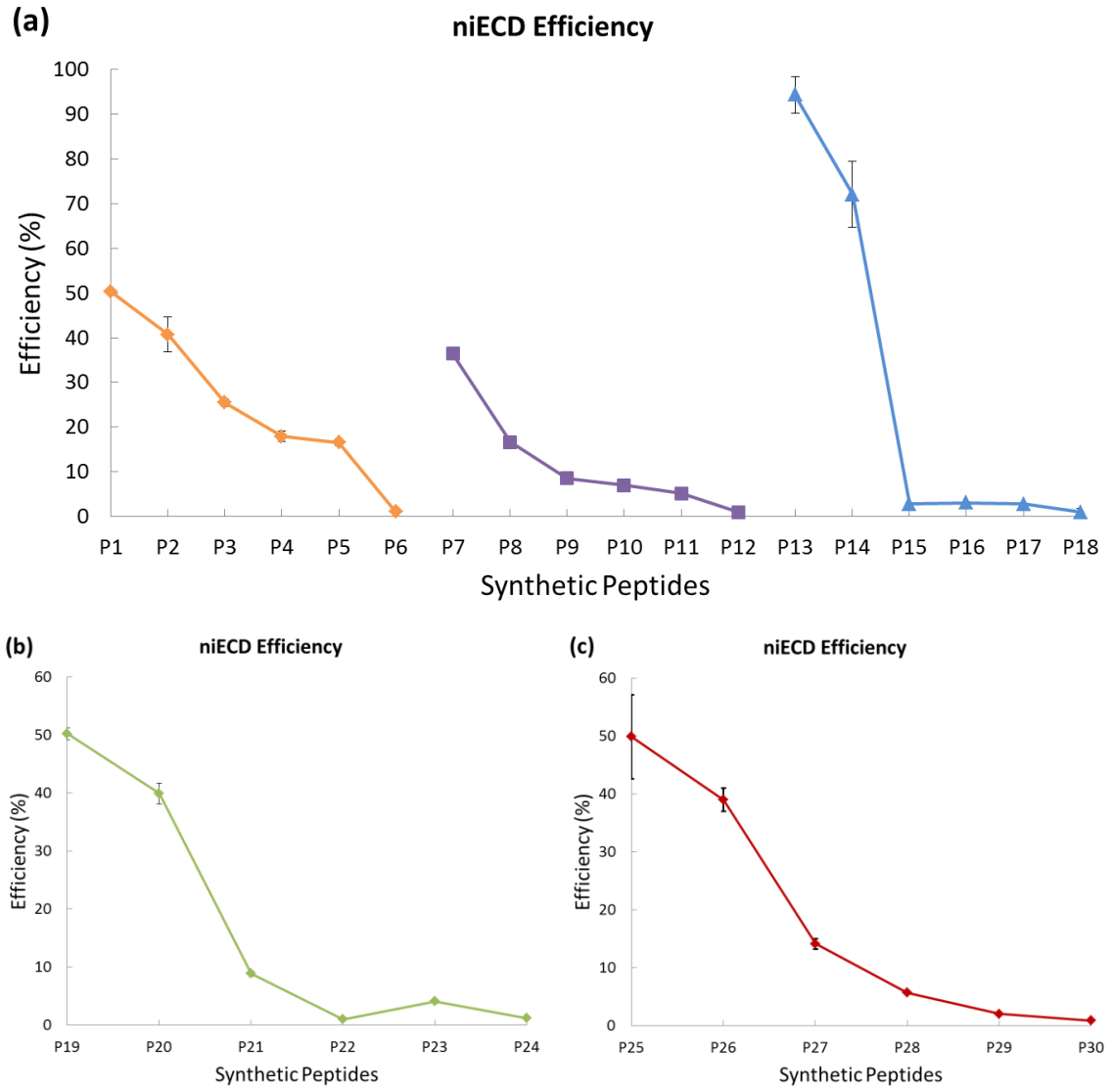

Figure 3.11. niECD efficiency of all five sets of synthetic peptides: (a) the first three sets P1-18, (b) P19-24, (c) P25-30. All niECD experiments were performed under the same conditions: 4.5 eV electron irradiation was applied for 5 s and the spectra were collected for 16 scans. niECD measurement of each peptide was repeated three times to obtain a standard deviation.

3.4 Conclusion

The proposed zwitterion mechanism of niECD was investigated by applying various chemical derivatization techniques and by synthesizing peptides with different zwitterion probabilities. Peptide N-terminal acetylation and dephosphorylation/desulfation, which may prevent zwitterion formation, decreased niECD efficiency. Addition of fixed-charge tags in the form of quaternary amine, i.e., TMAA, DABCO, and Girard's T-based tags, as well as N-terminal guanidination, which should promote zwitterion probability, enabled niECD of peptides and an oligosaccharide that were unable to capture electrons in their unmodified forms. Although not all the labeling strategies are analytically useful in generating structurally informative fragments, successful electron capture observed for most of the modified peptides and oligosaccharide strongly lends support to the hypothesis that niECD requires gas-phase zwitterionic structures. For synthetic peptides, niECD of five sets (30 peptides in total) was evaluated. All of the datasets followed the same decreasing niECD efficiency trend with decreasing zwitterionic propensity, again correlating with the proposed zwitterion mechanism.

However, it is worthwhile to point out that fixed-positive-charge derivatization/metal adduction to promote zwitterion formation did not consistently rescue the ability of a peptide to undergo niECD. Data points with unexpected niECD efficiency increase or decrease were also observed for synthetic peptides. Thus, the presence of a gas-phase zwitterionic structure does not appear to be the only criterion for successful niECD. The particular gas-phase zwitterion structure is likely also crucial: the influence of peptide gas-phase structure has been extensively studied in conventional cation ECD and is known to have a profound influence on fragmentation behavior.[65-68] Additional

mechanistic exploration, particularly regarding the effects of higher order gas-phase structure, is necessary to further elucidate the fundamental aspects of niECD.

3.5 References

1. Zubarev, R. A.; Kelleher, N. L.; McLafferty, F. W. Electron capture dissociation of multiply charged protein cations. A nonergodic process. *J. Am. Chem. Soc.* **1998**, *120*, 3265-3266.
2. Budnik, B. A.; Haselmann, K. F.; Zubarev, R. A. Electron detachment dissociation of peptide DI-ANIONS: an electron-hole recombination phenomenon. *Chem. Phys. Lett.* **2001**, *342*, 299-302.
3. Budnik, B. A.; Haselmann, K. F.; Elkin, Y. N.; Gorbach, V. I.; Zubarev, R. A. Applications of electron-ion dissociation reactions for analysis of polycationic chitooligosaccharides in fourier transform mass spectrometry. *Anal. Chem.* **2003**, *75*, 5994-6001.
4. Fung, Y. M. E.; Adams, C. M.; Zubarev, R. A. Electron ionization dissociation of singly and multiply charged peptides. *J. Am. Chem. Soc.* **2009**, *131*, 9977-9985.
5. Zubarev, R. A. Reactions of polypeptide ions with electrons in the gas phase. *Mass Spectrom. Rev.* **2003**, *22*, 57-77.
6. Cooper, H. J.; Hakansson, K.; Marshall, A. G. The role of electron capture dissociation in biomolecular analysis. *Mass Spectrom. Rev.* **2005**, *24*, 201-222.
7. Zubarev, R. A. Electron capture dissociation tandem mass spectrometry. *Curr. Opin. Biotechnol.* **2004**, *15*, 12-16.
8. Meng, F.; Forbes, A. J.; Miller, L. M.; Kelleher, N. L. Detection and localization of protein modifications by high resolution tandem mass spectrometry. *Mass Spectrom. Rev.* **2005**, *24*, 57-77.
9. Simons, J. Mechanisms for S-S and N-C-alpha bond cleavage in peptide ECD and ETD mass spectrometry. *Chem. Phys. Lett.* **2010**, *484*, 81-95.
10. Syrstad, E. A.; Turecek, F. Toward a general mechanism of electron capture dissociation. *J. Am. Soc. Mass Spectrom.* **2005**, *16*, 208-224.
11. Yoo, H. J.; Wang, N.; Zhuang, S.; Song, H.; Hakansson, K. Negative-ion electron capture dissociation: radical-driven fragmentation of charge-increased gaseous peptide anions. *J. Am. Chem. Soc.* **2011**, *133*, 16790-16793.
12. Song, H.; Hakansson, K. Electron Capture by Oligonucleotide Anions: Direct Dissociation and Further Radical Ion Activation. *J. Am. Soc. Mass Spectrom.* **2014**, in revision.
13. Paizs, B.; Suhai, S. Fragmentation pathways of protonated peptides. *Mass Spectrom. Rev.* **2005**, *24*, 508-548.
14. Reid, G. E.; Roberts, K. D.; Simpson, R. J.; O'Hair, R. A. Selective identification and quantitative analysis of methionine containing peptides by charge derivatization and tandem mass spectrometry. *J. Am. Soc. Mass. Spectrom.* **2005**, *16*, 1131-1150.
15. Creese, A. J.; Cooper, H. J. The effect of phosphorylation on the electron capture

dissociation of peptide ions. *J. Am. Soc. Mass Spectrom.* **2008**, *19*, 1263-1274.
16. Woods, A. S. The mighty arginine, the stable quaternary amines, the powerful aromatics, and the aggressive phosphate: Their role in the noncovalent minuet. *J. Proteome Res.* **2004**, *3*, 478-484.
17. Zubarev, R. A.; Kruger, N. A.; Fridriksson, E. K.; Lewis, M. A.; Horn, D. M.; Carpenter, B. K.; McLafferty, F. W. Electron capture dissociation of gaseous multiply-charged proteins is favored at disulfide bonds and other sites of high hydrogen atom affinity. *J. Am. Chem. Soc.* **1999**, *121*, 2857-2862.
18. Marchese, R.; Grandori, R.; Carloni, P.; Raugei, S. On the zwitterionic nature of gas-phase peptides and protein ions. *PLoS Comput. Biol.* **2010**, *6*, e1000775.
19. Chamot-Rooke, J.; Malosse, C.; Frison, G.; Turecek, F. Electron capture in charge-tagged peptides. Evidence for the role of excited electronic states. *J. Am. Soc. Mass. Spectrom.* **2007**, *18*, 2146-2161.
20. Chamot-Rooke, J.; van der Rest, G.; Dalleu, A.; Bay, S.; Lemoine, J. The combination of electron capture dissociation and fixed charge derivatization increases sequence coverage for O-glycosylated and O-phosphorylated peptides. *J. Am. Soc. Mass Spectrom.* **2007**, *18*, 1405-1413.
21. Xia, Y.; Gunawardena, H. P.; Erickson, D. E.; McLuckey, S. A. Effects of cation charge-site identity and position on electron-transfer dissociation of polypeptide cations. *J. Am. Chem. Soc.* **2007**, *129*, 12232-12243.
22. Gunawardena, H. P.; Gorenstein, L.; Erickson, D. E.; Xia, Y.; McLuckey, S. A. Electron transfer dissociation of multiply protonated and fixed charge disulfide linked polypeptides. *Int. J. Mass Spectrom.* **2007**, *265*, 130-138.
23. Roth, K. D.; Huang, Z. H.; Sadagopan, N.; Watson, J. T. Charge derivatization of peptides for analysis by mass spectrometry. *Mass Spectrom. Rev.* **1998**, *17*, 255-274.
24. Shen, T. L.; Allison, J. Interpretation of matrix-assisted laser desorption/ionization postsource decay spectra of charge-derivatized peptides: some examples of tris [(2, 4, 6-trimethoxyphenyl) phosphonium]-tagged proteolytic digestion products of phosphoenolpyruvate carboxykinase. *J. Am. Soc. Mass. Spectrom.* **2000**, *11*, 145-152.
25. Vath, J. E.; Biemann, K. Microderivatization of peptides by placing a fixed positive charge at the N-terminus to modify high-energy collision fragmentation. *Int. J. Mass Spectrom. Ion Processes* **1990**, *100*, 287-299.
26. Li, X. J.; Cournoyer, J. J.; Lin, C.; O'Connor, P. B. The effect of fixed charge modifications on electron capture dissociation. *J. Am. Soc. Mass Spectrom.* **2008**, *19*, 1514-1526.
27. Jones, J. W.; Sasaki, T.; Goodlett, D. R.; Turecek, F. Electron capture in spin-trap capped peptides. An experimental example of ergodic dissociation in peptide cation-radicals. *J. Am. Soc. Mass Spectrom.* **2007**, *18*, 432-444.
28. Ren, D. Y.; Julka, S.; Inerowicz, H. D.; Regnier, F. E. Enrichment of cysteine-containing peptides from tryptic digests using a quaternary amine tag. *Anal. Chem.* **2004**, *76*, 4522-4530.
29. Stults, J. T.; Lai, J.; McCune, S.; Wetzel, R. Simplification of high-energy collision spectra of peptides by amino-terminal derivatization. *Anal. Chem.* **1993**, *65*, 1703-1708.

30. Zaia, J.; Biemann, K. Comparison of charged derivatives for high energy collision-induced dissociation tandem mass spectrometry. *J. Am. Soc. Mass. Spectrom.* **1995**, *6*, 428-436.
31. Brancia, F. L.; Oliver, S. G.; Gaskell, S. J. Improved matrix-assisted laser desorption/ionization mass spectrometric analysis of tryptic hydrolysates of proteins following guanidination of lysine-containing peptides. *Rapid Commun. Mass Spectrom.* **2000**, *14*, 2070-2073.
32. Peters, E. C.; Horn, D. M.; Tully, D. C.; Brock, A. A novel multifunctional labeling reagent for enhanced protein characterization with mass spectrometry. *Rapid Commun. Mass Spectrom.* **2001**, *15*, 2387-2392.
33. Beardsley, R. L.; Reilly, J. P. Optimization of guanidination procedures for MALDI mass mapping. *Anal. Chem.* **2002**, *74*, 1884-1890.
34. Hennrich, M. L.; Boersema, P. J.; van den Toorn, H.; Mischerikow, N.; Heck, A. J. R.; Mohammed, S. Effect of chemical modifications on peptide fragmentation behavior upon electron transfer induced dissociation. *Anal. Chem.* **2009**, *81*, 7814-7822.
35. Miyashita, M.; Hanai, Y.; Awane, H.; Yoshikawa, T.; Miyagawa, H. Improving peptide fragmentation by N-terminal derivatization with high proton affinity. *Rapid Commun. Mass Spectrom.* **2011**, *25*, 1130-1140.
36. Lindh, I.; Sjovall, J.; Bergman, T.; Griffiths, W. J. Negative-ion electrospray tandem mass spectrometry of peptides derivatized with 4-aminonaphthalenesulphonic acid. *J. Mass Spectrom.* **1998**, *33*, 988-993.
37. Unterieser, I.; Cuers, J.; Voiges, K.; Enebro, J.; Mischnick, P. Quantitative aspects in electrospray ionization ion trap and matrix-assisted laser desorption/ionization time-of-flight mass spectrometry of malto-oligosaccharides. *Rapid Commun. Mass Spectrom.* **2011**, *25*, 2201-2208.
38. Beardsley, R. L.; Sharon, L. A.; Reilly, J. P. Peptide de novo sequencing facilitated by a dual-labeling strategy. *Anal. Chem.* **2005**, *77*, 6300-6309.
39. Yang, J.; Mo, J.; Adamson, J. T.; Hakansson, K. Characterization of oligodeoxynucleotides by electron detachment dissociation fourier transform ion cyclotron resonance mass spectrometry. *Anal. Chem.* **2005**, *77*, 1876-1882.
40. Tsybin, Y. O.; Witt, M.; Baykut, G.; Kjeldsen, F.; Hakansson, P. Combined infrared multiphoton dissociation and electron capture dissociation with a hollow electron beam in fourier transform ion cyclotron resonance mass spectrometry. *Rapid Commun. Mass Spectrom.* **2003**, *17*, 1759-1768.
41. Senko, M. W.; Canterbury, J. D.; Guan, S.; Marshall, A. G. A high-performance modular data system for FT-ICR mass spectrometry. *Rapid Commun. Mass Spectrom.* **1996**, *10*, 1839-1844.
42. Ledford Jr, E. B.; Rempel, D. L.; Gross, M. Space charge effects in fourier transform mass spectrometry. II. mass calibration. *Anal. Chem.* **1984**, *56*, 2744-2748.
43. Chung, T. W.; Moss, C. L.; Zimnicka, M.; Johnson, R. S.; Moritz, R. L.; Turecek, F. Electron-capture and -transfer dissociation of peptides tagged with tunable fixed-charge groups: Structures and dissociation energetics. *J. Am. Soc. Mass Spectrom.* **2011**, *22*, 13-30.
44. Clifford-Nunn, B.; Showalter, H. D. H.; Andrews, P. C. Quaternary diamines as

mass spectrometry cleavable crosslinkers for protein interactions. *J. Am. Soc. Mass. Spectrom.* **2012**, *23*, 201-212.
45. Jockusch, R. A.; Price, W. D.; Williams, E. R. Structure of cationized arginine (Arg-M+, M = H, Li, Na, K, Rb, and Cs) in the gas phase: further evidence for zwitterionic arginine. *J. Phys. Chem. A* **1999**, *103*, 9266-9274.
46. Adamson, J. T.; Hakansson, K. Electron capture dissociation of oligosaccharides ionized with alkali, alkaline earth, and transition metals. *Anal. Chem.* **2007**, *79*, 2901-2910.
47. Liu, H. C.; Hakansson, K. Electron capture dissociation of divalent metal-adducted sulfated oligosaccharides. *Int. J. Mass Spectrom.* **2011**, *305*, 170-177.
48. Adamson, J. T.; Hakansson, K. Electron detachment dissociation of neutral and sialylated oligosaccharides. *J. Am. Soc. Mass Spectrom.* **2007**, *18*, 2162-2172.
49. Wolff, J. J.; Laremore, T. N.; Aslam, H.; Linhardt, R. J.; Amster, I. J. Electron-Induced Dissociation of Glycosaminoglycan Tetrasaccharides. *J. Am. Soc. Mass. Spectrom.* **2008**, *19*, 1449-1458.
50. Devakumar, A.; Thompson, M. S.; Reilly, J. P. Fragmentation of oligosaccharide ions with 157 nm vacuum ultraviolet light. *Rapid Commun. Mass Spectrom.* **2005**, *19*, 2313-2320.
51. Fuster, M. M.; Esko, J. D. The sweet and sour of cancer: glycans as novel therapeutic targets. *Nat. Rev. Cancer* **2005**, *5*, 526-542.
52. Brockhausen, I. Mucin type O-glycans in human colon and breast cancer: glycodynamics and functions. *EMBO Rep.* **2006**, *7*, 599-604.
53. Dwek, M. V.; Brooks, S. A. Harnessing changes in cellular glycosylation in new cancer treatment strategies. *Curr. Cancer Drug Targ.* **2004**, *4*, 425-442.
54. Dube, D. H.; Bertozzi, C. R. Glycans in cancer and inflammation. Potential for therapeutics and diagnostics. *Nat. Rev. Drug Disc.* **2005**, *4*, 477-488.
55. Holligsworth, M. A.; Swanson, B. J. Mucins in cancer: protection and control of the cell surface. *Nat. Rev. Cancer* **2004**, *4*, 45-60.
56. Orntoft, T. F.; Vestergaard, E. M. Clinical aspects of altered glycosylation of glycoproteins in cancer. *Electrophoresis* **1999**, *20*, 362-371.
57. Byrd, J. C.; Bresalier, R. S. Mucins and mucin binding proteins in colorectal cancer. *Cancer. Met. Rev.* **2004**, *23*, 77-99.
58. Naven, T. J. P.; Harvey, D. J. Cationic derivatization of oligosaccharides with Girard's T reagent for improved performance in matrix-assisted laser desorption/ionization and electrospray mass spectrometry. *Rapid Commun. Mass Spectrom.* **1996**, *10*, 829-834.
59. Kim, Y. G.; Harvey, D. J.; Yang, Y. H.; Park, C. G.; Kim, B. G. Mass spectrometric analysis of the glycosphingolipid-derived glycans from miniature pig endothelial cells and islets: identification of NeuGc epitope in pig islets. *J. Mass Spectrom.* **2009**, *44*, 1489-1499.
60. Cagney, G.; Emili, A. De novo peptide sequencing and quantitative profiling of complex protein mixtures using mass-coded abundance tagging. *Nat. Biotechnol.* **2002**, *20*, 163-170.
61. Evans, R. L.; Saroff, H. A. A physiologically active guanidinated derivative of insulin. *J. Biol. Chem.* **1957**, *228*, 295-304.
62. Kimmel, J. R. [70] Guanidination of proteins. *Methods Enzymol.* **1967**, *11*, 584-

589.
63. Shaw, J. B.; Ledvina, A. R.; Zhang, X.; Julian, R. R.; Brodbelt, J. S. Tyrosine deprotonation yields abundant and selective backbone cleavage in peptide anions upon negative electron transfer dissociation and ultraviolet photodissociation. *J. Am. Chem. Soc.* **2012**, *134*, 15624-15627.
64. Kjeldsen, F.; Silivra, O. A.; Ivonin, I. A.; Haselmann, K. F.; Gorshkov, M.; Zubarev, R. A. C(alpha)-C backbone fragmentation dominates in electron detachment dissociation of gas-phase polypeptide polyanions. *Chem. Eur. J.* **2005**, *11*, 1803-1812.
65. Mihalca, R.; Kleinnijenhuis, A. J.; McDonnell, L. A.; Heck, A. J. R.; Heeren, R. M. A. Electron capture dissociation at low temperatures reveals selective dissociations. *J. Am. Soc. Mass Spectrom.* **2004**, *15*, 1869-1873.
66. Robinson, E. W.; Leib, R. D.; Williams, E. R. The role of conformation on electron capture dissociation of ubiquitin. *J. Am. Soc. Mass Spectrom.* **2006**, *17*, 1469-1479.
67. Ben Hamidane, H.; He, H.; Tsybin, O. Y.; Emmett, M. R.; Hendrickson, C. L.; Marshall, A. G.; Tsybin, Y. O. Periodic sequence distribution of product ion abundances in electron capture dissociation of amphipathic peptides and proteins. *J. Am. Soc. Mass Spectrom.* **2009**, *20*, 1182-1192.
68. Breuker, K.; Oh, H. B.; Lin, C.; Carpenter, B. K.; McLafferty, F. W. Nonergodic and conformational control of the electron capture dissociation of protein cations. *Proc. Natl. Acad. Sci. U.S.A.* **2004**, *101*, 14011-14016.

Chapter 4

Negative Ion Electron Capture Dissociation (niECD) of Disulfide-linked Peptide Anions

4.1 Introduction

Disulfide linkages constitute one of the most frequently encountered PTMs in extracellular proteins.[1] Disulfide bonds are critical for establishing and maintaining correct three-dimensional structures of proteins and, consequently, proper biological functions.[2-5] Unnatural disulfides are introduced by disulfide-containing cross-linkers in cross-linking experiments, which are utilized to map interfaces in protein complexes as well as to determine low resolution protein structures.[6-8] The customary approach for characterizing disulfide-containing peptides by mass spectrometry involves solution-phase chemical reduction of the disulfide bonds, often followed by alkylation of the thiol

group, prior to MS measurements. This approach involves rather lengthy analysis times and additional sample consumption compared with direct analysis.[9, 10]

An alternative approach is to cleave intact cystine bonds in the gas phase directly with tandem mass spectrometry (MS/MS). Many efforts have been made to develop gas-phase dissociation techniques as means of studying disulfide-linked peptides and proteins. Low-energy collision-activated dissociation (CAD) of cations, the typically used MS/MS technique, shows limited use for this purpose as it is often observed to lead to little disulfide cleavages.[11-13] High-energy CAD, on the other hand, has been utilized to cleave both native disulfide bridges and disulfides of 3,3'-dithiobis (sulfosuccinimidyl propionate) (DTSSP)-modified peptides.[14, 15] However, high energy CAD is mainly available on MALDI TOF/TOF mass spectrometers and involves significant ion scattering that reduces sensitivity. In ultraviolet photodissociation (UVPD), disulfide-linked peptide and protein polycations exhibit selective and efficient cleavage of the S-S bonds at 157 nm[16] and at 266 nm[17], as a result of electronic excitation by photon absorption.

Electron-mediated techniques, such as electron capture dissociation (ECD)[18, 19] and its ion-ion reaction analog electron transfer dissociation (ETD)[20], have seen a surge of interest as ion activation methods in tandem MS. They tend to produce *c*'- and $z^{\bullet}$-type backbone fragments, providing complementary, and usually more extensive, structural information compared with CAD. A significant attraction of ECD/ETD is that they can cleave backbone bonds without losing labile PTMs, such as phosphorylation and glycosylation, thus making them valuable techniques for PTM determination.[21-24] Another distinct feature of ECD/ETD is that they have been demonstrated to

preferentially fragment disulfide bonds over backbone bonds.[25-27] Thus, effective characterization of disulfide linkages can be obtained from ECD/ETD spectra for peptides and proteins. A study of intrachain disulfides reported that both disulfide and backbone cleavages could be induced in a single ETD experiment.[28] Several hypotheses have been proposed to explain the mechanism of specific disulfide bond cleavage in ECD. The "hot hydrogen" mechanism suggests that the capture of an electron occurs at a cationic site, which releases a hot hydrogen. Favored cleavage of S-S linkages has been proposed to be due to the high hydrogen affinity of the disulfide bond.[25] In alternative mechanisms, an electron can be directly captured into the σ* orbital of a disulfide bond through Coulomb stabilization by nearby positive charges,[29] or initially captured into a Rydberg state of a cationic site and then undergo through bond transfer to a disulfide linkage.[30] However, a more recent study by Ganisl and co-workers demonstrates that disulfide bonds of proteins are preserved, or not preferentially dissociated, during ECD, indicating that a more intricate mechanism may be involved in cleaving disulfide bonds by ECD than previously anticipated.[31] One drawback of ECD/ETD is that the precursor ions must be at least doubly charged in order to observe the products of ECD/ETD by mass spectrometry as capture or transfer of an electron by a singly-charged ion would result in a net charge of zero. Furthermore, the efficiency of ECD/ETD is dependent on charge state and high charge states are preferred.[32-34] However, generation of multiply-charged cations can be challenging for acidic molecules.

Although most mass spectrometric analysis focuses on peptide or protein cations, negative ion mode can provide complementary information and is particularly valuable for acidic proteins. In contrast to positive mode, disulfide bonds can undergo facile

cleavage during negative ion CAD.[35-37] Characteristic fragments arising from disulfide bond cleavages acquired with beam-type instruments allow fast mapping of disulfide linkage positions within proteins.[37] Recently, Calabrese and co-workers applied negative ion CAD to cross-linked peptides and proteins using the cystine-based cross-linking reagent dithiobis(succinimidyl) propionate (DSP).[38] Diagnostic MS/MS spectra were generated, allowing the identification of cross-linked peptides. Subsequent MS^3 analysis could be readily performed to sequence the peptides and localize the cross-linking site at a residue-specific level. Specific cleavage of S-S and C-S bonds has also been investigated by the electron-based technique operating in negative mode, electron detachment dissociation (EDD).[39] Ions arising from separation of the two peptide chains, at either the S-S or the C-S bonds, are apparent in EDD spectra. Negatively-charged peptides and proteins reacting with Fe^+ ions were examined by Glish and co-workers and was found to cause fragmentation near sulfur atoms, either adjacent to the cysteine residue or the disulfide bond between the two cysteines.[40]

Negative ion electron capture dissociation (niECD) is a novel MS/MS technique for anions, recently discovered in our lab.[41] In niECD, singly or multiply deprotonated precursor ions can capture electrons within a certain energy range (~3.5-6.5 eV) to generate charge-*increased* distonic radicals that undergo dissociation analogous to conventional ECD/ETD. A significant advantage of niECD is that ECD/ETD-like fragmentation, which is complementary to the more common CAD and thus generates valuable structural information, can be achieved in negative ion mode. niECD have been applied to phospho- and sulfopeptides (See Chapter 2).[41, 42] Just like ECD/ETD, niECD produces $c'/z^{\bullet}$ type backbone fragmentation and preserves the labile phosphorylation and

sulfation, while CAD typically does not. Similarities in terms of peptide backbone fragments and retention of labile PTMs led us to believe that niECD proceeds through a zwitterion mechanism related to positive ion ECD. We proposed that gas-phase zwitterionic structures are necessary for successful niECD and that a positive charge is required to serve as the site of electron capture, or to promote electron capture. This hypothesis is correlated with our experimental data: N-terminal acetylation, which should reduce the probability of zwitterion formation, results in decreased niECD efficiency and introduction of fixed positive charge tags, which should promote zwitterion formation, enables niECD of peptides which could not undergo niECD in their unmodified form.[41] niECD efficiency also decreases with decreased zwitterion propensity for five sets of synthetic peptides, further supporting the zwitterion mechanism (see details in Chapter 3).

Because another characteristic of ECD/ETD is that they cleave peptide cations preferentially at disulfide bonds in most cases, it is also of interest to examine the dissociation behavior of disulfide-linked peptides in niECD and to compare their fragmentation behavior to conventional ECD/ETD. In this Chapter, we employ the new method niECD to characterize systems with polypeptide chains bound by a disulfide bridge. Both natural protein disulfide bonds (in insulin and lysozyme) and disulfides introduced by the cystine-based cross-linker DTSSP are investigated. This work focuses on intermolecular disulfide linkages in singly- and doubly-deprotonated peptide anions. The analytical utility of niECD for disulfide analysis is also addressed. These experiments provide further insights into the degree to which ECD and niECD are analogous, and into the mechanism of niECD.

4.2 Experimental

4.2.1 Reagents

Insulin from bovine pancreas, chicken egg white lysozyme and ubiquitin were obtained from Sigma-Aldrich (St. Louis, MO). The cross-linking reagent, 3,3'-dithiobis (sulfosuccinimidyl propionate) DTSSP, was purchased from Pierce (Rockford, IL). Glu-C and trypsin were purchased from Roche (Indianapolis, IN) and Promega (Madison, WI), respectively. Isopropanol, formic acid, triethylamine, ammonium bicarbonate, and ammonium acetate were from Fisher Scientific (Fair Lawn, NJ).

4.2.2 Sample Preparation

For digestion, insulin was incubated with Glu-C at 1:40 enzyme to protein ratio for 10 h at 25 ℃. Lysozyme was digested with trypsin at a 1:20 enzyme to protein ratio for 12 h at 37 ℃. The digestion was quenched with 0.1% formic acid. For lysozyme, C18 reverse-phase micro-columns, Ziptip (Millipore, Billerica, MA), were used to desalt the resulting peptides, which were then diluted by 40% isopropanol and 15 mM ammonium bicarbonate for negative ion mode MS analysis. For insulin, the digestion was diluted with 40% isopropanol and 5 mM ammonium acetate without any purification.

For the cross-linking reaction, the protein ubiquitin was incubated with DTSSP in 15mM HEPES buffer (pH=7.6) at 1:100 protein to cross-linker ratio for 40 min at room temperature. The reaction was quenched with 1 M ammonium bicarbonate. The cross-linked protein was then denatured by heating (100 ℃) for 10 min followed by prompt placing on ice. The cross-linked protein was digested with trypsin or Glu-C at a 1:50 enzyme to protein ratio overnight at 37 ℃. The resulting peptides were desalted with

C18 Ziptips and diluted with H_2O/isopropanol (50/50 v/v) and 0.1% triethylamine as spraying solvent.

4.2.3 FT-ICR Mass Spectrometry

Negatively-charged peptide ions were generated by external electrospray ionization (ESI) at 70 μL/h (Apollo II ion source, Bruker Daltonics, Billerica, MA). All experiments were performed with an actively shielded 7 Tesla quadrupole (Q)-FT-ICR mass spectrometer (APEX-Q, Bruker Daltonics) as previously described.[43] All data were obtained in negative ion mode. For ESI, N_2 was used as both nebulizing gas (5 L/s) and drying gas (2.0 L/s). The drying gas temperature was set to 200˚C. Briefly, ions produced by ESI were mass-selectively accumulated in an external hexapole for 0.2-3 s, transferred via high voltage ion optics, and captured in the ICR cell by dynamic trapping. This accumulation sequence was looped three times to improve precursor ion abundance. For negative ion electron capture dissociation (niECD), mass selectively accumulated peptide ions were irradiated for 10 s with 4.5-5.5 eV electrons provided by an indirectly heated hollow dispenser cathode.[44] The cathode heating current was kept at 1.8 A. A lens electrode located in front of the hollow cathode was kept 1.5 V more positive than the cathode bias voltage.

4.2.4 Data Analysis

All mass spectra were acquired with XMASS software (version 6.1, Bruker Daltonics) in broadband mode from m/z 200 to 3000 with 256K data points and summed over 10-32 scans. Data processing was performed with the MIDAS analysis software.[45] Data were zero filled once, Hanning apodized, and exported to Microsoft Excel for internal

frequency-to-mass calibration with a two-term calibration equation.[46] Peaks in MS^n were assigned within 10 ppm error after internal calibration. Product ions were not assigned unless the S/N ratio was at least 3. Typically, internal calibration was performed with precursor ions and their electron-capture species as calibrants.

4.3 Results and Discussion

For the notation used in this study, R_1 and R_2 are used to indicate the two peptide chains bound by the disulfide bonds, respectively. The peptide backbone fragments are denoted as $R_1SSm_{n(R2)}$ if chain R_2 is fragmented to generate product ion m_n with retention of the intact chain R_1. Likewise, $R_2SSm_{n(R1)}$ indicates that the m_n product ion is from chain R_1 and is disulfide-bound to the intact chain R_2. RS• (odd electron species and RSH (even electron species) represent product ions resulting from cleavage of the S-S bond. Other product ion structures observed in niECD of natural disulfide-linked peptides and nomenclature are summarized in Scheme 4.1. For ease of discussion, similar notation of product ions to that for natural disulfide bonds is used for cross-linked peptides, as illustrated in Scheme 4.2(b).

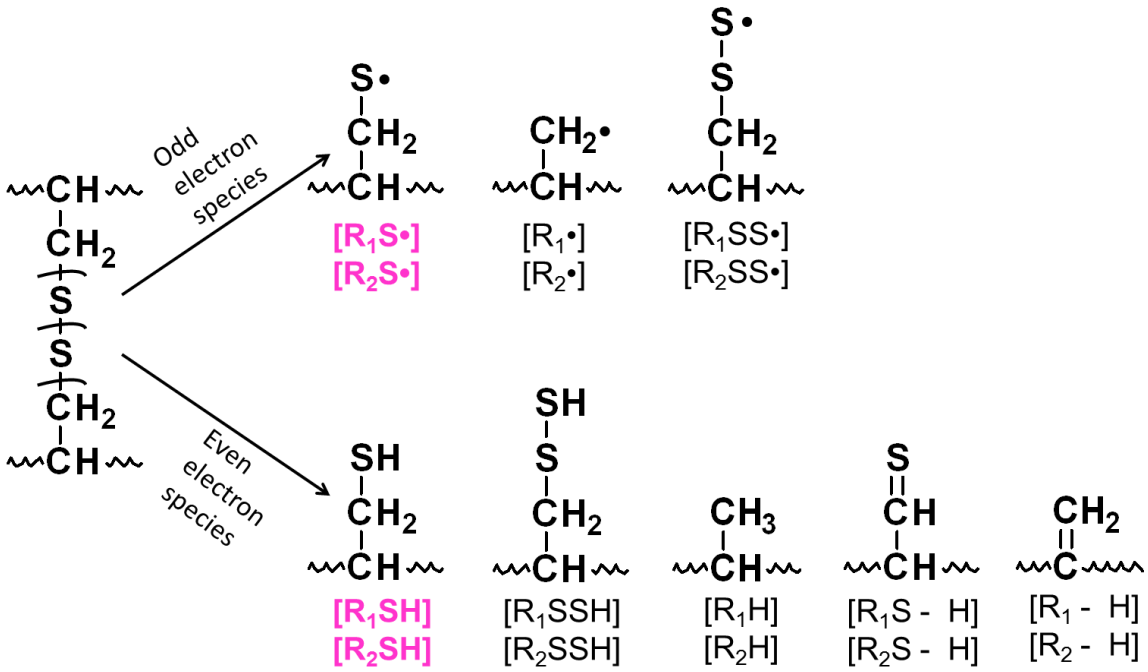

Scheme 4.1. Structures and nomenclature used for product ions of natural disulfide-linked peptides. The main fragmentation pathway, S-S bond cleavage, is labeled in purple.

4.3.1 niECD of Insulin Peptide Pairs

Figure 4.1(a) presents an niECD tandem mass spectrum of a singly-deprotonated ([M - H]$^-$) peptide pair, generated from insulin proteolysis and containing one intermolecular disulfide bond. Glu-C is chosen as the digestion enzyme to introduce acidic residues at the C-termini of each peptide chain and to increase the acidity of the molecule. The shorter peptide sequence NYCN, corresponding to residues 18-21, is termed chain R_1, and ALYLVCGE, residues 14-21, is termed chain R_2. Irradiation of the precursor ion, [M - H]$^-$, with 4.5 eV electrons yielded a charge-increased radical species, [M - H]$^{2-\bullet}$, consistent with the previously observed behavior of peptide anions in niECD.[41, 42] The two most dominant product ions observed in the mass spectrum correspond to cleavage of the S-S bond, resulting in two peptide monomers each containing one sulfur atom.

The insets in Figure 4.1 show a zoomed-in view of peptide chains R_1 and R_2. The isotopic distribution pattern indicates that both R_1 and R_2 chains are comprised of a mixture of two product ions, differing in mass by 1 Da, corresponding to one hydrogen atom. These products can be explained as the odd-electron product, $R_1S\bullet/R_2S\bullet$, and the even-electron species, R_1SH/R_2SH, with retention of the neutralized H• (from hydrogen migration).[47] Similar results have been reported from ECD and ETD of disulfide-linked peptides, which fragment to produce one odd electron species, S•, and one even electron species, SH.[25, 48] Thus, disulfide-bound peptides fragment analogously in niECD compared with ECD/ETD, generating both odd- and even-electron species.

In addition to the pronounced sulfur-sulfur bond cleavage, the neighboring carbon-sulfur bond cleavages, resulting in peptide chains containing none or two sulfur atoms, are also observed but with much lower efficiency (labeled as $[R_1SS\bullet]^-$, $[R_2SS\bullet]^-$ /$[R_2SSH]^-$, and $[R_2\bullet]^-/[R_2H]^-$). Inspection of the isotopic clusters reveals that some of these products are also mixtures of odd- and even-electron products. There is evidence for cleavages in the peptide backbone region as well: limited backbone fragments (three *c*' ions and one $z^\bullet$ ion with low abundance) are observed in the spectrum, in contrast to the predominant S-S disulfide bond cleavage. The specific backbone fragment types are in good agreement with the fact that niECD generally produces $c'/z^\bullet$ type ions.[41] Particularly, two doubly-charged backbone product ions, which have higher charge state than the precursor ion, are generated, whereas ECD/ETD results in charge reduction. This increase of charge is particularly useful for the FT-ICR instrument we use in this experiment, for which signal-to-noise ratios are proportional to charge state and increased charge states result in improved ion signal.[49] niECD also resulted in neutral ammonia

(NH_3) loss from the charge reduced species, constituting a ubiquitous fragmentation channel in niECD and also frequently occurring in ECD.[50, 51] NH_3 loss from one peptide monomer was also observed. Overall, the limited fragmentation at backbone bonds and abundant peptide chain ions following S-S cleavage observed in Figure 4.1 indicate that disulfide bonds are cleaved preferentially over backbone bonds in niECD for this insulin peptide pair, analogous to previously reported behavior of disulfide-bound peptides in ECD and ETD.

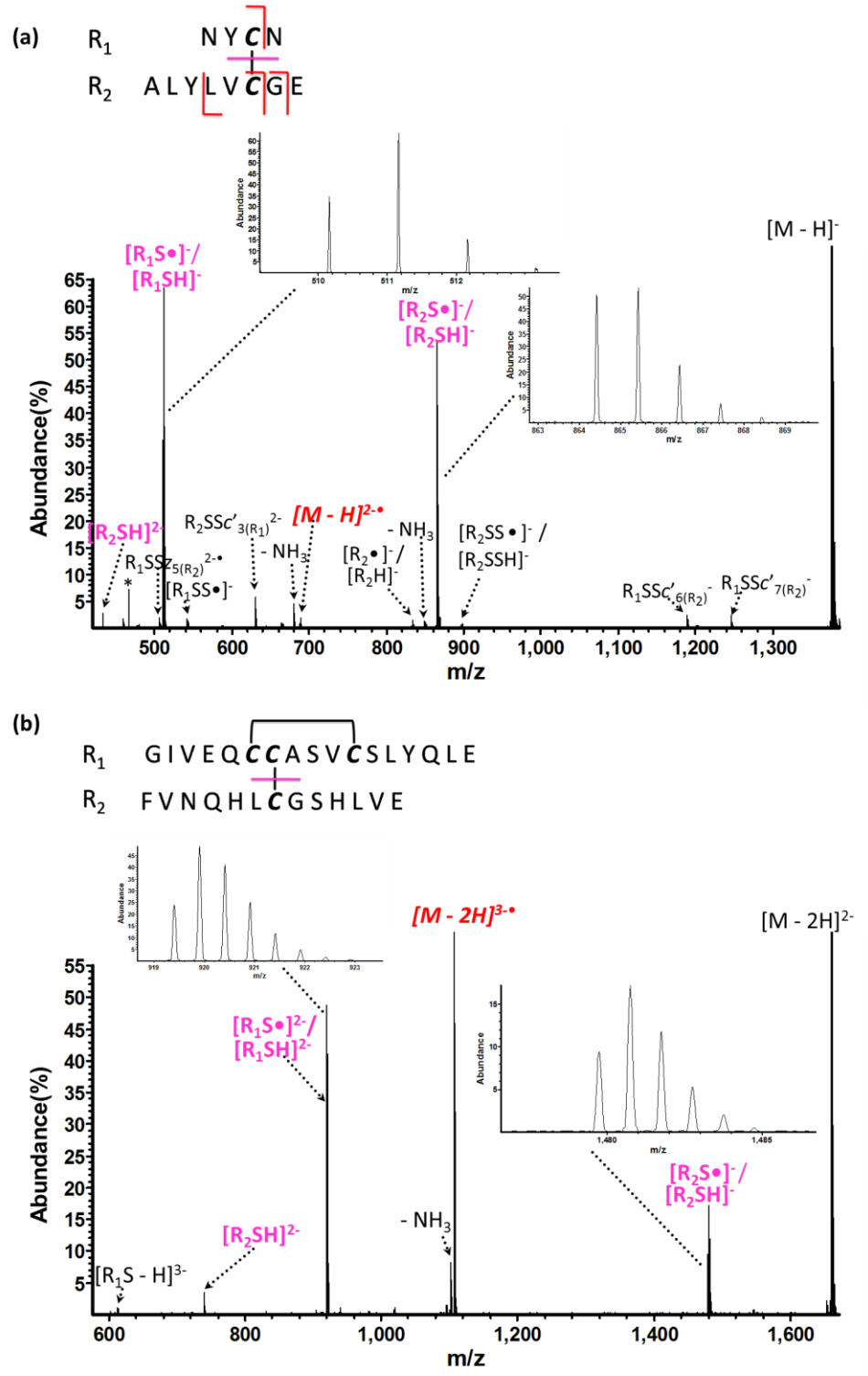

Figure 4.1. niECD of (a) singly- and (b) doubly-deprotonated Glu-C-derived disulfide-linked insulin peptide pairs. For the singly-deprotonated peptide pair, irradiation was performed with 4.5 eV electrons for 10 seconds; for the doubly-deprotonated species, 5.5 eV electrons were used for the same time. The charge-

increased product ion is marked in red and the dominant S-S cleavages marked in purple. Electronic noise is marked as *. The insets show a mixture of RSH and its radical form RS• for both the peptide chains.

niECD of a relatively larger Glu-C-digested insulin peptide pair, peptide GIVEQCCASVCSLYQLE (residues 1-13) of chain R_1 disulfide-linked to the peptide FVNQHLCGSHLVE (residues 1-17) of chain R_2, is shown in Figure 4.1(b). This analyte contains an intermolecular disulfide bridge at cysteine 7 of chain R_1 and cysteine 7 of chain R_2, as well as an intramolecular disulfide bridge formed between cysteine 6 and cysteine 11 of chain R_1. niECD was performed on a doubly-deprotonated precursor ion as a result of the increased peptide size. A charge state effect was observed. For the doubly charged precursor ion, higher electron energy (5.5 eV) was necessary to enable maximum electron capture, which can be explained by higher Coulomb repulsion between the precursor ion and electrons.[41] The increased charge state of the precursor ion also caused relatively lower fragmentation efficiency, indicating that capture of electrons by more highly charged anions is not as efficient as that by singly-charged ones. A charge-increased triply-charged radical, $[M - 2H]^{3-\bullet}$, is generated as a major product ion together with ammonia loss from this species, similar to niECD of peptide monomers.[41] However, unlike the singly-charged insulin peptide (Fig. 4.1a), only one bond is cleaved for the larger peptide pair, the S-S bond, leaving one sulfur atom within each peptide chain. The main dissociation products correspond to the singly-charged R_2 chain and doubly-charged R_1 chain, which has a relatively larger size and thus a higher tendency to contain multiple negative charges. For each of these two chains, is the products are a mixture of two species, the odd- and even-electron fragments (shown in the insets). These dominant characteristic fragment ions can be easily recognized and

thus used to identify the presence of disulfide bonds, and to define the constituent peptides. The abundant signal obtained in niECD makes it possible to subject the disulfide-cleaved products to MS^3 for sequencing of each peptide chain. In addition to the two major product ions, two small peaks were observed in the lower mass region, corresponding to the mass of the triply-charged R_1 chain and the doubly-charged R_2 chain. The increased charge state of the triply-charged product ion indicates that it must arise from the electron capture reaction. No C-S bond or backbone bond cleavages were noted in this spectrum. These data again show that cysteine-cysteine bond cleavage is the much preferred fragmentation pathway in niECD for disulfide-linked insulin peptides. The lack of other fragmentation pathways may be due to a higher energy barrier and the overall decreased fragmentation efficiency for doubly-charged precursor ions. It could not be determined if the intrachain disulfide was cleaved or not based on these data, as the disulfide cleavage will not yield a product ion of changed mass. Absence of other dissociation patterns leads to a highly simple and clean spectrum, rendering data interpretation straightforward.

4.3.2 niECD of Lysozyme Peptide Pairs

As a comparison, trypsin instead of Glu-C was utilized for lysozyme proteolysis, which should result in the presence of an arginine or lysine residue at each peptide C-terminus and, therefore, increased basicity of the precursor ions. Following digestion, two disulfide bond-containing species were investigated with niECD. niECD of the peptide GCR (denoted as chain R_1, corresponding to residues 5-7) connected via an intermolecular disulfide bond to the peptide CELAAAMK (denoted as chain R_2, corresponding to residues 127-134) is shown in Figure 4.2(a). The precursor ion

experienced lower ionization efficiency in negative ion electrospray compared to Glu-C-digested insulin peptide pairs due to its decreased acidity. The singly-deprotonated lysozyme peptide pair captured a 4.5 eV electron to generate a charge-increased radical intermediate. One and two ammonia neutral losses from the radical species are observed as well as one ammonia loss from peptide chain R_2. Similar to the niECD results for insulin peptides discussed above, the most predominant fragments correspond to S-S bond cleavage between the two peptide chains, generating product ions for both peptide halves. For this lysozyme peptide pair, the R_2 chain is an even-electron product ($[R_2SH]^-$) from hydrogen migration, retaining most of the hydrogen, whereas the R_1 chain is the odd-electron product ($[R_1S\bullet]^-$). In conventional ECD, it has been reported that even-electron products tend to originate from the peptide chain with higher charge state, presumably due to S-S polarization.[25] However, in our niECD experiment, both the odd- and the even-electron species are singly-charged ions. Thus, their distribution cannot be explained by the same mechanism. One feature shared between previous ECD and our current niECD results, though, is that the even-electron product is always the peptide chain with larger size, which may have some effect on the distribution between odd- and even-electron species. In addition to the primary cleavage at the S-S bond, weak signals corresponding to C-S bond cleavage in the R_2 chain are present in the spectrum. One backbone bond cleavage in the R_2 chain also resulted in the product ion c_6 disulfide-linked to the intact R_1 chain, as shown by the presence of the signal labeled as $R_1SSc'_{6(R2)}$. Again, this example demonstrates that disulfide bond cleavage constitutes the dominant dissociation process in niECD, analogous to positive ion ECD/ETD. Although relatively more basic peptides are examined here, the dissociation pattern is

virtually the same as those observed for Glu-C-digested peptide pairs, indicating that, other than ionization efficiency, the acidity does not have a large impact on fragmentation behavior in niECD.

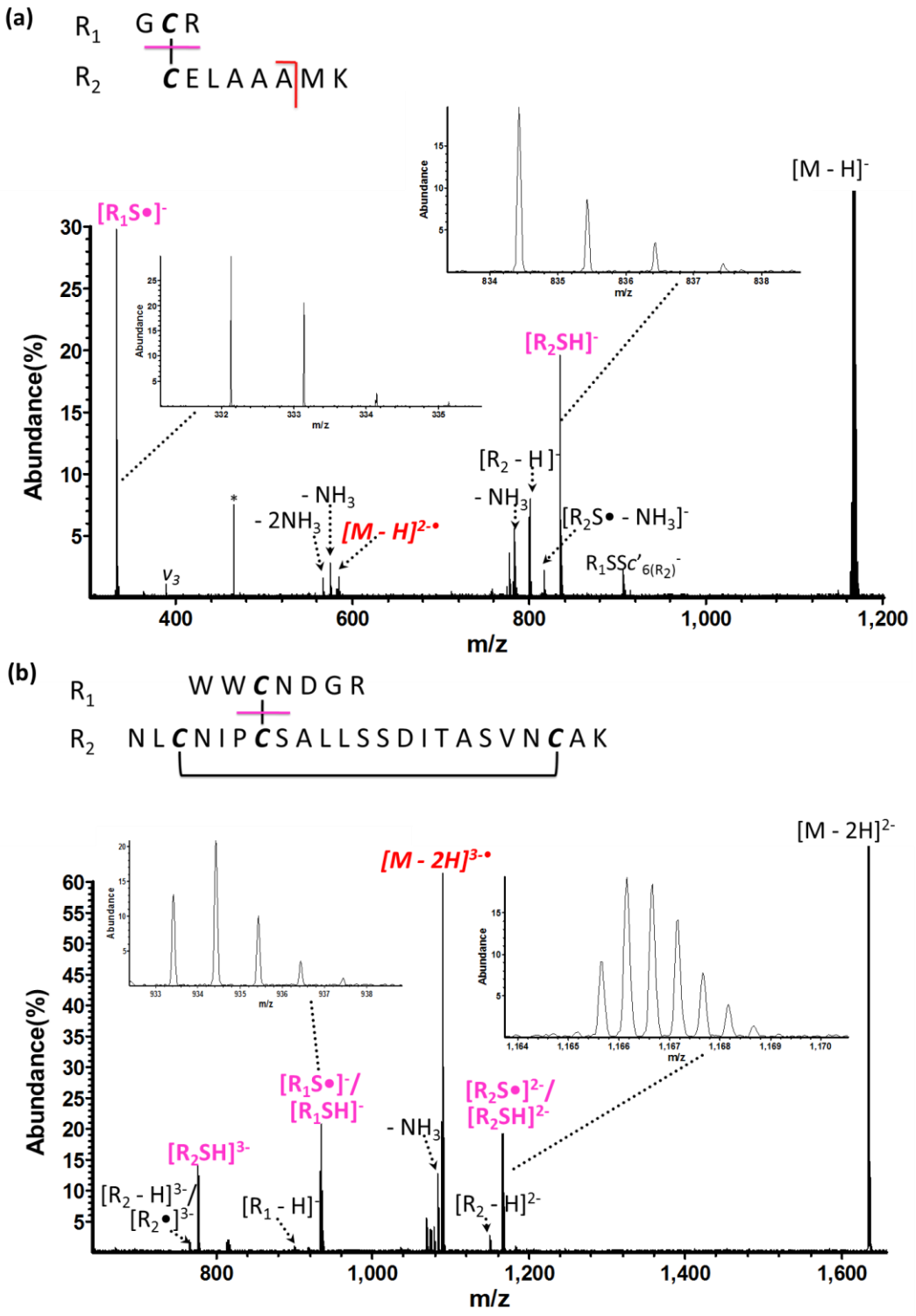

Figure 4.2. niECD of (a) singly- and (b) doubly-deprotonated trypsin-derived disulfide-linked insulin peptide pairs. For the singly-deprotonated peptide pair, irradiation was performed with 4.5 eV electrons for 10 seconds; for the doubly-deprotonated species, 5.5 eV electrons were used for the same time.

In the second species from lysozyme proteolysis, the peptide chain R_1 WWCNDGR (residues 62-68) is disulfide-linked to chain R_2 NLCNIPCSALLSSDITASVNCAK (residues 74-96) with an additional intramolecular disulfide bond between cysteine 3 and cysteine 21 of chain R_2, aside from the intermolecular disulfide bridge between cysteine 3 of chain R_1 and cysteine 7 of chain R_2. niECD of the doubly-charged peptide pair is demonstrated in Figure 4.2(b). Again, higher electron energy was necessary for the precursor ion with increased charge state. 5.5 eV electron irradiation yielded maximum electron capture signal $[M - 2H]^{3-\bullet}$. As expected, the spectrum looks very similar to that of the doubly-charged insulin peptide pair. Ammonia loss from the charge-increased radical intermediate is observed in the spectrum. niECD generates prominent signals corresponding to one singly-charged and one doubly-charged free monomer of the peptide pair and, thus, to cleavage of the S-S bond. Both the monomers are comprised of a mixture of odd- and even-electron fragments based on their isotopic patterns. Similar to the doubly-charged insulin peptide, these two characteristic product ion peaks can be easily identified, allowing facile detection of the disulfide-bound peptides within a complex proteolytic mixture. A triply-charged species of peptide chain R_2, containing higher charge state than the precursor ion is observed as well. Singly-charged peptide chain R_1, doubly- and triply-charged peptide chain R_2 with lack of a sulfur atom are also produced to a small extent in niECD, arising from cleavage at a C-S bond. No backbone fragmentation was obtained from niECD for this peptide pair, which again suggests that, similar to ECD/ETD, S-S disulfide bond cleavage is the more favored dissociation pathway in niECD, and this preference can serve as a suitable tool for identifying disulfide linkages in peptides. Taken collectively, all the data for the natural disulfides

described above are consistent with preferential cleavage of the S-S bond of the peptide pairs to yield free peptide monomers in niECD, analogous with conventional ECD/ETD.

4.3.3 niECD of Disulfide-Containing Cross-Linked Peptides

In addition to native disulfide bonds, the niECD fragmentation pathways of cross-linked peptides containing a disulfide-linked cross-linker is also of great interest. Ubiquitin was selected as the model protein and reacted with DTSSP, a cystine-like disulfide-containing cross-linker. DTSSP includes *N*-hydroxysuccinimide (NHS) esters at both ends, allowing reaction with lysine side chains in the protein. The structure of DTSSP is shown in Scheme 4.2(a). Following the cross-linking reaction, the cross-linked protein was enzymatically digested by trypsin and Glu-C, respectively. As expected, a series of intermolecularly cross-linked peptides, intramolecularly cross-linked peptides, and dead-end products were observed in the mass spectrum. Only intermolecularly cross-linked peptides can provide information on inter-protein interactions and are therefore the interest of the study here. The structures of niECD product ions from intermolecularly cross-linked peptides are shown in Scheme 4.2(b).

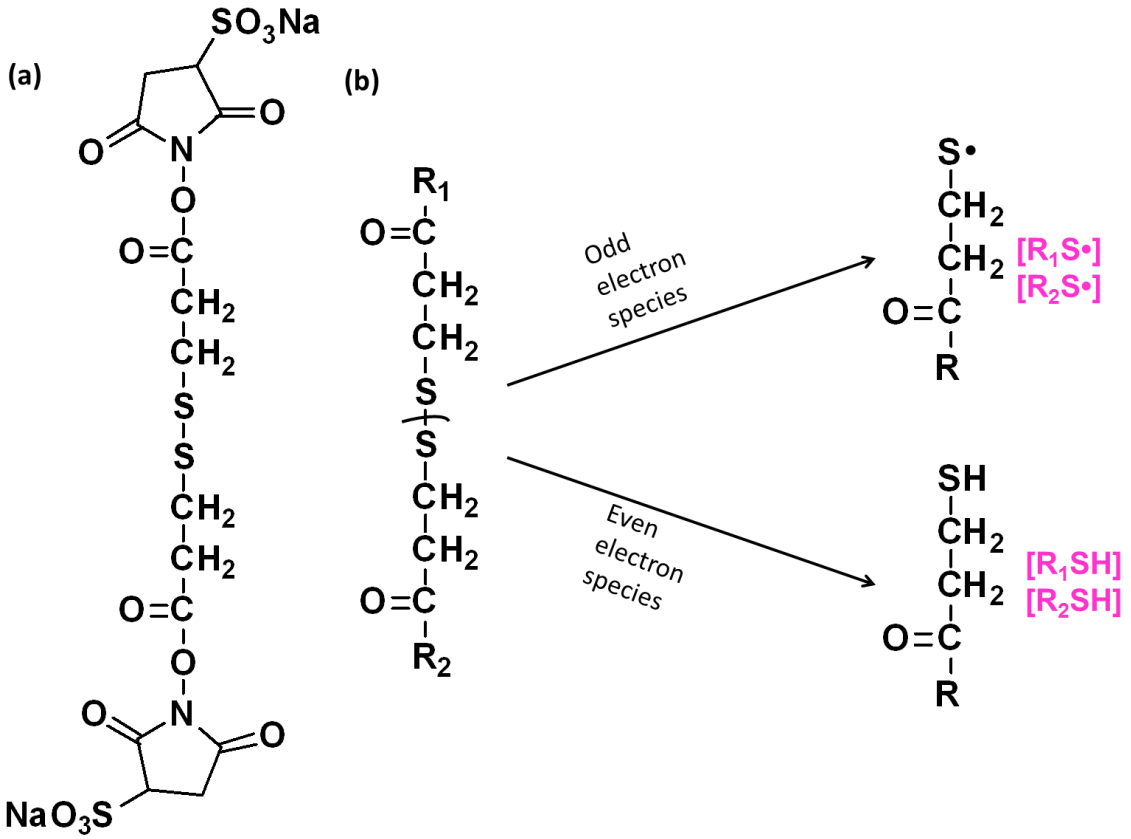

Scheme 4.2. (a) Structure of the cross-linker DTSSP. (b) Structures and nomenclature used for product ions of DTSSP cross-linked peptides. The only cleavage observed in the cross-linking region is the S-S bond, labeled in purple.

niECD of a tryptic ubiquitin peptide pair is shown in Figure 4.3. The peptide IQDKEGIPPDQQR (referred to as chain R_1), corresponding to residues 30-42, is intermolecularly cross-linked to LIFAGKQLEDGR (referred to as chain R_2), corresponding to residues 43-54, at lysine residues. In this example, the cross-links introduced by DTSSP dissociate in an analogous manner to native disulfide bridges. Similar to the doubly-charged precursor ions discussed above, irradiation with higher energy electrons (5.5 eV) was required for maximum electron capture. A charge-increased radical intermediate, $[M - 2H]^{3-\bullet}$, together with NH_3 deficient and CO_2 deficient radical ions were produced upon irradiation. With the exception of the electron capture species, doubly-charged R_1 chain and singly-charged R_2 chain, resulting from cleavage of

the S-S bond, are the most abundant product ions observed in the niECD spectrum. Similarly, the expanded views of these two peaks show that both of the peptide monomers correspond to a mixture of odd- and even-electron species. Particularly, a triply-charged R_1 chain ($[R_1SH]^{3-}$) is observed. It is interesting to note that C-S bond cleavage is absent for this cross-linked peptide pair, whereas low abundance C-S bond fragments could be observed for some naturally occurring cystine disulfides. Moreover, chain R_1 and chain R_2 are cleaved to generate some backbone fragments. z_5 and z_6 sequence ions from chain R_2 do not involve the cross-linked lysine. The z_{11} product ion from the R_1 chain and the c_6 product ion from the R_2 chain are cross-linked to the intact R_2 chain or R_1 chain, respectively, through the intact cross-linker. Therefore, niECD of peptides cross-linked by a disulfide-containing cross-linker generates similar fragmentation patterns to those of natural disulfide-containing peptides. One challenge remaining in chemical cross-linking experiments coupled with mass spectrometry is that low abundance cross-linked peptides are challenging to detect among the plenitude of other potentially higher ionizing proteolytic fragments. The unique niECD fragments observed here, associated with preferential and selective S-S bond cleavage, may be used to assign cross-linked peptides in a background of non cross-linked peptides.

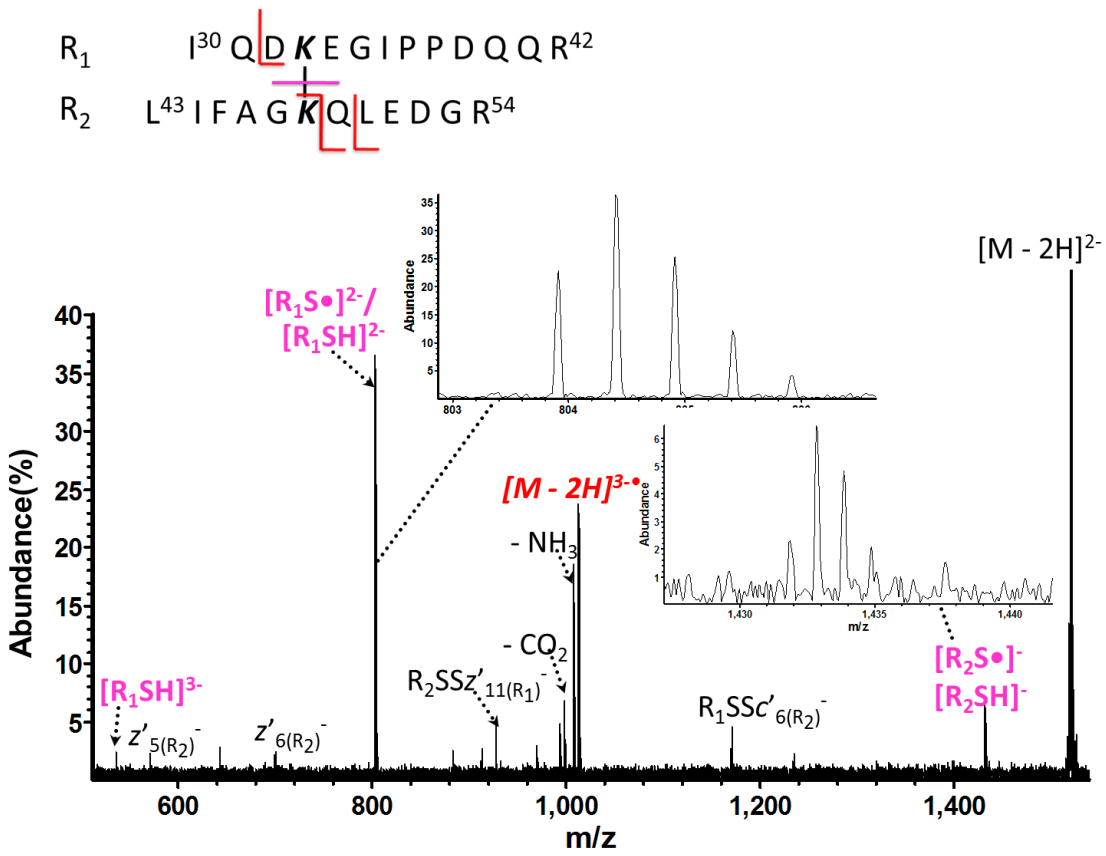

Figure 4.3. niECD of a doubly-deprotonated cross-linked ubiquitin peptide pair (DTSSP cross-linked ubiquitin was digested with trypsin). Precursor ions were irradiated with 5.5 eV electrons for 10 seconds.

An analogous niECD experiment was conducted on Glu-C-digested ubiquitin cross-linked peptides (Figure 4.4). Peptide chain R_1 GIPPDQQRLIFAGKQLE (residues 35-51) was cross-linked to peptide chain R_2 DGRTLSDYNIQKE (residues 52-64). This DTSSP-cross-linked peptide pair again yields similar niECD results to natural cystine disulfide-containing peptides, and to the tryptic cross-linked peptides shown above. Electron capture at 5.5 eV by the doubly-deprotonated precursor ion lead to dissociation of the resultant charge-increased distonic ion. Neutral losses such as NH_3 and CO_2 are also observed following the electron capture process. S-S bond cleavage is again the dominant dissociation pathway observed in niECD, resulting in the doubly-charged R_2

chain ($[R_2S\bullet]^{2-}$), and the singly- as well as doubly-charged R_1 chain ($[R_1SH]^-$ and $[R_1SH]^{2-}$) of the peptide dimer. Intriguingly, for this peptide pair, the R_2 chain is present only in the odd-electron form, while the R_1 chain only is observed in even-electron form. Because most of the R_2 chain is singly charged, a lower charge state compared with the doubly-charged R_1 chain, this finding is opposite to what would be expected according to the mechanism proposed for conventional ECD.[25] In contrast, the odd-electron R_1 chain is the longer peptide chain within the peptide dimer, consistent with the observation that longer peptides tend to retain the extra hydrogen, both in the niECD work shown above, and in previous ECD experiments.[52] A number of *c*' and $z^{\bullet}$ sequence ions, one of which is triply charged, were also produced for this peptide pair. Overall, niECD of cross-linked peptides results in efficient dissociation of disulfide bonds, and generates characteristic "signatures" in the resulting tandem mass spectra. Sequence information, including cross-linking sites, can be further obtained through MS^3 of the resulting fragment ions. Such information can subsequently be used to generate distance constraints, allowing approximation of the structure of the protein, and determination of the interaction site.

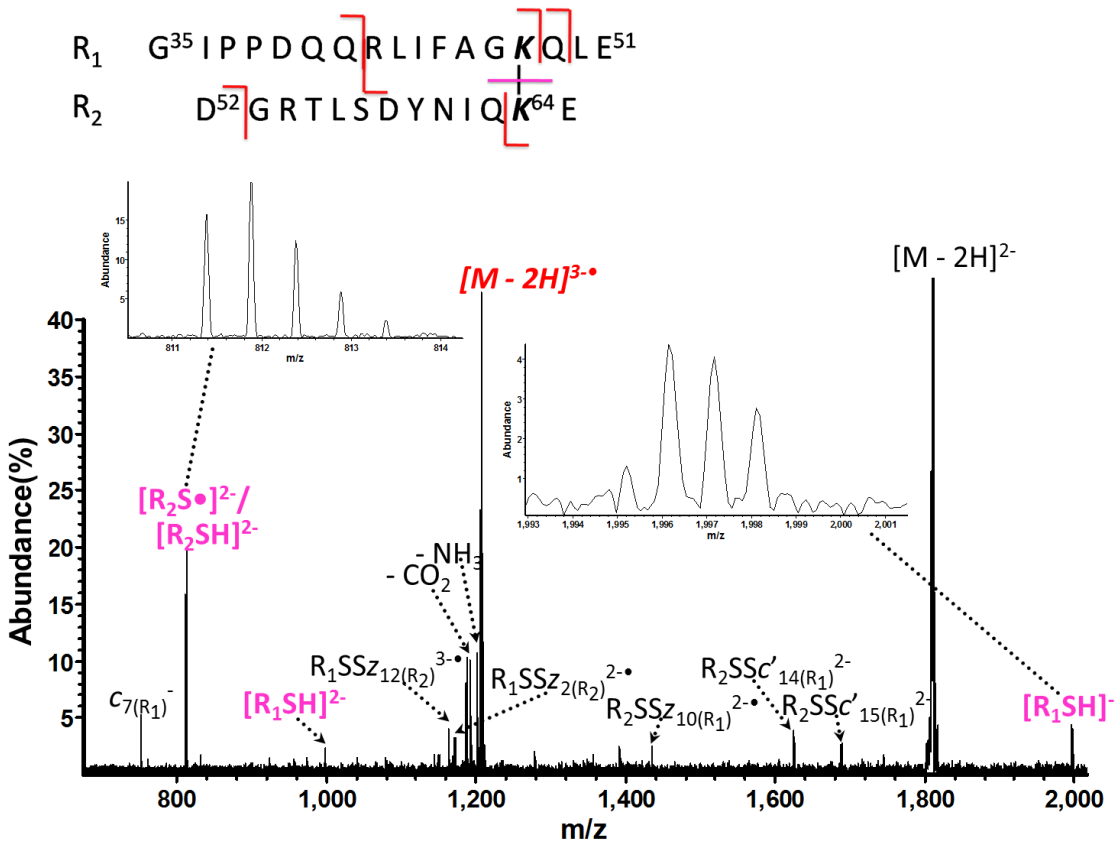

Figure 4.4. niECD of a doubly-deprotonated cross-linked ubiquitin peptide pair (DTSSP cross-linked ubiquitin was digested with Glu-C). Precursor ions were irradiated with 5.5 eV electrons for 10 seconds.

4.4 Conclusion

This Chapter shows that disulfide-bound peptide pairs, including both naturally occurring disulfides and cross-linked products from cystine-based reagents, exhibit niECD dissociation patterns very similar to those in positive ion ECD/ETD. S-S bond cleavage constitutes the dominant fragmentation pathway and can serve as "signature" fragments for rapid detection and identification of disulfide-linked peptides in complex mixtures. niECD also generates limited C-S bond cleavage and low abundance backbone bond cleavage. The preference for cleavage of the S-S bond in niECD renders it a promising tool for characterizing disulfide-bound peptides. This Chapter also sheds some

additional light onto the niECD mechanism. The dissociation chemistry in niECD is similar to ECD/ETD in many aspects, including competitive dissociation at disulfide bonds within peptides, both odd- and even-electron species generated from cleavage of an S-S bond, as well as *c*'/*z*˙ type backbone fragments. This observation further suggests that niECD proceeds through a similar mechanism as conventional ECD, –including both the hot hydrogen mechanism and direct electron capture through space or through bond.

4.5 References

1. Betz, S. F. Disulfide bonds and the stability of globular-proteins. *Protein Sci.* **1993**, *2*, 1551-1558.
2. Pace, C. N.; Grimsley, G.; Thomson, J.; Barnett, B. Conformational stability and activity of ribonuclease T1 with zero, one, and two intact disulfide bonds. *J. Biol. Chem.* **1988**, *263*, 11820-11825.
3. Wedemeyer, W. J.; Welker, E.; Narayan, M.; Scheraga, H. A. Disulfide bonds and protein folding. *Biochem.* **2000**, *39*, 4207-4216.
4. Creighton, T. E. Disulphide bonds and protein stability. *BioEssays.* **1988**, *8*, 57-63.
5. Clarke, J.; Fersht, A. R. Engineered disulfide bonds as probes of the folding pathway of barnase: increasing the stability of proteins against the rate of denaturation. *Biochem.* **1993**, *32*, 4322-4329.
6. Bennett, K. L.; Kussmann, M.; Mikkelsen, M.; Roepstorff, P.; Björk, P.; Godzwon, M.; Sörensen, P. Chemical cross‐linking with thiol‐cleavable reagents combined with differential mass spectrometric peptide mapping—A novel approach to assess intermolecular protein contacts. *Protein Sci.* **2000**, *9*, 1503-1518.
7. Peterson, J. J.; Young, M. M.; Takemoto, L. J. Probing alpha-crystallin structure using chemical cross-linkers and mass spectrometry. *Mol. Vis.* **2004**, *10*, 857-866.
8. Sinz, A. Chemical cross‐linking and mass spectrometry to map three‐dimensional protein structures and protein–protein interactions. *Mass Spectrom. Rev.* **2006**, *25*, 663-682.
9. Smith, D. L.; Zhou, Z. Strategies for locating disulfide bonds in proteins. *Methods Enzymol.* **1990**, *193*, 374.
10. Gorman, J. J.; Wallis, T. P.; Pitt, J. J. Protein disulfide bond determination by mass spectrometry. *Mass Spectrom. Rev.* **2002**, *21*, 183-216.
11. Loo, J. A.; Edmonds, C. G.; Udseth, H. R.; Smith, R. D. Effect of reducing disulfide-containing proteins on electrospray ionization mass spectra. *Anal. Chem.* **1990**, *62*, 693-698.
12. Hogan, J. M.; McLuckey, S. A. Charge state dependent collision‐induced dissociation of native and reduced porcine elastase. *J. Mass Spectrom.* **2003**, *38*,

245-256.
13. Stephenson, J. L.; Cargile, B. J.; McLuckey, S. A. Ion trap collisional activation of disulfide linkage intact and reduced multiply protonated polypeptides. *Rapid Commun. Mass Spectrom.* **1999**, *13*, 2040-2048.
14. Bean, M. F.; Carr, S. A. Characterization of disulfide bond position in proteins and sequence analysis of cystine-bridged peptides by tandem mass spectrometry. *Anal. Biochem.* **1992**, *201*, 216-226.
15. King, G. J.; Jones, A.; Kobe, B.; Huber, T.; Mouradov, D.; Hume, D. A.; Ross, I. L. Identification of disulfide-containing chemical cross-links in proteins using MALDI-TOF/TOF-mass spectrometry. *Anal. Chem.* **2008**, *80*, 5036-5043.
16. Fung, Y.; Kjeldsen, F.; Silivra, O. A.; Chan, T.; Zubarev, R. A. Facile disulfide bond cleavage in gaseous peptide and protein cations by ultraviolet photodissociation at 157 nm. *Angew. Chem.* **2005**, *117*, 6557-6561.
17. Agarwal, A.; Diedrich, J. K.; Julian, R. R. Direct elucidation of disulfide bond partners using ultraviolet photodissociation mass spectrometry. *Anal. Chem.* **2011**, *83*, 6455-6458.
18. Zubarev, R. A.; Kelleher, N. L.; McLafferty, F. W. Electron capture dissociation of multiply charged protein cations. A nonergodic process. *J. Am. Chem. Soc.* **1998**, *120*, 3265-3266.
19. Cooper, H. J.; Håkansson, K.; Marshall, A. G. The role of electron capture dissociation in biomolecular analysis. *Mass Spectrom. Rev.* **2005**, *24*, 201-222.
20. Syka, J. E.; Coon, J. J.; Schroeder, M. J.; Shabanowitz, J.; Hunt, D. F. Peptide and protein sequence analysis by electron transfer dissociation mass spectrometry. *Proc. Natl. Acad. Sci. U. S. A.* **2004**, *101*, 9528-9533.
21. Stensballe, A.; Jensen, O. N.; Olsen, J. V.; Haselmann, K. F.; Zubarev, R. A. Electron capture dissociation of singly and multiply phosphorylated peptides. *Rapid Commun. Mass Spectrom.* **2000**, *14*, 1793-1800.
22. Håkansson, K.; Cooper, H. J.; Emmett, M. R.; Costello, C. E.; Marshall, A. G.; Nilsson, C. L. Electron capture dissociation and infrared multiphoton dissociation MS/MS of an N-glycosylated tryptic peptide to yield complementary sequence information. *Anal. Chem.* **2001**, *73*, 4530-4536.
23. Mirgorodskaya, E.; Hassan, H.; Clausen, H.; Roepstorff, P. Mass spectrometric determination of O-glycosylation sites using β-elimination and partial acid hydrolysis. *Anal. Chem.* **2001**, *73*, 1263-1269.
24. Shi, S. D.-H.; Hemling, M. E.; Carr, S. A.; Horn, D. M.; Lindh, I.; McLafferty, F. W. Phosphopeptide/phosphoprotein mapping by electron capture dissociation mass spectrometry. *Anal. Chem.* **2001**, *73*, 19-22.
25. Zubarev, R. A.; Kruger, N. A.; Fridriksson, E. K.; Lewis, M. A.; Horn, D. M.; Carpenter, B. K.; McLafferty, F. W. Electron capture dissociation of gaseous multiply-charged proteins is favored at disulfide bonds and other sites of high hydrogen atom affinity. *J. Am. Chem. Soc.* **1999**, *121*, 2857-2862.
26. Ge, Y.; Lawhorn, B. G.; ElNaggar, M.; Strauss, E.; Park, J.-H.; Begley, T. P.; McLafferty, F. W. Top down characterization of larger proteins (45 kDa) by electron capture dissociation mass spectrometry. *J. Am. Chem. Soc.* **2002**, *124*, 672-678.
27. Gunawardena, H. P.; Gorenstein, L.; Erickson, D. E.; Xia, Y.; McLuckey, S. A.

Electron transfer dissociation of multiply protonated and fixed charge disulfide linked polypeptides. *Int. J. Mass Spectrom.* **2007**, *265*, 130-138.
28. Cole, S. R.; Ma, X.; Zhang, X.; Xia, Y. Electron transfer dissociation (ETD) of peptides containing intrachain disulfide bonds. *J. Am. Soc. Mass. Spectrom.* **2012**, *23*, 310-320.
29. Sawicka, A.; Skurski, P.; Hudgins, R. R.; Simons, J. Model calculations relevant to disulfide bond cleavage via electron capture influenced by positively charged groups. *J. Phys. Chem. B* **2003**, *107*, 13505-13511.
30. Sobczyk, M.; Neff, D.; Simons, J. Theoretical study of through-space and through-bond electron transfer within positively charged peptides in the gas phase. *Int. J. Mass Spectrom.* **2008**, *269*, 149-164.
31. Ganisl, B.; Breuker, K. Does Electron Capture Dissociation Cleave Protein Disulfide Bonds? *ChemistryOpen* **2012**, *1*, 260-268.
32. Good, D. M.; Wirtala, M.; McAlister, G. C.; Coon, J. J. Performance characteristics of electron transfer dissociation mass spectrometry. *Mol. Cell. Proteomics* **2007**, *6*, 1942-1951.
33. Kalli, A.; Håkansson, K. Comparison of the electron capture dissociation fragmentation behavior of doubly and triply protonated peptides from trypsin, Glu-C, and chymotrypsin digestion. *J. Proteome Res.* **2008**, *7*, 2834-2844.
34. Kalli, A.; Håkansson, K. Electron capture dissociation of highly charged proteolytic peptides from Lys N, Lys C and Glu C digestion. *Mol. Biosyst.* **2010**, *6*, 1668-1681.
35. Chrisman, P. A.; McLuckey, S. A. Dissociations of disulfide-linked gaseous polypeptide/protein anions: ion chemistry with implications for protein identification and characterization. *J. Proteome Res.* **2002**, *1*, 549-557.
36. Bilusich, D.; Maselli, V. M.; Brinkworth, C. S.; Samguina, T.; Lebedev, A. T.; Bowie, J. H. Direct identification of intramolecular disulfide links in peptides using negative ion electrospray mass spectra of underivatised peptides. A joint experimental and theoretical study. *Rapid Commun. Mass Spectrom.* **2005**, *19*, 3063-3074.
37. Zhang, M.; Kaltashov, I. A. Mapping of protein disulfide bonds using negative ion fragmentation with a broadband precursor selection. *Anal. Chem.* **2006**, *78*, 4820-4829.
38. Calabrese, A. N.; Good, N. J.; Wang, T.; He, J.; Bowie, J. H.; Pukala, T. L. A negative ion mass spectrometry approach to identify cross-linked peptides utilizing characteristic disulfide fragmentations. *J. Am. Soc. Mass. Spectrom.* **2012**, *23*, 1364-1375.
39. Kalli, A.; Håkansson, K. Preferential cleavage of SS and CS bonds in electron detachment dissociation and infrared multiphoton dissociation of disulfide-linked peptide anions. *Int. J. Mass Spectrom.* **2007**, *263*, 71-81.
40. Payne, A. H.; Glish, G. L. Gas-phase ion/ion interactions between peptides or proteins and iron ions in a quadrupole ion trap. *Int. J. Mass Spectrom.* **2001**, *204*, 47-54.
41. Yoo, H. J.; Wang, N.; Zhuang, S.; Song, H.; Håkansson, K. Negative-ion electron capture dissociation: radical-driven fragmentation of charge-increased gaseous peptide anions. *J. Am. Chem. Soc.* **2011**, *133*, 16790-16793.

42. Hersberger, K. E.; Håkansson, K. Characterization of O-Sulfopeptides by Negative Ion Mode Tandem Mass Spectrometry: Superior Performance of Negative Ion Electron Capture Dissociation. *Anal. Chem.* **2012**, *84*, 6370-6377.
43. Yang, J.; Mo, J.; Adamson, J. T.; Håkansson, K. Characterization of oligodeoxynucleotides by electron detachment dissociation Fourier transform ion cyclotron resonance mass spectrometry. *Anal. Chem.* **2005**, *77*, 1876-1882.
44. Tsybin, Y. O.; Witt, M.; Baykut, G.; Kjeldsen, F.; Håkansson, P. Combined infrared multiphoton dissociation and electron capture dissociation with a hollow electron beam in Fourier transform ion cyclotron resonance mass spectrometry. *Rapid Commun. Mass Spectrom.* **2003**, *17*, 1759-1768.
45. Senko, M. W.; Canterbury, J. D.; Guan, S.; Marshall, A. G. A high‐performance modular data system for Fourier transform ion cyclotron resonance mass spectrometry. *Rapid Commun. Mass Spectrom.* **1996**, *10*, 1839-1844.
46. Ledford Jr, E. B.; Rempel, D. L.; Gross, M. Space charge effects in fourier transform mass spectrometry. II. mass calibration. *Anal. Chem.* **1984**, *56*, 2744-2748.
47. O'Connor, P. B.; Lin, C.; Cournoyer, J. J.; Pittman, J. L.; Belyayev, M.; Budnik, B. A. Long-lived electron capture dissociation product ions experience radical migration via hydrogen abstraction. *J. Am. Soc. Mass. Spectrom.* **2006**, *17*, 576-585.
48. Chrisman, P. A.; Pitteri, S. J.; Hogan, J. M.; McLuckey, S. A. SO2- electron transfer ion/ion reactions with disulfide linked polypeptide ions. *J. Am. Soc. Mass. Spectrom.* **2005**, *16*, 1020-1030.
49. Fung, Y. E.; Adams, C. M.; Zubarev, R. A. Electron ionization dissociation of singly and multiply charged peptides. *J. Am. Chem. Soc.* **2009**, *131*, 9977-9985.
50. Cooper, H. J.; Hudgins, R. R.; Håkansson, K.; Marshall, A. G. Characterization of amino acid side chain losses in electron capture dissociation. *J. Am. Soc. Mass. Spectrom.* **2002**, *13*, 241-249.
51. Fälth, M.; Savitski, M. M.; Nielsen, M. L.; Kjeldsen, F.; Andren, P. E.; Zubarev, R. A. Analytical utility of small neutral losses from reduced species in electron capture dissociation studied using SwedECD database. *Anal. Chem.* **2008**, *80*, 8089-8094.
52. Greer, T. J.; Wang, B.; Hakansson, K. Characterization of peptides linked by disulfide-containing crosslinkers with various tandem mass spectrometric approaches, In Proc. *The 57th ASMS Conference on Mass Spectrometry and Allied Topics*, Philadelphia, PA, May 31-June 4, 2009.

Chapter 5

Negative Ion Electron Capture Dissociation (niECD) of N-linked and O-linked Glycopeptides with Neutral and Sialylated Glycans

5.1 Introduction

Among myriad post-translational modifications (PTMs), protein glycosylation, which involves the attachment of oligosaccharides to proteins, represents one of the most ubiquitous in eukaryotic cells, and it has been suggested that more than half of the proteins present are glycosylated.[1-3] Glycosylation serves key functions in an array of biological processes, including cell to cell recognition[4, 5], immune response[6, 7], protein folding[4, 8, 9], as well as protein solubility and stability[5]. Moreover, alternation in glycosylation can lead to protein malfunction and has been implicated in a variety of human diseases.[10-12] Particularly, due to its pivotal role in cancer biology, sialic acid-

containing glycoproteins have attracted a great deal of attention and have been extensively investigated as potential tumor markers for cancer detection.[13, 14] A general increase in sialylation and changes in sialic acid linkage type have been linked to cancer metastasis and inflammation.[15-21] Despite its frequency and significant influence on cellular systems, structural elucidation of glycosylation remains hindered due to its great complexity and diversity. In order to fully understand its relevance for cellular functions, complete glycosylation characterization requires different tiers of information with respect to protein identity, glycan composition as well as the site of glycosylation and its occupancy. Among these, site-specific glycosylation analysis presents one of the key obstacles in mass spectrometry (MS) analysis due to the lability of glycosidic bonds, which require less energy to cleave compared with the amide bonds in the peptide backbone.[22]

Though other forms have been reported,[1, 23] protein glycosylation can be categorized into two primary classes, N-linked and O-linked glycosylation.[24] In *N*-glycosylation, glycans with a common pentasaccharide core structure are covalently attached to asparagine residues through a nitrogen atom in the specific peptide sequence Asn-Xxx-Ser/Thr (Xxx may be any amino acid except proline). The presence of the consensus sequeon makes *N*-glycosylation site determination relatively predictable. More specific motifs such as D/E-X-N-X-S/T have been reported for *N*-glycosylation as well.[25, 26] By contrast, the more prevalent *O*-glycosylation exhibits a much higher degree of diversity and heterogeneity as O-linked glycosylation does not have a known amino acid sequence motif or one single saccharide core region for all O-linked glycans. *O*-glycans can be connected to the peptide backbone at any serine or threonine residue,

rendering structural analysis more intricate, and thus considerably less is understood about *O*-glycosylation compared with *N*-glycosylation. Moreover, *O*-glycans are frequently found in regions rich in serine and threonines, further complicating site-specific characterization.[27, 28] The variety of distinct oligosaccharide structures as well as the diversity of glycan attachment sites leads to a substantial degree of heterogeneity in *O*-glycosylation.

With the benefits of high selectivity, sensitivity and specificity, mass spectrometry has become increasingly attractive for structural elucidation of protein glycosylation.[2, 22, 29-31] In particular, tandem MS (MS/MS) has emerged as one of the most versatile and powerful techniques capable of providing glycan structural information from MS/MS data, depending on the specific activation method employed. The standard strategy for MS-based analysis of protein glycosylation typically involves a combination of enzymatic digestion of glycoproteins, separation or enrichment of glycopeptides, followed by glycopeptide analysis with MS and MS/MS.[32-37] Various MS/MS techniques have been utilized to characterize glycopeptides. In general, collision activated dissociation (CAD),[2, 38-42] infrared multiphoton dissociation (IRMPD)[43-45] and post-source decay (PSD)[46-48] primarily provide information about monosaccharide connectivity in the glycan, as preferential cleavages at glycosidic bonds in the glycan moiety are observed with little or no fragmentation at the peptide backbone. Consequently, these MS/MS activation techniques are effective tools for elucidating the carbohydrate portion of glycopeptides, while the peptide sequence remains undefined and the direct assignment of glycan attachment sites is hampered.[2, 39, 41, 44] For *N*-glycosylation, in certain cases, glycan sites can still be deduced as a result of its specific

peptide sequon.[2, 3, 39] Additionally, *N*-glycan structures are routinely released from glycoproteins using the selective glycosidic enzyme, peptide-N-glycosidase F (PNGase F), which cleaves the amide bond between the glycan and the asparagine residue, allowing structural analysis of glycans and peptides separately.[24, 49] Deduction of glycan attachment sites is also possible based on the mass change in the peptide portion introduced by converting asparagine residues to aspartic acid residues upon PNGase F-induced glycan release,[50, 51] however, this approach greatly increases analysis time and is labor intensive. Unlike *N*-glycosylation, a selective enzyme that can cleave all *O*-glycans is not available for global analysis of *O*-glycosylation, and hence, there is no universal method established for release of *O*-glycans.[52, 53] The lack of a reliable peptide consensus sequence and a specific enzyme to cleave the glycans, as well as the vast heterogeneity of *O*-glycan core structures, make structural characterization, particularly site determination of *O*-glycosylation, a formidable analytical task.[39]

In order to improve site-specific determination of relationships between glycans and proteins, electron-based MS/MS techniques have been applied as alternative activation strategies for glycopeptide analysis. Electron capture dissociation (ECD)[54, 55] and electron transfer dissociation (ETD),[56] which involve capture of a low-energy electron or electron transfer to multiply protonated precursor ions, respectively, are valuable tandem MS approaches for PTM characterization. These two radical-driven dissociation techniques are well-known to generate *c* and *z* type peptide backbone fragments without eliminating the thermolabile modifications.[44, 57-59] For glycosylated peptides, unlike CAD or IRMPD, ECD and ETD generally lead to dissociation at the polypeptide backbone with retention of the labile saccharide moiety, rendering localization of their

site of attachment possible.[41, 42, 44, 45, 60] Thus, ECD/ETD are well suited for direct assignment of protein-glycan connectivity. A combination of the slow-heating CAD/IRMPD and radical-driven ECD/ETD has also demonstrated to be a powerful strategy for glycoprotein studies by yielding orthogonal structural information.[41, 42, 45] However, one drawback with ECD and ETD is that they require positively charged precursor ions with at least two charges whereas acidic glycopeptides, e.g., sialylated ones, are readily deprotonated. Furthermore, ECD/ETD are charge-state dependent, favoring high charge states and a decrease in fragmentation efficiency has been reported for ETD as the precursor ion m/z increases.[61-63] Unfortunately, glycopeptides tend to have lower charge states and higher m/z ratios such that further activation is usually needed to improve the sequence coverage by combining IRMPD and ECD, or CAD and ETD.[42, 45]

The great majority of glycopeptide MS experiments in the current literature targets positively charged precursor ions.[2, 64] However, negative ion mode has compelling benefits that are worth pursuing, particularly for acidic glycopeptides. Acidic saccharides such as sialic acids render glycopeptides substantially less basic and preferentially deprotonated, thus exhibiting increased ionization efficiency, improved sensitivity, and less ion suppression in negative ion mode. Negative mode MS and MS/MS have proven beneficial for glycopeptide analysis, offering advantages such as enhanced detection of glycopeptides as anions, sialylated ones in particular, unique dissociation pathways and complementary structural information as compared with positive ion mode.[38, 39, 65] However, CAD of peptide anions often involves complex backbone fragmentations as well as side chain losses, yielding less predictable cleavages compared with positive ion

CAD.[66] Ion-electron and ion-ion methods, such as electron detachment dissociation (EDD)[67] and similar negative electron transfer dissociation (NETD),[68] can also be applied for negative precursor ion dissociation. EDD of glycosylated peptides induces extensive glycan (glycosidic and cross-ring cleavages) and peptide (*a*/*x*, *b*/*y* ions) fragments, providing rich structural information but rendering data interpretation difficult.[69] Ultraviolet photodissociation (UVPD) is also a feasible choice for characterizing deprotonated glycopeptides: 193 nm UVPD has been investigated for negative ion mode *O*-glycopeptide analysis, in which *a*/*x*-type peptide fragments with intact glycan attached as well as glycan-specific ions were produced.[70]

The novel MS/MS technique operating in negative ion mode, negative ion electron capture dissociation (niECD),[71] which involves peptide anions capturing an electron within a specific energy range (3.5-6.5 eV) and generating *c*/*z*-type cleavages at the peptide backbone, may also be of interest as an activation technique for glycopeptide structural analysis. The analytical merit of niECD lies in its ECD-like fragmentation. Previous studies of phospho- and sulfopeptides demonstrated that, in niECD, peptide anions are fragmented in a manner highly analogous to positive mode ECD with generation of *c*/*z* fragment ions and without loss of labile substituents.[71, 72] For disulfide-linked peptides, preferential disulfide bond cleavage is observed in niECD (see Chapter 4), a characteristic phenomenon in conventional ECD/ETD.[73] Gas-phase zwitterion structures were proposed to be important for successful niECD and a positive charge is necessary to either serve as the site to capture the electron, or to promote the capture (see Chapter 3).[74] Based on our promising results from niECD of different modified peptides together with the similarity observed between niECD and ECD, we

hypothesized that glycopeptides should also benefit from niECD analysis and valuable structural information may be extracted from niECD spectra of glycopeptides. Thus, here, we expand the applicability of niECD towards protein glycosylation. niECD fragmentation behaviors for both N-linked and O-linked glycopeptides with neutral and sialylated glycans are explored.

5.2 Experimental

5.2.1 Reagents

Lectin from *Erythrina cristagalli,* human apo-transferrin, bovine fetuin, and protease E from *Streptomyces griseus* Type XIVin (pronase E) were from Sigma-Aldrich (St. Louis, MO), and trypsin from Promega (Madison, WI). Ammonium bicarbonate, isopropanol, methanol, acetonitrile, water, triethylamine, and formic acid were purchased from Fisher (Fair Lawn, NJ)

5.2.2 Lectin Preparation

0.15 mg of the lectin from *Erythrina cristagalli* was dissolved in 100 µL buffer solution containing 200 mM ammonium bicarbonate. 10 µL of 0.1 mg/mL trypsin was then added to accomplish digestion and the protein solution was incubated for 12 hours at 37 ℃. After digestion, the resulting peptide mixture was desalted with a C18 reverse-phase micro-column, ZipTip (Millipore, Billerica, MA), dried down in a vacuum concentrator (Eppendorf, Hamberg, Germany), and reconstituted in 50:50 isopropanol/water with 0.1% triethylamine (v/v) prior to MS analysis.

5.2.3 Human Apo-transferrin and Bovine Fetuin Preparation

20 nmol of human apo-transferrin or bovine fetuin in 500 μL buffer solution containing 50 mM NH_4HCO_3 was mixed with pronase E. Different protein-to-enzyme ratios of 1:1, 25:1, or 50:1 (w/w) were used to generate glycopeptides with different peptide lengths. The digestion proceeded at 37 ℃ from 2h to overnight. After digestion, the peptide mixture was desalted with graphitized carbon solid-phase extraction (SPE) cartridges (Supelco, Bellefonte, PA). The carbon cartridge was first activated with 3 mL of 0.1% formic acid in 80% acetonitrile/H_2O (v/v) and then washed with 3 mL of deionized water. The digest solution was loaded onto the cartridge and washed with 3 mL to 4.5 mL of water. Glycopeptides were then eluted with 1.5 mL of 0.1% formic acid (v/v) in 20%, 40%, or 60% acetonitrile/water (v/v), dried in vacuo and dissolved in 50:50 isopropanol/water with 0.1% triethylamine (v/v) as spray solvent in negative ion mode. For positive ion mode analysis, the samples were diluted with electrospray solvent consisting of 50:50 methanol/water with 0.1% formic acid.

5.2.4 FT-ICR Mass Spectrometry

Peptide digests were directly infused via an external Apollo II electrospray ion source (Bruker Daltonics, Billerica, MA) at a flow rate of 70 μL/h. All experiments were performed with an actively shielded 7 Tesla hybrid quadrupole (Q)-FT-ICR mass spectrometer (APEX-Q, Bruker Daltonics), as previously described.[75] For ESI, N_2 was used as both nebulizing gas (5 L/s) and drying gas (2.5 L/s). The drying gas temperature was set to 180˚C. Briefly, ions produced by ESI were accumulated in the first hexapole for 0.05 s, mass-selectively accumulated in the second hexapole collision cell for 0.5-4 s, transferred through high voltage ion optics, and captured in an Infinity ICR cell by

dynamic trapping. This accumulation sequence was looped up to three times to improve precursor ion abundance. For MS/MS experiments, mass-selective external accumulation of negatively-charged peptide ions was performed. For niECD, electrons were provided by an indirectly heated hollow dispenser cathode.[76] The cathode heating current was kept at 1.8 A, and the cathode voltage was pulsed to a bias voltage of – 5 to – 7 V for 5 s. A lens electrode located in front of the hollow cathode was kept 0.5-1 V more positive than the cathode bias voltage.

5.2.5 Data Analysis

All mass spectra were acquired with XMASS software (version 6.1, Bruker Daltonics) in broadband mode from m/z 200 to 3000 with 256K data points and summed over 10-32 scans. Data processing was performed with the MIDAS analysis software.[77] Data were zero filled once, Hanning apodized, and exported to Microsoft Excel for internal frequency-to-mass calibration with a two-term calibration equation.[78] Typically, internal calibration was performed with precursor ions and their electron-capture species as calibrants. Peaks in MS^n were assigned within 10 ppm error after internal calibration. Product ions were not assigned unless the S/N ratio was at least 3.

5.3 Results and Discussion

Glycopeptide fragment ions generated in niECD experiments are designated by combining peptide fragmentation nomenclature adapted from Roepstorff and Fohlman.[79]with oligosaccharide fragmentation nomenclature from Domon and Costello.[80] Peptide fragments are labeled with lowercase letters, whereas glycan fragments with uppercase letters. Two varieties of cleavages are generally observed in

MS/MS of glycans: glycosidic cleavages (B-, C-, Y-, Z-type ions) and cross-ring cleavages (A- and X-type ions). The former occurs between saccharide units, and the latter are cleavages across the carbohydrate rings. A system of monosaccharide symbols are used to represent the glycans according to the nomenclature of Varki et al.[81]

5.3.1 Glycopeptide with a Neutral Glycan

First, in order to evaluate the general dissociation pattern associated with glycopeptide anions in niECD, an N-glycosylated peptide, well characterized in the literature was examined. The niECD fragmentation behavior was mapped with a tryptic glycopeptide from the lectin of *Erythrina cristagalli* (UniProtKB/Swiss-Port P83410), consisting of amino acid residues 100-116 and one *N*-glycosylation site at asparagine (Asn) 113 with a known neutral xylose-type glycan.[82] The monoisotopic mass of the glycopeptide is 2999.3281 Da, consistent with the trend that trypsin digestion of glycoproteins tends to generate large size peptides.[2] The peptide sequence and glycan structure of this *N*-glycopeptide are shown in Figure 5.1.

For niECD, the doubly-charged glycopeptide anion was subjected to irradiation with 5.5 eV electrons for 5 seconds. The niECD spectrum of this glycopeptide and its corresponding dissociation sites (illustrated by lines denoting the cleavage sites) are also shown in Figure 5.1. A major reaction product was the charge-increased radical anion, $[M - 2H]^{3-\bullet}$, generated from electron capture by the doubly-charged precursor ion. The only type of cleavage observed at the peptide backbone is between N-Cα bonds, producing a series of *c* ions and one odd-electron *z* ion. The occurrence of *c*/*z*-type fragments is in accordance with what was previously reported for unmodified, phosphorylated, sulfated, and disulfide-linked peptide anions in niECD.[71-73] More

importantly, similar to the dissociation behavior in positive ion ECD, the labile glycan substituent was preserved upon the peptide backbone, which allows facile inference of the glycosylation site. Six contiguous *c*-type products generated in the niECD spectrum forms a peptide sequence tag that could be potentially used for protein searching and identification in a database. The missing c_1 ion may be produced but failed to be detected due to its small m/z ratio. The c_2 fragment, which involves cleavage at the N-terminal side of proline, is not registered in the spectrum either. Similarly, this type of fragmentation is known to be a disfavored channel in positive ion mode ECD, attributed to the cyclic structure of proline and the concomitant necessity to cleave two bonds.[83] Absent from the spectrum are also peptide backbone cleavages in the proximity of the glycosylated asparagine residue. Similar dissociation preferences have been reported in ECD and ETD spectra of glycopeptides.[44, 60, 84] The proposed explanation is that the bulky glycan moiety prevents access to the backbone carbonyl oxygens and thus sterically hinders cleavage close to glycosylation sites. It is interesting to note that mostly N-terminal *c* ions and only a few complementary C-terminal *z* ions are present in the niECD spectrum, likely due to the lower stability of radical *z* ions.[54] This observation is analogous to what was reported in previous ECD work of a very similar lectin glycopeptide.[44] However, this result is opposite to what was shown for ETD, in which primarily *z* ions were produced for the same glycopeptide.[41] Preferred generation of even-electron *c* ions has also been observed in other ECD studies,[60, 84-86] supporting that niECD proceeds through similar fragmentation channels as compared with positive ion ECD. In this example, the glycan can be confidently assigned to the first asparagine residue based on the N-X-S/T sequon for *N*-glycosylation. However, in cases where

multiple glycosylation sites are present, more complete sequence coverage may be necessary to positively identify the modification location. Such identification becomes more problematic for *O*-glycopeptides, as they lack a consensus sequence and tend to occur in sequence tracts with a high density of threonines and serines.

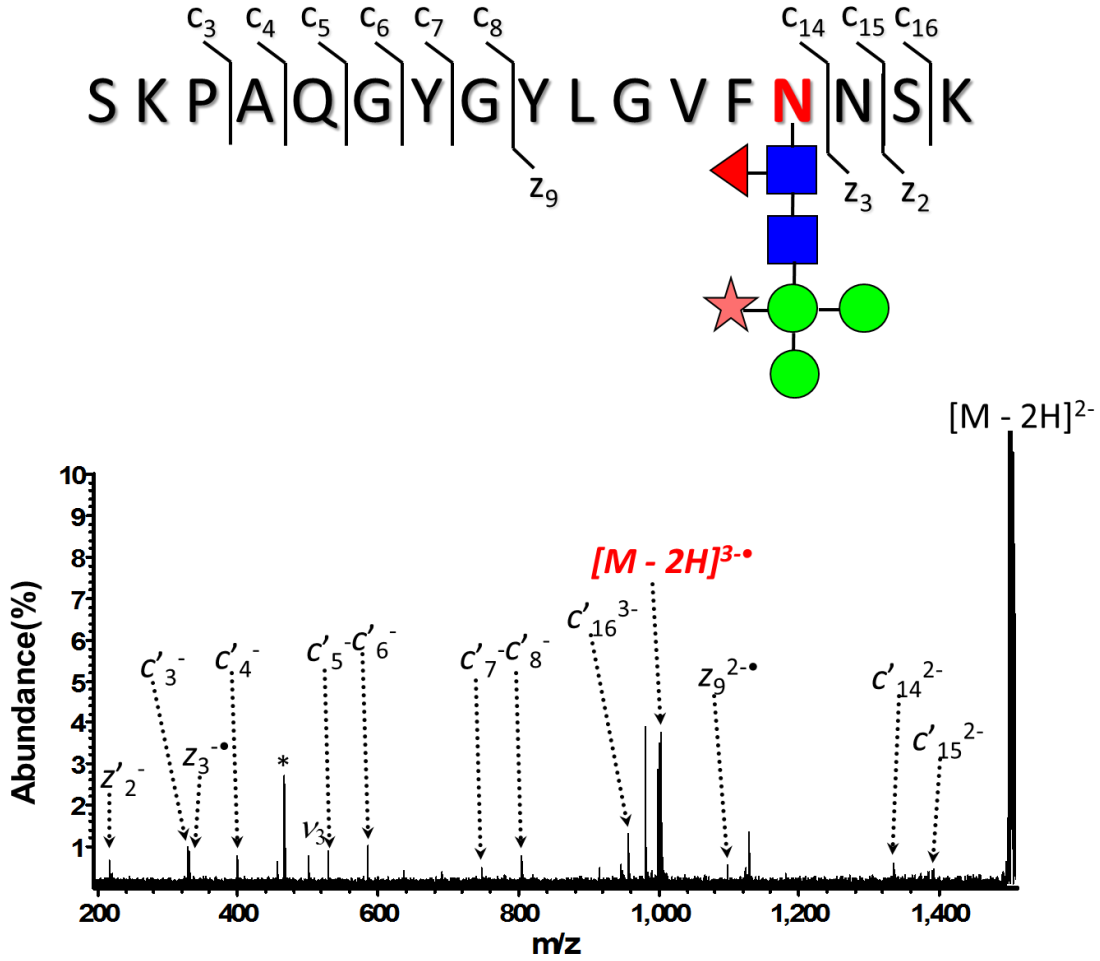

Figure 5.1. niECD (32scans, 5s irradiation, cathode bias -7.0 V) FT-ICR mass spectrum of a doubly-deprotonated *N*-glycopeptide obtained from trypsin digestion of *Erythrina cristagalli* lectin. The electron capture species is highlighted in red in the spectrum. ν_3 represents the third harmonic and * electronic noise. The fragmentation pattern is summarized on top of the spectrum. The glycosylation site in the peptide sequence is shown in red. In the diagram depicting glycopeptide structure, green circles indicate mannose, blue squares indicate *N*-acetylglucosamine, red triangles indicate fucose, and a rhombus indicates xylose.

This particular glycopeptide was also studied by the vibrational activation techniques CAD and IRMPD as well as the electron-mediated techniques ECD and ETD. The niECD fragmentation behavior was dramatically different from that in CAD and IRMPD, which primarily cleave glycosidic bonds in the glycan portion while leaving the peptide region intact.[41, 43] Conversely, the niECD data shown here looks almost identical to those observed in ECD by Hakansson et al.[44] and very similar to ETD results obtained by Hogan et al.[41] for the same glycopeptide, both in the appearance of various peptide backbone fragments as well as the absence of glycan-specific products. Therefore, for glycopeptides with neutral glycans, niECD appears to proceed very much like positive ion mode ECD/ETD.

5.3.2 MS Analysis of Sialyated Glycopeptides

Due to more abundant ion signal and less ion suppression, it is a more logical choice to perform negative ion mode analysis for acidic analytes. Thus, we moved on to investigate two model glycoproteins harboring acidic sialic acid oligosaccharides. Sialic acids (e.g., *N*-acetyl neuraminic acid, NeuAc) contain a carboxylic acid at the C-1 position of the six-member sugar ring and are frequently located at the terminal position of *N*- and *O*-glycans. Human apo-transferrin is a 77 kDa protein (UniProtKB/Swiss-Port P02787) and has several potential sites for both *N*- and *O*-glycosylation.[87, 88] Bovine fetuin (38 kDa protein, UniProtKB/Swiss-Port P12763) also has multiple putative sites for sialylated glycans.[89]

Both of these proteins were digested with pronase E, a protease mixture capable of cleaving every peptide bond in a protein nonspecifically, except for those near the glycosylation site.[90] The use of pronase takes advantage of steric hindrance from the

glycan moiety and hydrolyzes non-glycosylated portions of glycoproteins to free amino acids while leaving a short peptide tag surrounding the glycosylation site. This approach has the potential to determine glycan microheterogeneity at specific sites even in mixtures of proteins. On the other hand, traditional tryptic digestion primarily results in non-glycosylated peptides that tend to suppress glycopeptide signals. In addition, trypsin typically generates glycopeptides with large sizes that may not be optimal for MS analysis and do not fully represent the glycan heterogeneity. Trypsin also yields peptides with basic R or K residues at the C-terminus, decreasing the ionization efficiency in negative ion mode. Non-specific proteolysis by pronase followed by MS analysis has proven highly useful for site-specific glycosylation analysis of both *N*- and *O*-linked glycoproteins.[39, 65]

One example of MS analysis is provided in Figure 5.2, which depicts an ESI FT-ICR MS spectrum of human apo-transferrin digested by pronase E at 50:1 protein/enzyme ratio overnight. The top spectrum was obtained from electrospray ionization in positive ion mode using acidic spray solution (0.1% formic acid)routinely used in proteomics protocols. The bottom spectrum was obtained from spraying in negative ion mode using basic spray solution (0.1% triethylamine). The inverted triangles represent peaks of interest as they correspond to sialylated glycopeptides as determined by their accurate masses. In the positive mode analysis, acidic sialylated glycopeptides were generated at such low abundance that they are barely noticable. Non-glycopeptides and non-acidic glycopeptides dominate the spectrum, preventing detection of the less efficiently ionized acidic glycopeptides. With such signal abundance, it would be highly challenging to perform MS/MS techniques like ECD and ETD. In sharp contrast with the positive mode,

the same sialylated glycopeptides preferentially ionized and experienced a dramatic signal increase in negative ion mode (shown in Figure 5.2(b). This comparison strongly confirms that negative ion mode is superior to positive mode for detecting sialylated glycopeptides, by providing more intense ion signal, which further benefits the subsequent tandem MS analysis. In addition, it is worthwhile to point out that glycopeptides are known to appear at relatively high m/z ratios, as observed here. However, ECD and ETD exhibit poor fragmentation behavior at low charge states and high m/z ratios.[61, 62] As a result, additional activation (IRMPD or CAD) is often required for ECD and ETD analysis of glycopetides. Dissimilarly, niECD prefers high m/z ratios due to lower charge density and decreased Coulomb repulsion, which makes electron capture more viable. Overall, it appears that negative ion mode MS and niECD MS/MS are more suitable for characterization of sialylated glycopeptides compared with positive ion mode MS and ECD/ETD.

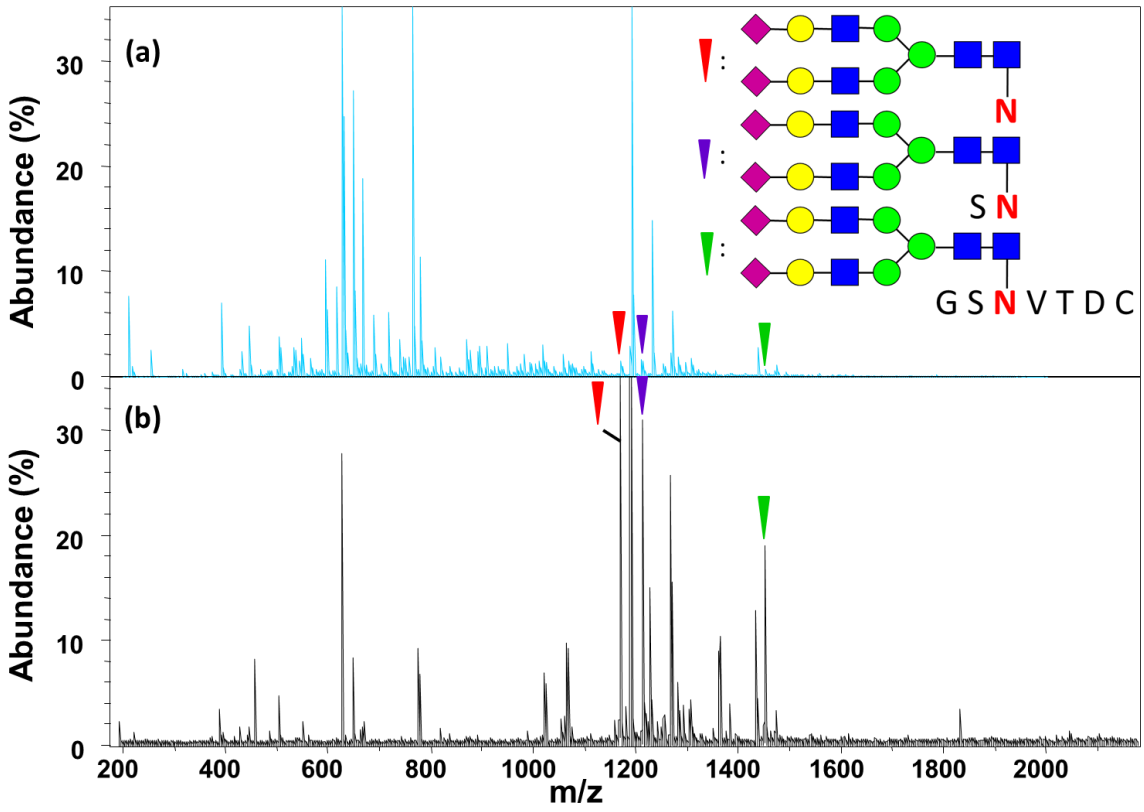

Figure 5.2. (a) Positive ion mode electrospray FT-ICR mass spectrum of human apo-transferrin glycoprotein after pronase E digestion at 1:1 protein/pronase ratio for 2 h. (b) Negative ion mode electrospray FT-ICR mass spectrum of the same digestion mixture. Inverted triangles with the same color represent the same sialylated glycopeptides. The corresponding structures of the sialylated glycopeptides are shown in the inset.

5.3.3 Sialyated O-Glycopeptides with One Potential Glycosylation Site

As mentioned above, *O*-glycoproteins are highly challenging to characterize and site-specific exploration of *O*-glycosylation has seen much less progress because there is no characterized peptide sequence motif. This problem is further compounded by the fact that *O*-glycans are often observed within domains rich in serine and threonine, introducing significant complications in assigning *O*-glycans to a specific site. With the aid of pronase digestion, glycopeptides harboring only a couple or even one threonine or serine in their sequences can be prepared, greatly facilitating determination of glycan

attachment sites. Figure 5.3 shows an *O*-glycopeptide with only one possible glycosylation site from pronase E digestion of bovine fetuin. Due to the presence of one acidic amino acid residue (aspartic acid) in the peptide and two sialic acids in the glycan, this glycopeptide has a very low pI, hence leading to improved ionization in the negative mode. There are two peptide sequences possible for this glycopeptide (shown in Figure 5.3). Without the aid of MS/MS, it is impossible to distinguish these structural isomers.

For niECD, 4.5 eV electron irradiation was applied to the singly-deprotonated *O*-glycopeptide. A major product corresponding to the charge-increased radical intermediate, a doubly charged *c*-type peptide fragment, and several singly charged *c*- and *z*-type peptide sequence ions are present in the spectrum (Figure 5.3). Some small molecule losses (water and CO_2), commonly observed in niECD, were also seen from the charge-increased radical anion. The presence of two prolines reduced the total number of possible cleavages at peptide backbone bonds to 4, out of which 3 were detected in the niECD spectrum. The missing cleavage at the N-terminal side of Ser may result from steric effects: this serine is located adjacent to the glycosylation site and the cleavage may be prevented by the nearby carbohydrate structure. Apart from the dissociation pathways yielding *c*- and *z*-type ions, one *y*-type peptide backbone cleavage was observed. Such cleavage has been previously reported as a minor reaction channel in conventional ECD as well.[83, 85] Similar to what was observed for the lectin glycopeptide, all the peptide fragments that contain the modified serine preserve the complete oligosaccharide moiety, thus rendering assignment of the glycan attachment site possible. It is noteworthy that c_4, z_3, c_6 ions in the niECD spectrum can be exclusively designated to the amino acid sequence APSAVPD, allowing unequivocal discrimination of the isomeric structure. The

structural information derived from the niECD spectrum is in agreement with what was obtained previously via EDD of the same glycopeptide.[69]

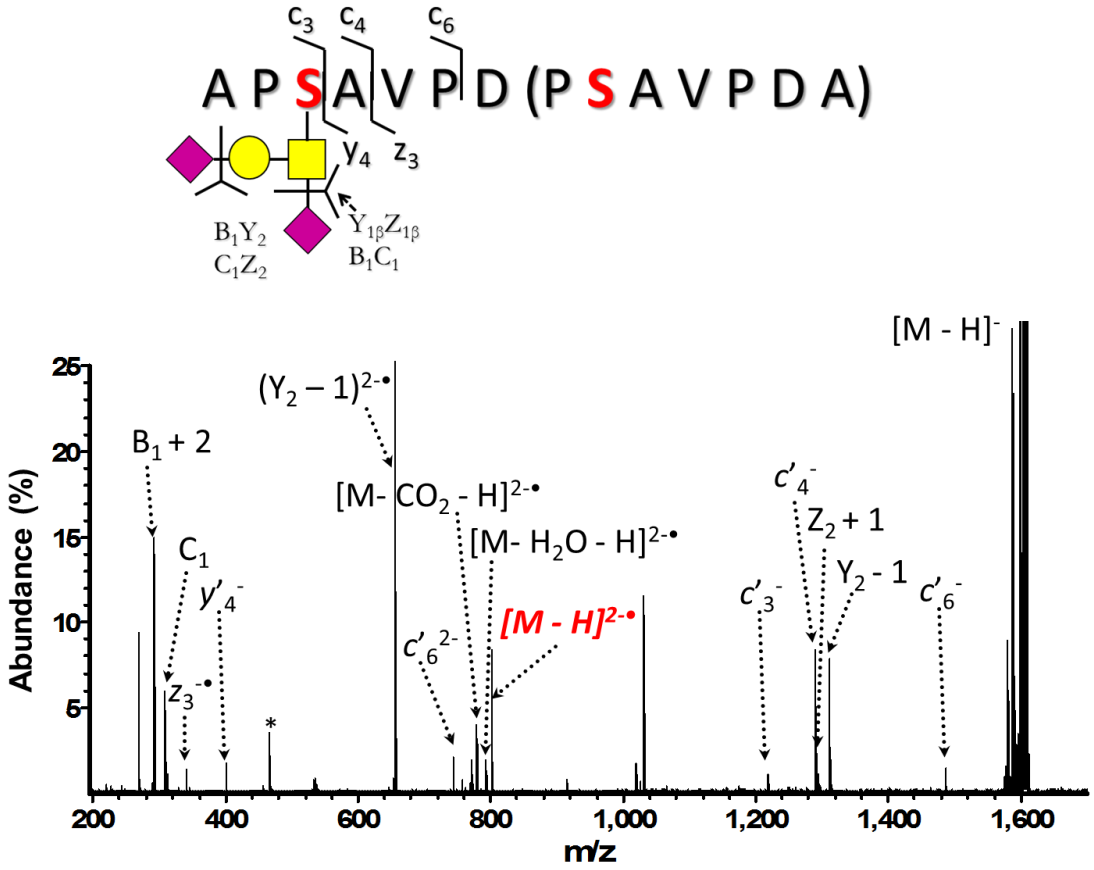

Figure 5.3. niECD (32scans, 5s irradiation, cathode bias -5.4 V) FT-ICR mass spectra of a singly-deprotonated sialylated *O*-glycopeptide containing one potential glycosylation site. The peptide was generated by pronase digestion of bovine fetuin at 1:1 protein/enzyme ratio overnight. The niECD fragmentation pattern is summarized on top of the spectrum. For branched oligosaccharides, the letter α refers to the largest branch and the letter β represents the second largest branch. An alternative assignment of the peptide sequence is shown in the brackets.

Interestingly, in addition to ion signals corresponding to regular peptide fragments, niECD of this acidic *O*-glycopeptide yielded some glycan-specific products formed through rupture of glycosidic bonds. B_1 and C_1 (B, C ions represent glycan-only products), Y_2 and Z_2 (Y, Z ions indicate the intact peptide losing parts of the glycan) ions,

arising from losing the sialic acid residue in the glycan moiety, were the most prominent in the spectrum. Remarkably, some of these sugar product ions are present as hydrogen-deficient (or hydrogen-abundant) species appearing at mass values 1 or 2 Da lower (or higher) than their expected masses. These atypical glycosidic cleavages as well as the observed mass shifts may be explained by a series of hydrogen-rearrangement reactions, induced by a radical site at the peptide backbone and prior to elimination of the sugar unit from the radical anion $[M - H]^{2-\bullet}$. $Y_2 - 1$ and $B_1 + 2$ ions could originate from one or two steps of hydrogen transfer processes from the peptide backbone to the leaving sialic acid residue, leading to cleavage of the glycosidic bond between sialic acid and its neighboring sugar residue. The formation of $Z_2 + 1$ ion may be interpreted through a similar process but with hydrogen transfer from the sugar moiety to the peptide chain. Although the provision of peptide sequence ions without fragmentation of the glycan portion is considered the most prevailing feature in glycopeptide ECD and ETD, exceptions to this general behavior have been reported in ECD of *O*-glycopeptides.[60, 84, 91] Mormann and co-workers applied ECD to mucin-derived glycopeptides and noted analogous Z-, Y-type glycan fragments along with hydrogen gains and losses.[84] A similar mechanism was proposed, involving a radical site-initiated process causing cleavage at glycosidic bonds, followed by a subsequent series of hydrogen migrations. With this evidence, we hypothesize that, when applied to *O*-glycopeptides, niECD involves similar dissociation processes.

Two more niECD examples of sialylated *O*-glycopeptides with only one putative glycosylation site are shown in Figures 5.4(a) and (b). These two glycopeptides also favor efficient ionization in negative ion mode by including two acidic amino acid

residues (aspartic acid and glutamic acid) and one sialic acid saccharide in their structures. As expected, the charge-increased electron capture species as well as a number of N-terminal *c*-type and C-terminal *z*-type peptide backbone fragments were produced in niECD. Each of these peptide sequence ions retains the intact glycan, except the z_3 ion in Figure 5.4(a), as it does not contain the modified serine. Similar to the previous example, niECD of these two *O*-glycopeptides exhibit ion signals corresponding to glycan fragmentation. Abundant loss of one or two sialic acid units from the precursor ions with hydrogen migration were observed in these two spectra. This pronounced and characteristic niECD fragmentation pathway within the glycan region can potentially serve as a screening method, allowing rapid detection and identification of sialylated glycopeptides in a digest mixture.

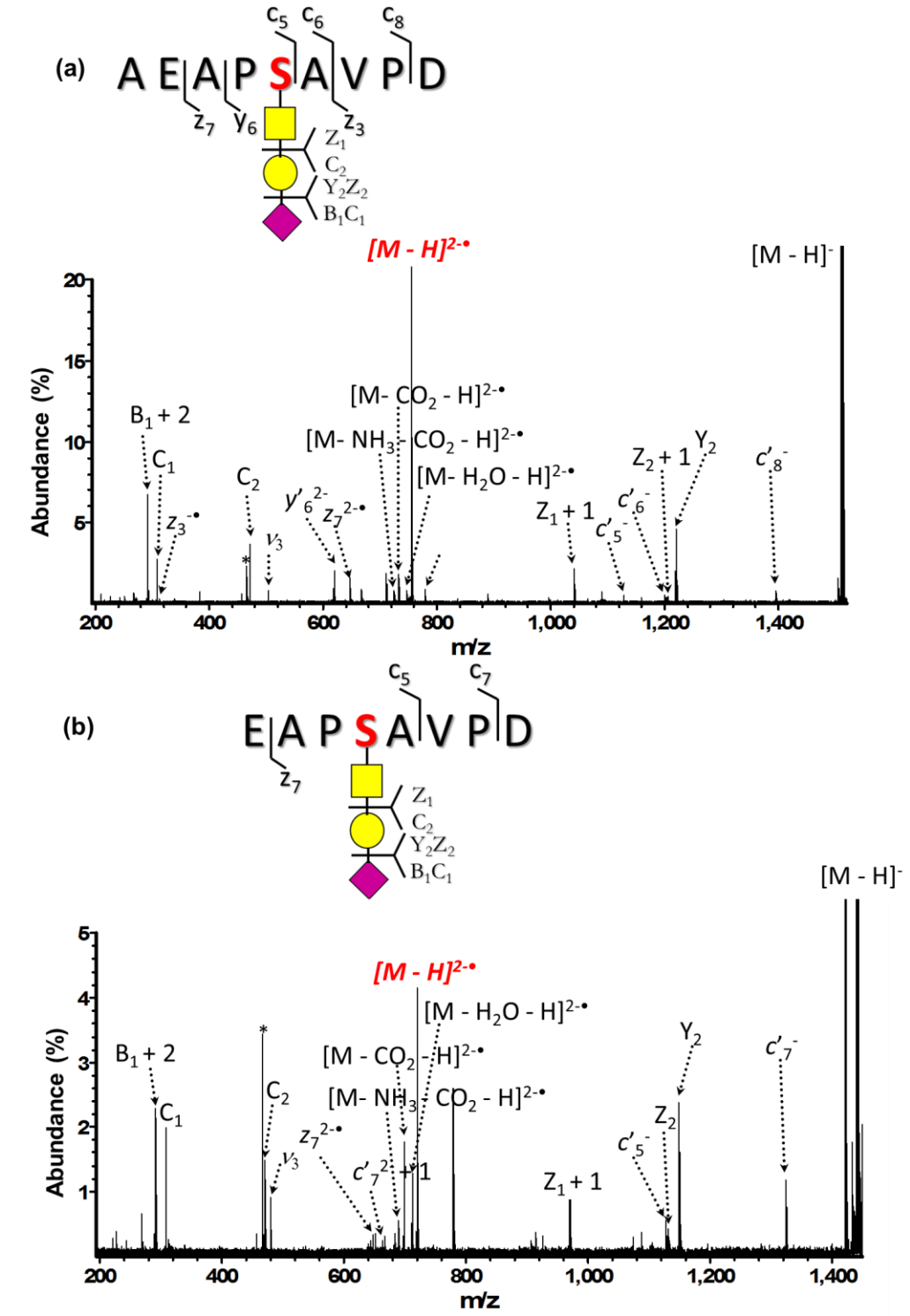

Figure 5.4. niECD (32scans, 5s irradiation, cathode bias -5.4 V) FT-ICR mass spectra of two singly-deprotonated sialylated *O*-glycopeptides derived from pronase digestion of bovine fetuin at 1:1 protein/enzyme ratio overnight. niECD fragmentation patterns of these sialylated *O*-glycopeptides are summarized on top of each spectrum, respectively.

The three *O*-glycopeptides shown in this section have overlapping peptide sequences, indicating that they originate from the same segment of bovine fetuin. However, the glycan structure in the first glycopeptide (Figure 5.3) is different from the latter two (Figure 5.4(a) and 5.4(b)), consistent with *O*-glycan structures being prone to having high structural heterogeneity. On the basis of similar and consistent fragmentation patterns for these three examples, niECD is again considered to proceed very similarly to ECD/ETD also in terms of *O*-glycopeptide analysis.

5.3.4 Sialyated O-Glycopeptides with Multiple Potential Glycosylation Sites

Even for nonspecific proteolysis with pronase, glycopeptides containing multiple potential sites for *O*-glycan attachment were produced, largely due to the tendency of *O*-glycosylation to occur in areas with a high frequency of threonine and serine residues. In Figure 5.5, an *O*-glycopeptide from a pronase digest of the glycoprotein bovine fetuin has two potential glycosylation sites, the threonine and serine residues in the sequence. On the basis of accurate mass, the structure of this *O*-glycopeptide could either be two trisaccharides attached to the serine and threonine separately, or one hexasaccharide attached to the serine or threonine.[92-94] Again, without tandem MS data, one cannot determine the specific structure of this glycopeptide. With 5.5 eV electron irradiation, niECD of the doubly-charged precursor anion resulted in a charge-increased electron capture species, $[M - 2H]^{3-\bullet}$, together with water loss from this intermediate as noted for other peptides upon niECD. As the main diagnostic ions produced in niECD, singly- and doubly-charged *c/z* type peptide sequence ions generated from peptide backbone cleavage were observed as well. No glycan detachment was observed from the peptide backbone

fragments. Although the complete peptide sequence cannot be derived from the niECD spectrum, the presence of z_6 and c_4 product ions is sufficient to differentiate these two isomeric structures. Because the two fragments each contain one trisaccharide, the glycopeptide could be assigned to the corresponding structure with two trisaccharides attached to threonine and serine respectively. In concert with the observation for sialylated *O*-glycopeptides in Figures 5.3 and 5.4, radical-driven fragmentation at the glycosidic bonds, resulting in neutral loss of the sialic acid residue, also occurred here. Appearance of these characteristic satellite peaks (sialic acid loss) in niECD again implies that this favored dissociation channel may be used as an important indicator of the presence of sialylated *O*-glycans.

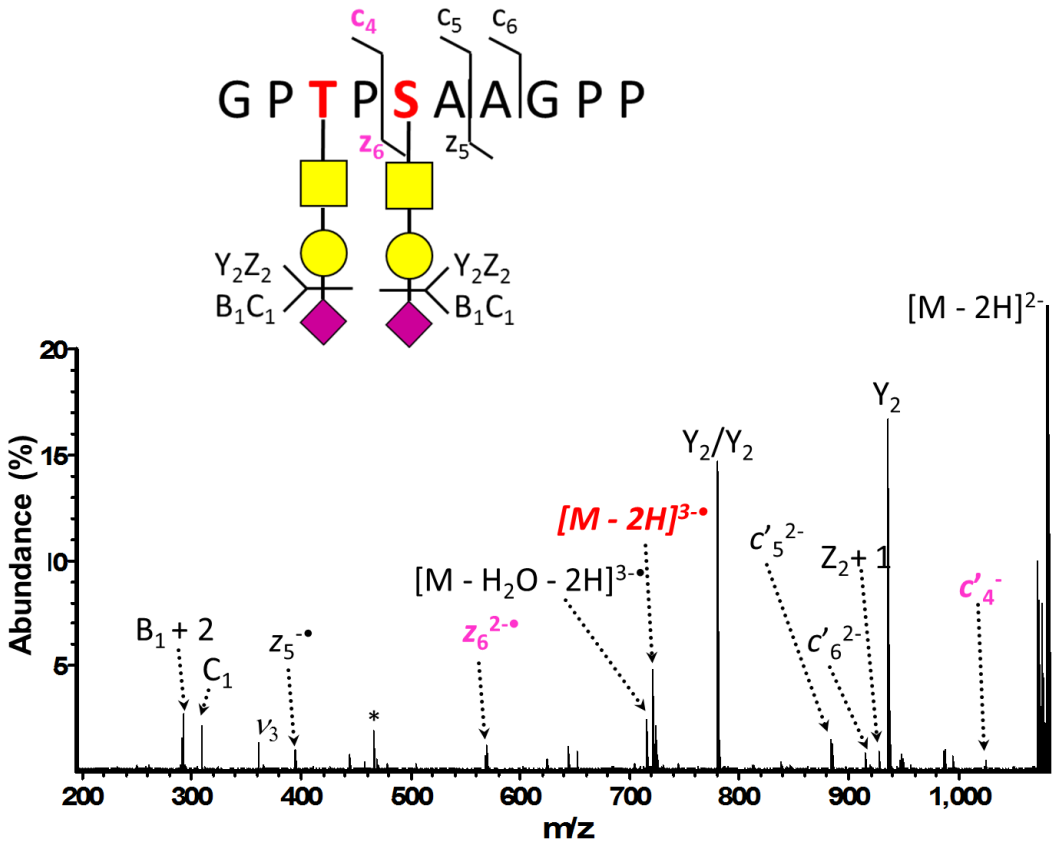

Figure 5.5. niECD (32scans, 5s irradiation, cathode bias -6.6 V) FT-ICR mass spectrum of a doubly-charged *O*-glycopeptide precursor anion from bovine fetuin. The pronase

digestion proceeded at 50:1 protein/enzyme ratio overnight. This sialylated glycopeptide has one threonine and one serine residue in the sequence, both of which are potential *O*-glycosylation sites. The two peptide sequence ions that could be utilized to differentiate the isomeric structures are highlighted in purple. If ions are generated due to multiple cleavage sites, they are designated with a slash between sites of cleavage.

5.3.5 Sialyated N-Glycopeptides with Long Peptide Length

Another glycopeptide type, deprotonated *N*-glycopeptides from the model glycoprotein human apo-transferrin, was characterized by negative ion ECD. According to previous studies, the length of the peptide portion in glycopeptides from pronase digestion is tunable via alteration of the mass ratios between pronase and protein, or the incubation time of the digestion. In order to evaluate the differences in dissociation behavior of glycopeptides varying in peptide length, a series of glycopeptides bearing different peptide moiety sizes but sharing the same N-linked glycan structure were prepared by adjusting mass ratios of protein and protease from 1:1 to 50:1. It appears that the fragmentation patterns of *N*-glycopeptides is highly sensitive to the peptide sequence length in niECD experiments.

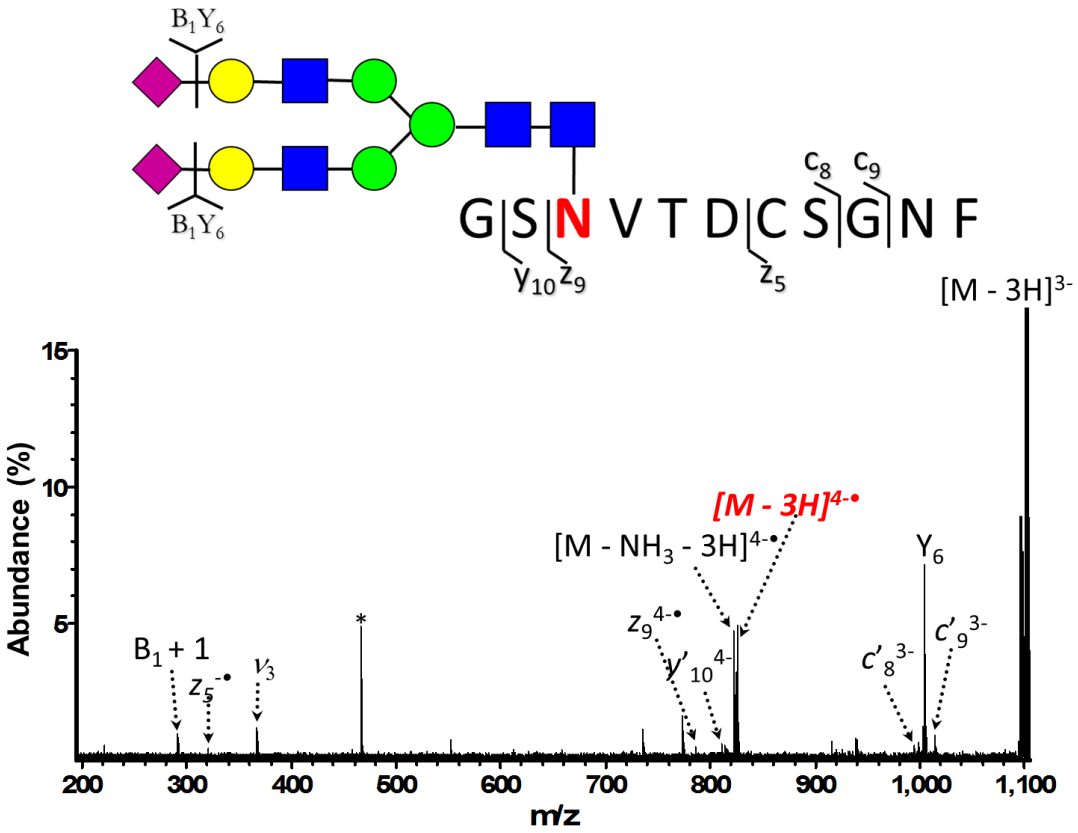

Figure 5.6. niECD (32scans, 5s irradiation, cathode bias -7.2 V) spectrum of a triply-charged sialylated *N*-glycopeptide prepared by incubating the glycoprotein with pronase E at 50:1 mass ratio for 2 h.

In Figure 5.6, the *N*-glycopeptide under inspection was generated by incubating the glycoprotein human apo-transferrin with pronase E at 50:1 ratio (w/w) for 2 h. This peptide comprises a relatively long amino acid portion (residues 628-638) and is glycosylated at asparagine 630 with a biantennary bisialylated oligosaccharide. Given its relatively large size (monoisotopic mass 3304.1965), triply-deprotonated precursor ions were generated upon negative mode electrospray ionization. It has been found previously that appropriate electron energy is key for successful niECD and appears to be substantially dependent on the charge state.[71] For peptides that are highly charged, electrons with relatively higher energy are required to overcome the increased Coulomb repulsion between the precursor anions and electrons. The fragmentation characteristics

of this sialylated *N*-glycopeptide in niECD are similar to other glycopeptides that have been investigated so far. Electron irradiation at 6 eV energy for 5 seconds gave rise to electron capture and the resulting radical species, $[M - 3H]^{4-\bullet}$. Signal due to neutral loss of ammonia from the molecular radical anion was also observed. Radical-driven fragmentation of the peptide chain was obtained, resulting in two c-type (c_8, c_9), two z-type (z_5, z_9), and one *y*-type (y_{10}) sequence ions without cleavages in the carbohydrate moiety. Again, this information can be readily used to confirm the amino acid sequence and the correct site of glycosylation. Analogous to the sialylated *O*-glycopeptides described above, the N-glycosylated peptide underwent some glycan cleavage processes: the major products present in the spectrum are glycan-specific fragments, i.e., B_1 and Y_6, which correspond to the loss of sialic acid. For *N*-glycopeptides, similar instances of ions originating from cleavages of the glycosidic bonds but not the peptide backbone bonds have been reported occasionally in ETD.[32] Wuhrer and co-workers performed ETD of several *N*-glycopeptides, and noticed that next to the apparent *c* and *z* peptide product ions, fragmentation of the glycosidic bonds as well as elimination of the entire *N*-glycan chain also occurred.[32] Similar to *O*-glycopeptides, a radical site-induced dissociation channel could probably account for the cleavages in the carbohydrate moiety for *N*-glycopeptides. Overall, the niECD fragmentation pathways for N-glycosylated peptides with high peptide length is very similar to those of *O*-glycopeptides.

5.3.6 Sialyated N-Glycopeptides with Short Peptide Length

For *N*-glycopeptides with shorter peptide length, niECD provides dissimilar fragmentation spectra as compared to the previous glycosylated peptides discussed above. By reducing the mass ratio between the protein and the protease to 25:1 and increasing

the digestion time to 12 h, glycopeptides with a shorter peptide sequence (and relatively larger glycan moiety compared to the peptide) were generated. Figure 5.7(a) illustrates the fragmentation pattern of the *N*-glycopeptide with five amino acid residues. The doubly-charged precursor anion was interacted with 5.5 eV electrons for 5 seconds. A charge-increased odd electron species and typical neutral loss of 17 Da (ammonia) from the precursor radical were observed. Two fragments that arose from peptide bond cleavages were observed as *c/z*-type ions. Consistently, the entire glycan remained intact on these peptide sequence ions, allowing mapping of the glycosylation site. Nonetheless, the dissociation pattern in this particular analysis is somewhat distinct from what have been found so far in niECD, and contains highly rich information with respect to the glycan structure. An extensive series of glycan-specific fragments, corresponding to cleavage of glycosidic bonds (B, C, Y, and Z ions) with retention of the intact peptide chain, was generated. The dominant glycan cleavages are probably due to the significantly increased glycan/peptide mass ratio. The fragmentation comprises complete coverage of monosaccharide composition and the entire structure of the glycan can be inferred from the niECD spectrum. The most abundant product ions again corresponded to the loss of the labile sialic acid unit. Similar to the sialylated *O*-glycopeptides, hydrogen migration was observed for this N-glycosylated peptide, indicating that elimination of the glycan residues is highly likely through the same radical-site induced process as described above. Concurrent with the glycosidic cleavages, niECD of this *N*-glycopeptide yielded one cross-ring cleavage (namely the $^{2,5}X_6$ ion), providing information regarding saccharide linkage positions. The dissociation behavior for this particular *N*-glycopeptide is not entirely surprising, as it has also been found that ECD or

ETD occasionally deviate from their "typical" dissociation behavior by eliminating the carbohydrate moiety as a whole or in part. Although the factors that influence loss or cleavage of the oligosaccharide during ECD and ETD of glycopeptides remain obscure, it has become clear that these pathways can contribute significantly to the overall dissociation behavior, similar to those observed in glycopeptide niECD.

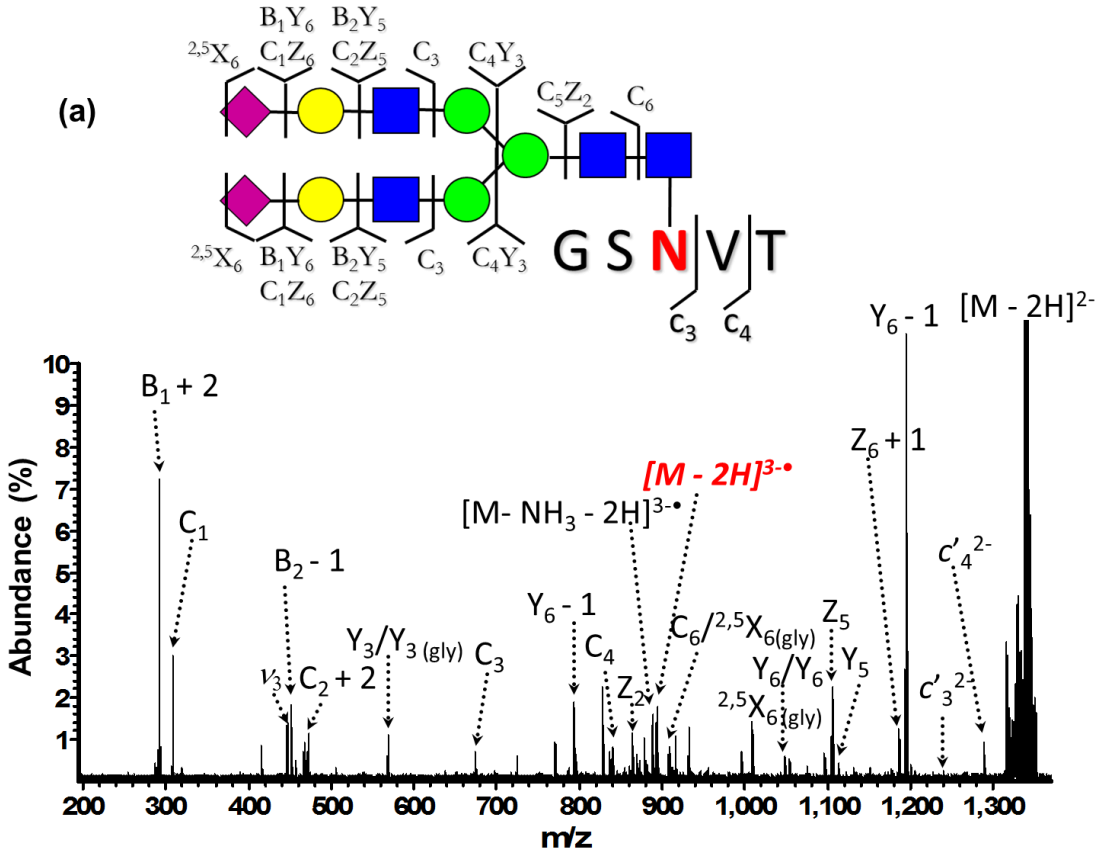

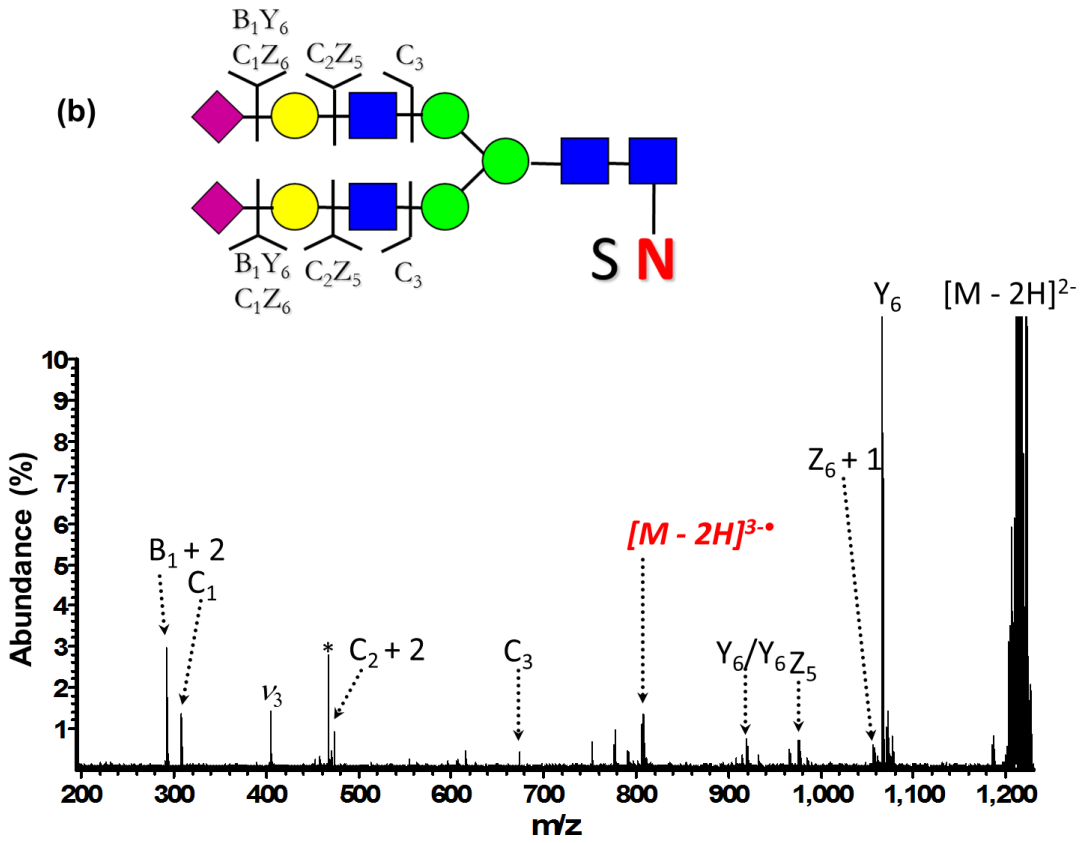
(b)
B1Y6
C1Z6
C2Z5
C3
S N
Y6
[M - 2H]2-
Z6 + 1
[M - 2H]3-•
B1 + 2
C1
C2 + 2
C3
Y6/Y6Z5
ν3
Abundance (%)
m/z

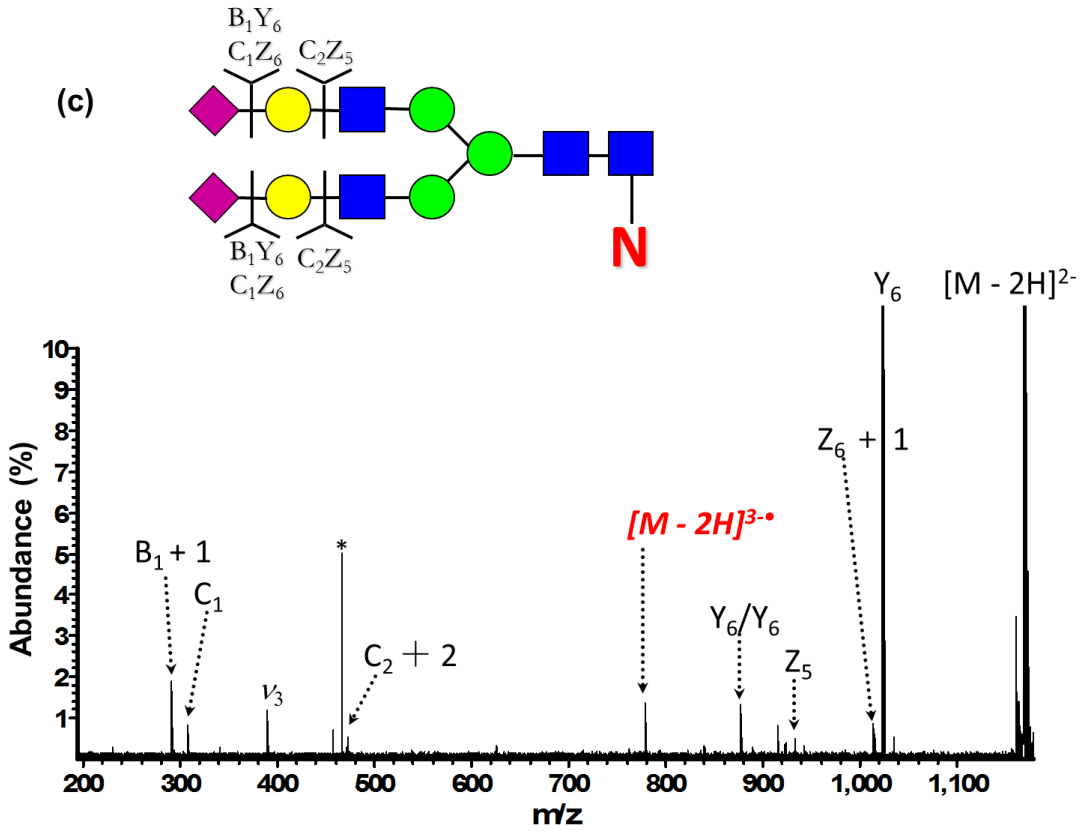
(c)
B1Y6
C1Z6
C2Z5
N
Y6
[M - 2H]2-
Z6 + 1
[M - 2H]3-•
B1 + 1
C1
C2 + 2
Y6/Y6
Z5
ν3
Abundance (%)
m/z

Figure 5.7. niECD (32scans, 5s irradiation, cathode bias -5.5 V) FT-ICR mass spectra of three doubly-charged *N*-glycopeptides from human apo-transferrin. The sialylated *N*-glycopeptide in (a) was generated through overnight pronase digestion at 25:1 mass ratio between the protein and the protease, whereas the glycopeptides in (b) and (c) were produced at 1:1 protein/enzyme ratio. Superscript numerals indicate between which bonds cross-ring cleavage occurred.

In Figures 5.7(b) and (c), two *N*-glycopeptides with even shorter peptide length were obtained by further decreasing the protein to protease ratio to 1:1 for overnight digestion. The glycan portion is much more massive than the peptide section in these two examples. The *N*-glycopeptides with rather small peptide moieties yielded a much simpler dissociation pattern, and therefore less information compared to the spectrum in Figure 5.7(a). The two niECD spectra look almost identical. With such a short peptide length, it is not surprising that neither of the glycopeptides gave rise to any peptide sequence ions upon electron capture (for the glycopeptide in Figure 5.7(c), peptide cleavage is not possible because it only contains one amino acid residue). Instead, glycan-specific fragment ions resulting from glycosidic cleavages were readily apparent in the spectra. The most abundant products were also generated by losing the terminal sialic acid residue. Neutral loss of two sugar residues was detected, but with a signal of minor abundance. For the *N*-glycopeptide containing two amino acid residues (shown in Figure 5.7(b)), loss of the three outermost sugar residues was present in the spectrum, whereas this particular fragment was missing for the *N*-glycopeptide with only one amino acid residue (Figure 5.7(c)). Notably, elimination of the sialic acid was observed on a consistent basis for all the sialylated glycopeptides studied here, confirming that the characteristic sialic acid ions could be potentially applied to distinguish sialylated glycopeptides from non-sialylated ones.

5.4 Conclusion

N-linked and O-linked glycopeptides with both neutral and acidic glycans were investigated by negative ion ECD. Similar to positive mode ECD and ETD, niECD of a glycopeptide with a neutral glycan showed cleavage of the peptide backbone, producing *c*- and *z*-type peptide fragments while the intact glycan was largely preserved. The retention of the labile glycan is critical for site-specific glycan determination in glycopeptide analysis. Amino acid sequence information as well as glycan occupancy site information could be obtained from niECD spectra directly and simultaneously, aiding the interpretation of glycopeptide structures. For sialylated glycopeptides, significantly enhanced detection was achieved in negative mode MS analysis. In the case of sialylated *O*-glycopeptides, which are far more challenging to study than *N*-glycopeptides, niECD generated peptide backbone fragments retaining the glycan. The peptide sequence and glycosylation site was confirmed via niECD. Analogous niECD results were acquired for sialylated *N*-glycopeptides with high peptide length. However, for *N*-glycopeptides with short peptide length, glycan cleavages are dominant in niECD spectra. Glycosidic bond cleavages have also been reported in ETD of *N*-glycopeptides. Abundant sialic acid loss was observed in all the sialylated glycopeptide examples in this study, suggesting its ability to constitute a characteristic signature in detecting sialylated glycopeptides in complex mixture.

5.5 References

1. Spiro, R. G. Protein glycosylation: Nature, distribution, enzymatic formation, and disease implications of glycopeptide bonds. *Glycobiology* **2002**, *12*, 43R-56R.
2. An, H. J.; Froehlich, J. W.; Lebrilla, C. B. Determination of glycosylation sites and site-specific heterogeneity in glycoproteins. *Curr. Opin. Chem. Biol.* **2009**, *13*,

421-426.
3. Apweiler, R.; Hermjakob, H.; Sharon, N. On the frequency of protein glycosylation, as deduced from analysis of the SWISS-PROT database. *Biochim. Biophys. Acta* **1999**, *1473*, 4-8.
4. Helenius, A.; Aebi, M. Intracellular functions of N-linked glycans. *Science* **2001**, *291*, 2364-2369.
5. Varki, A. Biological roles of oligosaccharides - all of the theories are correct. *Glycobiology* **1993**, *3*, 97-130.
6. Lowe, J. B. Glycosylation, immunity, and autoimmunity. *Cell* **2001**, *104*, 809-812.
7. Rudd, P. M.; Elliott, T.; Cresswell, P.; Wilson, I. A.; Dwek, R. A. Glycosylation and the immune system. *Science* **2001**, *291*, 2370-2376.
8. Wormald, M. R.; Dwek, R. A. Glycoproteins: glycan presentation and protein-fold stability. *Struct. Fold. Des.* **1999**, *7*, R155-R160.
9. Imperiali, B.; O'Connor, S. E. Effect of N-linked glycosylation on glycopeptide and glycoprotein structure. *Curr. Opin. Chem. Biol.* **1999**, *3*, 643-649.
10. Turner, G. A.; Goodarzi, M. T.; Thompson, S. Glycosylation of alpha-1-proteinase inhibitor and haptoglobin in ovarian-cancer - evidence for 2 different mechanisms. *Glycoconj. J.* **1995**, *12*, 211-218.
11. Okuyama, N.; Ide, Y.; Nakano, M.; Nakagawa, T.; Yamanaka, K.; Moriwaki, K.; Murata, K.; Ohigashi, H.; Yokoyama, S.; Eguchi, H. *et al*. Fucosylated haptoglobin is a novel marker for pancreatic cancer: A detailed analysis of the oligosaccharide structure and a possible mechanism for fucosylation. *Int. J. Cancer* **2006**, *118*, 2803-2808.
12. Kyselova, Z.; Mechref, Y.; Al Bataineh, M. M.; Dobrolecki, L. E.; Hickey, R. J.; Vinson, J.; Sweeney, C. J.; Novotny, M. V. Alterations in the serum glycome due to metastatic prostate cancer. *J. Proteome Res.* **2007**, *6*, 1822-1832.
13. Varki, N. M.; Varki, A. Diversity in cell surface sialic acid presentations: Implications for biology and disease. *Lab. Invest.* **2007**, *87*, 851-857.
14. Osorio, H.; Reis, C. A. Mass spectrometry methods for studying glycosylation in cancer. *Methods Mol. Biol.* **2013**, *1007*, 301-316.
15. Fuster, M. M.; Esko, J. D. The sweet and sour of cancer: glycans as novel therapeutic targets. *Nat. Rev. Cancer* **2005**, *5*, 526-542.
16. Tian, Y.; Esteva, F. J.; Song, J.; Zhang, H. Altered expression of sialylated glycoproteins in breast cancer using hydrazide chemistry and mass spectrometry. *Mol. Cell. Proteomics* **2012**, *11*, 10.
17. Pousset, D.; Piller, V.; Bureaud, N.; Monsigny, M.; Piller, F. Increased alpha 2,6 sialylation of N-glycans in a transgenic mouse model of hepatocellular carcinoma. *Cancer Res.* **1997**, *57*, 4249-4256.
18. Kim, Y. J.; Varki, A. Perspectives on the significance of altered glycosylation of glycoproteins in cancer. *Glycoconj. J.* **1997**, *14*, 569-576.
19. Pearlstein, E.; Salk, P. L.; Yogeeswaran, G.; Karpatkin, S. Correlation between spontaneous metastatic potential, platelet-aggregating activity of cell-surface extracts, and cell-surface sialylation in 10 metastatic-variant derivatives of a rat renal sarcoma cell-line. *Proc. Natl. Acad. Sci. U. S. A. Biol. Sci.* **1980**, *77*, 4336-4339.
20. Yogeeswaran, G.; Salk, P. L. Metastatic potential is positively correlated with

cell-surface sialylation of cultured murine tumor-cell lines. *Science* **1981**, *212*, 1514-1516.
21. Dennis, J.; Waller, C.; Timpl, R.; Schirrmacher, V. Surface sialic-acid reduces attachment of metastatic tumor-cells to collagen type-iv and fibronectin. *Nature* **1982**, *300*, 274-276.
22. Zaia, J. Mass spectrometry of oligosaccharides. *Mass Spectrom. Rev.* **2004**, *23*, 161-227.
23. Hofsteenge, J.; Muller, D. R.; Debeer, T.; Loffler, A.; Richter, W. J.; Vliegenthart, J. F. G. New-type of linkage between a carbohydrate and a protein - C-Glycosylation of a specific tryptophan residue in human rnase U-S. *Biochem.* **1994**, *33*, 13524-13530.
24. Mechref, Y.; Novotny, M. V. Structural investigations of glycoconjugates at high sensitivity. *Chem. Rev.* **2002**, *102*, 321-369.
25. Scott, N. E.; Parker, B. L.; Connolly, A. M.; Paulech, J.; Edwards, A. V. G.; Crossett, B.; Falconer, L.; Kolarich, D.; Djordjevic, S. P.; Hojrup, P. *et al*. Simultaneous glycan-peptide characterization using hydrophilic interaction chromatography and parallel fragmentation by CID, higher energy collisional dissociation, and electron transfer dissociation MS applied to the N-linked glycoproteome of campylobacter jejuni. *Mol. Cell. Proteomics* **2011**, *10*, 18.
26. Kowarik, M.; Young, N. M.; Numao, S.; Schulz, B. L.; Hug, I.; Callewaert, N.; Mills, D. C.; Watson, D. C.; Hernandez, M.; Kelly, J. F. *et al*. Definition of the bacterial N-glycosylation site consensus sequence. *EMBO J.* **2006**, *25*, 1957-1966.
27. Renfrow, M. B.; Mackay, C. L.; Chalmers, M. J.; Julian, B. A.; Mestecky, J.; Kilian, M.; Poulsen, K.; Emmett, M. R.; Marshall, A. G.; Novak, J. Analysis of O-glycan heterogeneity in iga1 myeloma proteins by fourier transform ion cyclotron resonance mass spectrometry: implications for IgA nephropathy. *Anal. Bioanal. Chem.* **2007**, *389*, 1397-1407.
28. Sihlbom, C.; Hard, I. V.; Lidell, M. E.; Noll, T.; Hansson, G. C.; Backstrom, M. Localization of O-glycans in MUC1 glycoproteins using electron-capture dissociation fragmentation mass spectrometry. *Glycobiology* **2009**, *19*, 375-381.
29. Peterkatalinic, J. Analysis of glycoconjugates by fast-atom-bombardment mass-spectrometry and related MS techniques. *Mass Spectrom. Rev.* **1994**, *13*, 77-98.
30. Harvey, D. J. Identification of protein-bound carbohydrates by mass spectrometry. *Proteomics* **2001**, *1*, 311-328.
31. Kuster, B.; Krogh, T. N.; Mortz, E.; Harvey, D. J. Glycosylation analysis of gel-separated proteins. *Proteomics* **2001**, *1*, 350-361.
32. Catalina, M. I.; Koeleman, C. A. M.; Deelder, A. M.; Wuhrer, M. Electron transfer dissociation of N-glycopeptides: loss of the entire N-glycosylated asparagine side chain. *Rapid Commun. Mass Spectrom.* **2007**, *21*, 1053-1061.
33. Huddleston, M. J.; Bean, M. F.; Carr, S. A. Collisional fragmentation of glycopeptides by electrospray ionization LC/MS and LC/MS/MS - methods for selective detection of glycopeptides in protein digests. *Anal. Chem.* **1993**, *65*, 877-884.
34. Zhao, J.; Simeone, D. M.; Heidt, D.; Anderson, M. A.; Lubman, D. M. Comparative Serum Glycoproteomics Using Lectin Selected Sialic Acid Glycoproteins with Mass Spectrometric Analysis: Application to Pancreatic

Cancer Serum. *J. Proteome Res.* **2006**, *5*, 1792-1802.
35. Hirabayashi, J.; Kasai, K. Separation technologies for glycomics. *J. Chromatogr. B Analyt. Technol. Biomed. Life Sci.* **2002**, *771*, 67-87.
36. Pan, S.; Chen, R.; Aebersold, R.; Brentnall, T. A. Mass spectrometry based glycoproteomics-from a proteomics perspective. *Mol. Cell. Proteomics* **2011**, *10*, 14.
37. Wuhrer, M.; Deelder, A. M.; Hokke, C. H. Protein glycosylation analysis by liquid chromatography-mass spectrometry. *J. Chromatogr. B Analyt. Technol. Biomed. Life Sci.* **2005**, *825*, 124-133.
38. Deguchi, K.; Ito, H.; Takegawa, Y.; Shinji, N.; Nakagawa, H.; Nishimura, S. I. Complementary structural information of positive- and negative-Ion MSn spectra of glycopeptides with neutral and sialylated N-glycans. *Rapid Commun. Mass Spectrom.* **2006**, *20*, 741-746.
39. Seipert, R. R.; Dodds, E. D.; Lebrilla, C. B. Exploiting differential dissociation chemistries of O-linked glycopeptide ions for the localization of mucin-type protein glycosylation. *J. Proteome Res.* **2009**, *8*, 493-501.
40. Huberty, M. C.; Vath, J. E.; Yu, W.; Martin, S. A. Site-specific carbohydrate identification in recombinant proteins using MALD-TOF MS. *Anal. Chem.* **1993**, *65*, 2791-2800.
41. Hogan, J. M.; Pitteri, S. J.; Chrisman, P. A.; McLuckey, S. A. Complementary structural information from a tryptic N-linked glycopeptide via electron transfer ion/ion reactions and collision-induced dissociation. *J. Proteome Res.* **2005**, *4*, 628-632.
42. Han, H.; Xia, Y.; Yang, M.; McLuckey, S. A. Rapidly alternating transmission mode electron-transfer dissociation and collisional activation for the characterization of polypeptide ions. *Anal. Chem.* **2008**, *80*, 3492-3497.
43. Adamson, J. T.; Hakansson, K. Infrared multiphoton dissociation and electron capture dissociation of high-mannose type glycopeptides. *J. Proteome Res.* **2006**, *5*, 493-501.
44. Hakansson, K.; Cooper, H. J.; Emmett, M. R.; Costello, C. E.; Marshall, A. G.; Nilsson, C. L. Electron capture dissociation and infrared multiphoton dissociation MS/MS of an N-glycosylated tryptic peptide yield complementary sequence information. *Anal. Chem.* **2001**, *73*, 4530-4536.
45. Hakansson, K.; Chalmers, M. J.; Quinn, J. P.; McFarland, M. A.; Hendrickson, C. L.; Marshall, A. G. Combined electron capture and infrared multiphoton dissociation for multistage MS/MS in an FT-ICR mass spectrometer. *Anal. Chem.* **2003**, *75*, 3256-3262.
46. Bezouska, K.; Sklenar, J.; Novak, P.; Halada, P.; Havlicek, V.; Kraus, M.; Ticha, M.; Jonakova, V. Determination of the complete covalent structure of the major glycoform of DQH sperm surface protein, a novel trypsin-resistant boar seminal plasma O-glycoprotein related to pB1 protein. *Protein Sci.* **1999**, *8*, 1551-1556.
47. Tsarbopoulos, A.; Bahr, U.; Pramanik, B. N.; Karas, M. Glycoprotein analysis by delayed extraction and post-source decay MALDI-TOF-MS. *Int. J. Mass Spectrom.* **1997**, *169*, 251-261.
48. Goletz, S.; Thiede, B.; Hanisch, F. G.; Schultz, M.; PeterKatalinic, J.; Muller, S.; Seitz, O.; Karsten, U. A sequencing strategy for the localization of O-

glycosylation sites of MUC1 tandem repeats by PSD-MALDI mass spectrometry. *Glycobiology* **1997**, *7*, 881-896.

49. Tarentino, A. L.; Plummer, T. H. Enzymatic deglycosylation of asparagine-linked glycans - purification, properties, and specificity of oligosaccharide-cleaving enzymes from flavobacterium-meningosepticum. *Method Enzymol.* **1994**, *230*, 44-57.
50. An, H. J.; Peavy, T. R.; Hedrick, J. L.; Lebrilla, C. B. Determination of N-glycosylation sites and site heterogeneity in glycoproteins. *Anal. Chem.* **2003**, *75*, 5628-5637.
51. Khoshnoodi, J.; Hill, S.; Tryggvason, K.; Hudson, B.; Friedman, D. B. Identification of N-linked glycosylation sites in human nephrin using mass spectrometry. *J. Mass Spectrom.* **2007**, *42*, 370-379.
52. Wada, Y.; Dell, A.; Haslam, S. M.; Tissot, B.; Canis, K.; Azadi, P.; Backstrom, M.; Costello, C. E.; Hansson, G. C.; Hiki, Y. *et al*. Comparison of methods for profiling O-glycosylation human proteome organisation human disease glycomics/proteome initiative multi-institutional study of IgA1. *Mol. Cell. Proteomics* **2010**, *9*, 719-727.
53. Takahashi, K.; Wall, S. B.; Suzuki, H.; Smith, A. D.; Hall, S.; Poulsen, K.; Kilian, M.; Mobley, J. A.; Julian, B. A.; Mestecky, J. *et al*. Clustered O-glycans of IgA1. *Mol. Cell. Proteomics* **2010**, *9*, 2545-2557.
54. Zubarev, R. A.; Kelleher, N. L.; McLafferty, F. W. Electron capture dissociation of multiply charged protein cations. A nonergodic process. *J. Am. Chem. Soc.* **1998**, *120*, 3265-3266.
55. Cooper, H. J.; Hakansson, K.; Marshall, A. G. The role of electron capture dissociation in biomolecular analysis. *Mass Spectrom. Rev.* **2005**, *24*, 201-222.
56. Syka, J. E. P.; Coon, J. J.; Schroeder, M. J.; Shabanowitz, J.; Hunt, D. F. Peptide and protein sequence analysis by electron transfer dissociation mass spectrometry. *Proc. Natl. Acad. Sci. U. S. A.* **2004**, *101*, 9528-9533.
57. Shi, S. D.-H.; Hemling, M. E.; Carr, S. A.; Horn, D. M.; Lindh, I.; McLafferty, F. W. Phosphopeptide/phosphoprotein mapping by electron capture dissociation mass spectrometry. *Anal. Chem.* **2001**, *73*, 19-22.
58. Stensballe, A.; Norregaard-Jensen, O.; Olsen, J. V.; Haselmann, K. F.; Zubarev, R. A. Electron capture dissociation of singly and multiply phosphorylated peptides. *Rapid Commun. Mass Spectrom.* **2000**, *14*, 1793-1800.
59. Mirgorodskaya, E.; Hassan, H.; Clausen, H.; Roepstorff, P. Mass spectrometric determination of o-glycosylation sites using beta-elimination and partial acid hydrolysis. *Anal. Chem.* **2001**, *73*, 1263-1269.
60. Mirgorodskaya, E.; Roepstorff, P.; Zubarev, R. A. Localization of O-glycosylation sites in peptides by electron capture dissociation in a fourier transform mass spectrometer. *Anal. Chem.* **1999**, *71*, 4431-4436.
61. Good, D. M.; Wirtala, M.; McAlister, G. C.; Coon, J. J. Performance characteristics of electron transfer dissociation mass spectrometry. *Mol. Cell. Proteomics* **2007**, *6*, 1942-1951.
62. Kalli, A.; Hakansson, K. Comparison of the electron capture dissociation fragmentation behavior of doubly and triply protonated peptides from trypsin, GLU-C, and chymotrypsin digestion. *J. Proteome Res.* **2008**, *7*, 2834-2844.

63. Pitteri, S. J.; Chrisman, P. A.; Hogan, J. M.; McLuckey, S. A. Electron transfer ion/ion reactions in a three-dimensional quadrupole ion trap: Reactions of doubly and triply protonated peptides with SO2 center dot. *Anal. Chem.* **2005**, *77*, 1831-1839.
64. Parker, B. L.; Thaysen-Andersen, M.; Solis, N.; Scott, N. E.; Larsen, M. R.; Graham, M. E.; Packer, N. H.; Cordwell, S. J. Site-specific glycan-peptide analysis for determination of N-glycoproteome heterogeneity. *J. Proteome Res.* **2013**, *12*, 5791-5800.
65. Nwosu, C. C.; Strum, J. S.; An, H. J.; Lebrilla, C. B. Enhanced detection and identification of glycopeptides in negative ion mode mass spectrometry. *Anal. Chem.* **2010**, *82*, 9654-9662.
66. Bowie, J. H.; Brinkworth, C. S.; Dua, S. Collision-induced fragmentations of the (M-H)(-) parent anions of underivatized peptides: an aid to structure determination and some unusual negative ion cleavages. *Mass Spectrom. Rev.* **2002**, *21*, 87-107.
67. Budnik, B. A.; Haselmann, K. F.; Zubarev, R. A. Electron detachment dissociation of peptide DI-ANIONS: an electron-hole recombination phenomenon. *Chem. Phys. Lett.* **2001**, *342*, 299-302.
68. Coon, J. J.; Shabanowitz, J.; Hunt, D. F.; Syka, J. E. P. Electron transfer dissociation of peptide anions. *J. Am. Soc. Mass Spectrom.* **2005**, *16*, 880-882.
69. Zhou, W.; Hakansson, K. Influence of peptide length on the gas-phase fragmentation of pronase-derived glycopeptides, In Proc. *58th ASMS Conference on Mass Spectrometry and Allied Topics*, Salt Lake City, UT, 2010.
70. Madsen, J. A.; Ko, B. J.; Xu, H.; Iwashkiw, J. A.; Robotham, S. A.; Shaw, J. B.; Feldman, M. F.; Brodbelt, J. S. Concurrent automated sequencing of the glycan and peptide portions of O-linked glycopeptide anions by ultraviolet photodissociation mass spectrometry. *Anal. Chem.* **2013**, *85*, 9253-9261.
71. Yoo, H. J.; Wang, N.; Zhuang, S.; Song, H.; Hakansson, K. Negative-ion electron capture dissociation: radical-driven fragmentation of charge-increased gaseous peptide anions. *J. Am. Chem. Soc.* **2011**, *133*, 16790-16793.
72. Hersberger, K. E.; Hakansson, K. Characterization of O-sulfopeptides by negative ion mode tandem mass spectrometry: Superior performance of negative ion electron capture dissociation. *Anal. Chem.* **2012**, *84*, 6370-6377.
73. Wang, N.; Hakansson, K. Negative ion electron capture dissociation (niECD) of disulfide-linked peptide anions, In Proc. *59th ASMS Conference on Mass Spectrometry and Allied Topics*, Denver, CO, 2011.
74. Wang, N.; Hakansson, K. Systematic niECD mechanistic exploration with synthetic peptides and fixed-charge tags, In Proc. *61st ASMS Conference on Mass Spectrometry and Allied Topics*, Minneapolis, MN, 2013.
75. Yang, J.; Mo, J.; Adamson, J. T.; Hakansson, K. Characterization of oligodeoxynucleotides by electron detachment dissociation fourier transform ion cyclotron resonance mass spectrometry. *Anal. Chem.* **2005**, *77*, 1876-1882.
76. Tsybin, Y. O.; Witt, M.; Baykut, G.; Kjeldsen, F.; Hakansson, P. Combined infrared multiphoton dissociation and electron capture dissociation with a hollow electron beam in fourier transform ion cyclotron resonance mass spectrometry. *Rapid Commun. Mass Spectrom.* **2003**, *17*, 1759-1768.

77. Senko, M. W.; Canterbury, J. D.; Guan, S.; Marshall, A. G. A high-performance modular data system for FT-ICR mass spectrometry. *Rapid Commun. Mass Spectrom.* **1996**, *10*, 1839-1844.
78. Ledford, E. B., Jr.; Rempel, D. L.; Gross, M. L. Space charge effects in fourier transform mass spectrometry mass calibration. *Anal. Chem.* **1984**, *56*, 2744-2748.
79. Roepstorff, P.; Fohlman, J. Proposal for a common nomenclature for sequence ions in mass-spectra of peptides. *Biomed. Mass Spectrom.* **1984**, *11*, 601-601.
80. Domon, B.; Costello, C. E. A systematic nomenclature for carbohydrate fragmentations in FAB-MS/MS spectra of glycoconjugates. *Glycoconj. J.* **1988**, *5*, 397-409.
81. Varki, A.; Cummings, R. D.; Esko, J. D.; Freeze, H. H.; Stanley, P.; Marth, J. D.; Bertozzi, C. R.; Hart, G. W.; Etzler, M. E. Symbol nomenclature for glycan representation. *Proteomics* **2009**, *9*, 5398-5399.
82. Ashford, D.; Dwek, R. A.; Welply, J. K.; Atamayakul, S.; Homans, S. W.; Lis, H.; Taylor, G. N.; Sharon, N.; Rademacher, T. W. The beta-1-2-d-xylose and alpha-1-3-fucose substituted N-linked oligosaccharides from erythrina cristagalli lectin - isolation, characterization and comparison with other legume lectins. *Eur. J. Biochem.* **1987**, *166*, 311-320.
83. Zubarev, R. A. Reactions of polypeptide ions with electrons in the gas phase. *Mass Spectrom. Rev.* **2003**, *22*, 57-77.
84. Mormann, M.; Paulsen, H.; Peter-Katalinic, J. Electron capture dissociation of O-glycosylated peptides: Radical site-induced fragmentation of glycosidic bonds. *Eur. J. Mass Spectrom.* **2005**, *11*, 497-511.
85. Zubarev, R. A.; Kruger, N. A.; Fridriksson, E. K.; Lewis, M. A.; Horn, D. M.; Carpenter, B. K.; McLafferty, F. W. Electron capture dissociation of gaseous multiply-charged proteins is favored at disulfide bonds and other sites of high hydrogen atom affinity. *J. Am. Chem. Soc.* **1999**, *121*, 2857-2862.
86. Axelsson, J.; Palmblad, M.; Hakansson, K.; Hakansson, P. Electron capture dissociation of substance P using a commercially available fourier transform ion cyclotron resonance mass spectrometer. *Rapid Commun. Mass Spectrom.* **1999**, *13*, 474-477.
87. Spik, G.; Bayard, B.; Fournet, B.; Strecker, G.; Bouquelet, S.; Montreuil, J. Studies on glycoconjugates .64. complete structure of 2 carbohydrate units of human serotransferrin. *FEBS Lett.* **1975**, *50*, 296-299.
88. Coddeville, B.; Strecker, G.; Wieruszeski, J. M.; Vliegenthart, J. F. G.; Vanhalbeek, H.; Peterkatalinic, J.; Egge, H.; Spik, G. Heterogeneity of bovine lactotransferrin glycans - characterization of alpha-d-galp-(1- 3)-beta-d-gal and alpha-neuac-(2- 6)-beta-d-galpnac-(1- 4)-beta-d-glcnac-substituted N-linked glycans. *Carbohydr. Res.* **1992**, *236*, 145-164.
89. Green, E. D.; Adelt, G.; Baenziger, J. U.; Wilson, S.; Vanhalbeek, H. The asparagine-linked oligosaccharides on bovine fetuin - structural analysis of N-glycanase-released oligosaccharides by 500 megahertz H-1 NMR spectroscopy. *J. Biol. Chem.* **1988**, *263*, 18253-18268.
90. Narahashi, Y. Pronase. *Methods Enzymol.* **1970**, 651-664.
91. Mormann, M.; Peter-Katalinic, J. Improvement of electron capture dissociation efficiency by resonant excitation. *Rapid Commun. Mass Spectrom.* **2003**, *17*,

2208-2214.
92. Medzihradszky, K. F.; GilleceCastro, B. L.; Townsend, R. R.; Burlingame, A. L.; Hardy, M. R. Structural elucidation of O-linked glycopeptides by high energy collision-induced dissociation. *J. Am. Soc. Mass. Spectrom.* **1996**, *7*, 319-328.
93. Zauner, G.; Koeleman, C. A. M.; Deelder, A. M.; Wuhrer, M. Protein glycosylation analysis by HILIC-LC-MS of proteinase K-generated N- and O-glycopeptides. *J. Sep. Sci.* **2010**, *33*, 903-910.
94. Edge, A. S. B.; Spiro, R. G. Presence of an O-glycosidically linked hexasaccharide in fetuin. *J. Biol. Chem.* **1987**, *262*, 16135-16141.

Chapter 6

Conclusions and Future Directions

6.1 Summary of Results

The electron-based ion activation techniques, ECD and ETD, involve electron attachment/transfer to multiply-charged peptide and protein cations and have found broad applications in the structural analysis of biomolecules. In Chapter 2, we demonstrated that negatively charged peptide ions ($[M - nH]^{n-}$, $n \geq 1$) can also capture electrons, resulting in charge-increased radical intermediates that undergo further fragmentation analogous to that observed in positive ion mode ECD and ETD. We termed this phenomenon niECD. A rather narrow electron energy range (~3.5-6.5 eV) appears acceptable for niECD. The acidic and biologically important PTMs, phosphorylation and sulfation, were investigated by this new MS/MS technique. For all examined phosphorylated and sulfated peptides, predictable c' and $z^{\bullet}$ product ions from N-C_{α}

backbone bond cleavage were observed with retention of the labile modifications. In addition, higher sequence coverage was obtained in niECD compared with negative ion mode CAD. Thus, niECD holds great promise for characterization of acidic peptides that show improved ionization efficiency and less ion suppression in negative mode, and for localization of PTMs. However, niECD is not universal. Electron capture did not occur for several unmodified peptides which do not contain either strongly acidic or strongly basic residues in their sequences. This shared characteristic among these peptides led us to hypothesize that gas-phase zwitterionic structures may play an important role in successful niECD.

In Chapter 3, the proposed zwitterion mechanism of niECD was first explored by implementing a variety of chemical derivatization techniques with the goal to either prevent or promote gaseous zwitterionic structures. Peptide N-terminal acetylation and dephosphorylation/desulfation remove potential protonation and deprotonation sites, respectively, and thus may inhibit zwitterion formation. Consistently, both of these reactions resulted in decreased peptide niECD efficiency. Enhancement of gas-phase zwitterion structures was achieved by introducing positive charge-carrying or readily chargeable groups to the molecules. Attachment of fixed-charge tags in the form of quaternary amine (i.e., TMAA, DABCO, and Girard's T-based tags), as well as peptide N-terminal guanidination, rescued niECD ability of peptides and an oligosaccharide that were unable to capture an electron in their unmodified forms. Although structurally uninformative fragments such as partial and entire tag losses were dominant in the niECD spectra, successful electron capture upon derivatization correlates with our hypothesis that niECD requires zwitterionic gas-phase structures. In order to examine the

mechanism more systematically, niECD was applied to five sets of synthetic peptides with varying propensities for zwitterion formation. All the five datasets followed the same decreasing niECD efficiency trend with decreasing zwitterionic probability, thus supporting the zwitterion niECD mechanism.

In Chapter 4, application of niECD was expanded towards disulfide-linked peptide pairs. Both natural protein disulfide bonds in insulin and lysozyme and disulfides introduced by the cystine-based cross-linker DTSSP were investigated. When subjected to niECD, disulfide-bound peptides exhibited dissociation patterns highly analogous to those in conventional ECD/ETD. S-S bonds are preferentially cleaved in niECD, rendering it a promising tool for rapid detection of disulfide-linked peptides in complex mixtures. Limited C-S bond cleavage and N-Cα backbone bond cleavage were also generated in niECD. This work also sheds some light on the niECD mechanism. Selective dissociation at disulfide bonds observed in both ECD and niECD further indicates that niECD proceeds through a mechanism related to that of conventional peptide ECD/ETD.

The applicability of niECD towards another important PTM, glycosylation, was explored in Chapter 5. Site-specific characterization of glycosylation by mass spectrometry remains challenging due to the lability of glycosidic bonds. Both N-linked and O-linked glycopeptides with neutral and acidic glycans were examined by niECD. For a lectin glycopeptide with a neutral glycan, niECD exclusively cleaved the peptide backbone bonds while preserving the labile glycan, analogous to cation ECD and ETD. Thus, peptide sequence information as well as glycan attachment site information could be extracted simultaneously from the niECD spectrum. For sialylated glycopeptides, a

dramatic signal increase was achieved in negative ion mode electrospray due to their acidic nature. In the cases of sialylated *O*-glycopeptides, which are far more challenging to analyze than *N*-glycopeptides, similar peptide backbone fragments with retention of the intact glycans were produced in niECD. Analogous niECD results were obtained for sialylated *N*-glycopeptides with high peptide length. However, for *N*-glycopeptides with short peptide length, niECD spectra were dominated by glycan cleavages. Similar radical site-induced glycosidic bond fragmentation has also been reported in positive ion mode ECD and ETD experiments.

6.2 Prospects for Future Work

6.2.1 Further Mechanistic Exploration of niECD

As discussed in Chapter 3, fixed-positive charge tags (quaternary amine groups) successfully enabled niECD for peptide anions failing to capture an electron in their unmodified forms. However, abundant tag losses were observed for the chosen derivatization techniques, precluding peptide/oligosaccharide sequence analysis. Additional charge tags could be investigated to promote peptide gas-phase zwitterion formation in negative ion mode. Fixed-negative charge tags are also of interest, particularly for peptides with multiple basic sites (e.g., tryptic peptides). Two tag candidates providing a negative charge are shown in Scheme 6.1. The first example is 4-aminonaphtalene sulfonic acid (ANSA), previously used to invoke charge-remote fragmentation in negative ion CAD.[1] ANSA reacts with peptide C-termini and acidic side chains, replacing the carboxylic acids with a more acidic sulfonic acid. Introduction of a negative charge may also be achieved by derivatization with 4-sulfophenyl

isothiocyanate (SPITC).[2, 3] In this case, the N-terminal amino group is modified to a highly acidic/negatively charged sulfonate derivative.

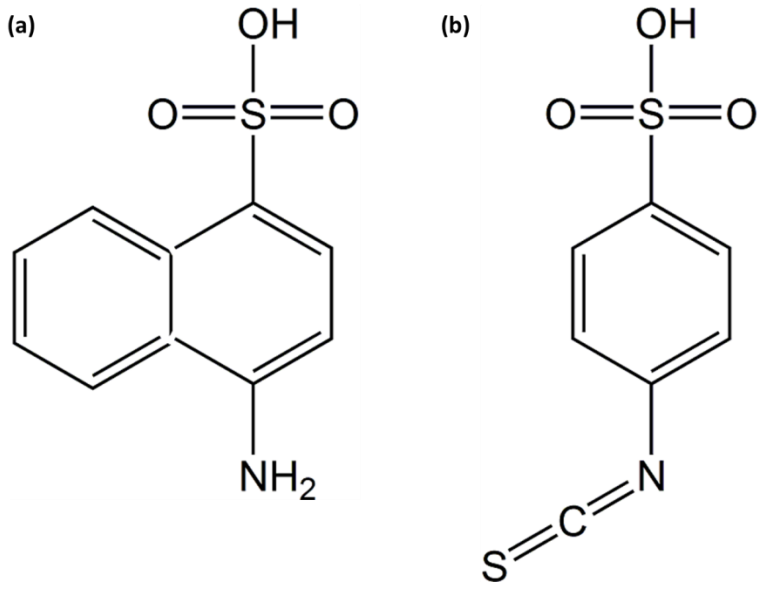

Scheme 6.1. Negative-charge tags to be explored for promoting peptide zwitterions in negative ion mode. (a) 4-aminonaphtalene sulfonic acid (ANSA) (b) 4-sulfophenyl isothiocyanate (SPITC).

The synthetic peptide data shown in Chapter 3 also indicate that higher-order structure may influence the niECD process. We proposed that the unexpected decrease in niECD fragmentation efficiency upon replacing C-terminal glutamine with lysine (the second series of synthetic peptides) is due to salt bridge formation between the lysine side chain and the C-terminal carboxylic acid. To address this problem, an infrared laser pulse before or after electron irradiation could be applied to break these potential non-covalent bonds, thus unfolding the peptide gas-phase structures, and presumably enhance niECD fragmentation. Further experiments with activated ion niECD will lend more insights into the structural effects in niECD. Another approach to investigate gaseous zwitterion structure is through computational modelling, which will be conducted in collaboration with Dr. Charles Brooks' group in the Department of Chemistry, University of Michigan.

Calculations of the gas-phase structures of the synthetic peptides will be performed and theoretical zwitterion propensity will be compared for peptides within the same sets as well as corresponding peptides in different sets. These computational data will be important for comparison with our experimental work and to verify the zwitterion hypothesis.

6.2.2 Optimization of niECD

It has been shown that niECD efficiency decreases with increasing charge state with maximum efficiency at an overall negative charge of one. However, for peptides, ESI favors higher charge states (2- or higher depending on peptide mass and sequence). In niECD experiments, mass spectral scan times are often lengthened due to the necessity to acquire sufficient signal from low abundance singly-charged precursor anions. Thus, charge state manipulation techniques to promote low precursor ion charge states may be necessary for optimum niECD.

Proton transfer reactions (PTR), which involve gas-phase reactions between precursor ions and reagent ions of opposite polarity, have shown utility for reducing precursor ion charge[4-6], charge-state purification[7], and even charge inversion[8]. PTR can be carried out in the external collision cell of our SolariX FT-ICR mass spectrometer. The external CI source is used to generate protonated fluoranthene ions, which provide efficient proton transfer to multiply charged peptide anions. PTR has been successfully applied in our lab to peptide anions and enhanced the signal of the singly-charged species. Experimental data demonstrate that niECD is achieved in a shorter time and more extensive structural information is generated when PTR is employed. However, there is still room for improvement. Further exploration of PTR, including reagent ion type, ion

mixing time, and ion introduction time could be performed in order to optimize this process. Alternative PTR reagents will include protonated isobutylene, pyridine, qunioline, isoqunioline, and benzoquinoline, all of which have been shown to predominantly affect proton transfer in reactions with multiply deprotonated oligonucleotides.[9, 10] Protonated reagent molecular ions should be relatively straightforward to produce with the existing CI source. Alternative CI reagent gases, including isobutane and ammonia rather than methane, could also be used as needed.

In addition to gas-phase charge state manipulation, solution-phase manipulation could be performed to improve niECD. Solution pH may play a role in affecting precursor charge states. Currently, basic pH is used to promote anion generation, however, lower pH may be ideal for generation of lower charge states. Furthermore, different solvent additives could be explored, such as piperidine/imidazole as reported by Taucher and Breuker for lowering charge states of RNA.[11]

6.2.3 niECD of Intact Proteins

One major contribution of conventional ECD is its utility for protein top-down analysis.[12-14] Given the extent of backbone fragmentation and retention of PTMs associated with ECD of intact proteins, it provides great benefits in protein characterization during top-down analysis. However, for acidic proteins, the high acidity affects protonation during positive mode ESI. In particular for phosphoproteins, salt bridges between the negatively charged phosphates and protonated groups may be induced, potentially affecting their fragmentation behavior.

Alternatively, negative ion mode may be valuable for acidic proteins, as reported by Breuker and co-workers for EDD of unmodified acidic proteins.[15] EDD and negative

ion IRMPD were applied in our lab to a phosphoprotein (β-casein) and valuable complementary information was generated.[16] Particularly, additional backbone cleavage was observed in the highly acidic multiply-phosphorylated region compared to conventional ECD, possibly due to salt-bridge formation in positive ion mode as discussed above. Thus, further exploration of negative ion mode for top-down MS/MS is of interest. Because niECD is very similar to regular ECD, it should also be advantageous in dissociating intact proteins and directly localizing labile PTMs. Moreover, niECD should be complementary to both negative mode IRMPD and EDD because IRMPD yields a variety of product ions, EDD yields *a*/*x*-type ions, and niECD should provide *c*/*z*-type ions.

Preliminary data for quadruply deprotonated, $[M - 4H]^{4-}$, ubiquitin (8.5 kDa) precursor ions from niECD are illustrated in Figure 6.1. Successful electron capture resulting in charge-increased $[M - 4H]^{5-\bullet}$ ions was observed but no backbone fragments were generated. For positive ion mode ECD or negative ion mode EDD, when applied to proteins, "activated ion" ECD or EDD (AI-ECD or AI-EDD) are often utilized to maximize the amount of informative backbone fragments. A similar precursor ion pre- or post-activation strategy may also be necessary for niECD, i.e., activated ion niECD. IR laser irradiation could be applied before or after electron capture to help unfold the sterically constrained structure and increase backbone cleavage coverage. Since the pI of ubiquitin is around neutral, investigation of more acidic standard proteins such as calmodulin and standard phosphoproteins such as caseins may also be valuable future work.

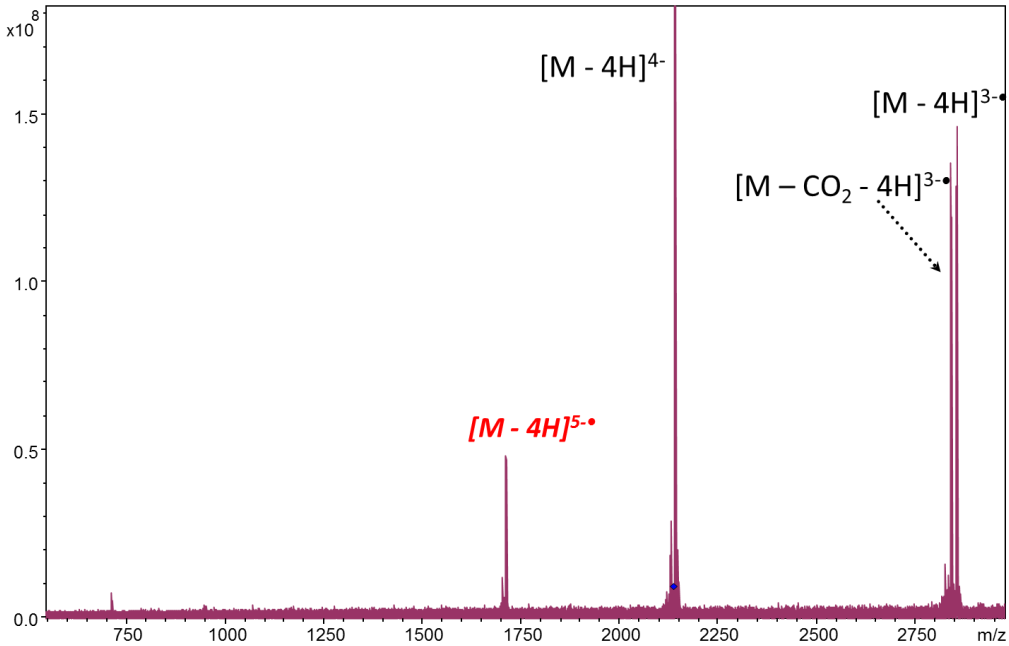

Figure 6.1. niECD of ubiquitin (SolariX FT-ICR MS instrument). $[M - 4H]^{4-}$ precursor ions were irradiated with electrons for 5 s. The cathode voltage was set to – 7.1 V. The spectrum was accumulated for 32 scans.

The approaches proposed to be developed in the previous section for charge state manipulation will be employed for maximizing niECD outcome as well. PTR prior to niECD could be applied to lower the charge state of precursor ions, decrease Coulomb repulsion and thus increase niECD efficiency. Nano ESI and native ESI, where proteins are sprayed in an aqueous solution containing a volatile salt, e.g., ammonium acetate, could also be utilized to shift charge state distribution of proteins. Ionization conditions in both cases are much gentler than regular ESI, and thus, more native-like proteins could be generated, which usually carry fewer charges. It also makes niECD a promising technique for investigating non-covalent interactions in protein complexes, as low charge states are preferred to retain solution-phase higher order structure into the gas phase.

6.3 References

1. Lindh, I.; Sjovall, J.; Bergman, T.; Griffiths, W. J. Negative-ion electrospray tandem mass spectrometry of peptides derivatized with 4-aminonaphthalenesulphonic acid. *J. Mass Spectrom.* **1998**, *33*, 988-993.
2. Madsen, J. A.; Brodbelt, J. S. Simplifying fragmentation patterns of multiply charged peptides by N-terminal derivatization and electron transfer collision activated dissociation. *Anal. Chem.* **2009**, *81*, 3645-3653.
3. Wang, D.; Kalb, S. R.; Cotter, R. J. Improved procedures for N-terminal sulfonation of peptides for matrix-assisted laser desorption/ionization post-source decay peptide sequencing. *Rapid Commun. Mass Spectrom.* **2004**, *18*, 96-102.
4. Stephenson, J. L.; McLuckey, S. A. Ion/Ion Reactions in the Gas Phase: Proton Transfer Reactions Involving Multiply-Charged Proteins. *J. Am. Chem. Soc.* **1996**, *118*, 7390-7397.
5. Stephenson, J. L.; McLuckey, S. A. Simplification of Product Ion Spectra Derived from Multiply-Charged Parent Ions via Ion/Ion Chemistry. *Anal. Chem. 70*, 3533–3544.
6. Coon, J. J.; Ueberheide, B.; Syka, J. E. P.; Dryhurst, D. D.; Ausio, J.; Shabanowitz, J.; Hunt, D. F. Protein identification using sequential ion/ion reactions and tandem mass spectrometry. *Proc. Natl. Acad. Sci. U. S. A.* **2005**, *102*, 9463-9468.
7. McLuckey, S. A.; Reid, G. E.; Wells, J. M. Ion Parking during Ion/Ion Reactions in Electrodynamic Ion Traps. *Anal. Chem.* **2002**, *74*, 336–346.
8. He, M.; Emory, J. F.; McLuckey, S. A. Reagent Anions for Charge Inversion of Polypeptide/Protein Cations in the Gas Phase. *Anal. Chem.* **2005**, *77*, 3173–3182.
9. Herron, W. J.; Goeringer, D. E.; McLuckey, S. A. Ion-Ion Reactions in the Gas Phase - Proton Transfer Reactions of Protonated Pyridine wiht Multiply-Charged Oligonucleotide Anions. *J. Am. Soc. Mass Spectrom.* **1995**, *6*, 529-532.
10. Wu, J.; McLuckey, S. A. Ion/ion Reactions of Multiply Charged Nucleic Acid Anions: Electron Transfer, Proton Transfer, and Ion Attachment. *Int. J. Mass Spectrom.* **2003**, *228*.
11. Taucher, M.; Breuker, K. Top-Down Mass Spectrometry for Sequencing of Larger (up to 61 nt) RNA by CAD and EDD. *J. Am. Soc. Mass Spectrom.* **2010**, *21*, 918-929.
12. Siuti, N.; Kelleher, N. L. Decoding protein modifications using top-down mass spectrometry. *Nat. Methods* **2007**, *4*, 817-821.
13. Cooper, H. J.; Hakansson, K.; Marshall, A. G. The role of electron capture dissociation in biomolecular analysis. *Mass Spectrom. Rev.* **2005**, *24*, 201-222.
14. Lanucara, F.; Eyers, C. E. Top-down mass spectrometry for the analysis of combinatorial post-translational modifications. *Mass Spectrom. Rev.* **2013**, *32*, 27-42.
15. Ganisl, B.; Valovka, T.; Hartl, M.; Taucher, M.; Bister, K.; Breuker, K. Electron Detachment Dissociation for Top-Down Mass Spectrometry of Acidic Proteins. *Chem. Eur. J.* **2011**, *17*, 4460-4469.
16. Song, H. T.; Hakansson, K. Electron Detachment Dissociation and Negative on Infrared Multiphoton Dissociation of Electrosprayed Intact Proteins. *Anal. Chem.* **2012**, *84*, 871-876.